UNIVERSIDAD NACIONAL AUTÓNOMA DE MÉXICO

POSGRADO EN CIENCIAS FÍSICAS

CLASSICAL AND QUANTUM DESCRIPTIONS OF THE PARAMETER SPACE GEOMETRY

TESIS

QUE PARA OPTAR POR EL GRADO DE:
DOCTOR EN CIENCIAS (FÍSICA)
PRESENTA:

DANIEL GUTIÉRREZ RUIZ

TUTOR PRINCIPAL

DR. JOSÉ DAVID VERGARA OLIVER
Instituto de Ciencias Nucleares

COMITÉ TUTOR

DR. HERNANDO QUEVEDO CUBILLOS
Instituto de Ciencias Nucleares

DRA. GABRIELA MURGUÍA ROMERO
Facultad de Ciencias

CIUDAD UNIVERSITARIA, CD. MX., MARZO DE 2021

Contents

Abstract

This thesis deals with the geometrical structures that underlie the parameter space of a physical system. We begin by introducing the Berry phase, connection and curvature. The Berry phase is the flux of the Berry curvature and emerges in a quantum system when we traverse adiabatically a circuit in parameter space. After understanding this object, we present the quantum metric tensor which encodes how distances are measured in parameter space in a gauge-invariant manner. It turns out that both the Berry curvature and the quantum metric tensor can be obtained, respectively, as the imaginary and real part of the quantum geometric tensor. The description can be broadened to include also a non-Abelian gauge structure that appears when considering degenerate quantum states. All these results are then cast in terms of Hermitian operators that generate displacements in parameter space, which will later turn out to be of special importance. Later, we introduce a path integral approach to treat the quantum geometric tensor and prove the equivalence between this description and the initial perspective based on the Hilbert space.

Once the basic tools have been presented, we introduce a novel phase space formulation of the parameter space geometry whose protagonist is the Wigner function. We establish the Abelian and non-Abelian descriptions and illustrate the approach with two examples.

In the following part, with the help of the classical analogs of the generators of displacements in parameter space, we reformulate the Hannay curvature, which is the classical analog of the Berry curvature. After this, we reach the central part of the work by introducing the classical analog of the quantum metric tensor, a novel object that measures the distance in the parameter space of a classical integrable system. Then, we present an equivalent time-dependent approach that arises from the semiclassical approximation of the path integral approach to the quantum geometric tensor.

We devote a good part of this thesis to the presentation of examples that illustrate the use of the different formulations and help us establish a comparison between the quantum and classical results. This will form the basis for the analysis of the Dicke and Lipkin-Meshkov-Glick models, where we use the quantum and classical metric tensors and their scalar curvatures to study quantum phase transitions in the thermodynamic limit, as well as their precursors for finite sizes of the system.

Finally, we find a relativistic Runge-Lenz vector for a modified Klein-Gordon equation that preserves the SO(4) symmetry. We describe its extraction from the $\mathcal{N} = 4$ super

Yang-Mills theory through a particular Higgs mechanism and connect its symmetries with those of the relativistic harmonic oscillator.

Resumen

Esta tesis trata sobre las estructuras geométricas subyacentes al espacio de parámetros de un sistema físico. Comenzamos presentando la fase de Berry, su conexión y curvatura. La fase de Berry es el flujo de la curvatura de Berry y aparece en un sistema cuántico cuando recorremos adiabáticamente un circuito en el espacio de parámetros. Después de entender este objeto, introducimos el tensor métrico cuántico, el cual codifica cómo se miden las distancias en el espacio de parámetros en una forma invariante de norma. Vemos que tanto la curvatura de Berry como el tensor métrico cuántico pueden obtenerse, respectivamente, como la parte imaginaria y real del tensor geométrico cuántico. Esta descripción puede ampliarse para incluir una estructura de norma no Abeliana que aparece al considerar estados cuánticos degenerados. Todos estos resultados se formulan luego en términos de operadores Hermitianos que generan desplazamientos en el espacio de parámetros, que serán luego de especial importancia. Posteriormente, introducimos el enfoque de integral de trayectoria del tensor geométrico cuántico y demostramos la equivalencia entre esta descripción y el enfoque inicial basado en el espacio de Hilbert.

Ya que las herramientas básicas fueron introducidas, presentamos una nueva formulación en el espacio fase de la geometría del espacio de parámetros cuyo protagonista es la función de Wigner. Establecemos las descripciones Abelianas y no Abelianas e ilustramos el enfoque con dos ejemplos.

En la siguiente parte, mediante los análogos clásicos de los generadores de desplazamientos en el espacio de parámetros, reformulamos la curvatura de Hannay, que es el análogo clásico de la curvatura de Berry. Después, llegamos a la parte central del trabajo al introducir el análogo clásico del tensor métrico cuántico, un objeto nuevo que mide la distancia en el espacio de parámetros de un sistema integrable clásico. Luego, presentamos una fomulación equivalente dependiente del tiempo y que surge de la aproximación semiclásica del enfoque de integral de trayectoria del tensor geométrico cuántico.

Dedicamos una buena parte de esta tesis a presentar ejemplos que ilustren el uso de las diferentes formulaciones y nos ayuden a establecer una comparación entre los resultados cuánticos y clásicos. Esto formará la base para el análisis de los modelos de Dicke y de Lipkin-Meshkov-Glick, donde usamos el tensor métrico cuántico y clásico y sus curvaturas escalares para estudiar las transiciones de fase cuánticas en el límite termodinámico, así como sus precursores para tamaños finitos del sistema.

Finalmente, encontramos un vector relativista de Runge-Lenz para una ecuación de Klein-Gordon modificada que preserva la simetría SO(4). Describimos su obtención

a partir de la teoría super Yang-Mills $\mathcal{N} = 4$ mediante cierto mecanismo de Higgs y conectamos sus simetrías con las del oscilador armónico relativista.

Acknowledgments

I wish to thank:

- God for filling me with his grace and blessing me with the opportunity to get through my studies.
- Dr. José David Vergara for being an admirable supervisor. Your valuable help, patience and comprehension allowed me to finish this work.
- Drs. Hernando Quevedo and Gabriela Murguía for their advice and always being attentive to my progress.
- Drs. Jorge Hirsch, Andrea Valdés, and David José Fernández for their suggestions and comments to improve this work.
- Dr. Diego González for his support and patience. Without your help and ideas, I am sure that this thesis would be half its length.
- Drs. Jorge Hirsch, Antonio García, and Jorge Chávez for wonderful collaborations together.
- Dr. Eduardo Rosas for his wise advice that was essential during this long journey. I am truly indebted to you.
- My family for their unconditional love and support. This thesis is dedicated to you, mom.
- Ema, the most wonderful person in the universe. I could write two hundred more pages telling how much you mean to me.
- All my friends and partners for always putting a smile on my face.
- The staff of the ICN and the PCF for their help with administrative matters.
- CONACYT for supporting me with the four-year scholarship No. 463765.
- The DGAPA-PAPIIT Grant No. IN103919 provided by UNAM.

List of publications

The results of this thesis have been published on the following peer-reviewed articles:

- J. Alvarez-Jimenez, I. Cortese, J. Antonio García, D. Gutiérrez-Ruiz, and J. David Vergara, "Relativistic Runge-Lenz vector: from $\mathcal{N} = 4$ SYM to SO(4) scalar field theory", Journal of High Energy Physics **2018**, 153 (2018)

- Diego Gonzalez, D. Gutiérrez-Ruiz, and J. David Vergara, "Classical analog of the quantum metric tensor", Physical Review E **99**, 032144 (2019)

- J. Alvarez-Jimenez, Diego Gonzalez, D. Gutiérrez-Ruiz, and J. David Vergara, "Geometry of the parameter space of a quantum system: Classical point of view", Annalen der Physik **532**, 1900215 (2020)

- Diego Gonzalez, D. Gutiérrez-Ruiz, and J. David Vergara, "Phase space formulation of the Abelian and non-Abelian quantum geometric tensor", Journal of Physics A: Mathematical and Theoretical **53**, 505305 (2020)

and on the conference article:

- J. Alvarez-Jimenez, I. Cortese, J. Antonio García, D. Gutiérrez-Ruiz, and J. David Vergara, "Reestablishment of SO(4) symmetry in the relativistic Coulomb problem from $\mathcal{N} = 4$ SYM", Journal of Physics: Conference Series **1194**, 012057 (2019).

Additional peer-reviewed collaborations:

- J. Antonio García, D. Gutiérrez-Ruiz, and R. Abraham Sánchez-Isidro, "Vertical extension of Noether theorem for scaling symmetries", European Physical Journal Plus **136**, 3 (2021).

- D. Gutiérrez-Ruiz, Diego Gonzalez, Jorge Chávez-Carlos, Jorge G. Hirsch, and J. David Vergara, "Quantum geometric tensor and quantum phase transitions in the Lipkin-Meshkov-Glick model", Physical Review B (sent).

- Diego Gonzalez, D. Gutiérrez-Ruiz, and J. David Vergara, "Classical and quantum descriptions of the parameter space geometry in the Dicke and Lipkin-Meshkov-Glick models", Physical Review E (sent).

Introduction

There is a deep interplay between geometry, information theory and quantum mechanics [1]. A fundamental element in geometry is the metric tensor which allows to measure distances. A metric of great interest that is defined for statistical spaces is the Fisher metric. This metric plays an important role in the study of information in quantum mechanics [2], where it is called Bures metric [3] for mixed states, and Fubini-Study metric, or quantum geometric tensor for pure states [4]. When the real part of this tensor is taken, the quantum metric tensor is obtained; Provost and Vallee [5] motivated the definition of this quantum metric by requiring that the distance induced by the inner product in Hilbert state space be gauge independent with respect to the parameter space. On the other hand, the imaginary part of the quantum geometric tensor gives rise to the Berry curvature [6], which was given a formal geometric interpretation by Simon [7] and is central in the study of adiabatic phenomena. The celebrated Berry phase appears as the flux of the Berry curvature through the enclosed area of a circuit in parameter space that is adiabatically traversed. The Berry phase was seen to possess a classical counterpart, the Hannay angle [8], and the relation between them was established by Berry through the semiclassical approximation of the wave function [9]. The Berry phase was later generalized for a non-adiabatic evolution and for general quantum states in the framework of the projective Hilbert space [10]. Likewise, the Fubini-Study distance was shown to induce a measure of speed in the projective Hilbert space for a general evolution [11, 12].

Nowadays, the quantum metric tensor and the Berry curvature have found a broad range of applicability in quantum mechanics, as well as in other areas of physics like condensed matter and information theory. For example, information theory concepts like fidelity are deeply related to the quantum metric tensor and can be used to predict phase transitions in quantum systems [13]. Also, divergences that appear in the components of the quantum metric metric tensor are intimately related to quantum phase transitions [14–20]; for instance, there is a complete study of the Riemannian geometry associated with the spin XY chain in a transverse field [15, 21], where different types of singularities in the metric and curvature are described, and experiments that can account for these phenomena are suggested [21]. The quantum metric tensor has also great relevance in the study of superfluids [22], Bogoliubov quasiparticles [23], and more recently, it has proven to be an essential element in quantum computation [24–26] and complexity [27].

The geometric perspective has also been fruitful in the understanding of other branches

of physics. For instance, in thermodynamics it has evolved since the proposals of Weinhold and Ruppeiner [28–31], until the more recent geometrothermodynamics [32, 33], which has even been applied to black holes and cosmology. Therefore, the relation between geometric objects and physical properties has been successfully implemented and has been found to possess a great predictive power. It also leads to a deeper insight of the physical phenomena under consideration. In this spirit, different experiments have been proposed to measure the quantum metric [34–38].

Another area of interest that departs from the previous topics is the study of $\mathcal{N} = 4$ super Yang-Mills theory (SYM), which is central to theoretical high energy physics. Recent developments in the integrability of $\mathcal{N} = 4$ SYM have made possible the complete calculation of all tree-level amplitudes as well as up to fourth order loops in perturbation theory [39]. This was accomplished by using a duality symmetry in momentum space. The integrability has its origins in the existence of generators of symmetries that transform the fields in the internal space of the theory. In this context, in [40] it was raised the question about the possibility of constructing a consistent relativistic quantum field theory that preserves the analogous of the Runge-Lenz vector of the attractive Coulomb potential in classical mechanics. The answer to this question is that it is indeed possible and that the theory is precisely $\mathcal{N} = 4$ SYM processed by a Higgs mechanism that gives mass to some scalars fields.

In this work, our first purpose is to delve deeper into the study of the quantum geometric tensor. To do this, we will relate and illustrate two approaches to its computation and introduce a new formulation in terms of the Wigner function formalism. A second purpose is the investigation of a classical analog of the quantum metric tensor. Our motivation is that information from parameter space can be retrieved through classical methods since quantum systems may possess features that are attainable through the computation of classical geometric objects that have a similar structure as the quantum ones. This will lead us to the application of the quantum and classical methods to the analysis of many-body systems that are important in quantum optics and nuclear physics. Our last purpose is to obtain a relativistic hydrogen-like theory from $\mathcal{N} = 4$ SYM which will preserve the SO(4) symmetry that is lost in the usual minimal-coupling prescription. This will motivate the consideration of a Higgs mechanism on the Lagrangian of $\mathcal{N} = 4$ SYM, and then to the application of the enhanced symmetry to the solution of the resulting equation.

The structure of the thesis is as follows. Chapter 1 provides an overview of the fidelity approach to quantum phase transitions and summarizes some geometrical concepts that are relevant for this work. Chapter 2 deals with the quantum construction of the parameter space geometry. The Berry phase, connection, curvature, as well as the quantum metric tensor and quantum geometric tensor are described. Two approaches are introduced and are proved to be equivalent. In Chapter 3, we present a Wigner function formulation of the Abelian and non-Abelian quantum geometric tensors and complement the concepts with two examples. In Chapter 4, we introduce the Hannay angle, connection and curvature, and propose the classical analog of the quantum metric

tensor. These classical objects are obtained from a semiclassical approximation of their quantum counterparts and different expressions to compute them are presented. Chapters 5 and 6 treat several examples using the two approaches to the quantum and classical geometric quantities. In Chapters 7, 8 and 9, we study the quantum phase transitions in the Dicke and Lipkin-Meshkov-Glick models through the use of the quantum metric tensor, its classical analog, and their scalar curvatures. In Chapter 10, we introduce a Higgs mechanism on the $\mathcal{N} = 4$ super Yang-Mills theory that yields a relativistic equation for the Coulomb potential that preserves the SO(4) symmetry, and thus, allows us to build a relativistic Runge-Lenz vector to find the solutions. We illustrate the Kustaanheimo-Stiefel duality between this system and the relativistic harmonic oscillator and relate their constants of motion. Finally, some conclusions and directions for future research are laid out in Chapter 11.

Chapter 1

Quantum phase transitions and geometry

The goal of this chapter is to provide a brief account of the basic tools to understand the fidelity approach to quantum phase transitions, as well as some notions of Riemannian geometry that will be used throughout this work. These two apparently different subjects will be seen to merge in the next chapter, where important concepts such as the Berry curvature and the quantum metric tensor appear.

1.1 Fidelity approach to quantum phase transitions

A quantum phase transition is characterized by a change in the analytic properties of the ground state. As opposed to classical phase transitions (thermodynamic phase transitions), it is usually said that quantum phase transitions occur at zero temperature to remark that they are not driven by thermal fluctuations, but by fluctuations associated with the Heisenberg uncertainty principle [41]. In this sense, a quantum phase transition can occur when the parameters that appear in the Hamiltonian are varied.

In the context of quantum many-body systems, the main focus is on second-order phase transitions, also known as continuous phase transitions. In terms of the Ehrenfest classification scheme, we say that an nth-order quantum phase transition occurs when the nth derivative is the lowest order derivative which is discontinuous. Usually, second-order phase transitions occur in many-body systems in the limit where the system's extension becomes infinite (thermodynamic limit), thus leading to a non-analyticity at a critical value $x = x_c$ in the ground state energy. The non-analyticity could be either the limiting case of an avoided level-crossing or an actual level-crossing [41].

Given that drastic changes in the ground state occur at a quantum phase transition, we expect that a measure of the degree of similarity between quantum states can provide a characterization of that phenomenon. In this respect, we can use a concept borrowed from quantum information: the fidelity. This quantity measures the closeness between two quantum states, yielding the value of unity if both states are the same, or zero in

case they are orthogonal. Given two pure quantum states, denoted as $|\psi_1\rangle$ and $|\psi_2\rangle$, the fidelity $\mathcal{F}$ is the modulus of their overlap, i.e. [13],

$$\mathcal{F}(\psi_1, \psi_2) := |\langle\psi_1|\psi_2\rangle|. \tag{1.1}$$

It is worth noting that unlike the overlap, the fidelity is the same regardless of the phases of each state[1]. The fidelity has the following properties:

$$\begin{aligned} 0 \leq \mathcal{F}(\psi_1, \psi_2) &\leq 1, \\ \mathcal{F}(\psi_1, \psi_2) &= \mathcal{F}(\psi_2, \psi_1), \\ \mathcal{F}(\hat{U}\psi_1, \hat{U}\psi_2) &= \mathcal{F}(\psi_1, \psi_2), \\ \mathcal{F}(\psi_1 \otimes \varphi_1, \psi_2 \otimes \varphi_2) &= \mathcal{F}(\psi_1, \psi_2)\mathcal{F}(\varphi_1, \varphi_2), \end{aligned} \tag{1.2}$$

where $\hat{U}$ represents a unitary transformation and $|\psi\rangle$, $|\varphi\rangle$ are the states of different subsystems. Fidelity can also be used to compare mixed states described by the density matrices $\hat{\rho}_1$ and $\hat{\rho}_2$. The most widely-used definition in this case is the Uhlmann fidelity [44] given by

$$\mathcal{F}(\rho_1, \rho_2) := \mathrm{Tr}\sqrt{\sqrt{\hat{\rho}_1}\hat{\rho}_2\sqrt{\hat{\rho}_1}}. \tag{1.3}$$

This definition satisfies the properties (1.2). For pure states, we have $\hat{\rho}_1 = |\psi_1\rangle\langle\psi_1|$ and $\hat{\rho}_2 = |\psi_2\rangle\langle\psi_2|$, and the Uhlmann fidelity reduces to (1.1).

A closely related concept to fidelity is the Fubini-Study distance [45, 46]. Consider the quantum states $|\psi_1\rangle$ and $|\psi_2\rangle$, then the Fubini-Study distance between them is defined as

$$d_{FS}(\psi_1, \psi_2) := \sqrt{2 - 2|\langle\psi_1|\psi_2\rangle|} = \sqrt{2 - 2\mathcal{F}(\psi_1, \psi_2)}. \tag{1.4}$$

It can be shown that it satisfies the three axioms of a distance function [1]:

$$\begin{aligned} d_{FS}(\psi_1, \psi_2) = 0 &\iff |\psi_1\rangle = |\psi_2\rangle, \\ d_{FS}(\psi_2, \psi_1) &= d_{FS}(\psi_1, \psi_2), \\ d_{FS}(\psi_1, \psi_3) &\leq d_{FS}(\psi_1, \psi_2) + d_{FS}(\psi_2, \psi_3). \end{aligned} \tag{1.5}$$

To gain more intuition about the fidelity and the Fubini-Study distance, we can easily establish an analogy with basic concepts of Euclidean geometry. Let $\boldsymbol{x}$ and $\boldsymbol{y}$ be two unit vectors in $\mathbb{R}^2$. The Euclidean distance between these two vectors can be obtained as

$$||\boldsymbol{x} - \boldsymbol{y}|| = \sqrt{(\boldsymbol{x} - \boldsymbol{y}) \cdot (\boldsymbol{x} - \boldsymbol{y})} = \sqrt{2 - 2\boldsymbol{x} \cdot \boldsymbol{y}}, \tag{1.6}$$

where $\boldsymbol{x} \cdot \boldsymbol{y}$ denotes the scalar product. If θ is the angle between the vectors, we know that $\boldsymbol{x} \cdot \boldsymbol{y} = \cos\theta$. Therefore, comparing (1.6) with (1.4), we see that the fidelity is analogous to the cosine of the angle between the vectors, whereas the Fubini-Study distance is analogous to the Euclidean distance.

[1] There is an alternative definition of fidelity given by $|\langle\psi_1|\psi_2\rangle|^2$ (see [42, 43]). However, in this work we will employ (1.1) only

Now, when the states under consideration in the evaluation of the Fubini-Study distance (1.4) are infinitesimally separated such that $|\psi_1\rangle = |\psi\rangle$ and $|\psi_2\rangle = |\psi\rangle + |\delta\psi\rangle$, then the Fubini-Study metric, also known as the quantum metric tensor, is obtained. We will see the emergence of this object in the next chapter following the work of Provost and Valle [5]. It is worth mentioning that the Fubini-Study metric can also be shown to appear when the Fisher metric, which is used in information theory to provide a measure of distance in a statistical manifold, is extended to a complex projective space [2].

Finally, regarding the generalization to mixed states, if equation (1.4) is evaluated with the Ulhmann fidelity (1.3) instead of (1.1), then we obtain the so-called Bures distance [47]. The infinitesimal expansion of this distance results in the Bures metric, which is in general not easy to calculate due to the presence of the symmetric logarithm derivative operator [3].

1.2 Elements of Riemannian geometry

We now provide a brief account of the basic geometric tools that will later be useful for analyzing the parameter space of a given system. The differential-geometric construction begins with the concept of manifold. A (differentiable) manifold $\mathcal{M}$ of dimension N is a topological space that locally resembles $\mathbb{R}^N$. In this sense, we can assign coordinates $x_\alpha = \{x^i_\alpha\}$, $(i = 1, ..., N)$ to an open subset $A_\alpha \subset \mathcal{M}$ that provide a one-to-one map $\phi_\alpha : A_\alpha \to \mathbb{R}^N$ such that the image $\phi_\alpha(A_\alpha)$ is open in $\mathbb{R}^N$. The pair $\{A_\alpha, \phi_\alpha\}$ is called a chart. We further require that the union of all the charts $\bigcup_\alpha A_\alpha$ cover the manifold, and that where two charts intersect, the map $(\phi_\alpha \circ \phi_\beta^{-1})$ is infinitely differentiable, meaning that the charts are smoothly sewn together [48].

At this point, we introduce the Einstein summation convention to write compact expressions for sums by omitting the symbol Σ. In this way, when the same index appears two times, one as a subscript and the other as a superscript, a sum is implied. We call this a contraction. For example, the expression $V^i\omega_i$ means $\sum_{i=1}^N V^i\omega_i$.

We now proceed to the introduction of tensors on a manifold. We begin with the concept of a vector. A (contravariant) vector at a point P is an object whose N components $\{V^i\}$ transform as

$$V^i \to V'^i = \frac{\partial x'^i}{\partial x^j} V^j \tag{1.7}$$

under a change of coordinates $x \to x' = x'(x)$. Here, the derivatives are evaluated at P. The set of all the vectors that are defined at P is known as the tangent space T_P. The (coordinate) basis of this vector space is the set of directional derivatives at P, therefore, a vector V is written as $V = V^i\partial_i$, where $\partial_i := \frac{\partial}{\partial x^i}$.

Analogously, we define a covariant vector, or one-form, as an object whose N components $\{\omega_i\}$ transform as

$$\omega_i \to \omega'_i = \frac{\partial x^j}{\partial x'^i} \omega_j \tag{1.8}$$

under the change of coordinates $x \to x' = x'(x)$. The set of all the one-forms at a given point P is called the cotangent space T_p^* and its (coordinate) basis is formed by the differential displacements $\mathrm{d}x^i$, thus, a one-form is expanded as $\omega = \omega_i \mathrm{d}x^i$.

More generally, we define a tensor of rank (m, n) as an object whose components $T^{i_1 \cdots i_m}{}_{j_1 \cdots j_n}$ transform as

$$T^{i_1 \cdots i_m}{}_{j_1 \cdots j_n} \to T'^{i_1 \cdots i_m}{}_{j_1 \cdots j_n} = \frac{\partial x'^{i_1}}{\partial x^{k_1}} \cdots \frac{\partial x'^{i_m}}{\partial x^{k_m}} \frac{\partial x^{l_1}}{\partial x'^{j_1}} \cdots \frac{\partial x^{l_n}}{\partial x'^{j_n}} T^{k_1 \cdots k_m}{}_{l_1 \cdots l_n} \tag{1.9}$$

under the change of coordinates $x \to x' = x'(x)$. In this case, the tensor is expressed as $T = T^{i_1 \cdots i_m}{}_{j_1 \cdots j_n} \partial_{i_1} \otimes \cdots \otimes \partial_{i_m} \otimes \mathrm{d}x^{j_1} \otimes \cdots \otimes \mathrm{d}x^{j_n}$. We readily recognize that vectors are $(1, 0)$ tensors and one-forms are $(0, 1)$ tensors. It is important to note that an object with no free indices, like the contraction $V^i \omega_i$, is invariant under coordinate transformations due to the properties (1.7) and (1.8). Such an object is called a scalar and is a $(0, 0)$ tensor.

A fundamental object in Riemannian geometry is the metric tensor $g_{ij}(x)$, which allows us to measure distances on the manifold $\mathcal{M}$. The metric is a symmetric $(0, 2)$ tensor, hence, its components transform as

$$g_{ij} \to g'_{ij} = \frac{\partial x^k}{\partial x'^i} \frac{\partial x^l}{\partial x'^j} g_{kl} \tag{1.10}$$

under the change $x \to x' = x'(x)$. The metric tensor defines an inner product over $\mathcal{M}$ which is invariant under coordinate transformations: $V \cdot W = g_{ij} V^i W^j$. This, in turn, allows us to define the (squared) norm $||V||^2 = V \cdot V$, and as a consequence, to measure distances. The metric is also non-degenerate, i.e., $V \cdot W = 0$ for all V only if $W = 0$. In particular, this means that the matrix with elements g_{ij} is invertible at every point. Denoting the components of the inverse metric as g^{ij}, we have that $g^{ik} g_{kj} = \delta^i_j$. With this at hand, we can find the infinitesimal (squared) distance between two points whose coordinates are x and $x + \mathrm{d}x$ as

$$\mathrm{d}s^2 = g_{ij}(x) \mathrm{d}x^i \mathrm{d}x^j. \tag{1.11}$$

Other tensors of interest are differential forms, or n-forms, which are completely antisymmetric $(0, n)$ tensors. To discuss their properties, we first introduce the wedge product defined as

$$\mathrm{d}x^i \wedge \mathrm{d}x^j = \frac{1}{2}(\mathrm{d}x^i \otimes \mathrm{d}x^j - \mathrm{d}x^j \otimes \mathrm{d}x^i) = -\mathrm{d}x^j \wedge \mathrm{d}x^i. \tag{1.12}$$

Naturally, $\mathrm{d}x^i \wedge \mathrm{d}x^i = 0$. Under the coordinate transformation $x \to x' = x'(x)$, we see that $\mathrm{d}x^i \wedge \mathrm{d}x^j$ transforms as [49]

$$\mathrm{d}x^i \wedge \mathrm{d}x^j \to \mathrm{d}x'^i \wedge \mathrm{d}x'^j = \left(\frac{\partial x'^i}{\partial x^k} \frac{\partial x'^j}{\partial x^l} - \frac{\partial x'^i}{\partial x^l} \frac{\partial x'^j}{\partial x^k} \right) \mathrm{d}x^k \wedge \mathrm{d}x^l, \tag{1.13}$$

which is precisely the transformation rule of an area element. An n-form ω defined on the manifold $\mathcal{M}$ is then expressed as

$$\omega = \frac{1}{n!}\omega_{i_1\cdots i_n}\mathrm{d}x^{i_1}\wedge\cdots\wedge\mathrm{d}x^{i_n}, \tag{1.14}$$

where the coefficients $\omega_{i_1\cdots i_n}$ are completely antisymmetric. The dimension of the vector space $\Lambda^n(x)$, which contains all the n-forms at a point P with coordinates x, is $\binom{N}{n} = \frac{N!}{n!(N-n)!}$. The wedge product can be used to operate between differential forms. If ω is an m-form and η is an n-form, then

$$\omega\wedge\eta = \frac{(m+n)!}{m!n!}\omega_{[i_1\cdots i_m}\eta_{i_{m+1}\cdots i_{m+n}]}\mathrm{d}x^{i_1}\wedge\cdots\wedge\mathrm{d}x^{i_m}\wedge\mathrm{d}x^{i_{m+1}}\wedge\cdots\wedge\mathrm{d}x^{i_{m+n}} \tag{1.15}$$

gives as a result an $(m+n)$-form, where $[\cdots]$ performs the antisymmetrization of the indices contained inside the brackets. Also,

$$\omega\wedge\eta = (-1)^{mn}\eta\wedge\omega. \tag{1.16}$$

The n-forms can be differentiated with the aid of the exterior derivative. This operation takes n-forms into $(n+1)$-forms as

$$\mathrm{d}\left(\frac{1}{n!}\omega_{i_1\cdots i_n}\mathrm{d}x^{i_1}\wedge\cdots\wedge\mathrm{d}x^{i_n}\right) = (n+1)\partial_{[i_{n+1}}\omega_{i_1\cdots i_n]}\mathrm{d}x^{i_{n+1}}\wedge\mathrm{d}x^{i_1}\wedge\cdots\wedge\mathrm{d}x^{i_n}, \tag{1.17}$$

The exterior derivative of the wedge product of an m-form ω and an n-form η is

$$\mathrm{d}(\omega\wedge\eta) = \mathrm{d}\omega\wedge\eta + (-1)^m\omega\wedge\mathrm{d}\eta. \tag{1.18}$$

Furthermore, $\mathrm{d}(\mathrm{d}\omega) = 0$. The exterior derivative allows us to state an important result that generalizes the fundamental theorem of calculus: the Stokes theorem. It says that given an $(n-1)$-form ω and an orientable n-dimensional manifold Ω, then

$$\int_{\Omega}\mathrm{d}\omega = \int_{\partial\Omega}\omega, \tag{1.19}$$

where $\partial\Omega$ is the boundary of Ω.

Finally, we can characterize the local behavior of our manifold $\mathcal{M}$ with the Riemann tensor $R^i{}_{jkl}$. This object can be constructed from second derivatives of the metric combined in a specific way and it contains all the information about the curvature in the vicinity of a given point. Essentially, it arises from the commutator of the covariant derivatives which are formed from a metric-compatible and symmetric connection, i.e., the Levi-Civita connection (for more details, see [48]). In two dimensions, which will be the case for the models that we analyze in Chapters 7, 8, and 9, the Riemann tensor has only one independent component, and thus, its contraction $R = g^{ij}R^k{}_{ikj}$ known as the

scalar curvature (or Ricci scalar) provides an invariant measure of the curvature. Using local coordinates $x = (x^1, x^2)$, the scalar curvature can be computed as [50]

$$R = \frac{1}{\sqrt{g}}(\mathcal{A} + \mathcal{B}) \tag{1.20}$$

where

$$\begin{aligned} \mathcal{A} &= \frac{\partial}{\partial x^1}\left[\frac{1}{\sqrt{g}}\left(\frac{g_{12}}{g_{11}}\frac{\partial g_{11}}{\partial x^2} - \frac{\partial g_{22}}{\partial x^1}\right)\right], \\ \mathcal{B} &= \frac{\partial}{\partial x^2}\left[\frac{1}{\sqrt{g}}\left(2\frac{\partial g_{12}}{\partial x^1} - \frac{\partial g_{11}}{\partial x^2} - \frac{g_{12}}{g_{11}}\frac{\partial g_{11}}{\partial x^1}\right)\right], \end{aligned} \tag{1.21}$$

and g is the determinant of the metric.

As a first example to illustrate the concept of scalar curvature, let our manifold $\mathcal{M}$ be a sphere with radius a. We take as our coordinates the polar and azimuthal angles, hence, $x = \{x^i\} = (\theta, \phi)$, $(i = 1, 2)$. The infinitesimal squared distance between two points on the sphere is given by

$$\mathrm{d}s^2 = a^2\mathrm{d}\theta^2 + a^2 \sin^2\theta\, \mathrm{d}\phi^2, \tag{1.22}$$

from which we can extract the metric tensor

$$g_{ij} = \begin{pmatrix} a^2 & 0 \\ 0 & a^2\sin^2\theta \end{pmatrix}. \tag{1.23}$$

Using equation (1.20), we find the scalar curvature

$$R = \frac{2}{a^2}. \tag{1.24}$$

This result indicates that a sphere has a positive constant curvature. Furthermore, increasing the radius makes the curvature smaller, as we intuitively expect, and in the limit $a \to \infty$ the scalar curvature approaches to zero, which is the curvature of a plane.

As our second example, we consider the Lobachevsky space H^2 [51]. Taking as our coordinates $x = \{x^i\} = (\rho, \theta)$, $(i = 1, 2)$, the distance element is

$$\mathrm{d}s^2 = a^2(\mathrm{d}\rho^2 + \sinh^2\rho\, \mathrm{d}\theta^2), \tag{1.25}$$

where $a > 0$ is a constant. The metric tensor is

$$g_{ij} = \begin{pmatrix} a^2 & 0 \\ 0 & a^2\sinh^2\rho \end{pmatrix}, \tag{1.26}$$

and its resulting scalar curvature is

$$R = -\frac{2}{a^2}. \tag{1.27}$$

The negative scalar curvature means that this manifold has hyperbolic geometry, thus having a saddle-like shape at each point.

Chapter 2

Quantum geometric tensor

In this chapter, we summarize the basic results concerning the emerge of the Berry phase [6] and the quantum metric tensor, and the associated geometric structure that naturally appears. We remark the important feature that all the geometric quantities can be rewritten in terms of the generators of translations in parameter space, and note that this will later prove to possess great relevance. Then, we introduce the path integral approach to the quantum geometric tensor and prove our first result: that the expressions obtained under this formulation are the same that those obtained with the generator approach. Finally, we provide the different ways of computing the objects that encode the geometry of the parameter space.

2.1 The Berry phase, connection and curvature

The notion of adiabaticity is usually introduced through a system with a Hamiltonian $\hat{H}(x)$ that depends on some parameters $x(t) = \{x^i\}$, $i = 1, ..., M$, which at the same time have a dependence on time[1]. We say that we are in the adiabatic regime when the time it takes the parameters to change appreciably is much longer compared to the natural time scale of the system [4]. Moreover, the parameters change in a form which is independent of the dynamics of the system. The adiabatic theorem states that if a quantum system begins in the Hamiltonian's eigenstate $|n(x)\rangle$, then after an adiabatic evolution where the parameters change from x to $x + \mathrm{d}x$, the system will remain in the same state eigenstate, assuming that the nth energy level is non degenerate. In this work, we restrict ourselves to the consideration of the adiabatic regime. Generalizations of some of the geometric structures that will be introduced and some aspects of the parameters' choice can be found in [10] and [52], respectively.

The time evolution in the adiabatic approximation is obtained by solving the instantaneous Schrödinger equation

$$\hat{H}(x)|n(x)\rangle = E_n(x)|n(x)\rangle. \tag{2.1}$$

[1]Along this work, the parameters $x(t)$ will be denoted as x to simplify notation.

The result is that during evolution, the state will acquire a dynamic phase

$$\alpha_n(t) = \exp\left[-\frac{i}{\hbar}\int_0^t \mathrm{d}t'\, E_n(t')\right], \tag{2.2}$$

and a so-called geometric phase

$$\gamma_n(t) = \int_0^t \mathrm{d}t'\, i\left\langle n\middle|\frac{\mathrm{d}n}{\mathrm{d}t'}\right\rangle = \int_0^t \mathrm{d}t'\, i\langle n|\dot{n}\rangle. \tag{2.3}$$

If the system is taken through a closed curve $C : \{x^i = x^i(t)\,|\,t \in [0,T]\}$ in parameter space, the geometric phase can be written as

$$\gamma_n(C) = \oint_C \mathrm{d}x^i\, A_i^{(n)}, \tag{2.4}$$

where

$$A_i^{(n)} = i\left\langle n\middle|\frac{\partial n}{\partial x^i}\right\rangle = i\langle n|\partial_i n\rangle. \tag{2.5}$$

We see that this introduces a one-form $A^{(n)}$ that in local coordinates is expressed as $A^{(n)} = A_i^{(n)}\mathrm{d}x^i$ (we use the Einstein summation convention), and thus,

$$\gamma_n(C) = \oint_C A^{(n)}. \tag{2.6}$$

This geometric phase $\gamma_n(C)$ is known as Berry phase [6]. Using Stokes theorem, we can cast it in the form

$$\gamma_n(C) = \int_\Sigma F^{(n)}, \tag{2.7}$$

with $F^{(n)} = \mathrm{d}A^{(n)}$ and Σ a surface such that $C = \partial\Sigma$. In local coordinates, the two-form $F^{(n)}$ is

$$F^{(n)} = \frac{1}{2}F_{ij}^{(n)}\mathrm{d}x^i \wedge \mathrm{d}x^j, \tag{2.8}$$

where

$$F_{ij}^{(n)} = \partial_i A_j^{(n)} - \partial_j A_i^{(n)}. \tag{2.9}$$

We assume that we are working with an orthonormal set of states such that $\langle m|n\rangle = \delta_{mn}$. Taking the derivative of this condition with respect to x^i, we see that

$$\langle \partial_i m|n\rangle = -\langle m|\partial_i n\rangle, \tag{2.10}$$

and letting $m = n$, we conclude that

$$\mathrm{Re}\langle n|\partial_i n\rangle = 0. \tag{2.11}$$

This indicates that $A_i^{(n)} = i\langle n|\partial_i n\rangle$ is real, hence,

$$A_i^{(n)} = -\mathrm{Im}\langle n|\partial_i n\rangle. \tag{2.12}$$

Of course, this also entails that $F_{ij}^{(n)}$ is real and can be written as

$$F_{ij}^{(n)} = i\left(\langle\partial_i n|\partial_j n\rangle - \langle\partial_j n|\partial_i n\rangle\right) = -\mathrm{Im}\left(\langle\partial_i n|\partial_j n\rangle - \langle\partial_j n|\partial_i n\rangle\right). \tag{2.13}$$

We know that two states differing by a phase are equivalent, so the state $|n'\rangle = e^{i\lambda_n}|n\rangle$ yields the same expectation value as $|n\rangle$ for any observable. We see that both $A_i^{(n)}$, and $F_{ij}^{(n)}$, and thus the Berry phase, remain invariant under this phase transformation. However, if we allow the phase to depend on the parameters x, i.e., we perform the local phase transformation

$$|n\rangle \to |n'\rangle = e^{i\lambda_n(x)}|n\rangle, \tag{2.14}$$

we see that

$$A_i^{(n)} \to A_i'^{(n)} = A_i^{(n)} - \partial_i\lambda_n, \tag{2.15}$$

$$F_{ij}^{(n)} \to F_{ij}'^{(n)} = F_{ij}^{(n)}. \tag{2.16}$$

This transformation is reminiscent of the Abelian U(1) gauge transformation of electromagnetism, thus $A^{(n)}$ is really a connection one-form (Berry connection), and $F^{(n)}$ is its curvature two-form (Berry curvature) [7, 53]. Notice that the Berry phase remains invariant too.

2.2 Quantum metric tensor

We can easily see that the distance in Hilbert space naturally induces a metric. The square of this distance between quantum spaces infinitesimally close is given by

$$\mathrm{d}L^2(n(x), n(x+\delta x)) = \langle n(x+\delta x) - n(x)|n(x+\delta x) - n(x)\rangle. \tag{2.17}$$

Expanding this function to second order, we see that

$$\mathrm{d}L^2(n(x), n(x+\delta x)) = \gamma_{ij}^{(n)}\delta x^i \delta x^j, \tag{2.18}$$

where $\gamma_{ij}^{(n)} = \frac{1}{2}\left(\langle\partial_i n|\partial_j n\rangle + \langle\partial_j n|\partial_i n\rangle\right)$. This might lead us into thinking that the symmetric matrix $\gamma_{ij}^{(n)}$ is the natural choice of metric for our parameter space. However, this "metric" is not invariant under the U(1) gauge transformation

$$|n\rangle \to |n'\rangle = e^{i\lambda_n(x)}|n\rangle. \tag{2.19}$$

Provost and Valle [5] noticed that another term can be added to $\gamma_{ij}^{(n)}$ such that now we have a gauge invariant metric, also known as the quantum metric tensor:

$$g_{ij}^{(n)} = \mathrm{Re}\left(\langle\partial_i n|\partial_j n\rangle - \langle\partial_i n|n\rangle\langle n|\partial_j n\rangle\right), \tag{2.20}$$

and hence, the appropriate (squared) distance $\mathrm{d}s^2$ between the two infinitesimally near quantum states is now given by

$$\mathrm{d}s^2 = g_{ij}^{(n)} \delta x^i \delta x^j, \tag{2.21}$$

which can also be written in terms of the quantum fidelity $\mathcal{F}(x, x+\delta x) = |\langle n(x+\delta x)|n(x)\rangle|$ as

$$\mathrm{d}s^2 = 2 - 2\mathcal{F}(x, x+\delta x). \tag{2.22}$$

Therefore, as anticipated in Chapter 1, $\mathrm{d}s = \sqrt{2-2\mathcal{F}(x,x+\delta x)}$ is the infinitesimal version of the Fubini-Study distance which is why $g_{ij}^{(n)}$ is also called the Fubini-Study metric.

The fact that $g_{ij}^{(n)}$ is actually a tensor of rank $(0,2)$ is easily proved, since it is evident from (2.20) that under the change of parameters $x^i \to x'^i = x'^i(x)$, it transforms as

$$g_{ij}'^{(n)} = \frac{\partial x^k}{\partial x'^i} \frac{\partial x^l}{\partial x'^j} g_{kl}^{(n)}. \tag{2.23}$$

Besides, it is positive semidefinite [4], so that the length of any curve C on the parameter space is

$$I(C) = \int_C \sqrt{g_{ij}^{(n)} \delta x^i \delta x^j} \geq 0. \tag{2.24}$$

2.3 Abelian and non-Abelian quantum geometric tensor

The (Abelian) quantum geometric tensor for the nth non-degenerate quantum state is defined as

$$G_{ij}^{(n)} = \langle \partial_i n | \partial_j n \rangle - \langle \partial_i n | n \rangle \langle n | \partial_j n \rangle. \tag{2.25}$$

It is easily seen that it can be separated as

$$G_{ij}^{(n)} = g_{ij}^{(n)} - \frac{i}{2} F_{ij}^{(n)}, \tag{2.26}$$

so that the metric and the Berry curvature can be extracted from the quantum geometric tensor as

$$g_{ij}^{(n)} = \mathrm{Re} G_{ij}^{(n)}, \quad F_{ij}^{(n)} = -2\mathrm{Im} G_{ij}^{(n)}. \tag{2.27}$$

We can as well introduce the non-Abelian quantum geometric tensor [54]. This object is a generalization of the quantum geometric tensor (2.25) to degenerate states of a quantum system. Let us consider a Hamiltonian $\hat{H}$ that depends on a set of M adiabatic parameters $x = \{x^i\}$, and suppose that the nth energy level is g_n times degenerate, i.e.,

$$\hat{H}(x)|n_I(x)\rangle = E_n(x)|n_I(x)\rangle, \quad I = 1, 2, ..., g_n, \tag{2.28}$$

Assuming that we have chosen an orthonormal set of eigenstates on the nth subspace, $\langle n_I(x)|n_J(x)\rangle = \delta_{IJ}$, the non-Abelian quantum geometric tensor is defined as

$$G^{(n)}_{ijIJ} = \langle \partial_i n_I| \left(1 - \sum_{K=1}^{g_n} |n_K\rangle\langle n_K|\right) |\partial_j n_J\rangle. \tag{2.29}$$

Of course, in the non-degenerate case $g_n = 1$, this non-Abelian tensor reduces to the Abelian one (2.25). Under the unitary phase transformation

$$|n_I(x)\rangle \to |n'_I(x)\rangle = \sum_{J=1}^{g_n} |n_J(x)\rangle U^{(n)}_{JI}(x), \tag{2.30}$$

where $U^{(n)}_{JI}(x)$ are the entries of a unitary matrix of dimension $g_n \times g_n$, the geometric tensor (2.29) transforms as

$$G^{(n)}_{ijIJ} \to G^{(n)\prime}_{ijIJ} = \sum_{K,L=1}^{g_n} U^{(n)*}_{KI} G^{(n)}_{ijKL} U^{(n)}_{LJ}. \tag{2.31}$$

From this tensor, we can extract the non-Abelian quantum metric tensor

$$g^{(n)}_{ijIJ} = \frac{1}{2}\left(G^{(n)}_{ijIJ} + G^{(n)*}_{ijJI}\right), \tag{2.32}$$

and the non-Abelian Wilczek-Zee curvature [55]

$$F^{(n)}_{ijIJ} = i\left(G^{(n)}_{ijIJ} - G^{(n)*}_{ijJI}\right). \tag{2.33}$$

In the degenerate case, the application of the adiabatic theorem gives as a result that at the end of a cyclic evolution, the system will remain in the nth subspace acquiring a dynamical phase (the same as in the Abelian case), and a geometric phase (Wilczek-Zee factor [55]) which now is

$$V = \mathcal{P} \exp\left(i \oint_C A^{(n)}\right), \tag{2.34}$$

where $\mathcal{P}$ denotes path-ordering and $A^{(n)}$ is the matrix one-form

$$A^{(n)} = A^{(n)}_i \mathrm{d}x^i \tag{2.35}$$

with elements

$$A^{(n)}_{iIJ} = i\langle n_I|\partial_i n_J\rangle. \tag{2.36}$$

It is easily found that under the unitary transformation (2.30), the one-form $A^{(n)}$ transforms as

$$A^{(n)} \to A'^{(n)} = U^{(n)\dagger} A^{(n)} U^{(n)} + i U^{(n)\dagger}(\mathrm{d}U^{(n)}), \tag{2.37}$$

or in component form,

$$A_i^{(n)} \to A_i'^{(n)} = U^{(n)\dagger} A_i^{(n)} U^{(n)} + iU^{(n)\dagger}(\partial_i U^{(n)}). \tag{2.38}$$

This is precisely the transformation associated with a connection of the non-Abelian gauge group SU(N). The corresponding non-Abelian curvature two-form $F^{(n)}$ is written as

$$F^{(n)} = \frac{1}{2} F_{ij}^{(n)} \mathrm{d}x^i \wedge \mathrm{d}x^j, \tag{2.39}$$

where the matrix elements of $F_{ij}^{(n)}$ are given by (2.33). In differential-form notation, the Wilczek-Zee curvature takes on the familiar form

$$F^{(n)} = \mathrm{d}A^{(n)} - iA^{(n)} \wedge A^{(n)}, \tag{2.40}$$

or, in terms of components,

$$F_{ij}^{(n)} = \partial_i A_j^{(n)} - \partial_j A_i^{(n)} - i[A_i^{(n)}, A_j^{(n)}]. \tag{2.41}$$

The Wilczek-Zee curvature is not gauge-invariant, as opposed to the Abelian case; it transforms as

$$F^{(n)} \to F'^{(n)} = U^{(n)\dagger} F^{(n)} U^{(n)}. \tag{2.42}$$

However, due to the cyclic property of the trace, $\mathrm{Tr} F^{(n)}$ is gauge-invariant.

From now on, when using the term quantum geometric tensor, we only refer to the Abelian tensor (2.25), except in Chapter 3, where both the Abelian and non-Abelian geometric tensors are treated.

2.4 Generator approach to the quantum geometric tensor

Now, we introduce the concept of generator of translations in parameter space, also known as adiabatic gauge potentials [56]. First, note that the displaced state $|n(x+\delta x)\rangle$ is given, to first order in δx by

$$|n(x+\delta x)\rangle = |n(x)\rangle + \partial_i |n(x)\rangle \delta x^i, \tag{2.43}$$

so we can rewrite this displacement in terms of the unitary translation operator $\hat{\mathcal{T}}(\delta x) = 1 - \frac{i}{\hbar}\hat{G}_i \delta x^i$. Notice that the unitarity of $\hat{\mathcal{T}}(\delta x)$ implies that all $\hat{G}_i$, which we shall call generators of translations in parameter space (or simply, generators), are Hermitian. Thus, our $\hat{G}_i$ will satisfy the differential equation

$$i\hbar \partial_i |n(x)\rangle = \hat{G}_i |n(x)\rangle. \tag{2.44}$$

This simple, but crucial observation, enables us to rewrite all the geometric quantities we have defined so far in terms of the $\hat{G}_i$:

$$A_i^{(n)} = \frac{1}{\hbar}\langle \hat{G}_i \rangle_n, \tag{2.45}$$

$$F_{ij}^{(n)} = \frac{i}{\hbar^2}\langle [\hat{G}_i, \hat{G}_j] \rangle_n = \mathrm{Im}\left(-\frac{1}{\hbar^2}\langle [\hat{G}_i, \hat{G}_j] \rangle_n \right), \tag{2.46}$$

$$g_{ij}^{(n)} = \frac{1}{\hbar^2}\left(\frac{1}{2}\langle \{\hat{G}_i, \hat{G}_j\} \rangle_n - \langle \hat{G}_i \rangle_n \langle \hat{G}_j \rangle_n \right) = \mathrm{Re}\left[\frac{1}{\hbar^2}\left(\langle \hat{G}_i \hat{G}_j \rangle_n - \langle \hat{G}_i \rangle_n \langle \hat{G}_j \rangle_n \right) \right], \tag{2.47}$$

where $\langle \hat{X} \rangle_n = \langle n | \hat{X} | n \rangle$ is the expectation value of the operator $\hat{X}$ with respect to the state $|n\rangle$. Notice that the Hermiticity of the generators is consistent with the reality of the Berry connection, the curvature, and the metric. Furthermore, if we define

$$\Delta \hat{G}_i = \hat{G}_i - \langle \hat{G}_i \rangle_n, \tag{2.48}$$

and $\Delta \hat{G} = \Delta \hat{G}_i \delta x^i$, we can see that the distance takes the form

$$\mathrm{d}L^2 = \mathrm{Re}\left[\frac{1}{\hbar^2}\langle (\Delta \hat{G})^2 \rangle_n \right], \tag{2.49}$$

i.e., the distance is the variance of the complete generator $\hat{G} = \hat{G}_i \delta x^i$. Finally, we note that by virtue of (2.44), the action of the operator $\Delta \hat{G}_j$ on the state $|n\rangle$ can be written as

$$\Delta \hat{G}_j |n\rangle = \left(i\hbar \partial_j - \langle \hat{G}_j \rangle_n \right) |n\rangle = i\hbar \left(\partial_j + i A_j^{(n)} \right) |n\rangle, \tag{2.50}$$

which resembles the structure of a covariant derivative $D_j^{(n)} = \partial_j + i A_j^{(n)}$ with connection $A_j^{(n)}$.

2.5 Path integral approach to the quantum geometric tensor

In this section, we briefly present a path integral approach to the quantum geometric tensor. This approach was first introduced in [57] for the quantum metric tensor in the context of gauge-gravity duality, and was later generalized to include both the metric and the Berry curvature in [58].

Consider a quantum system in the time interval $t \in (-\infty, 0)$ which is described through the path integral formulation by a Hamiltonian $H(q(t), p(t); x)$, where $q = \{q^a\}$ and $p = \{p_a\}$, $a = 1, ..., N$ are the coordinates and the momenta, and $x = \{x^i\}$ with $i = 1, ..., M$ is a set of M adiabatic parameters. Suppose that at $t = 0$, a perturbation is turned on such that the system will now be described by a Hamiltonian $H' = H + \mathcal{O}_i \delta x^i$

during the time interval $t \in (0, \infty)$. The functions $\mathcal{O}_i(t)$ are known as Hamiltonian deformations and are given by

$$\mathcal{O}_i(t) = \left(\frac{\partial H}{\partial x^i}\right)_{q,p}. \tag{2.51}$$

In order to compare the ground states $|0\rangle$ and $|0'\rangle$ of H and H', respectively, we use the fidelity $\mathcal{F}(x, x+\delta x) = |\langle 0'|0\rangle|$. A treatment of the kernel $\langle q', \infty | q, -\infty\rangle$ in the path integral formalism leads to [58]

$$\langle 0'|0\rangle = \frac{\left\langle \exp\left(\frac{i}{\hbar}\int_0^\infty \mathrm{d}t\, \mathcal{O}_i \delta x^i\right)\right\rangle_0}{\left\langle \exp\left(\frac{i}{\hbar}\int_{-\infty}^\infty \mathrm{d}t\, \mathcal{O}_i \delta x^i\right)\right\rangle_0^{1/2}}, \tag{2.52}$$

where the expectation value $\langle \hat{A}\rangle_0$ is taken in the ground state of H as

$$\langle \hat{A}\rangle_0 = \frac{1}{Z_0}\int \mathcal{D}q\mathcal{D}p\, A(q,p;x) \exp\left[\frac{i}{\hbar}\int_{-\infty}^{\infty} \mathrm{d}t\, (p\dot{q} - H)\right], \tag{2.53}$$

and $Z_0 = \int \mathcal{D}q\mathcal{D}p \exp\left[\frac{i}{\hbar}\int_{-\infty}^{\infty} \mathrm{d}t\, (p\dot{q} - H)\right]$. An expansion of the fidelity $\mathcal{F}(x, x+\delta x)$ to second order yields [58]

$$\mathcal{F}(x, x+\delta x) = 1 - \frac{1}{2} G^{(0)}_{ij}(x) \delta x^i \delta x^j, \tag{2.54}$$

where

$$G^{(0)}_{ij}(x) = -\frac{1}{\hbar^2}\int_{-\infty}^{0} \mathrm{d}t_1 \int_0^\infty \mathrm{d}t_2 \left(\langle \hat{\mathcal{O}}_i(t_1)\hat{\mathcal{O}}_j(t_2)\rangle_0 - \langle \hat{\mathcal{O}}_i(t_1)\rangle_0 \langle \hat{\mathcal{O}}_j(t_2)\rangle_0\right) \tag{2.55}$$

is the quantum geometric tensor for the ground state $|0\rangle$. Assuming time-reversal symmetry for the two-point functions, $\langle \hat{\mathcal{O}}_i(-t_1)\hat{\mathcal{O}}_j(-t_2)\rangle_0 = \langle \hat{\mathcal{O}}_i(t_1)\hat{\mathcal{O}}_j(t_2)\rangle_0$, the quantum metric tensor can be obtained as the real part of (2.55):

$$g^{(0)}_{ij}(x) = -\frac{1}{\hbar^2}\int_{-\infty}^{0} \mathrm{d}t_1 \int_0^\infty \mathrm{d}t_2 \left(\frac{1}{2}\langle \{\hat{\mathcal{O}}_i(t_1), \hat{\mathcal{O}}_j(t_2)\}\rangle_0 - \langle \hat{\mathcal{O}}_i(t_1)\rangle_0 \langle \hat{\mathcal{O}}_j(t_2)\rangle_0\right), \tag{2.56}$$

where $\{\cdot,\cdot\}$ is the anticommutator. On the other hand, taking the imaginary part of (2.55) as $F^{(0)}_{ij}(x) = -2\mathrm{Im}G^{(0)}_{ij}(x)$, we get the Berry curvature:

$$F^{(0)}_{ij}(x) = \frac{1}{i\hbar^2}\int_{-\infty}^{0} \mathrm{d}t_1 \int_0^\infty \mathrm{d}t_2\, \langle [\hat{\mathcal{O}}_i(t_1), \hat{\mathcal{O}}_j(t_2)]\rangle_0, \tag{2.57}$$

with $[\cdot,\cdot]$ the commutator.

We must mention that equation (2.55) was obtained under a path integral formulation, however, it may be as well evaluated traditionally using operators acting on states of the Hilbert space of the system. As a matter of fact, it turns out that (2.55) can be used to find the quantum geometric tensor not only for the ground state, but for any excited state $|n\rangle$ as follows:

$$G_{ij}^{(n)}(x) = -\frac{1}{\hbar^2}\int_{-\infty}^{0} \mathrm{d}t_1 \int_{0}^{\infty} \mathrm{d}t_2 \left(\langle \hat{\mathcal{O}}_i(t_1)\hat{\mathcal{O}}_j(t_2)\rangle_n - \langle \hat{\mathcal{O}}_i(t_1)\rangle_n \langle \hat{\mathcal{O}}_j(t_2)\rangle_n \right). \tag{2.58}$$

The expectation values that appear here are naturally taken in the nth eigenstate of the Hamiltonian, i.e., $\langle\cdot\rangle_n = \langle n|\cdot|n\rangle$. The following section is devoted to prove this fact and to establish the relation between expressions (2.25) and (2.58).

2.6 Equivalence between the two approaches

Here, we present the first result of our work: the proof that equations (2.25) and (2.58) are indeed the same. This was not proved in reference [58]; the equivalence between these two approaches was only shown through some examples.

Let us start with equation (2.58) and try to get to (2.25). First, we move to the Schrödinger picture where the operators are time-independent. This means that the Heisenberg operator $\hat{\mathcal{O}}_i(t)$ will be written as $\hat{\mathcal{O}}_i(t) = e^{\frac{i}{\hbar}\hat{H}t}\hat{\mathcal{O}}_i e^{-\frac{i}{\hbar}\hat{H}t}$, where $\hat{\mathcal{O}}_i$ is the Schrödinger operator $\hat{\mathcal{O}}_i(t=0)$. From the second term in the above expression, we clearly see that $\langle \hat{\mathcal{O}}_i(t_1)\rangle_n = \langle n|e^{\frac{i}{\hbar}\hat{H}t_1}\hat{\mathcal{O}}_i e^{-\frac{i}{\hbar}\hat{H}t_1}|n\rangle = \langle n|\hat{\mathcal{O}}_i|n\rangle$, since we can apply the first exponential to the left and the second to the right, canceling each other out. Now, we use the same manipulation and we find that the first term takes the form

$$\langle \hat{\mathcal{O}}_i(t_1)\hat{\mathcal{O}}_j(t_2)\rangle_n = e^{-\frac{i}{\hbar}E_n(t_2-t_1)}\langle n|\hat{\mathcal{O}}_i e^{-\frac{i}{\hbar}\hat{H}t_1} e^{\frac{i}{\hbar}\hat{H}t_2}\hat{\mathcal{O}}_j|n\rangle. \tag{2.59}$$

We now insert the identity operator $\hat{\mathbb{1}} = \sum_m |m\rangle\langle m|$ between the two exponentials inside the bracket, which results in

$$\langle \hat{\mathcal{O}}_i(t_1)\hat{\mathcal{O}}_j(t_2)\rangle_n = \sum_m e^{\frac{i}{\hbar}(E_m-E_n)(t_2-t_1)}\langle n|\hat{\mathcal{O}}_i|m\rangle\langle m|\hat{\mathcal{O}}_j|n\rangle. \tag{2.60}$$

The sum in this expression runs over all the allowed values of m, however, if we split the sum as $\sum_{m\neq n} e^{\frac{i}{\hbar}(E_m-E_n)(t_2-t_1)}\langle n|\hat{\mathcal{O}}_i|m\rangle\langle m|\hat{\mathcal{O}}_j|n\rangle + \langle n|\hat{\mathcal{O}}_i|n\rangle\langle n|\hat{\mathcal{O}}_j|n\rangle$, it is obvious that the integrand in (2.58) reduces to

$$\langle \hat{\mathcal{O}}_i(t_1)\hat{\mathcal{O}}_j(t_2)\rangle_n - \langle \hat{\mathcal{O}}_i(t_1)\rangle_n\langle \hat{\mathcal{O}}_j(t_2)\rangle_n = \sum_{m\neq n} e^{\frac{i}{\hbar}(E_m-E_n)(t_2-t_1)}\langle n|\hat{\mathcal{O}}_i|m\rangle\langle m|\hat{\mathcal{O}}_j|n\rangle, \tag{2.61}$$

and thus, the quantum geometric tensor takes the form

$$G_{ij}^{(n)} = -\frac{1}{\hbar^2}\sum_{m\neq n}\left(\int_{-\infty}^{0} \mathrm{d}t_1 \int_{0}^{\infty} \mathrm{d}t_2\, e^{\frac{i}{\hbar}(E_m-E_n)(t_2-t_1)}\right)\langle n|\hat{\mathcal{O}}_i|m\rangle\langle m|\hat{\mathcal{O}}_j|n\rangle. \tag{2.62}$$

We have completely isolated the time-dependence and now we wish to integrate it. We notice that the integrand is oscillatory, and therefore, it is not well-defined in the limits $-\infty$ and ∞, however, it is possible to apply a convenient regularization that is often used in field theory. Having in mind the ranges of t_1 and t_2, we establish the following prescription to make sense of the integral:

$$\int_{-\infty}^{0} \mathrm{d}t_1 \int_{0}^{\infty} \mathrm{d}t_2\, e^{\frac{i}{\hbar}(E_m-E_n)(t_2-t_1)} = \lim_{\epsilon\to 0^+}\int_{-\infty}^{0} \mathrm{d}t_1 \int_{0}^{\infty} \mathrm{d}t_2\, e^{\frac{i}{\hbar}(E_m-E_n+i\epsilon)(t_2-t_1)} = -\frac{\hbar^2}{(E_m-E_n)^2}. \tag{2.63}$$

This prescription will be used along this work multiple times. Taking this result into account, (2.62) turns into

$$G_{ij}^{(n)} = \sum_{m\neq n}\frac{\langle n|\hat{\mathcal{O}}_i|m\rangle\langle m|\hat{\mathcal{O}}_j|n\rangle}{(E_m-E_n)^2}. \tag{2.64}$$

This is known as the perturbative form of the quantum geometric tensor [13]. This expression is relevant because divergences are explicitly seen to occur when level-crossing takes place, i.e., when there is some value of the parameters $x = x^*$ such that $E_m(x^*) = E_n(x^*)$, which may be a signature of a quantum phase transition [41]. In (2.64), we have removed the time-dependence of the operators, but a disadvantage of this formulation is that we now have to take the expectation values of the Hamiltonian deformations over all the quantum states of the system, which is not in general an easy task.

From (2.64), it is straightforward to arrive at the quantum geometric tensor that Provost and Vallee [5] first obtained. Differentiating the Schrödinger equation, we get that $\langle\partial_i n|m\rangle = \frac{\langle n|\partial_i\hat{H}|m\rangle}{E_n-E_m}$ and $\langle m|\partial_j n\rangle = \frac{\langle m|\partial_j\hat{H}|n\rangle}{E_n-E_m}$ for $m\neq n$, which leads to

$$G_{ij}^{(n)} = \sum_{m\neq n}\langle\partial_i n|m\rangle\langle m|\partial_j n\rangle = \sum_{m}\langle\partial_i n|m\rangle\langle m|\partial_j n\rangle - \langle\partial_i n|n\rangle\langle n|\partial_j n\rangle. \tag{2.65}$$

We have added and subtracted one term to complete the sum. In this expression, we readily recognize the identity operator $\hat{\mathbb{1}} = \sum_m |m\rangle\langle m|$, hence, the quantum geometric tensor finally takes the form

$$G_{ij}^{(n)} = \langle\partial_i n|\partial_j n\rangle - \langle\partial_i n|n\rangle\langle n|\partial_j n\rangle, \tag{2.66}$$

which is just equation (2.25).

Summarizing, the expressions to compute the quantum geometric tensor for the nth state are:

1. Provost and Vallee

$$G_{ij}^{(n)}(x) = \langle \partial_i n | \partial_j n \rangle - \langle \partial_i n | n \rangle \langle n | \partial_j n \rangle. \tag{2.67}$$

2. Generator approach

$$G_{ij}^{(n)}(x) = \frac{1}{\hbar^2} \left(\langle \hat{G}_i \hat{G}_j \rangle_n - \langle \hat{G}_i \rangle_n \langle \hat{G}_j \rangle_n \right). \tag{2.68}$$

3. Perturbative form

$$G_{ij}^{(n)}(x) = \sum_{m \neq n} \frac{\langle n | \hat{\mathcal{O}}_i | m \rangle \langle m | \hat{\mathcal{O}}_j | n \rangle}{(E_m - E_n)^2}. \tag{2.69}$$

4. Path integral approach

$$G_{ij}^{(n)}(x) = -\frac{1}{\hbar^2} \int_{-\infty}^{0} \mathrm{d}t_1 \int_{0}^{\infty} \mathrm{d}t_2 \left(\langle \hat{\mathcal{O}}_i(t_1) \hat{\mathcal{O}}_j(t_2) \rangle_n - \langle \hat{\mathcal{O}}_i(t_1) \rangle_n \langle \hat{\mathcal{O}}_j(t_2) \rangle_n \right). \tag{2.70}$$

Each of these expressions possesses advantages and disadvantages, and it depends on the system at hand to decide which one will be used. Naturally, once the quantum geometric tensor has been obtained, the quantum metric and the Berry curvature can be extracted from its real and imaginary parts as (2.27). In the next chapter, we introduce yet another approach to arrive at the quantum geometric tensor in both the Abelian and non-Abelian cases.

Chapter 3

Phase space formulation of the quantum geometric tensor

In this chapter, we present another important result of this work: the Wigner function formulation of the Berry and Wilczek-Zee connections, as well as of the Abelian and non-Abelian quantum geometric tensor. We briefly describe the Wigner function formalism, and then, tackle the issue of incorporating in this description the geometric objects that describe the parameter space. As an illustration of the phase space formulation, we provide two illustrative examples: the generalized harmonic oscillator and two symmetric coupled harmonic oscillators. The results presented here have been published in [59].

3.1 Wigner function formalism

Let us first introduce the basic elements of the phase space formulation of quantum mechanics, also known as the Wigner function formalism [60–63]. Given an operator $\hat{Q}(\hat{q},\hat{p};x)$ that depends on $\hat{q}=\{\hat{q}^a\}$, $\hat{p}=\{\hat{p}_a\}$, $(a=1,...,N)$ and a set of parameters $x=\{x^i\}$, $(i=1,...,M)$, its Wigner transform is

$$\mathcal{Q}(q,p;x)=\int_{-\infty}^{\infty}\mathrm{d}^N y\, e^{-\frac{ip\cdot y}{\hbar}}\left\langle q+\frac{y}{2}\middle|\hat{Q}(\hat{q},\hat{p};x)\middle|q-\frac{y}{2}\right\rangle, \tag{3.1}$$

where the variables $q=\{q^a\}$, $p=\{p_a\}$ are the eigenvalues of the operators $\hat{q}$ and $\hat{p}$, respectively, and $p\cdot y=\sum_{a=1}^{N}p_a y^a$. The Wigner transform has the following property of composition of two operators $\hat{Q}_1$ and $\hat{Q}_2$:

$$\mathrm{Tr}(\hat{Q}_1\hat{Q}_2)=\frac{1}{(2\pi\hbar)^N}\int_{-\infty}^{\infty}\mathrm{d}^N q\mathrm{d}^N p\,\mathcal{Q}_1\mathcal{Q}_2, \tag{3.2}$$

where $\mathcal{Q}_1$ and $\mathcal{Q}_2$ are the corresponding Wigner transforms of $\hat{Q}_1$ and $\hat{Q}_2$.

The Wigner function $W_n(q,p;x)$ of a quantum state $|n(x)\rangle$ is defined as the Wigner transform of the density operator $\hat{\rho}_n(x) = |n(x)\rangle\langle n(x)|$ modulo a constant, i.e.,

$$\begin{aligned} W_n(q,p;x) &= \frac{1}{(2\pi\hbar)^N} \int_{-\infty}^{\infty} \mathrm{d}^N y \, e^{-\frac{ip\cdot y}{\hbar}} \left\langle q + \frac{y}{2} \middle| n(x) \right\rangle \left\langle n(x) \middle| q - \frac{y}{2} \right\rangle \\ &= \frac{1}{(2\pi\hbar)^N} \int_{-\infty}^{\infty} \mathrm{d}^N y \, e^{-\frac{ip\cdot y}{\hbar}} \psi_n\left(q + \frac{y}{2}; x\right) \psi_n^*\left(q - \frac{y}{2}; x\right). \end{aligned} \tag{3.3}$$

Using (3.2) with $\hat{Q}_1 \to \hat{\rho}_n$ and $\hat{Q}_2 \to \hat{O}$, we immediately see that the expectation value of the operator $\hat{O}$ can be written as

$$\langle \hat{O} \rangle_n = \mathrm{Tr}(\hat{\rho}_n \hat{O}) = \int_{-\infty}^{\infty} \mathrm{d}^N q \mathrm{d}^N p \, W_n(q,p;x) \mathcal{O}(q,p;x), \tag{3.4}$$

which resembles the average of the function $\mathcal{O}(q,p;x)$ over the phase space variables. This is why the Wigner function is dubbed as a quasiprobability distribution, since it is real but not positive everywhere. Two last properties that we need are

$$\int_{-\infty}^{\infty} \mathrm{d}^N q \mathrm{d}^N p \, W_n(q,p;x) = 1, \tag{3.5}$$

and

$$\int_{-\infty}^{\infty} \mathrm{d}^N q \mathrm{d}^N p \, W_n^2(q,p;x) = \frac{1}{(2\pi\hbar)^N}. \tag{3.6}$$

The first is obtained setting $\hat{O} \to \hat{\mathbb{1}}$ in (3.4) and recognizing that the Wigner transform of the identity operator is 1, whereas the second one can be derived setting $\hat{O} \to \hat{\rho}_n$ in (3.4).

3.2 Phase space formulation of the parameter space geometry

We now use the Wigner function formalism to provide expressions for the quantum metric tensor and the Berry curvature in both the Abelian and non-Abelian cases. Some years ago, in reference [64], the author conjectured a phase-space formulation of the Berry curvature but did not prove it. Moreover, his treatment requires the use of action-angle variables, and thus, is restricted to the treatment of integrable systems. In contrast to this, we provide a step-by-step deduction which does not incorporate action-angle variables. The basic tool is a function of phase space that encodes all the relevant

information about the parameter space geometry and gives rise to the quantum geometric tensor. An advantage of our approach is that we can get the quantum metric without recourse to the wave function, since it only requires the Wigner function of the system which can be experimentally measured [65].

3.2.1 Abelian case

We first consider the Berry connection for a non-degenerate energy E_n that corresponds to the $|n\rangle$ state. As we have seen in Section 2.3, this gives rise to an Abelian gauge structure where the group U(1) underlies the construction. The Berry connection is given by

$$A_i^{(n)} = i\langle n|\partial_i n\rangle. \tag{3.7}$$

It is easily recognized that it can be rewritten as

$$A_i^{(n)} = \mathrm{Tr}\hat{A}_i^{(n)}, \tag{3.8}$$

where the operator $\hat{A}_i^{(n)}$ is defined by

$$\hat{A}_i^{(n)} \equiv i|\partial_i n\rangle\langle n|. \tag{3.9}$$

This operator is non-Hermitian, and therefore, its Wigner transform

$$\begin{aligned}\mathcal{A}_i^{(n)}(q,p;x) &= i\int_{-\infty}^{\infty} \mathrm{d}^N y\, e^{-\frac{ip\cdot y}{\hbar}} \left\langle q+\frac{y}{2}\middle|\partial_i n\right\rangle\left\langle n\middle|q-\frac{y}{2}\right\rangle \\ &= i\int_{-\infty}^{\infty} \mathrm{d}^N y\, e^{-\frac{ip\cdot y}{\hbar}} \partial_i\psi_n\left(q+\frac{y}{2};x\right)\psi_n^*\left(q-\frac{y}{2};x\right)\end{aligned} \tag{3.10}$$

is a complex function of phase space coordinates. If we take the derivative of equation (3.3) with respect to the parameter x^i, we find that

$$\begin{aligned}\partial_i W_n =& \frac{1}{(2\pi\hbar)^N}\int_{-\infty}^{\infty} \mathrm{d}^N y\, e^{-\frac{ip\cdot y}{\hbar}} \partial_i\psi_n\left(q+\frac{y}{2};x\right)\psi_n^*\left(q-\frac{y}{2};x\right) \\ &+ \frac{1}{(2\pi\hbar)^N}\int_{-\infty}^{\infty} \mathrm{d}^N y\, e^{-\frac{ip\cdot y}{\hbar}} \psi_n\left(q+\frac{y}{2};x\right)\partial_i\psi_n^*\left(q-\frac{y}{2};x\right).\end{aligned} \tag{3.11}$$

Thus, comparing with (3.10), we arrive at

$$\begin{aligned}\partial_i W_n &= \frac{1}{i(2\pi\hbar)^N}\mathcal{A}_i^{(n)} - \frac{1}{i(2\pi\hbar)^N}\mathcal{A}_i^{(n)*} \\ &= \frac{2}{(2\pi\hbar)^N}\mathrm{Im}\mathcal{A}_i^{(n)}.\end{aligned} \tag{3.12}$$

We can now use (3.2) with $\hat{Q}_1 \to \hat{\mathbb{1}}$ and $\hat{Q}_2 \to \hat{A}_i^{(n)}$ to relate the phase space function $\mathcal{A}_i^{(n)}$ with the Berry connection $A_i^{(n)}$ as

$$A_i^{(n)} = \frac{1}{(2\pi\hbar)^N} \int_{-\infty}^{\infty} \mathrm{d}^N q \mathrm{d}^N p \, \mathcal{A}_i^{(n)}(q,p;x). \tag{3.13}$$

This is precisely the expression of the Berry connection in the phase space formalism. Under the U(1) gauge transformation $|n(x)\rangle \to |n'(x)\rangle = e^{i\lambda_n(x)}|n(x)\rangle$, the function $\mathcal{A}_i^{(n)}$ transforms as

$$\mathcal{A}_i^{(n)} \to \mathcal{A}_i'^{(n)} = \mathcal{A}_i^{(n)} - (2\pi\hbar)^N W_n \partial_i \lambda_n, \tag{3.14}$$

and as a consequence, the Berry connection $A_i^{(n)}$ has the expected gauge transformation property (2.15)

$$A_i^{(n)} \to A_i'^{(n)} = A_i^{(n)} - \partial_i \lambda_n. \tag{3.15}$$

We must point out that only the real part of the function $\mathcal{A}_i^{(n)}$ contributes to the Berry connection $A_i^{(n)}$. This is straightforward to prove:

$$\begin{aligned} A_i^{(n)} &= \frac{1}{(2\pi\hbar)^N} \int_{-\infty}^{\infty} \mathrm{d}^N q \mathrm{d}^N p \, \mathrm{Re}\mathcal{A}_i^{(n)} + \frac{i}{(2\pi\hbar)^N} \int_{-\infty}^{\infty} \mathrm{d}^N q \mathrm{d}^N p \, \mathrm{Im}\mathcal{A}_i^{(n)} \\ &= \frac{1}{(2\pi\hbar)^N} \int_{-\infty}^{\infty} \mathrm{d}^N q \mathrm{d}^N p \, \mathrm{Re}\mathcal{A}_i^{(n)} + \frac{i}{2}\partial_i \left(\int_{-\infty}^{\infty} \mathrm{d}^N q \mathrm{d}^N p \, W_n \right) \\ &= \frac{1}{(2\pi\hbar)^N} \int_{-\infty}^{\infty} \mathrm{d}^N q \mathrm{d}^N p \, \mathrm{Re}\mathcal{A}_i^{(n)}, \end{aligned} \tag{3.16}$$

where we used (3.12) and the normalization of the Wigner function (3.5).

Now, we analyze the quantum geometric tensor. We define the operator $\hat{G}_{ij}^{(n)}$ as

$$\hat{G}_{ij}^{(n)} \equiv \left(\hat{A}_i^{(n)\dagger} - \hat{A}_i^{(n)} \right) \hat{A}_j^{(n)}, \tag{3.17}$$

and see that the (Abelian) quantum geometric tensor can be obtained as

$$G_{ij}^{(n)} = \mathrm{Tr}\hat{G}_{ij}^{(n)}. \tag{3.18}$$

From here, if we use the relation $\hat{A}_i^{(n)\dagger} - \hat{A}_i^{(n)} = -i\partial_i\hat{\rho}_n$ and in equation (3.2) we set $\hat{Q}_1 \to -i\partial_i\hat{\rho}_n$ and $\hat{Q}_2 \to \hat{A}_j^{(n)}$, we find that

$$G_{ij}^{(n)} = -i \int_{-\infty}^{\infty} \mathrm{d}^N q \mathrm{d}^N p \, \partial_i W_n \mathcal{A}_j^{(n)}, \tag{3.19}$$

or, using (3.12),

$$G_{ij}^{(n)} = -\frac{2i}{(2\pi\hbar)^N}\int_{-\infty}^{\infty} \mathrm{d}^N q \mathrm{d}^N p \,\mathrm{Im}\left(\mathcal{A}_i^{(n)}\right)\mathcal{A}_j^{(n)}. \tag{3.20}$$

Thus, we have a formulation of the quantum geometric tensor in terms of the phase space functions $\mathcal{A}_i^{(n)}$ only. Therefore, the $\mathcal{A}_i^{(n)}$ encode the relevant information of the parameter space of a system.

With the quantum geometric tensor at hand, we can extract its real and imaginary parts to get the quantum metric and the Berry curvature. Hence, the metric tensor takes the form

$$g_{ij}^{(n)} = \mathrm{Re}G_{ij}^{(n)} = \frac{2}{(2\pi\hbar)^N}\int_{-\infty}^{\infty} \mathrm{d}^N q \mathrm{d}^N p \,\mathrm{Im}\left(\mathcal{A}_i^{(n)}\right)\mathrm{Im}\left(\mathcal{A}_j^{(n)}\right), \tag{3.21}$$

or, by virtue of (3.12),

$$g_{ij}^{(n)} = \frac{(2\pi\hbar)^N}{2}\int_{-\infty}^{\infty} \mathrm{d}^N q \mathrm{d}^N p \,\partial_i W_n \partial_j W_n. \tag{3.22}$$

On the other hand, the Berry curvature can be written as

$$F_{ij}^{(n)} = -2\mathrm{Im}G_{ij}^{(n)} = \frac{4}{(2\pi\hbar)^N}\int_{-\infty}^{\infty} \mathrm{d}^N q \mathrm{d}^N p \,\mathrm{Im}\left(\mathcal{A}_i^{(n)}\right)\mathrm{Re}\left(\mathcal{A}_j^{(n)}\right). \tag{3.23}$$

We want to remark that the phase space formulation to find the quantum metric tensor (equation (3.22)), does not require the wave functions, it is sufficient to know the Wigner functions which can actually be obtained from certain functional equations in phase space [66]. On the other hand, the Berry connection and curvature do require the knowledge of the wave function.

3.2.2 Non-Abelian case

To treat the non-Abelian case, we define an operator $\hat{A}_{iIJ}^{(n)}$ such that the Wilczek-Zee connection can be obtained from its trace as

$$A_{iIJ}^{(n)} = \mathrm{Tr}\hat{A}_{iIJ}^{(n)}. \tag{3.24}$$

The operator turns out to be

$$\hat{A}_{iIJ}^{(n)} = i|\partial_i n_J\rangle\langle n_I|, \tag{3.25}$$

and its Wigner transform is

$$\mathcal{A}_{iIJ}^{(n)}(q,p;x) = i\int_{-\infty}^{\infty} \mathrm{d}^N y\, e^{-\frac{ip\cdot y}{\hbar}}\partial_i\psi_{nJ}\left(q+\frac{y}{2};x\right)\psi_{nI}^*\left(q-\frac{y}{2};x\right). \tag{3.26}$$

Through the use of (3.24) and (3.2), we get the Wilczek-Zee connection in terms of the phase space function $\mathcal{A}^{(n)}_{iIJ}$ as

$$A^{(n)}_{iIJ} = \frac{1}{(2\pi\hbar)^N} \int_{-\infty}^{\infty} \mathrm{d}^N q \mathrm{d}^N p \, \mathcal{A}^{(n)}_{iIJ}(q,p;x). \tag{3.27}$$

This expression is the non-Abelian counterpart of (3.13). The $A^{(n)}_{iIJ}$ are the entries of a Hermitian matrix of dimension $g_n \times g_n$. To see this, we first present the definition of the non-diagonal Wigner functions W_{nIJ}:

$$W_{nIJ} = \frac{1}{(2\pi\hbar)^N} \int_{-\infty}^{\infty} \mathrm{d}^N y \, e^{-\frac{ip\cdot y}{\hbar}} \psi_{nI}\left(q + \frac{y}{2}; x\right) \psi^*_{nJ}\left(q - \frac{y}{2}; x\right). \tag{3.28}$$

Thus, from equation (3.27), it follows that

$$\mathcal{A}^{(n)}_{iIJ} = \mathcal{A}^{(n)*}_{iJI} + i(2\pi\hbar)^N \partial_i W_{nJI}. \tag{3.29}$$

Substituting this in (3.27) and using the normalization of the non-diagonal Wigner functions [66],

$$\int_{-\infty}^{\infty} \mathrm{d}^N q \mathrm{d}^N p \, W_{nIJ} = \delta_{IJ}, \tag{3.30}$$

we find that $A^{(n)}_{iIJ} = A^{(n)*}_{iJI}$.

Now, under the SU(N) gauge transformation (2.30), the phase space function $\mathcal{A}^{(n)}_{iIJ}$ transforms as

$$\mathcal{A}^{(n)}_{iIJ} \to \mathcal{A}'^{(n)}_{iIJ} = \sum_{K,L=1}^{g_n} \left[U^{(n)*}_{KI} \mathcal{A}^{(n)}_{iKL} U_{LJ} + i(2\pi\hbar)^N U^{(n)*}_{KI} W_{nLK} \partial_i U^{(n)}_{LJ} \right], \tag{3.31}$$

and, as a consequence, the Wilczek-Zee connection has the expected transformation law (2.38)

$$A^{(n)}_{iIJ} \to A'^{(n)}_{iIJ} = \sum_{K,L=1}^{g_n} U^{(n)*}_{KI} A^{(n)}_{iKL} U^{(n)}_{LI} + i \sum_{K=1}^{g_n} U^{(n)*}_{KI} \partial_i U^{(n)}_{KJ}. \tag{3.32}$$

Now, the non-Abelian quantum geometric tensor (2.29) can be written as

$$G^{(n)}_{ijIJ} = \mathrm{Tr}\hat{G}^{(n)}_{ijIJ}, \tag{3.33}$$

where the operator $\hat{G}^{(n)}_{ijIJ}$ is defined as

$$\hat{G}^{(n)}_{ijIJ} \equiv -i\partial_i \hat{\boldsymbol{P}}_n \hat{A}^{(n)}_{jIJ}, \tag{3.34}$$

and $\hat{\boldsymbol{P}}_n = \sum_{I=1}^{g_n} |n_I\rangle\langle n_I|$ is the projection operator onto the nth subspace. Setting $\hat{Q}_1 \to -i\partial_i \hat{\boldsymbol{P}}_n$ and $\hat{Q}_2 \to \hat{A}^{(n)}_{jIJ}$ in (3.2), we find

$$G^{(n)}_{ijIJ} = -i \int_{-\infty}^{\infty} \mathrm{d}^N q \mathrm{d}^N p \sum_{K=1}^{g_n} \partial_i W_{nKK} \mathcal{A}^{(n)}_{jIJ}. \tag{3.35}$$

To cast this expression entirely in terms of $\mathcal{A}^{(n)}_{iIJ}$, we use the relation

$$\mathrm{Im}\mathcal{A}^{(n)}_{iKK} = \frac{(2\pi\hbar)^N}{2} \partial_i W_{nKK}, \tag{3.36}$$

which stems from (3.26) and (3.28). Therefore, substituting (3.36) in (3.35), we arrive at the non-Abelian quantum geometric tensor:

$$G^{(n)}_{ijIJ} = -\frac{2i}{(2\pi\hbar)^N} \int_{-\infty}^{\infty} \mathrm{d}^N q \mathrm{d}^N p \sum_{K=1}^{g_n} \mathrm{Im}\left(\mathcal{A}^{(n)}_{iKK}\right) \mathcal{A}^{(n)}_{jIJ}. \tag{3.37}$$

Now, we can extract the non-Abelian quantum metric tensor using (2.32) and get

$$g^{(n)}_{ijIJ} = \frac{-i}{(2\pi\hbar)^N} \int_{-\infty}^{\infty} \mathrm{d}^N q \mathrm{d}^N p \sum_{K=1}^{g_n} \mathrm{Im}\left(\mathcal{A}^{(n)}_{iKK}\right) \left(\mathcal{A}^{(n)}_{jIJ} - \mathcal{A}^{(n)*}_{jJI}\right), \tag{3.38}$$

or, we can cast it entirely in terms of Wigner functions through (3.29) and (3.36) as

$$g^{(n)}_{ijIJ} = \frac{(2\pi\hbar)^N}{2} \int_{-\infty}^{\infty} \mathrm{d}^N q \mathrm{d}^N p \sum_{K=1}^{g_n} \partial_i W_{nKK} \partial_J W_{nIJ}. \tag{3.39}$$

On the other hand, the Wilczek-Zee curvature is obtained from (3.37) using (2.33), and it takes the form

$$F^{(n)}_{ijIJ} = \frac{2}{(2\pi\hbar)^N} \int_{-\infty}^{\infty} \mathrm{d}^N q \mathrm{d}^N p \sum_{K=1}^{g_n} \mathrm{Im}\left(\mathcal{A}^{(n)}_{iKK}\right) \left(\mathcal{A}^{(n)}_{jIJ} + \mathcal{A}^{(n)*}_{jJI}\right). \tag{3.40}$$

In this way, we have formulated the basic geometric structures that underlie the parameter space in both the non-degenerate and degenerate systems.

3.3 Illustrative examples

In this section, our aim is to present two simple systems that can be treated with the phase space formulation. First, we analyze the generalized harmonic oscillator whose geometric tensor has an Abelian geometrical structure, and then, we study a set of three coupled harmonic oscillators that has a degenerate spectrum, and thus, gives rise to a non-Abelian quantum geometric tensor.

3.3.1 Generalized harmonic oscillator

The Hamiltonian of the generalized harmonic oscillator is

$$\hat{H} = \frac{1}{2}\left[X\hat{q}^2 + Y(\hat{q}\hat{p} + \hat{p}\hat{q}) + Z\hat{p}^2\right], \tag{3.41}$$

where the adiabatic parameters are $x = \{x^i\} = (X, Y, Z)$ with $i = 1, 2, 3$. The Schrödinger equation takes the form

$$-\frac{Z\hbar^2}{2}\frac{\mathrm{d}^2\psi_n}{\mathrm{d}q^2} - i\hbar Yq\frac{\mathrm{d}\psi_n}{\mathrm{d}q} + \left(\frac{Xq^2}{2} - i\hbar\frac{Y}{2}\right)\psi_n = E_n\psi_n, \tag{3.42}$$

and the resulting wave function is

$$\psi_n(q;x) = \left(\frac{\omega}{Z\hbar}\right)^{1/4}\chi_n\left(q\sqrt{\frac{\omega}{Z\hbar}}\right)\exp\left(-\frac{iYq^2}{2Z\hbar}\right), \tag{3.43}$$

where $\omega = \sqrt{XZ - Y^2}$ is the frequency, so this system has an oscillatory behavior as long as $XZ - Y^2 > 0$. Moreover, $\chi_n(\xi)$ are the Hermite functions

$$\chi_n(\xi) = \left(2^n n!\sqrt{\pi}\right)^{-1/2} e^{-\xi^2/2}H_n(\xi), \tag{3.44}$$

with $H_n(\xi)$ the nth Hermite polynomial. The energy is restricted to take the values $E_n = (n + 1/2)\hbar\omega$ $(n = 0, 1, 2, ...)$, and of course, no degeneracy exists.

The Wigner function of the generalized harmonic oscillator can be obtained from that of the simple harmonic oscillator through the transformation

$$Q = \frac{q}{\sqrt{Z}}, \quad P = \sqrt{Z}\left(p + \frac{Y}{Z}q\right), \tag{3.45}$$

which casts the associated classical Hamiltonian $H = \frac{1}{2}(Xq^2 + 2Yqp + Zp^2)$ into the standard form

$$H = \frac{1}{2}(P^2 + \omega^2 Q^2). \tag{3.46}$$

Thus, the Wigner function is [66]

$$W_n(q, p; x) = \frac{(-1)^n}{\pi\hbar}e^{-\lambda/2}L_n(\lambda), \tag{3.47}$$

where $\lambda = 4H/(\hbar\omega)$ and $L_n(\lambda)$ are the Laguerre polynomials.

We now compute the phase space function $\mathcal{A}_i^{(n)}$ using equation (3.10). Through the use of the following properties of the Hermite functions,

$$\begin{aligned}\frac{\mathrm{d}\chi_n}{\mathrm{d}\xi} &= \sqrt{\frac{n}{2}}\chi_{n-1} - \sqrt{\frac{n+1}{2}}\chi_{n+1},\\ \xi\chi_n &= \sqrt{\frac{n}{2}}\chi_{n-1} + \sqrt{\frac{n+1}{2}}\chi_{n+1},\end{aligned} \tag{3.48}$$

we arrive at

$$\mathcal{A}_i^{(n)} = \frac{\pi\hbar Z}{2\omega}\left[i\partial_i\left(\frac{\omega}{Z}\right)\Xi_n^{(-)} + \partial_i\left(\frac{Y}{Z}\right)\left(\Xi_n^{(+)} + (2n+1)W_n\right)\right]. \tag{3.49}$$

Here, W_n is the Wigner function (3.47), and the $\Xi_n^{(\pm)}$ are

$$\Xi_n^{(\pm)} = \sqrt{n(n-1)}W_{n-2,n} \pm \sqrt{(n+1)(n+2)}W_{n+2,n}, \tag{3.50}$$

where

$$W_{n\pm2,n} = \frac{1}{2\pi\hbar}\int_{-\infty}^{\infty} \mathrm{d}y\, e^{-\frac{ipy}{\hbar}}\psi_{n\pm2}\left(q+\frac{y}{2};x\right)\psi_n^*\left(q-\frac{y}{2};x\right), \quad n \geq 2 \tag{3.51}$$

are the non-diagonal Wigner functions [66]

$$\begin{aligned} W_{n-2,n} &= \frac{(-1)^{n+1}2(P-i\omega Q)^2}{\sqrt{n(n-1)}\pi\hbar^2\omega}e^{-\frac{\lambda}{2}}L_{n-2}^{(2)}(\lambda), \\ W_{n+2,n} &= \frac{(-1)^{n+1}2(P+i\omega Q)^2}{\sqrt{(n+1)(n+2)}\pi\hbar^2\omega}e^{-\frac{\lambda}{2}}L_{n}^{(2)}(\lambda), \end{aligned} \tag{3.52}$$

with $L_n^{(\alpha)}(\lambda)$ the associated Laguerre polynomials. Substituting (3.49) in (3.13) and using the orthogonality of the non-diagonal Wigner functions,

$$\int_{-\infty}^{\infty} \mathrm{d}q\mathrm{d}p\, W_{n\pm2,n} = 0, \tag{3.53}$$

we find the Berry connection $A^{(n)} = A_i^{(n)}\mathrm{d}x^i$, whose three components are

$$A_1^{(n)} = 0, \quad A_2^{(n)} = \left(n+\frac{1}{2}\right)\frac{1}{2\omega}, \quad A_3^{(n)} = -\left(n+\frac{1}{2}\right)\frac{Y}{2Z\omega}. \tag{3.54}$$

Moreover, the components of the Berry curvature are found as $F_{ij}^{(n)} = \partial_i A_j^{(n)} - \partial_j A_i^{(n)}$, resulting in

$$F_{23}^{(n)} = -\left(n+\frac{1}{2}\right)\frac{X}{4\omega^3}, \quad F_{31}^{(n)} = -\left(n+\frac{1}{2}\right)\frac{Y}{4\omega^3}, \quad F_{12}^{(n)} = -\left(n+\frac{1}{2}\right)\frac{Z}{4\omega^3}. \tag{3.55}$$

We finally find the quantum metric tensor. The derivative of the Wigner function (3.47) with respect to the parameter x^i is

$$\partial_i W_n = -\frac{(-1)^n}{2\pi\hbar}e^{-\lambda/2}\left[L_n(\lambda) - 2\frac{\mathrm{d}L_n(\lambda)}{\mathrm{d}\lambda}\right]\partial_i\lambda, \tag{3.56}$$

thus, substituting it in (3.22) we find that

$$g_{ij}^{(n)} = \frac{2\pi\hbar}{2}\int_{-\infty}^{\infty} \mathrm{d}q\mathrm{d}p\, \partial_i W_n \partial_j W_n$$
$$= \frac{1}{4\pi\hbar}\int_{-\infty}^{\infty} \mathrm{d}q\mathrm{d}p\, e^{-\frac{\lambda}{2}} \left(L_n - 2\frac{\mathrm{d}L_n}{\mathrm{d}\lambda}\right)^2 \partial_i\lambda\partial_j\lambda. \tag{3.57}$$

Taking the required partial derivatives, and then, applying the transformation

$$q = \sqrt{\frac{\hbar\lambda Z}{2\omega}}\sin\phi, \quad p = \sqrt{\frac{\hbar\lambda Z}{2\omega}}\left(-\frac{Y}{Z}\sin\phi + \frac{\omega}{Z}\cos\phi\right), \tag{3.58}$$

and the fact that

$$\int_{-\infty}^{\infty}\mathrm{d}q\int_{-\infty}^{\infty}\mathrm{d}p = \frac{\hbar}{4}\int_0^{2\pi}\mathrm{d}\phi\int_0^{\infty}\mathrm{d}\lambda, \tag{3.59}$$

we can recast the integral in terms of the variables (ϕ, λ). The integral in ϕ is easily carried out, and for the integral in λ we need to use the relation

$$\int_0^{\infty}\mathrm{d}\lambda\,\lambda^2 e^{-\lambda}\left(L_n - 2\frac{\mathrm{d}L_n}{\mathrm{d}\lambda}\right)^2 = 2(n^2+n+1), \tag{3.60}$$

after which we find the quantum metric tensor:

$$g_{ij}^{(n)} = \frac{n^2+n+1}{32\omega^4}\begin{pmatrix} Z^2 & -2YZ & 2Y^2 - XZ \\ -2YZ & 4XZ & -2XY \\ 2Y^2 - XZ & -2XY & X^2 \end{pmatrix}. \tag{3.61}$$

3.3.2 Three coupled harmonic oscillators

We now analyze a system of coupled harmonic oscillators which possesses a non-Abelian parameter space structure for excited states. Our aim here is to compute the non-Abelian quantum metric tensor.

Let us consider the Hamiltonian

$$\hat{H} = \frac{1}{2}\sum_{a=1}^{3}(\hat{p}_a^2 + k\hat{q}_a^2) + \frac{k'}{2}\left[(\hat{q}_1 - \hat{q}_2)^2 + (\hat{q}_2 - \hat{q}_3)^2 + (\hat{q}_3 - \hat{q}_1)^2\right], \tag{3.62}$$

where the parameters are $x = \{x^i\} = (k, k')$, $i = 1, 2$. We begin by uncoupling the oscillators by means of the transformation

$$\begin{pmatrix}\hat{Q}_1\\ \hat{Q}_2\\ \hat{Q}_3\end{pmatrix} = \begin{pmatrix} \frac{1}{\sqrt{3}} & \frac{1}{\sqrt{3}} & \frac{1}{\sqrt{3}} \\ -\frac{1}{\sqrt{2}} & 0 & \frac{1}{\sqrt{2}} \\ \frac{1}{\sqrt{6}} & -\sqrt{\frac{2}{3}} & \frac{1}{\sqrt{6}} \end{pmatrix}\begin{pmatrix}\hat{q}_1\\ \hat{q}_2\\ \hat{q}_3\end{pmatrix}, \tag{3.63}$$

and similarly for the momenta. The resulting Hamiltonian reads

$$\hat{H} = \frac{1}{2}\sum_{a=1}^{3}(\hat{P}_a^2 + \omega_a^2\hat{Q}_a^2), \tag{3.64}$$

where the frequencies are $\omega_1 = \sqrt{k}$, $\omega_2 = \omega_3 = \sqrt{k+3k'}$. The system is then separable, and thus, the wave function is

$$\psi_{n_1,n_2,n_3}(q_1,q_2,q_3;x) = \psi_{n_1}(Q_1;x)\psi_{n_2}(Q_2;x)\psi_{n_3}(Q_3;x), \tag{3.65}$$

with $n_a = 1, 2, ...$ The individual wave functions ψ_a have the form

$$\psi_a(Q_a;x) = \left(\frac{\omega_a}{\pi\hbar}\right)^{1/4}\frac{1}{\sqrt{2^{n_a}n_a!}}H_{n_a}\left(\sqrt{\frac{\omega_a}{\hbar}}Q_a\right)\exp\left(-\frac{\omega_a}{2\hbar}Q_a^2\right), \tag{3.66}$$

where $H_{n_a}(\xi)$ are the Hermite polynomials, and the energy takes the values

$$E_{n_1,n_2,n_3} = \left(n_1 + \frac{1}{2}\right)\hbar\omega_1 + (n_2+n_3+1)\hbar\omega_2. \tag{3.67}$$

To compute the non-Abelian quantum metric tensor, we choose the first excited-state wave functions $\psi_{0,0,1}$ and $\psi_{0,1,0}$ which have the same energy $E_1 = \frac{1}{2}\hbar\omega_1 + 2\hbar\omega_2$, and therefore, constitute a degenerate set with $g_1 = 2$. Using the notation $\{\psi_{(1)I}\} = (\psi_{0,0,1}, \psi_{0,1,0})$ with $I, J = 1, 2$, we obtain the non-diagonal Wigner functions using equation (3.28):

$$W_{(1)IJ} = \frac{1}{(2\pi\hbar)^3}\int_{-\infty}^{\infty}\mathrm{d}^3y\, e^{-\frac{ip\cdot y}{\hbar}}\psi_{(1)I}\left(q+\frac{y}{2};x\right)\psi^*_{(1)J}\left(q-\frac{y}{2};x\right). \tag{3.68}$$

At this point, it is useful to make the change of integration variables $y \to Y$ as

$$\begin{pmatrix}Y_1\\Y_2\\Y_3\end{pmatrix} = \begin{pmatrix}\frac{1}{\sqrt{3}} & \frac{1}{\sqrt{3}} & \frac{1}{\sqrt{3}}\\ -\frac{1}{\sqrt{2}} & 0 & \frac{1}{\sqrt{2}}\\ \frac{1}{\sqrt{6}} & -\sqrt{\frac{2}{3}} & \frac{1}{\sqrt{6}}\end{pmatrix}\begin{pmatrix}y_1\\y_2\\y_3\end{pmatrix}, \tag{3.69}$$

so that the integral can be separated into three independent pieces which are easily performed. The resulting non-diagonal Wigner functions are

$$\begin{aligned}
W_{(1)11} &= \frac{1}{(\pi\hbar)^3}(\lambda_3 - 1)e^{-\frac{\lambda_1+\lambda_2+\lambda_3}{2}},\\
W_{(1)12} &= \frac{2}{\pi^3\hbar^4\omega_2}(P_2 - i\omega_2 Q_2)(P_3 + i\omega_2 Q_3)e^{-\frac{\lambda_1+\lambda_2+\lambda_3}{2}},\\
W_{(1)21} &= \frac{2}{\pi^3\hbar^4\omega_2}(P_2 + i\omega_2 Q_2)(P_3 - i\omega_2 Q_3)e^{-\frac{\lambda_1+\lambda_2+\lambda_3}{2}},\\
W_{(1)22} &= \frac{1}{(\pi\hbar)^3}(\lambda_2 - 1)e^{-\frac{\lambda_1+\lambda_2+\lambda_3}{2}},
\end{aligned} \tag{3.70}$$

where $\lambda_a = 4H_a/(\hbar\omega_a)$ and $H_a = (P_a^2+\omega_a^2 Q_a^2)/2$. We substitute these functions in (3.39) and find the non-Abelian quantum geometric tensor, whose components are

$$g^{(1)}_{ij11}(x) = g^{(1)}_{ij22}(x) = \frac{1}{32}\begin{pmatrix} \frac{1}{\omega_1^4}+\frac{4}{\omega_2^4} & \frac{12}{\omega_2^4} \\ \frac{12}{\omega_2^4} & \frac{36}{\omega_2^4} \end{pmatrix},$$
$$g^{(1)}_{ij12}(x) = g^{(1)}_{ij21}(x) = \begin{pmatrix} 0 & 0 \\ 0 & 0 \end{pmatrix}. \tag{3.71}$$

Chapter 4

Classical analog of the quantum geometric tensor

We devote this chapter to the description of the classical counterparts of the geometric objects that appeared in the quantum realm. First, we review the Hannay angle, connection, and curvature. Then, we introduce one of the most important results of this work: the notion of the classical generator of translations in parameter space which will allow us to find the classical analog of the metric tensor. We corroborate that our proposed classical metric tensor satisfies the desired properties and then obtain it from the semiclassical approximation of the path integral approach introduced in Chapter 2. After this, we prove the equivalence of the generator and time-dependent approaches which parallels that of their quantum counterpart, and finally, we provide the different expressions to compute the Hannay curvature and the classical metric tensor. The results of this chapter have been published in references [67] and [68].

4.1 The Hannay angle, connection and curvature

To formulate the adiabatic theorem in classical mechanics, we require an integrable system with a Hamiltonian $H(q,p;x)$ that depends on the parameters $x=\{x^i\}$, $i=1,...,M$, where $q=\{q^a\}$ and $p=\{p_a\}$, $a=1,...,N$ are the coordinates and their canonical momenta, respectively. Since we have an integrable system, we can introduce action-angle variables $I=\{I_a\}$ and $\phi=\{\phi^a\}$ that satisfy Hamilton's equations with respect to the transformed Hamiltonian [69]

$$K(\phi,I;x)=H(I;x)+\frac{\partial S^{(\alpha)}(q,I;x)}{\partial t}=H(I;x)+(\partial_i S^{(\alpha)})_{q,I}\dot{x}^i, \tag{4.1}$$

where $H(I;x)=H(q(\phi,I;x),p(\phi,I;x);x)$ and $S^{(\alpha)}(q,I;x)$ is the generating function of the canonical transformation $(q,p)\to(\phi,I)$. The subscript indicates that the derivative is taken with respect to the parameters leaving (q,I) fixed, and the superscript α labels different branches of the multivalued generating function. Also, we have used the Einstein

summation convention over the index i. Using the chain rule and selecting the branch $0 \leq \phi < 2\pi$, we can easily see that

$$(\partial_i S)_{q,I} = -G_i, \tag{4.2}$$

with

$$G_i(\phi, I; x) \equiv p_a(\partial_i q^a)_{\phi,I} - (\partial_i S)_{\phi,I}. \tag{4.3}$$

Here, too, we are using the Einstein summation convention over a. The adiabatic theorem states that the action variables I_a remain invariant during the slow evolution of the parameters and that the angle variables change while the system is taken through a closed curve in parameter space is

$$\Delta\phi^a = \int_0^T \mathrm{d}t'\, \omega^a(I; x) - \frac{\partial}{\partial I_a} \oint_C \mathrm{d}x^i \, \langle G_i(\phi, I; x)\rangle, \tag{4.4}$$

where $\omega^a(I; x) = \partial H(I; x)/\partial I_a$ and

$$\langle f(\phi, I; x)\rangle = \frac{1}{(2\pi)^N} \int_0^{2\pi} \mathrm{d}^N\phi\, f(\phi, I; x) \tag{4.5}$$

is the torus average of the function f. The first term in (4.4) represents a dynamical change, while the second is a geometric change called the Hannay angle [8] and denoted as $\Delta\phi^a_H$. In analogy to the quantum case, we introduce the one-form

$$A = A_i \mathrm{d}x^i = \langle G_i\rangle \mathrm{d}x^i, \tag{4.6}$$

so that using Stokes theorem, the ath Hannay angle can be written as

$$\Delta\phi^a_H(C) = -\frac{\partial}{\partial I_a} \int_\Sigma F, \tag{4.7}$$

where F is a two-form such that $F = \mathrm{d}A$ and $C = \partial\Sigma$. In terms of components,

$$F = \frac{1}{2} F_{ij} \mathrm{d}x^i \wedge \mathrm{d}x^j, \tag{4.8}$$

with

$$F_{ij} = \partial_i A_j - \partial_j A_i = \langle (\partial_i p_a)_{\phi,I} (\partial_j q^a)_{\phi,I} - (\partial_j p_a)_{\phi,I} (\partial_i q^a)_{\phi,I}\rangle. \tag{4.9}$$

Now, consider the infinitesimal canonical transformation

$$q^a(x) \to q^a(x + \delta x) = q^a(x) + \overline{\delta} q^a, \tag{4.10}$$

$$p_a(x) \to p_a(x + \delta x) = p_a(x) + \overline{\delta} p_a, \tag{4.11}$$

where

$$\overline{\delta}q^a \equiv q^a(x') - q^a(x) = (\partial_i q^a)_{\phi,I}\delta x^i, \tag{4.12}$$

$$\overline{\delta}p_a \equiv p_a(x') - p_a(x) = (\partial_i p_a)_{\phi,I}\delta x^i, \tag{4.13}$$

with $x' = x + \delta x$. Note that the variation $\overline{\delta}q^a$ leaves the action-angle variables fixed, and can be written in terms of the more familiar virtual and total variations, $\tilde{\delta}q^a = q'^a(x) - q^a(x)$ and $\delta q^a = q'^a(x') - q^a(x)$, respectively, as

$$\overline{\delta}q^a = \delta q^a - \tilde{\delta}q^a. \tag{4.14}$$

We set out to prove the crucial result that the G_i are the generators of this infinitesimal canonical transformation, i.e.,

$$(\partial_i q^a)_{\phi,I} = \{q^a, G_i\}_{q,p} = \frac{\partial G_i}{\partial p_a}, \tag{4.15}$$

$$(\partial_i p_a)_{\phi,I} = \{p_a, G_i\}_{q,p} = -\frac{\partial G_i}{\partial q^a}. \tag{4.16}$$

In the first place, we differentiate the defining relation of a canonical transformation,

$$p_a\tilde{\delta}q^a - I_a\tilde{\delta}\phi^a = \tilde{\delta}f, \tag{4.17}$$

with respect to x^i leaving (ϕ, I) fixed. Here, $f = S(q, I; x) - \phi^a I_a$, and the virtual variation $\tilde{\delta}$ is taken at fixed time (frozen parameters). We get

$$(\partial_i p_a)_{\phi,I}\tilde{\delta}q^a + p_a\tilde{\delta}(\partial_i q^a)_{\phi,I} = \tilde{\delta}(\partial_i S)_{\phi,I}, \tag{4.18}$$

where we used the fact that $\tilde{\delta}$ commutes with ∂_i. Next, we perform the virtual variation of (4.3) which yields

$$\tilde{\delta}G_i = \tilde{\delta}p_a(\partial_i q^a)_{\phi,I} + p_a\tilde{\delta}(\partial_i q^a)_{\phi,I} - \tilde{\delta}(\partial_i S)_{\phi,I}. \tag{4.19}$$

Now, we combine this equation with (4.18), resulting in

$$\tilde{\delta}G_i = -(\partial_i p_a)_{\phi,I}\tilde{\delta}q^a + (\partial_i q^a)_{\phi,I}\tilde{\delta}p_a. \tag{4.20}$$

On the other hand, if we consider G_i as a function of (q, p), it follows that

$$\tilde{\delta}G_i = \frac{\partial G_i}{\partial q^a}\tilde{\delta}q^a + \frac{\partial G_i}{\partial p_a}\tilde{\delta}p_a. \tag{4.21}$$

Comparing these two previous equations, we find (4.15) and (4.16). Therefore, since the G_i generate translations in parameter space, they are the classical analogs of the quantum operators $\hat{G}_i$. Furthermore, using (4.15) and (4.16), we can write the components of the two-form F (4.9) as

$$F_{ij} = -\langle\{G_i, G_j\}\rangle. \tag{4.22}$$

Notice that written in this form, we can clearly see that F_{ij} is the classical analog of the Berry curvature (2.46), and that the torus average $\langle\cdot\rangle$ is the classical analog of the expectation value $\langle\cdot\rangle_n$.

Finally, we address the issue of gauge transformations. In this case, the analog of the quantum local phase transformation (2.19) is a parameter-dependent angle shift [9] given by the canonical transformation

$$I'_a = I_a, \quad \phi'^a = \phi^a + \frac{\partial\lambda(I;x)}{\partial I_a}, \tag{4.23}$$

which has the generating function [69]

$$F_2(\phi, I'; x) = \phi^a I'_a + \lambda(I'; x). \tag{4.24}$$

Note that this angle variable shift may depend on I, which is analogous to having a different Berry phase for each n. The transformation from (q,p) to (ϕ, I) gives the Hamiltonian (4.1)

$$K(\phi, I; x) = H(I; x) - G_i(\phi, I; x)\dot{x}^i. \tag{4.25}$$

Then, the transformation $(\phi, I) \to (\phi', I')$ yields

$$K'(\phi', I'; x) = K(\phi', I'; x) + \left(\frac{\partial F_2(\phi, I'; x)}{\partial t}\right)_{\phi=\phi(\phi', I'; x)}, \tag{4.26}$$

where $K(\phi', I'; x) = K(\phi(\phi', I'; x), I'; x)$. Hence, combining both Hamiltonians, we get

$$K'(\phi', I'; x) = H - \left[G_i - \left(\frac{\partial F_2}{\partial x^i}\right)\right]\dot{x}^i. \tag{4.27}$$

This expression defines the generator $G'(\phi', I'; x)$ as

$$G'(\phi', I'; x) = G_i - \left(\frac{\partial F_2}{\partial x^i}\right). \tag{4.28}$$

Applying the chain rule on (4.24), we find

$$G'_i(\phi', I'; x) = G_i - \partial_i\lambda. \tag{4.29}$$

The new components of the one-form are then

$$A'_i(I'; x) = \langle G'_i\rangle', \tag{4.30}$$

where $G'_i = G'_i(\phi', I'; x)$ and $\langle\cdot\rangle'$ indicates the torus average over the angle variable ϕ'. Using (4.29) we can see that

$$\begin{aligned}
\langle G'_i\rangle' =& \frac{1}{(2\pi)^N}\int_0^{2\pi} \mathrm{d}^N\phi' \ [G_i(\phi', I'; x) - (\partial_i\lambda(I'; x))_{I'}] \\
=& \frac{1}{(2\pi)^N}\int_{-b^1}^{2\pi-b^1} \mathrm{d}\phi^1 \cdots \int_{-b^N}^{2\pi-b^N} \mathrm{d}\phi^N \ [G_i(\phi, I; x) - (\partial_i\lambda(I; x))_I] \\
=& \langle G_i\rangle - \partial_i\lambda,
\end{aligned} \tag{4.31}$$

where we performed the change of angle variables $\phi'^a \to \phi^a$, defined $b^a = \partial\lambda(I;x)/\partial I_a$, and used the periodicity of p_a, $(\partial_i q^a)_{\phi,I}$ and $(\partial_i S)_{\phi,I}$ in each angle variable which implies the periodicity of G_i. The function $(\partial_i S)_{\phi,I}$ is seen to be periodic by writing

$$S(q,I;x) = \sum_{a=1}^{N} S_a(q_a,I;x). \tag{4.32}$$

If we use the definition of the action variable I_a,

$$S_a(\phi+2\pi,I;x) - S_a(\phi,I;x) = 2\pi I_a, \tag{4.33}$$

where $S_a(\phi,I;x) = S_a(q(\phi,I;x),I;x)$, and differentiate with respect to x^i, the periodicity $(\partial_i S)_{\phi,I}$ is evident. We have found that the one-form components A_i transform as

$$A_i \to A'_i = A_i - \partial_i\lambda, \tag{4.34}$$

so the one-form A defines an Abelian connection [9]. On the other hand, $F = \mathrm{d}A$ is the curvature associated with this connection and it is left gauge invariant, since

$$F' = \mathrm{d}A' = \mathrm{d}A - \mathrm{d}^2\lambda = \mathrm{d}A. \tag{4.35}$$

4.2 Classical analog of the quantum metric tensor

Now that we have introduced the classical generators G_i, and in complete analogy with the quantum case (2.49), it is natural to define the distance between the points $(q(x),p(x))$ and $(q(x)+\overline{\delta}q, p(x)+\overline{\delta}p)$ of phase space as

$$\mathrm{d}s^2 = \langle(\Delta G)^2\rangle, \tag{4.36}$$

where $\Delta G = \Delta G_i \delta x^i$, with $\Delta G_i = G_i - \langle G_i\rangle$. Hence, expanding (4.36), we find that the distance takes the form

$$\mathrm{d}s^2 = \left(\langle G_i G_j\rangle - \langle G_i\rangle\langle G_j\rangle\right)\delta x^i \delta x^j. \tag{4.37}$$

Therefore, we define the classical analog of the quantum metric tensor as

$$g_{ij}(I;x) = \langle G_i G_j\rangle - \langle G_i\rangle\langle G_j\rangle. \tag{4.38}$$

From now on, we will refer to it as classical metric.

We can easily verify that our classical metric: (i) transforms as a tensor under the change of parameters, (ii) it is gauge invariant, and (iii) it is positive semidefinite. To prove the first property, we note from (4.3) that given the transformation $x^i \to x'^i = x'^i(x)$, the generator G_i changes as

$$G_i(\phi,I;x) \to G'_i(\phi,I;x') = \frac{\partial x^j}{\partial x'^i} G_j(\phi,I;x(x')). \tag{4.39}$$

This result, together with the definition (4.38) leads to

$$g'_{ij}(I;x') = \frac{\partial x^k}{\partial x'^i}\frac{\partial x^l}{\partial x'^j} g_{kl}(I;x). \tag{4.40}$$

The proof of property (ii) is readily carried out by considering the transformations (4.29) and (4.31). We find that the first term of the classical metric transforms as

$$\langle G'_i G'_j\rangle' = \langle G_i G_j\rangle - \langle G_i\rangle(\partial_j\lambda) - \langle G_j\rangle(\partial_i\lambda) + (\partial_i\lambda)(\partial_j\lambda). \tag{4.41}$$

Despite this term being a symmetric tensor, it should not be considered as a classical metric candidate, since it is clearly not gauge invariant. We see that, analogously to the Provost quantum metric (2.20), the second term $\langle G_i\rangle\langle G_j\rangle$ compensates this change and we are left with

$$g'_{ij}(I';x) = \langle G_i G_j\rangle - \langle G_i\rangle\langle G_j\rangle = g_{ij}(I;x). \tag{4.42}$$

Regarding the third property, it is easy to see from expression (4.36) that $\mathrm{d}L^2 \geq 0$ since the variance $(\Delta G)^2$ is non-negative. Thus, our classical metric (4.38) is positive semidefinite. Moreover, we observe that the classical analog of the quantum persistence of the system in the state $|n\rangle$, is the invariance of the action variable I. Finally, note that from (4.15) we can see that

$$\{q^a, \Delta G_i\} = (\partial_i - A_i)q^a, \tag{4.43}$$

which, in an analogous manner to the quantum case (cf. (2.50)), resembles the structure of a covariant derivative $D_i = \partial_i - A_i$ with connection A_i.

4.2.1 Behavior under canonical transformations

So far, we have seen how the classical metric tensor behaves under parameter transformations $x^i \to x'^i = x'^i(x)$, however, nothing has been said about the transformation properties of the generators and the classical metric under canonical transformations. In some problems, it may be easier to work with a special set of phase space coordinates, thus, the rule for the transformation of generators constitutes a crucial result of this work. We must say that the quantum counterpart of this problem was not considered, although it might be developed through the use of unitary transformations, at least those that correspond to linear canonical transformations [70].

As we know, the generators of displacements in the parameters of phase space coordinates (q,p) are (4.2)

$$G_i = -\left(\frac{\partial S}{\partial x^i}\right)_{q,I}, \tag{4.44}$$

where the function $S(q,I;x)$ effects the transformation from the original variables (q,p) to the action-angle variables (ϕ,I). Now, consider the canonical transformation $(q,p)\to(Q,P)$ performed by a type-2 generating function $F = F(q,P;x)$. We might as well

introduce the generator of displacements in the parameters of the variables (Q, P), which are given by

$$\tilde{G}_i = -\left(\frac{\partial \tilde{S}}{\partial x^i}\right)_{Q,I}, \tag{4.45}$$

where $\tilde{S}(Q, I; x)$ is the generating function of the transformation $(Q, P) \to (\phi, I)$. Our goal is to find the relation between the functions G_i and $\tilde{G}_i$. Given that there are three transformations involved in the process, we need to know the rule for composing canonical transformations through their generating functions. It turns out that the resulting generating function S is [71, 72]

$$S(q, I; x) = \tilde{S}(Q, I; x) + F(q, P; x) - Q^a P_a. \tag{4.46}$$

For our purposes, it is convenient to cast this composition rule as a function of the variables $(Q, I; x)$ as follows:

$$\tilde{S}(Q, I; x) = S(q(Q, I; x), I; x) - F(q(Q, I; x), P(Q, I; x); x) + Q^a P_a(Q, I; x). \tag{4.47}$$

We take the derivative of this expression with respect to x^i with the aid of the chain rule and find that

$$\begin{aligned}\left(\frac{\partial \tilde{S}}{\partial x^i}\right)_{Q,I} = &\left(\frac{\partial S}{\partial q^a}\right)_{I,x}\left(\frac{\partial q^a}{\partial x^i}\right)_{Q,I} + \left(\frac{\partial S}{\partial x^i}\right)_{q,I} - \left[\left(\frac{\partial F}{\partial q^a}\right)_{P,x}\left(\frac{\partial q^a}{\partial x^i}\right)_{Q,I}\right. \\ &\left. + \left(\frac{\partial F}{\partial P_a}\right)_{q,x}\left(\frac{\partial P_a}{\partial x^i}\right)_{Q,I} + \left(\frac{\partial F}{\partial x^i}\right)_{q,P}\right] + Q^a\left(\frac{\partial P_a}{\partial x^i}\right)_{Q,I}.\end{aligned} \tag{4.48}$$

Using the following equations of a type-2 canonical transformation

$$p_a = \left(\frac{\partial S}{\partial q^a}\right)_{I,x}, \quad p_a = \left(\frac{\partial F}{\partial q^a}\right)_{P,x}, \quad Q^a = \left(\frac{\partial F}{\partial P_a}\right)_{q,x}, \tag{4.49}$$

we arrive at

$$\begin{aligned}\left(\frac{\partial \tilde{S}}{\partial x^i}\right)_{Q,I} = &p_a\left(\frac{\partial q^a}{\partial x^i}\right)_{Q,I} + \left(\frac{\partial S}{\partial x^i}\right)_{q,I} - \left[p_a\left(\frac{\partial q^a}{\partial x^i}\right)_{Q,I} + Q^a\left(\frac{\partial P_a}{\partial x^i}\right)_{Q,I}\right. \\ &\left. + \left(\frac{\partial F}{\partial x^i}\right)_{q,P}\right] + Q^a\left(\frac{\partial P_a}{\partial x^i}\right)_{Q,I},\end{aligned} \tag{4.50}$$

which simplifies to

$$\left(\frac{\partial \tilde{S}}{\partial x^i}\right)_{Q,I} = \left(\frac{\partial S}{\partial x^i}\right)_{q,I} - \left(\frac{\partial F}{\partial x^i}\right)_{q,P}. \tag{4.51}$$

Identifying the generators G_i and $\tilde{G}_i$ through (4.44) and (4.45), we arrive at the desired formula

$$G_i = \tilde{G}_i - \left(\frac{\partial F}{\partial x^i}\right)_{q,P}. \tag{4.52}$$

This apparently simple relation contains a powerful result: if the generating function of the transformation $(q,p) \to (Q,P)$ does not depend on the parameters x, then the classical metric resulting from G_i is the same as that obtained with $\tilde{G}_i$. Thus, if the description of the system in question is simpler in terms of the coordinates (Q,P) rather than in coordinates (q,p), and the type-2 generating function of the $(q,p) \to (Q,P)$ transformation does not depend on parameters, then the metric can be found through the formula $g_{ij} = \langle \tilde{G}_i \tilde{G}_j \rangle - \langle \tilde{G}_i \rangle \langle \tilde{G}_j \rangle$. It is worth noting the inhomogeneous character of equation (4.52), as opposed to the homogeneous tensor transformation rule for parameters (4.39).

4.3 Time-dependent approach to the classical metric and curvature

In this section, we introduce a time-dependent approach to the classical metric and the Hannay curvature [68]. This formulation is the classical analog of the path integral approach of Section 2.5, and actually stems from the semiclassical approximation of equations (2.56) and (2.57), as we will show next.

Let us recall the expressions for the quantum metric tensor and the Berry curvature:

$$g_{ij}^{(0)}(x) = -\frac{1}{\hbar^2} \int_{-\infty}^{0} \mathrm{d}t_1 \int_{0}^{\infty} \mathrm{d}t_2 \left(\frac{1}{2} \langle [\hat{\mathcal{O}}_i(t_1) \hat{\mathcal{O}}_j(t_2)]_+ \rangle_0 - \langle \hat{\mathcal{O}}_i(t_1) \rangle_0 \langle \hat{\mathcal{O}}_j(t_2) \rangle_0 \right), \tag{4.53}$$

$$F_{ij}^{(0)}(x) = \frac{1}{i\hbar^2} \int_{-\infty}^{0} \mathrm{d}t_1 \int_{0}^{\infty} \mathrm{d}t_2 \, \langle [\hat{\mathcal{O}}_i(t_1), \hat{\mathcal{O}}_j(t_2)]_- \rangle_0, \tag{4.54}$$

where $[\cdot,\cdot]_+$ stands for the anticommutator and $[\cdot,\cdot]_-$ for the commutator. We assume that the Heisenberg equations of motion for the N position and N momentum operators,

$$\frac{\mathrm{d}\hat{q}^a}{\mathrm{d}t} = -\frac{i}{\hbar}[\hat{q}^a, \hat{H}], \qquad \frac{\mathrm{d}\hat{p}_a}{\mathrm{d}t} = -\frac{i}{\hbar}[\hat{p}_a, \hat{H}], \qquad , a = 1, ..., N \tag{4.55}$$

can be integrated, so that $\hat{q}(t) = \{\hat{q}^a(t)\}$ and $\hat{p}(t) = \{\hat{p}_a(t)\}$ can be expressed as functions of the initial (Schrödinger) operators $\hat{q} = \hat{q}(t=0)$ and $\hat{p} = \hat{p}(t=0)$, and time. In this way, the Hamiltonian deformation $\hat{\mathcal{O}}_i(t)$ will read

$$\hat{\mathcal{O}}_i(t) = \hat{\mathcal{O}}_i(\hat{q}(\hat{q}_0, \hat{p}_0, t; x), \hat{p}(\hat{q}_0, \hat{p}_0, t; x), t; x). \tag{4.56}$$

Thus, the expectation values appearing in (4.53) and (4.54) can be written as

$$\begin{aligned} \langle \hat{\mathcal{O}}_i(t) \rangle_0 &= \langle \psi_0(x) | \hat{\mathcal{O}}_i(t) | \psi_0(x) \rangle \\ &= \int \mathrm{d}q_0 \, \psi_0^*(q_0; x) \mathcal{O}_i \left(q_0, -i\hbar \frac{\partial}{\partial q_0}, t; x \right) \psi_0(q_0; x), \end{aligned} \tag{4.57}$$

and as

$$\begin{aligned}\langle[\hat{\mathcal{O}}_i(t_1)\hat{\mathcal{O}}_j(t_2)]_\pm\rangle_0 &= \langle\psi_0(x)|[\hat{\mathcal{O}}_i(t_1),\hat{\mathcal{O}}_j(t_2)]_\pm|\psi_0(x)\rangle \\ &= \int \mathrm{d}^N q_0\, \psi_0^*(q_0;x) \\ &\quad\times\left[\mathcal{O}_i\left(q_0,-i\hbar\frac{\partial}{\partial q_0},t_1;x\right),\mathcal{O}_j\left(q_0,-i\hbar\frac{\partial}{\partial q_0},t_2;x\right)\right]_\pm \psi_0(q_0;x).\end{aligned} \tag{4.58}$$

In the spirit of Berry's work [9], we use the semiclassical approximation of the wave function for an integrable system with N degrees of freedom [73, 74]:

$$\psi_0(q_0;x) \simeq \sum_\alpha a_{(\alpha)}(q_0,I_0;x)\exp\left[\frac{i}{\hbar}S^{(\alpha)}(q_0,I_0;x)\right], \tag{4.59}$$

where

$$\left(a_{(\alpha)}(q_0,I_0;x)\right)^2 = \frac{1}{(2\pi)^N}\det\left[\frac{\partial\phi^a_{0(\alpha)}(q_0,I_0;x)}{\partial q_0^b}\right], \tag{4.60}$$

and α denotes the branch of the multi-valued function $S^{(\alpha)}(q_0,I_0;x)$ which generates the transformation $(q_0,p_0)\to(\phi_0,I_0)$. Since the action I_0 remains constant, we may set $I_0 = I$. Substituting (4.59) in (4.57) and (4.58), and taking into account that terms coming from different branches are suppressed due to a strongly oscillating behavior, we arrive at

$$\langle\hat{\mathcal{O}}_i(t)\rangle_0 = \int\frac{\mathrm{d}^N q_0}{(2\pi)^N}\sum_\alpha\det\left[\frac{\partial\phi^a_{0(\alpha)}(q_0,I;x)}{\partial q_0^b}\right]\mathcal{O}_i\left(q_0,\frac{\partial S^{(\alpha)}}{\partial q_0},t;x\right)+O(\hbar), \tag{4.61}$$

and

$$\begin{aligned}\langle[\hat{\mathcal{O}}_i(t_1)\hat{\mathcal{O}}_j(t_2)]_\pm\rangle_0 &= \int\frac{\mathrm{d}^N q_0}{(2\pi)^N}\sum_\alpha\det\left[\frac{\partial\phi^a_{0(\alpha)}(q_0,I;x)}{\partial q_0^b}\right] \\ &\quad\times\left[\mathcal{O}_i\left(q_0,\frac{\partial S^{(\alpha)}}{\partial q_0},t_1;x\right),\mathcal{O}_j\left(q_0,\frac{\partial S^{(\alpha)}}{\partial q_0},t_2;x\right)\right]_\pm + O(\hbar).\end{aligned} \tag{4.62}$$

We replace $\frac{\partial S^{(\alpha)}}{\partial q_0}$ by $p_0^{(\alpha)}$, following the transformation equations of the canonical transformation to action-angle variables. For bosonic operators, we must replace the anticommutators by products of functions, and the commutators by $i\hbar$ times the non-equal-time Poisson brackets

$$\{\mathcal{O}_i(t_1),\mathcal{O}_j(t_2)\} = \sum_{a=1}^N\left(\frac{\partial\mathcal{O}_i(t_1)}{\partial q_0^a}\frac{\partial\mathcal{O}_j(t_2)}{\partial p_{0a}^{(\alpha)}}-\frac{\partial\mathcal{O}_i(t_1)}{\partial p_{0a}^{(\alpha)}}\frac{\partial\mathcal{O}_j(t_2)}{\partial q_0^a}\right). \tag{4.63}$$

If, on the other hand, we are dealing with fermionic operators, we replace the anticommutators by Poisson brackets, and the commutators by products. Assuming the bosonic case and neglecting terms of order $O(\hbar)$, we have that

$$\langle\hat{\mathcal{O}}_i(t)\rangle_0 \simeq \int \frac{\mathrm{d}^N q_0}{(2\pi)^N} \sum_\alpha \det\left[\frac{\partial\phi^a_{0(\alpha)}(q_0,I;x)}{\partial q_0^b}\right] \mathcal{O}_i\left(q_0, p_0^{(\alpha)}, t; x\right), \tag{4.64}$$

$$\begin{aligned}\langle[\hat{\mathcal{O}}_i(t_1)\hat{\mathcal{O}}_j(t_2)]_+\rangle_0 \simeq 2\int \frac{\mathrm{d}^N q_0}{(2\pi)^N} \sum_\alpha \det\left[\frac{\partial\phi^a_{0(\alpha)}(q_0,I;x)}{\partial q_0^b}\right] \\ \times \mathcal{O}_i\left(q_0, p_0^{(\alpha)}, t_1; x\right) \mathcal{O}_j\left(q_0, p_0^{(\alpha)}, t_2; x\right),\end{aligned} \tag{4.65}$$

and

$$\begin{aligned}\langle[\hat{\mathcal{O}}_i(t_1)\hat{\mathcal{O}}_j(t_2)]_-\rangle_0 \simeq i\hbar\int \frac{\mathrm{d}^N q_0}{(2\pi)^N} \sum_\alpha \det\left[\frac{\partial\phi^a_{0(\alpha)}(q_0,I;x)}{\partial q_0^b}\right] \\ \times \left\{\mathcal{O}_i\left(q_0, p_0^{(\alpha)}, t_1; x\right), \mathcal{O}_j\left(q_0, p_0^{(\alpha)}, t_2; x\right)\right\}.\end{aligned} \tag{4.66}$$

We now choose the branch defined by $0 \leq \phi_0 < 2\pi$ which makes $\phi_{0(\alpha)}$, and therefore, $p_0^{(\alpha)}$ single-valued. In addition to this, we effect the change to the angle variable in the integrals. Thus,

$$\langle\hat{\mathcal{O}}_i(t)\rangle_0 \simeq \frac{1}{(2\pi)^N}\int \mathrm{d}^N\phi_0\, \mathcal{O}_i(q_0,p_0,t;x), \tag{4.67}$$

$$\langle[\hat{\mathcal{O}}_i(t_1)\hat{\mathcal{O}}_j(t_2)]_+\rangle_0 \simeq \frac{2}{(2\pi)^N}\int \mathrm{d}^N\phi_0\, \mathcal{O}_i(q_0,p_0,t_1;x)\mathcal{O}_j(q_0,p_0,t_2;x), \tag{4.68}$$

$$\langle[\hat{\mathcal{O}}_i(t_1)\hat{\mathcal{O}}_j(t_2)]_-\rangle_0 \simeq i\hbar\frac{1}{(2\pi)^N}\int \mathrm{d}^N\phi_0\, \{\mathcal{O}_i(q_0,p_0,t_1;x), \mathcal{O}_j(q_0,p_0,t_2;x)\}. \tag{4.69}$$

Denoting by $\langle\cdot\rangle_0$ the torus average of over the initial angle variables $\frac{1}{(2\pi)^N}\int \mathrm{d}^N\phi_0\,(\cdot)$, we can cast the above equations as

$$\langle\hat{\mathcal{O}}_i(t)\rangle_0 \simeq \langle\mathcal{O}_i(t)\rangle_0, \tag{4.70}$$

$$\langle[\hat{\mathcal{O}}_i(t_1)\hat{\mathcal{O}}_j(t_2)]_+\rangle_0 \simeq 2\langle\mathcal{O}_i(t_1)\mathcal{O}_j(t_2)\rangle_0, \tag{4.71}$$

$$\langle[\hat{\mathcal{O}}_i(t_1)\hat{\mathcal{O}}_j(t_2)]_-\rangle_0 \simeq i\hbar\langle\{\mathcal{O}_i(t_1), \mathcal{O}_j(t_2)\}\rangle_0, \tag{4.72}$$

where $\mathcal{O}_i(t) = \mathcal{O}_i(q_0,p_0,t;x)$ are the deformation functions

$$\mathcal{O}_i = \left(\frac{\partial H}{\partial x^i}\right)_{q,p} \tag{4.73}$$

obtained solving Hamilton's equations and then expressing the solutions in terms of initial conditions (q_0, p_0) and time, which in turn, must be written in terms of initial action-angle variables (ϕ_0, I) and time.

Plugging (4.70) and (4.71) into (4.53), we arrive at

$$g_{ij}^{(0)}(x) \simeq \frac{1}{\hbar^2} g_{ij}(I;x), \tag{4.74}$$

where

$$g_{ij}(I;x) = -\int_{-\infty}^{0} \mathrm{d}t_1 \int_{0}^{\infty} \mathrm{d}t_2 \left(\langle \mathcal{O}_i(t_1)\mathcal{O}_j(t_2)\rangle_0 - \langle \mathcal{O}_i(t_1)\rangle_0 \langle \mathcal{O}_j(t_2)\rangle_0 \right) \tag{4.75}$$

is the classical metric. Substituting (4.70) and (4.72) in (4.54), we find

$$F_{ij}^{(0)}(x) \simeq \frac{1}{\hbar} F_{ij}(I;x), \tag{4.76}$$

where

$$F_{ij}(I;x) = \int_{-\infty}^{0} \mathrm{d}t_1 \int_{0}^{\infty} \mathrm{d}t_2 \, \langle \{\mathcal{O}_i(t_1), \mathcal{O}_j(t_2)\}\rangle_0, \tag{4.77}$$

is the Hannay curvature. In these expressions, it is understood that the action variable I is quantized according to the corrected Bohr-Sommerfeld rule, also called the Einstein-Brillouin-Keller (EBK) rule [74]

$$I_a = \left(n_a + \frac{\mu_a}{4}\right)\hbar, \tag{4.78}$$

where μ_a are the Maslov indices [73]. Previous works [9, 75] had already obtained the relation (4.76), however, neither of them tackled the classical analog of the quantum metric tensor.

4.4 Equivalence between the two approaches

In this section, we prove a crucial result of our work: the equivalence between the time-dependent approach to the classical metric and the Hannay curvature, and the generator approach. This justifies our initial proposal of the classical metric (4.38).

Consider an integrable system of N degrees of freedom with Hamiltonian $H(q,p;x)$, where $q = \{q^a\}$ and $p = \{p_a\}$ with $a = 1, ..., N$ are the phase space coordinates and $x = \{x^i\}$ with $i = 1, ..., M$ is a set of M adiabatic parameters. The classical deformation functions

$$\mathcal{O}_i = \left(\frac{\partial H}{\partial x^i}\right)_{q,p} \tag{4.79}$$

are functions of q, p and the parameters x. In the periodic motion regime, action-angle variables (ϕ, I) can be introduced and any function of q and p will be itself periodic [76], thus, it can be expanded in Fourier series in terms of the angle variables ϕ. Using the compact notation $\mathcal{O}_i(t) \equiv \mathcal{O}_i(q(t), p(t); x)$, we have that

$$\mathcal{O}_i(t) = \sum_n \beta_n^{(i)} e^{in\cdot(\phi_0+\omega t)}, \tag{4.80}$$

where $\phi_0 = (\phi_0^1, ...\phi_0^N)$ are the initial angle variables, $\omega = (\omega^1, ..., \omega^N)$ are the frequencies derived as $\omega^a = \partial H/\partial I_a$, and the $\beta_n^{(i)}$ are the Fourier coefficients of the time-independent deformation functions $\mathcal{O}_i \equiv \mathcal{O}_i(q_0, p_0; x)$, i.e.,

$$\beta_n^{(i)} \equiv \beta_n^{(i)}(I; x) = \frac{1}{(2\pi)^N} \int_0^{2\pi} \mathrm{d}^N\phi_0 \, \mathcal{O}_i e^{-in\cdot\phi_0}, \tag{4.81}$$

where $n = (n_1, ..., n_N)$, and every n_a runs over all the integers.

4.4.1 Classical metric

We begin with the classical metric (4.75). We first consider the torus average of the $\mathcal{O}_i(t)$:

$$\begin{aligned}
\langle \mathcal{O}_i(t)\rangle_0 &= \frac{1}{(2\pi)^N} \int_0^{2\pi} \mathrm{d}^N\phi_0 \sum_n \beta_n^{(i)} e^{in\cdot(\phi_0+\omega t)} \\
&= \sum_n \beta_n^{(i)} e^{in\cdot\omega t} \left[\frac{1}{(2\pi)^N} \int_0^{2\pi} \mathrm{d}^N\phi_0 \, e^{in\cdot\phi_0} \right] \\
&= \sum_n \beta_n^{(i)} e^{in\cdot\omega t} \delta_{n,0} = \beta_0^{(i)}.
\end{aligned} \tag{4.82}$$

From equation (4.81), we conclude that

$$\langle \mathcal{O}_i(t)\rangle_0 = \frac{1}{(2\pi)^N} \int_0^{2\pi} \mathrm{d}^N\phi_0 \, \mathcal{O}_i = \langle \mathcal{O}_i\rangle_0. \tag{4.83}$$

Therefore, as in the quantum case, the average of a single deformation function turns out to be time-independent.

Now, we consider the two-time average and expand it as follows:

$$\begin{aligned}\langle \mathcal{O}_i(t_1)\mathcal{O}_j(t_2)\rangle_0 &= \frac{1}{(2\pi)^N}\int_0^{2\pi} \mathrm{d}^N\phi_0 \sum_n \beta_n^{(i)} e^{in\cdot(\phi_0+\omega t_1)} \sum_{n'} \beta_{n'}^{(j)} e^{in'\cdot(\phi_0+\omega t_2)} \\ &= \sum_{n,n'} \beta_n^{(i)}\beta_{n'}^{(j)} e^{in\cdot\omega t_1} e^{in'\cdot\omega t_2} \left[\frac{1}{(2\pi)^N}\int_0^{2\pi} \mathrm{d}^N\phi_0\, e^{i(n+n')\cdot\phi_0}\right] \\ &= \sum_{n,n'} \beta_n^{(i)}\beta_{n'}^{(j)} e^{in\cdot\omega t_1} e^{in'\cdot\omega t_2}\delta_{n',-n} \\ &= \beta_0^{(i)}\beta_0^{(j)} + \sum_{n\neq 0} \beta_n^{(i)}\beta_{-n}^{(j)} e^{in\cdot\omega(t_1-t_2)}. \end{aligned} \tag{4.84}$$

Thus, equations (4.83) and (4.84) lead to

$$\langle \mathcal{O}_i(t_1)\mathcal{O}_j(t_2)\rangle_0 - \langle \mathcal{O}_i(t)\rangle_0\langle \mathcal{O}_j(t)\rangle_0 = \sum_{n\neq 0} \beta_n^{(i)}\beta_{-n}^{(j)} e^{in\cdot\omega(t_1-t_2)}. \tag{4.85}$$

Substituting (4.85) in (4.75), it is now easy to isolate the time dependence, just as in the quantum case. Hence,

$$g_{ij} = -\sum_{n\neq 0} \beta_n^{(i)}\beta_{-n}^{(j)} \int_{-\infty}^{0} \mathrm{d}t_1 \int_0^{\infty} \mathrm{d}t_2\, e^{in\cdot\omega(t_1-t_2)}, \tag{4.86}$$

and upon using the regularization (2.63)

$$\int_{-\infty}^{0} \mathrm{d}t_1 \int_0^{\infty} \mathrm{d}t_2\, e^{in\cdot\omega(t_1-t_2)} = -\frac{1}{(n\cdot\omega)^2}, \tag{4.87}$$

we find that

$$g_{ij} = \sum_{n\neq 0} \frac{\beta_n^{(i)}\beta_{-n}^{(j)}}{(n\cdot\omega)^2}. \tag{4.88}$$

This expression tells us that from the Fourier coefficients of the time-independent deformation functions $\mathcal{O}_i$, and the frequencies ω_a, we can compute the classical metric. To better understand the result, let us use (4.81) and rewrite it as

$$g_{ij} = \sum_{n\neq 0} \frac{\langle \mathcal{O}_i e^{-in\cdot\phi_0}\rangle_0 \langle \mathcal{O}_j e^{in\cdot\phi_0}\rangle_0}{(n\cdot\omega)^2}. \tag{4.89}$$

Remarkably, this expression for the classical metric is similar to equation (2.64) that corresponds to the quantum metric. Now, we consider the following relation

$$H(q_0(\phi_0, I; x), p_0(\phi_0, I; x); x) = H(I; x), \tag{4.90}$$

and differentiate it with respect to x^i. We get

$$\sum_{a=1}^{N}\left[\left(\frac{\partial H}{\partial q_0^a}\right)_{p_0,x}\left(\frac{\partial q_0^a}{\partial x^i}\right)_{\phi_0,I}+\left(\frac{\partial H}{\partial p_{0a}}\right)_{q_0,x}\left(\frac{\partial p_{0a}}{\partial x^i}\right)_{\phi_0,I}\right]+\left(\frac{\partial H}{\partial x^i}\right)_{q_0,p_0}=\left(\frac{\partial H}{\partial x^i}\right)_I. \quad (4.91)$$

The generators of parameter displacements G_i are readily identified through equations (4.15) and (4.16). Thus,

$$\sum_{a=1}^{N}\left[\left(\frac{\partial H}{\partial q_0^a}\right)_{p_0,x}\left(\frac{\partial G_i}{\partial p_{0a}}\right)_{q_0,x}-\left(\frac{\partial H}{\partial p_{0a}}\right)_{q_0,x}\left(\frac{\partial G_i}{\partial q_0^a}\right)_{p_0,x}\right]+\mathcal{O}_i=\left(\frac{\partial H}{\partial x^i}\right)_I. \quad (4.92)$$

The first term is the Poisson bracket of H with the generator G_i, hence,

$$\mathcal{O}_i=\left(\frac{\partial H}{\partial x^i}\right)_I-\{H,G_i\}_{(q_0,p_0)}. \quad (4.93)$$

Next, we take advantage of the canonical invariance of Poisson brackets and compute them in terms of action-angle variables to get

$$\mathcal{O}_i=\left(\frac{\partial H}{\partial x^i}\right)_I+\sum_{a=1}^{N}\omega^a\left(\frac{\partial G_i}{\partial \phi_0^a}\right)_{I,x}, \quad (4.94)$$

where we have used the fact that $\omega^a=\partial H/\partial I$. With this at hand, we can rewrite one of the averages that appear in (4.89) as

$$\begin{aligned}\langle\mathcal{O}_i e^{-in\cdot\phi_0}\rangle_0&=\left(\frac{\partial H}{\partial x^i}\right)_I\langle e^{-in\cdot\phi_0}\rangle_0+\sum_{a=1}^{N}\omega^a\left\langle\frac{\partial G_i}{\partial\phi_0^a}e^{-in\cdot\phi_0}\right\rangle_0\\&=\left(\frac{\partial H}{\partial x^i}\right)_I\delta_{n,0}+\sum_{a=1}^{N}\omega^a\left\langle\frac{\partial G_i}{\partial\phi_0^a}e^{-in\cdot\phi_0}\right\rangle_0. \quad (4.95)\end{aligned}$$

Now, we separate the ath degree of freedom in the average of the second term and perform an integration by parts as follows:

$$\begin{aligned}\left\langle\frac{\partial G_i}{\partial\phi_0^a}e^{-in\cdot\phi_0}\right\rangle_0&=\frac{1}{(2\pi)^N}\int_0^{2\pi}\mathrm{d}^{N-1}\phi_0\,e^{-i\sum_{b\neq a}n_b\phi_0^b}\int_0^{2\pi}\mathrm{d}\phi_0^a\,\frac{\partial G_i}{\partial\phi_0^a}e^{-in_a\phi_0^a}\\&=\frac{1}{(2\pi)^N}\int_0^{2\pi}\mathrm{d}^{N-1}\phi_0\,e^{-i\sum_{b\neq a}n_b\phi_0^b}\left[G_i e^{-in_a\phi_0^a}\Big|_0^{2\pi}+in_a\int_0^{2\pi}\mathrm{d}\phi_0^a\,G_i e^{-in_a\phi_0^a}\right]\\&=\frac{in_a}{(2\pi)^N}\int_0^{2\pi}\mathrm{d}^N\phi_0\,G_i e^{-in\cdot\phi_0}\\&=in_a\langle G_i e^{-in\cdot\phi_0}\rangle_0, \quad (4.96)\end{aligned}$$

where in the third line we have used the fact that G_i is periodic in every ϕ_0^a. Therefore, substituting this into (4.95), we find that

$$\begin{aligned}\langle \mathcal{O}_i e^{-in\cdot\phi_0}\rangle_0 &= \left(\frac{\partial H}{\partial x^i}\right)_I \delta_{n,0} + \left(\sum_{a=1}^{N} in_a\omega^a\right)\langle G_i e^{-in\cdot\phi_0}\rangle_0 \\ &= \left(\frac{\partial H}{\partial x^i}\right)_I \delta_{n,0} + i(n\cdot\omega)\langle G_i e^{-in\cdot\phi_0}\rangle_0. \end{aligned} \tag{4.97}$$

Similarly, the other average appearing in (4.89) turns out to be

$$\langle \mathcal{O}_j e^{in\cdot\phi_0}\rangle_0 = \left(\frac{\partial H}{\partial x^j}\right)_I \delta_{n,0} - i(n\cdot\omega)\langle G_j e^{in\cdot\phi_0}\rangle_0. \tag{4.98}$$

Substituting these averages in (4.89) and noticing that $n \neq 0$, we arrive at

$$g_{ij} = \sum_{n\neq 0}\langle G_i e^{-in\cdot\phi_0}\rangle_0\langle G_j e^{in\cdot\phi_0}\rangle_0, \tag{4.99}$$

so adding and subtracting the term with $n = 0$, we get

$$g_{ij} = \sum_{n}\langle G_i e^{-in\cdot\phi_0}\rangle_0\langle G_j e^{in\cdot\phi_0}\rangle_0 - \langle G_i\rangle_0\langle G_j\rangle_0. \tag{4.100}$$

Expanding the first term, we find that

$$\begin{aligned}\sum_n \langle G_i e^{-in\cdot\phi_0}\rangle_0\langle G_j e^{in\cdot\phi_0}\rangle_0 &= \sum_n \frac{1}{(2\pi)^N}\int_0^{2\pi} \mathrm{d}^N\phi_0\, G_i e^{-in\cdot\phi_0}\frac{1}{(2\pi)^N}\int_0^{2\pi}\mathrm{d}^N\phi_0'\, G_j' e^{in\cdot\phi_0'} \\ &= \frac{1}{(2\pi)^N}\frac{1}{(2\pi)^N}\int_0^{2\pi}\mathrm{d}^N\phi_0\int_0^{2\pi}\mathrm{d}^N\phi_0'\, G_i G_j' \sum_n e^{in\cdot(\phi_0'-\phi_0)} \\ &= \frac{1}{(2\pi)^N}\frac{1}{(2\pi)^N}\int_0^{2\pi}\mathrm{d}^N\phi_0\int_0^{2\pi}\mathrm{d}^N\phi_0'\, G_i G_j' (2\pi)^N\delta^{(N)}(\phi_0'-\phi_0) \\ &= \frac{1}{(2\pi)^N}\int_0^{2\pi}\mathrm{d}^N\phi_0\, G_i G_j \\ &= \langle G_i G_j\rangle_0. \end{aligned} \tag{4.101}$$

Putting this result in (4.100), we arrive at

$$g_{ij} = \langle G_i G_j\rangle_0 - \langle G_i\rangle_0\langle G_j\rangle_0. \tag{4.102}$$

Finally, due to the gauge invariance of the metric, we can pick any angle to carry out the torus average, not necessarily the initial angle ϕ_0. Thus,

$$g_{ij} = \langle G_i G_j\rangle - \langle G_i\rangle\langle G_j\rangle, \tag{4.103}$$

which is precisely equation (4.38).

4.4.2 The Hannay curvature

Now, we consider the Hannay curvature. Naturally, due to (4.80) being expressed in terms of action-angle variables, we compute the Poisson bracket as

$$\{\mathcal{O}_i(t_1), \mathcal{O}_j(t_2)\} = \sum_{a=1}^{N} \left[\frac{\partial \mathcal{O}_i(t_1)}{\partial \phi_0^a} \frac{\partial \mathcal{O}_j(t_2)}{\partial I_a} - \frac{\partial \mathcal{O}_i(t_1)}{\partial I_a} \frac{\partial \mathcal{O}_j(t_2)}{\partial \phi_0^a} \right]. \tag{4.104}$$

The average of the first term is

$$\begin{aligned} \left\langle \sum_{a=1}^{N} \frac{\partial \mathcal{O}_i(t_1)}{\partial \phi_0^a} \frac{\partial \mathcal{O}_j(t_2)}{\partial I_a} \right\rangle_0 &= \sum_{n,n'} \sum_{a=1}^{N} \beta_n^{(i)} e^{in\cdot\omega t_1} i n_a \frac{\partial}{\partial I_a} \left(\beta_{n'}^{(j)} e^{in'\cdot\omega t_2} \right) \langle e^{i(n+n')\cdot\phi_0} \rangle_0 \\ &= \sum_{n,n'} \sum_{a=1}^{N} \beta_n^{(i)} e^{in\cdot\omega t_1} i n_a \frac{\partial}{\partial I_a} \left(\beta_{n'}^{(j)} e^{in'\cdot\omega t_2} \right) \delta_{n',-n} \\ &= \sum_{n} \sum_{a=1}^{N} \beta_n^{(i)} e^{in\cdot\omega t_1} i n_a \frac{\partial}{\partial I_a} \left(\beta_{-n}^{(j)} e^{-in\cdot\omega t_2} \right), \end{aligned} \tag{4.105}$$

and the average of the second term is obtained with $t_1 \leftrightarrow t_2$ and $i \leftrightarrow j$:

$$\begin{aligned} \left\langle \sum_{a=1}^{N} \frac{\partial \mathcal{O}_i(t_1)}{\partial I_a} \frac{\partial \mathcal{O}_j(t_2)}{\partial \phi_0^a} \right\rangle_0 &= \sum_{n} \sum_{a=1}^{N} \beta_n^{(j)} e^{in\cdot\omega t_2} i n_a \frac{\partial}{\partial I_a} \left(\beta_{-n}^{(i)} e^{-in\cdot\omega t_1} \right) \\ &= -\sum_{n} \sum_{a=1}^{N} \beta_{-n}^{(j)} e^{-in\cdot\omega t_2} i n_a \frac{\partial}{\partial I_a} \left(\beta_n^{(i)} e^{in\cdot\omega t_1} \right), \end{aligned} \tag{4.106}$$

where in the last line we made change $n \to -n$. Now, subtracting (4.106) from (4.105), we recognize the derivative of a product, hence,

$$\begin{aligned} \langle \{\mathcal{O}_i(t_1), \mathcal{O}_j(t_2)\} \rangle_0 &= \sum_{n} \sum_{a=1}^{N} i n_a \frac{\partial}{\partial I_a} \left(\beta_n^{(i)} \beta_{-n}^{(j)} e^{in\cdot\omega(t_1-t_2)} \right) \\ &= \sum_{n\neq 0} \sum_{a=1}^{N} i n_a \frac{\partial}{\partial I_a} \left(\beta_n^{(i)} \beta_{-n}^{(j)} e^{in\cdot\omega(t_1-t_2)} \right). \end{aligned} \tag{4.107}$$

The Hannay curvature then is

$$F_{ij} = \sum_{n\neq 0} \sum_{a=1}^{N} i n_a \frac{\partial}{\partial I_a} \left(\beta_n^{(i)} \beta_{-n}^{(j)} \int_{-\infty}^{0} \mathrm{d}t_1 \int_{0}^{\infty} \mathrm{d}t_2 \, e^{in\cdot\omega(t_1-t_2)} \right), \tag{4.108}$$

and using the result of the time integral (4.87) we arrive at

$$F_{ij} = -\sum_{n\neq 0} \sum_{a=1}^{N} i n_a \frac{\partial}{\partial I_a} \left[\frac{\beta_n^{(i)} \beta_{-n}^{(j)}}{(n\cdot\omega)^2} \right], \tag{4.109}$$

or

$$F_{ij} = -\sum_{n\neq 0}\sum_{a=1}^{N} in_a \frac{\partial}{\partial I_a}\left[\frac{\langle \mathcal{O}_i e^{-in\cdot\phi_0}\rangle_0 \langle \mathcal{O}_j e^{in\cdot\phi_0}\rangle_0}{(n\cdot\omega)^2}\right]. \tag{4.110}$$

Taking into account equations (4.97) and (4.98), the Hannay curvature takes the form

$$F_{ij} = -\sum_{n\neq 0}\sum_{a=1}^{N} in_a \frac{\partial}{\partial I_a}\Big(\langle G_i e^{-in\cdot\phi_0}\rangle_0 \langle G_j e^{in\cdot\phi_0}\rangle_0\Big). \tag{4.111}$$

Considering again the null $n = 0$ term and expanding the product, we get

$$F_{ij} = A_{ij} + B_{ij}, \tag{4.112}$$

where

$$A_{ij} = -\sum_{n}\sum_{a=1}^{N} in_a \left\langle \frac{\partial G_i}{\partial I_a} e^{-in\cdot\phi_0}\right\rangle_0 \langle G_j e^{in\cdot\phi_0}\rangle_0 \tag{4.113}$$

and

$$B_{ij} = -\sum_{n}\sum_{a=1}^{N} in_a \langle G_i e^{-in\cdot\phi_0}\rangle_0 \left\langle \frac{\partial G_j}{\partial I_a} e^{in\cdot\phi_0}\right\rangle_0. \tag{4.114}$$

We manipulate the first term as follows:

$$\begin{aligned}
A_{ij} &= -\sum_{n}\sum_{a=1}^{N} in_a \frac{1}{(2\pi)^N}\int_0^{2\pi} \mathrm{d}^N\phi_0\, \frac{\partial G_i}{\partial I_a} e^{-in\cdot\phi_0} \frac{1}{(2\pi)^N}\int_0^{2\pi} \mathrm{d}^N\phi_0'\, G_j' e^{in\cdot\phi_0'} \\
&= \sum_{n}\sum_{a=1}^{N} \frac{1}{(2\pi)^N}\int_0^{2\pi} \mathrm{d}^N\phi_0\, \left[\frac{\partial G_i}{\partial I_a}\frac{\partial}{\partial \phi_0^a}(e^{-in\cdot\phi_0})\right] \frac{1}{(2\pi)^N}\int_0^{2\pi} \mathrm{d}^N\phi_0'\, G_j' e^{in\cdot\phi_0'} \\
&= \sum_{a=1}^{N} \frac{1}{(2\pi)^N}\int_0^{2\pi} \mathrm{d}^N\phi_0\, \left[\frac{\partial G_i}{\partial I_a}\frac{\partial}{\partial \phi_0^a}\left(\frac{1}{(2\pi)^N}\int_0^{2\pi} \mathrm{d}^N\phi_0'\, G_j'\left(\sum_n e^{in\cdot(\phi_0'-\phi_0)}\right)\right)\right] \\
&= \sum_{a=1}^{N} \frac{1}{(2\pi)^N}\int_0^{2\pi} \mathrm{d}^N\phi_0\, \left[\frac{\partial G_i}{\partial I_a}\frac{\partial}{\partial \phi_0^a}\left(\frac{1}{(2\pi)^N}\int_0^{2\pi} \mathrm{d}^N\phi_0'\, G_j'(2\pi)^N\delta^{(N)}(\phi_0'-\phi_0)\right)\right] \\
&= \sum_{a=1}^{N} \frac{1}{(2\pi)^N}\int_0^{2\pi} \mathrm{d}^N\phi_0\, \frac{\partial G_i}{\partial I_a}\frac{\partial G_j}{\partial \phi_0^a} \\
&= \left\langle \sum_{a=1}^{N} \frac{\partial G_i}{\partial I_a}\frac{\partial G_j}{\partial \phi_0^a}\right\rangle_0.
\end{aligned} \tag{4.115}$$

Similarly, the second term yields

$$B_{ij} = -\left\langle \sum_{a=1}^{N} \frac{\partial G_i}{\partial \phi_0^a} \frac{\partial G_j}{\partial I_a} \right\rangle_0 . \tag{4.116}$$

Thus, the Hannay curvature turns out to be

$$F_{ij} = A_{ij} + B_{ij} = \left\langle \sum_{a=1}^{N} \left(\frac{\partial G_i}{\partial I_a} \frac{\partial G_j}{\partial \phi_0^a} - \frac{\partial G_i}{\partial \phi_0^a} \frac{\partial G_j}{\partial I_a} \right) \right\rangle_0 , \tag{4.117}$$

which reduces to

$$F_{ij} = -\langle \{G_i, G_j\} \rangle_0 . \tag{4.118}$$

Once again, due to gauge invariance, we have

$$F_{ij} = -\langle \{G_i, G_j\} \rangle , \tag{4.119}$$

which is equation (4.22).

Summarizing, the different ways of computing the classical metric and the Hannay curvature are

1. Generator approach

$$g_{ij}(I;x) = \langle G_i G_j \rangle - \langle G_i \rangle \langle G_j \rangle , \tag{4.120}$$
$$F_{ij}(I;x) = -\langle \{G_i, G_j\} \rangle . \tag{4.121}$$

2. Decomposition in Fourier modes

$$g_{ij}(I;x) = \sum_{n \neq 0} \frac{\langle \mathcal{O}_i e^{-in\cdot\phi_0} \rangle_0 \langle \mathcal{O}_j e^{in\cdot\phi_0} \rangle_0}{(n\cdot\omega)^2} , \tag{4.122}$$

$$F_{ij}(I;x) = -\sum_{n \neq 0} \sum_{a=1}^{N} i n_a \frac{\partial}{\partial I_a} \left[\frac{\langle \mathcal{O}_i e^{-in\cdot\phi_0} \rangle_0 \langle \mathcal{O}_j e^{in\cdot\phi_0} \rangle_0}{(n\cdot\omega)^2} \right] . \tag{4.123}$$

3. Time-dependent approach

$$g_{ij}(I;x) = -\int_{-\infty}^{0} \mathrm{d}t_1 \int_{0}^{\infty} \mathrm{d}t_2 \left(\langle \mathcal{O}_i(t_1) \mathcal{O}_j(t_2) \rangle_0 - \langle \mathcal{O}_i(t_1) \rangle_0 \langle \mathcal{O}_j(t_2) \rangle_0 \right), \tag{4.124}$$

$$F_{ij}(I;x) = \int_{-\infty}^{0} \mathrm{d}t_1 \int_{0}^{\infty} \mathrm{d}t_2 \, \langle \{\mathcal{O}_i(t_1), \mathcal{O}_j(t_2)\} \rangle_0 . \tag{4.125}$$

It is worth noticing the remarkable similarity between these expressions and those on the quantum side (2.68 - 2.70).

Chapter 5

Examples of the generator approach to the classical metric

In this chapter, we illustrate the application of the formulas to compute the quantum connection, curvature, and metric as well as their classical counterparts. The classical results are obtained under the generator approach and every system that is considered presents a distinctive feature. We see how the classical metric contains all, or almost all the information of the parameter space provided that we establish some identification rules for the action variables. Furthermore, in some cases, the Berry curvature is zero, and as a consequence, information about the parameter space cannot be read from this quantity. Therefore, in these cases the quantum metric tensor and its classical analog come into play and help one see the underlying parameter geometry. The results of this chapter have been published in [67].

5.1 Generalized harmonic oscillator

The generalized harmonic oscillator is the archetypal system where one can exactly calculate the connection, curvature, and metric. It was analyzed by Berry and Hannay in their seminal works [8, 9]. In the first subsection, we present the standard results of the generalized harmonic oscillator. In the second subsection, we add a linear term in the position and show that the system is still exactly solvable regardless of the magnitude of the coupling parameter.

5.1.1 Standard generalized harmonic oscillator

The Hamiltonian of this system is

$$\hat{H} = \frac{1}{2}\left[X\hat{q}^2 + Y(\hat{q}\hat{p} + \hat{p}\hat{q}) + Z\hat{p}^2\right]. \tag{5.1}$$

The parameters are $x = \{x^i\} = (X, Y, Z)$ with $i = 1, 2, 3$, and in order to have periodic motion we restrict ourselves to the subspace defined by $XZ - Y^2 > 0$. The wave function

is found to be

$$\psi_n(q;x) = \left(\frac{\omega}{Z\hbar}\right)^{1/4} \chi_n\left(q\sqrt{\frac{\omega}{Z\hbar}}\right) \exp\left(-\frac{iYq^2}{2Z\hbar}\right), \tag{5.2}$$

where $\omega = \sqrt{XZ - Y^2}$ and

$$\chi_n(\xi) = \left(2^n n!\sqrt{\pi}\right)^{-1/2} e^{-\xi^2/2} H_n(\xi) \tag{5.3}$$

with $H_n(\xi)$ the nth Hermite polynomial. The energy eigenvalues are $E_n = (n + 1/2)\hbar\omega$ $(n = 0, 1, 2, ...)$.

Now, the quantum connection, curvature, and metric can be computed using the following property of the Hermite functions:

$$\int_{-\infty}^{\infty} \mathrm{d}\xi\, \xi^2 \chi_n^2(\xi) = n + \frac{1}{2}. \tag{5.4}$$

The components of the Berry connection (2.5) are

$$A_1^{(n)} = 0, \quad A_2^{(n)} = \left(n + \frac{1}{2}\right)\frac{1}{2\omega}, \quad A_3^{(n)} = -\left(n + \frac{1}{2}\right)\frac{Y}{2Z\omega}. \tag{5.5}$$

From these, we get the components of the Berry curvature (2.9),

$$F_{23}^{(n)} = -\left(n + \frac{1}{2}\right)\frac{X}{4\omega^3}, \quad F_{31}^{(n)} = -\left(n + \frac{1}{2}\right)\frac{Y}{4\omega^3}, \quad F_{12}^{(n)} = -\left(n + \frac{1}{2}\right)\frac{Z}{4\omega^3}. \tag{5.6}$$

And, finally, using (5.2) we get the components of the quantum metric tensor,

$$g_{ij}^{(n)} = \frac{n^2 + n + 1}{32\omega^4} \begin{pmatrix} Z^2 & -2YZ & 2Y^2 - XZ \\ -2YZ & 4XZ & -2XY \\ 2Y^2 - XZ & -2XY & X^2 \end{pmatrix}. \tag{5.7}$$

We see that these results agree with those found for the same system in Chapter 3 using the Wigner function formalism.

On the other hand, for the classical calculation we need first to express the solution of the equations of motion in terms of action-angle variables. We get [69]

$$q(\phi, I; x) = \sqrt{\frac{2IZ}{\omega}}\sin\phi, \quad p(\phi, I; x) = \sqrt{\frac{2IZ}{\omega}}\left(-\frac{Y}{Z}\sin\phi + \frac{\omega}{Z}\cos\phi\right), \tag{5.8}$$

so that in terms of these variables the Hamiltonian has the form $H = I\omega$. In order to find the generators G_i, we can integrate their defining equations (4.15,4.16) which yields

$$\begin{aligned} G_1 &= -\frac{Y}{4\omega^2}q^2 - \frac{Z}{4\omega^2}qp, \\ G_2 &= \frac{X}{2\omega^2}q^2 + \frac{Y}{2\omega^2}qp, \\ G_3 &= -\frac{XY}{4Z\omega^2}q^2 + \frac{XZ - 2Y^2}{4Z\omega^2}qp. \end{aligned} \tag{5.9}$$

Of course, we could have found the generating function $S(q, I, x)$ of the canonical transformation $(q, p) \to (\phi, I)$, and then use $G_i = (p\partial_i q)_{\phi,I} - \partial_i S_{\phi,I}$. The generating function in terms of action-angle variables is [69]

$$S(\phi, I; x) = -\frac{IY}{\omega}\sin^2\phi + I(\phi + \sin\phi\cos\phi). \tag{5.10}$$

Thus, the generators are

$$\begin{aligned} G_1 =& -\frac{IZ}{2\omega^2}\sin\phi\cos\phi, \\ G_2 =& \frac{I\sin\phi}{\omega^2}\left(Y\cos\phi + \omega\sin\phi\right), \\ G_3 =& \frac{I\sin\phi}{2Z\omega^2}\left[(XZ - 2Y^2)\cos\phi - 2Y\omega\sin\phi\right]. \end{aligned} \tag{5.11}$$

Upon substitution of $q(\phi, I; x)$ and $p(\phi, I; x)$ into (5.9) we reproduce the above expressions. The components of the classical Hannay connection $A_i = \langle G_i\rangle$ are

$$A_1 = 0, \quad A_2 = \frac{I}{2\omega}, \quad , A_3 = -\frac{IY}{2Z\omega}. \tag{5.12}$$

Thus, the curvature turns out to be

$$F_{23} = -\frac{IX}{4\omega^3}, \quad F_{31} = -\frac{IY}{4\omega^3}, \quad F_{12} = -\frac{IZ}{4\omega^3}, \tag{5.13}$$

and the metric tensor has the form

$$g_{ij} = \frac{I^2}{32\omega^4}\begin{pmatrix} Z^2 & -2YZ & 2Y^2 - XZ \\ -2YZ & 4XZ & -2XY \\ 2Y^2 - XZ & -2XY & X^2 \end{pmatrix}. \tag{5.14}$$

Some observations are in order:

1. The quantum results might have been obtained using the expressions for the generators in terms of q and p and quantizing with the appropriate symmetrization taking care of the Hermitian nature of the generators $\hat{G}_i$.

2. We could have also found the curvature directly by taking the Poisson brackets of the generators in the form of (5.9) or (5.11) since they are canonical invariants.

3. The action variable is quantized as $I = (n + 1/2)\hbar$. The substitution of this result in the classical Hannay connection and curvature yields

$$A_i^{(n)} = \frac{A_i}{\hbar}, \quad F_{ij}^{(n)} = \frac{F_{ij}}{\hbar}, \tag{5.15}$$

which are precisely the relations found by Berry in [9]. See also (4.76).

4. For the metrics, we have to use the identification $I^2 \to (n^2+n+1)\hbar^2$ to get

$$g_{ij}^{(0)} = \frac{g_{ij}}{\hbar^2}, \tag{5.16}$$

which is the relation (4.74). The quantization rule $I = (n+1/2)\hbar$ does not give the correct result for the metric tensor since $I^2 = (n^2+n+1/4)\hbar^2$. We will see that this mismatch is a common feature to all the examples that we consider, indicating that powers of the action variable should be quantized by adding some correction. It is important to remark that even in the case of the harmonic oscillator $H = (p^2/2m + kq^2/2)$ this effect is observed.

5. The determinants of both the quantum and classical metric are zero, which indicates that the Hamiltonian involves more parameters than the effective ones. This can be seen through a change of parameters $x \to x'$ that has the same form as that of the Cartesian to spherical coordinates. The effect of this transformation in parameter space is to make zero one row and column of the metric tensors. In fact, the metrics have rank two and hence, in order to have non-vanishing determinants, we must leave one of the parameters fixed (but different from zero).

5.1.2 Linear term

Now, we add a linear term in the position with coupling parameter W to the previous Hamiltonian:

$$\hat{H} = \frac{1}{2}\left[X\hat{q}^2 + Y(\hat{q}\hat{p}+\hat{p}\hat{q}) + Z\hat{p}^2\right] + W\hat{q}. \tag{5.17}$$

If we set $W = 0$, we recover the generalized harmonic oscillator. We take as our parameters $x = \{x^i\} = (W, X, Y, Z)$ with $i = 0, 1, 2, 3$. Now, the Schrödinger equation acquires an extra term

$$-\frac{Z\hbar^2}{2}\frac{\mathrm{d}^2\psi_n}{\mathrm{d}q^2} - i\hbar Yq\frac{\mathrm{d}\psi_n}{\mathrm{d}q} + \left(\frac{Xq^2}{2} - i\hbar\frac{Y}{2}\right)\psi_n + Wq\psi_n = E_n\psi_n, \tag{5.18}$$

and this modifies the wave function

$$\psi_n(q;x) = \left(\frac{\omega}{Z\hbar}\right)^{1/4}\chi_n\left[\left(q+\frac{WZ}{\omega^2}\right)\sqrt{\frac{\omega}{Z\hbar}}\right]\exp\left(-\frac{iYq^2}{2Z\hbar}\right). \tag{5.19}$$

Through the use of the properties of Hermite polynomials we calculate the connection, curvature, and metric. The connection is

$$A_0^{(n)} = A_1^{(n)} = 0, \quad A_2^{(n)} = \frac{n+\frac{1}{2}}{2\omega} + \frac{W^2Z}{2\hbar\omega^4}, \quad A_3^{(n)} = -\frac{\left(n+\frac{1}{2}\right)Y}{2Z\omega} - \frac{W^2Y}{2\hbar\omega^4}. \tag{5.20}$$

From here, we get the six independent components of the curvature which are displayed in matrix form as

$$F_{ij}^{(n)} = \frac{n+\frac{1}{2}}{4\omega^3}\begin{pmatrix} 0 & 0 & 0 & 0 \\ 0 & 0 & -Z & Y \\ 0 & Z & 0 & -X \\ 0 & -Y & X & 0 \end{pmatrix} + \frac{1}{\hbar\omega^6}\begin{pmatrix} 0 & 0 & WZ\omega^2 & -WY\omega^2 \\ 0 & 0 & -W^2Z^2 & W^2YZ \\ -WZ\omega^2 & W^2Z^2 & 0 & -W^2Y^2 \\ WY\omega^2 & -W^2YZ & W^2Y^2 & 0 \end{pmatrix}. \tag{5.21}$$

The metric tensor turns out to be

$$\begin{aligned} g_{ij}^{(n)} = &\frac{n^2+n+1}{32\omega^4}\begin{pmatrix} 0 & 0 & 0 & 0 \\ 0 & Z^2 & -2YZ & 2Y^2-XZ \\ 0 & -2YZ & 4XZ & -2XY \\ 0 & 2Y^2-XZ & -2XY & X^2 \end{pmatrix} \\ &+ \frac{n+\frac{1}{2}}{\hbar\omega^7}\begin{pmatrix} Z\omega^4 & -WZ^2\omega^2 & 2WYZ\omega^2 & -WY^2\omega^2 \\ -WZ^2\omega^2 & W^2Z^3 & -2W^2YZ^2 & W^2Y^2Z \\ 2WYZ\omega^2 & -2W^2YZ^2 & W^2Z(3Y^2+XZ) & -W^2Y(Y^2+XZ) \\ -WY^2\omega^2 & W^2Y^2Z & -W^2Y(Y^2+XZ) & W^2XY^2 \end{pmatrix}. \end{aligned} \tag{5.22}$$

We see that taking $W = 0$ in the above expressions and eliminating the corresponding row and column of the tensors, the results match the standard generalized harmonic oscillator.

For the classical analogs, we use the position and momentum in terms of action-angle variables which can be found almost in the same way as in the previous example.

$$q(\phi, I; x) = \sqrt{\frac{2IZ}{\omega}}\sin\phi - \frac{WZ}{\omega^2}, \quad p(\phi, I; x) = \sqrt{\frac{2IZ}{\omega}}\left(-\frac{Y}{Z}\sin\phi + \frac{\omega}{Z}\cos\phi\right) + \frac{WY}{\omega^2}, \tag{5.23}$$

so that the Hamiltonian now reads $H = I\omega - W^2Z/2\omega^2$, with $\omega = \sqrt{XZ - Y^2}$. The generating function S of the transformation to action-angle variables is

$$S(\phi, I; x) = -\frac{Y}{2Z}\left(\sqrt{\frac{2IZ}{\omega}}\sin\phi - \frac{WZ}{\omega^2}\right)^2 + I(\phi + \sin\phi\cos\phi), \tag{5.24}$$

and the generators G_i written in compact form are

$$G_i(\phi, I; x) = f_i(x)qp + g_i(x)q^2 + h_i(x)p + \frac{Y}{Z}h_i(x)q, \tag{5.25}$$

where $q = q(\phi, I; x)$ and $p = p(\phi, I; x)$ are given by (5.23) and

$$\begin{aligned} f_i(x) =& \frac{\omega}{2Z}\frac{\partial}{\partial x^i}\left(\frac{Z}{\omega}\right), \\ g_i(x) =& \frac{Y}{Z}f_i(x) + \frac{1}{2}\frac{\partial}{\partial x^i}\left(\frac{Y}{Z}\right), \\ h_i(x) =& \frac{W}{2\omega}\frac{\partial}{\partial x^i}\left(\frac{Z}{\omega}\right) - \frac{\partial}{\partial x^i}\left(\frac{WZ}{\omega^2}\right). \end{aligned} \tag{5.26}$$

It can readily be verified that if the parameter W is fixed to zero, we recover the generators (5.9). With these expressions at hand, we can get the connection,

$$A_0 = A_1 = 0, \quad A_2 = \frac{I}{2\omega} + \frac{W^2 Z}{2\omega^4}, \quad A_3 = -\frac{IY}{2Z\omega} - \frac{W^2 Y}{2\omega^4}, \tag{5.27}$$

the curvature,

$$F_{ij} = \frac{I}{4\omega^3}\begin{pmatrix} 0 & 0 & 0 & 0 \\ 0 & 0 & -Z & Y \\ 0 & Z & 0 & -X \\ 0 & -Y & X & 0 \end{pmatrix} + \frac{1}{\omega^6}\begin{pmatrix} 0 & 0 & WZ\omega^2 & -WY\omega^2 \\ 0 & 0 & -W^2Z^2 & W^2YZ \\ -WZ\omega^2 & W^2Z^2 & 0 & -W^2Y^2 \\ WY\omega^2 & -W^2YZ & W^2Y^2 & 0 \end{pmatrix}, \tag{5.28}$$

and the metric tensor,

$$\begin{aligned} g_{ij} = {} & \frac{I^2}{32\omega^4}\begin{pmatrix} 0 & 0 & 0 & 0 \\ 0 & Z^2 & -2YZ & 2Y^2 - XZ \\ 0 & -2YZ & 4XZ & -2XY \\ 0 & 2Y^2 - XZ & -2XY & X^2 \end{pmatrix} \\ & + \frac{I}{\omega^7}\begin{pmatrix} Z\omega^4 & -WZ^2\omega^2 & 2WYZ\omega^2 & -WY^2\omega^2 \\ -WZ^2\omega^2 & W^2Z^3 & -2W^2YZ^2 & W^2Y^2Z \\ 2WYZ\omega^2 & -2W^2YZ^2 & W^2Z(3Y^2 + XZ) & -W^2Y(Y^2 + XZ) \\ -WY^2\omega^2 & W^2Y^2Z & -W^2Y(Y^2 + XZ) & W^2XY^2 \end{pmatrix}. \end{aligned} \tag{5.29}$$

Notice again the different quantization of powers of the action variable. In this case, the action variable in the metric tensor appears both linearly and squared, but only the squared action is quantized in a distinct manner. Finally, it is easy to find that the determinants of the metrics (5.22) and (5.29) are zero and their rank is three.

5.2 Quartic anharmonic oscillator

Here, we consider the Hamiltonian of the quartic anharmonic oscillator

$$\hat{H} = \frac{\hat{p}^2}{2m} + \frac{k}{2}\hat{q}^2 + \frac{\lambda}{4!}\hat{q}^4 \tag{5.30}$$

with parameters $x = \{x^i\} = (m, k, \lambda)$, $i = 1, 2, 3$. We focus on a perturbative treatment for $0 < \lambda \ll 1$, since the analytical solutions for the eigenvalue problem cannot be obtained. Also, we restrict ourselves to considering only the ground state wave function and its energy in powers of λ up to third order.

First of all, notice that the definition of the Berry connection (2.12) and curvature (2.13) requires that we take the imaginary part of an inner product [4]. However, since the wave function that we consider is real, we have as a result a zero connection, and thus, a zero curvature. This will happen too in the remaining examples.

The ground state energy and wave function of Hamiltonian (5.30) can be obtained using the standard perturbation theory [77, 78]. Nevertheless, through the more efficient non-linearization method [79] we can easily find corrections to arbitrarily large powers of λ. The dimensionless form of the eigenvalue problem considered in [79] is

$$\left(-\frac{\mathrm{d}^2}{\mathrm{d}X^2}+X^2+\gamma X^4\right)\psi(X)=\epsilon\psi(X). \tag{5.31}$$

Of course, we can return to our eigenvalue problem with all the dimensions through the following change of variables

$$\gamma=\frac{\hbar\lambda}{12m^2\omega_0^3},\quad X=\sqrt{\frac{m\omega_0}{\hbar}}q,\quad \epsilon=\frac{2E}{\hbar\omega_0}, \tag{5.32}$$

where $\omega_0=\sqrt{k/m}$. The non-normalized ground state wave function for the dimensionless Hamiltonian is, to third order in γ,

$$\begin{aligned}\psi(X)=e^{-\frac{X^2}{2}}\Bigg[1-\frac{1}{8}\gamma X^2\left(X^2+3\right)+\frac{1}{384}\gamma^2X^2\left(3X^6+26X^4+93X^2+252\right)\\ -\frac{1}{3072}\gamma^3X^2\left(X^{10}+17X^8+141X^6+813X^4+2916X^2+7992\right)\Bigg]+\mathcal{O}(\gamma^4),\end{aligned} \tag{5.33}$$

and the corresponding energy is

$$\epsilon=1+\frac{3}{4}\gamma-\frac{21}{16}\gamma^2+\frac{333}{64}\gamma^3+\mathcal{O}(\gamma^4). \tag{5.34}$$

For more details about the features of the asymptotic series, we refer the reader to the standard references of Bender and Wu [80, 81]. After returning to our original variables and normalizing, we find that

$$\begin{aligned}\psi(q;x)=e^{-\frac{m\omega_0}{2\hbar}q^2}\Bigg[\sqrt[4]{\frac{m\omega_0}{\pi\hbar}}-\lambda\frac{P_1(q;x)}{384\sqrt[4]{\pi m^7\omega_0^{11}\hbar^5}}+\lambda^2\frac{P_2(q;x)}{884736\sqrt[4]{\pi m^{15}\omega_0^{23}\hbar^9}}\\ -\lambda^3\frac{P_3(q;x)}{339738624\sqrt[4]{\pi m^{23}\omega_0^{35}\hbar^{13}}}\Bigg]+\mathcal{O}(\lambda^4),\end{aligned} \tag{5.35}$$

$$E_0=\frac{\hbar\omega_0}{2}+\lambda\frac{\hbar^2}{32m^2\omega_0^2}-\lambda^2\frac{7\hbar^3}{1536m^4\omega_0^5}+\lambda^3\frac{37\hbar^4}{24576m^6\omega_0^8}+\mathcal{O}(\lambda^4). \tag{5.36}$$

where

$$\begin{aligned}P_1(q;x)=&4m^2\omega_0^2q^4+12\hbar m\omega_0q^2-9\hbar^2,\\ P_2(q;x)=&48m^4\omega_0^4q^8+416\hbar m^3\omega_0^3q^6+1272\hbar^2m^2\omega_0^2q^4+3384\hbar^3m\omega_0q^2-4677\hbar^4,\\ P_3(q;x)=&\,64m^6\omega_0^6q^{12}+1088\hbar m^5\omega_0^5q^{10}+8592\hbar^2m^4\omega_0^4q^8\\ &+48288\hbar^3m^3\omega_0^3q^6+154524\hbar^4m^2\omega_0^2q^4+419076\hbar^5m\omega_0q^2-729153\hbar^6.\end{aligned} \tag{5.37}$$

To compute the quantum metric tensor, it is sufficient to consider the expression

$$g_{ij}^{(0)} = \langle \partial_i \psi | \partial_j \psi \rangle - \langle \partial_i \psi | \psi \rangle \langle \psi | \partial_j \psi \rangle \tag{5.38}$$

due to the reality of the wave function. We find the components

$$\begin{aligned}
g_{11}^{(0)} =& \frac{1}{32m^2} - \lambda \frac{3\hbar}{512\sqrt{m^5k^3}} + \lambda^2 \frac{59\hbar^2}{16384m^3k^3} + \mathcal{O}(\lambda^3), \\
g_{12}^{(0)} =& \frac{1}{32mk} - \lambda \frac{7\hbar}{512\sqrt{m^3k^5}} + \lambda^2 \frac{143\hbar^2}{16384m^2k^4} + \mathcal{O}(\lambda^3), \\
g_{13}^{(0)} =& \frac{\hbar}{128\sqrt{m^3k^3}} - \lambda \frac{21\hbar^2}{4096m^2k^3} + \lambda^2 \frac{2353\hbar^3}{589824\sqrt{m^5k^9}} + \mathcal{O}(\lambda^3), \\
g_{22}^{(0)} =& \frac{1}{32k^2} - \lambda \frac{11\hbar}{512\sqrt{mk^7}} + \lambda^2 \frac{785\hbar^2}{49152mk^5} + \mathcal{O}(\lambda^3), \\
g_{23}^{(0)} =& \frac{\hbar}{128\sqrt{mk^5}} - \lambda \frac{89\hbar^2}{12288mk^4} + \lambda^2 \frac{3841\hbar^3}{589824\sqrt{m^3k^{11}}} + \mathcal{O}(\lambda^3), \\
g_{33}^{(0)} =& \frac{13\hbar^2}{6144mk^3} - \lambda \frac{31\hbar^3}{12288\sqrt{m^3k^9}} + \lambda^2 \frac{57227\hbar^4}{21233664m^2k^6} + \mathcal{O}(\lambda^3).
\end{aligned} \tag{5.39}$$

It is important to remark that the metric tensor is correct up to one order less than the wave function since there are components which require the calculation of a derivative with respect to λ. Another observation can be made regarding the determinant of the metric. We can easily find that

$$\det g_{ij}^{(0)} = \mathcal{O}(\lambda^3). \tag{5.40}$$

However, if we fix the mass and only take as our parameters $x = \{x^i\} = (k, \lambda)$ with $i = 1, 2$, the determinant of this reduced 2×2 metric is

$$\det g_{ij}^{(0)\text{red}} = \frac{\hbar^2}{196608mk^5} - \lambda \frac{35\hbar^3}{3145728\sqrt{m^3k^{13}}} + \lambda^2 \frac{48935\hbar^4}{2717908992m^2k^8} + \mathcal{O}(\lambda^3). \tag{5.41}$$

Let us now turn to the classical calculation. The tool that we use is canonical perturbation theory [76, 82]. The central idea of this method is that we can divide our Hamiltonian in two parts:

$$H = H_0 + \lambda H_1, \tag{5.42}$$

where $0 < \lambda \ll 1$. It is assumed that we can find the position and momentum for the system with unperturbed Hamiltonian H_0 in terms of action-angle variables (ϕ_0, I_0). In this case, we take

$$H_0 = \frac{p^2}{2m} + \frac{k}{2}q^2, \tag{5.43}$$

and

$$H_1 = \frac{q^4}{4!}. \tag{5.44}$$

The solution (q, p) in terms of old action-angle variables (ϕ_0, I_0) is well-known:

$$q(\phi_0, I_0; x) = \sqrt{\frac{2I_0}{m\omega_0}} \sin\phi_0, \quad p(\phi_0, I_0; x) = \sqrt{2m\omega_0 I_0} \cos\phi_0, \tag{5.45}$$

where $\omega_0 = \sqrt{k/m}$ is the unperturbed frequency. The problem is to find the canonical transformation from old action-angle variables (ϕ_0, I_0) to the new set (ϕ, I) such that now the perturbed Hamiltonian H can be written only in terms of I, i.e.,

$$H(q(\phi, I; x), p(\phi, I; x); x) = E(I; x). \tag{5.46}$$

This canonical transformation is generated by the type 2 function $W(\phi_0, I; x)$,

$$W(\phi_0, I; x) = \phi_0 I + \lambda W_1(\phi_0, I; x) + \lambda^2 W_2(\phi_0, I; x) + \lambda^3 W_3(\phi_0, I; x) + \mathcal{O}(\lambda^4), \tag{5.47}$$

and the Hamiltonian $E(I; x)$ will be expressed as

$$E(I; x) = E_0(I; x) + \lambda E_1(I; x) + \lambda^2 E_2(I; x) + \lambda^3 E_3(I; x) + \mathcal{O}(\lambda^4). \tag{5.48}$$

From the equations of the canonical transformation, $\phi = \partial W/\partial I$ and $I_0 = \partial W/\partial\phi_0$, we can find that

$$\phi(\phi_0, I; x) = \phi_0 + \lambda \frac{\partial W_1(\phi_0, I; x)}{\partial I} + \lambda^2 \frac{\partial W_2(\phi_0, I; x)}{\partial I} + \lambda^3 \frac{\partial W_3(\phi_0, I; x)}{\partial I} + \mathcal{O}(\lambda^4) \tag{5.49}$$

and

$$I_0(\phi_0, I; x) = I + \lambda \frac{\partial W_1(\phi_0, I; x)}{\partial \phi_0} + \lambda^2 \frac{\partial W_2(\phi_0, I; x)}{\partial \phi_0} + \lambda^3 \frac{\partial W_3(\phi_0, I; x)}{\partial \phi_0} + \mathcal{O}(\lambda^4). \tag{5.50}$$

The results of canonical perturbation theory are

$$E_\mu(I; x) = \langle \Phi_\mu(\phi_0, I; x) \rangle_0, \tag{5.51}$$

$$\omega_0(I; x) \frac{\partial W_\mu(\phi_0, I; x)}{\partial \phi_0} = \langle \Phi_\mu(\phi_0, I; x) \rangle_0 - \Phi_\mu(\phi_0, I; x), \quad \mu = 1, 2, \ldots, \tag{5.52}$$

where $\omega_0(I; x) = (\partial H_0/\partial I_0)_{I_0 = I}$ and the symbol $\langle \cdot \rangle_0$ denotes the average with respect to the angle variable ϕ_0. In our case, $\omega_0(I; x) = \omega_0 = \sqrt{k/m}$. The function Φ_0 is just the unperturbed Hamiltonian H_0 evaluated at the new action variable I, which is $\Phi_0(I; x) = I\omega_0$. The function Φ_1 is the perturbation H_1 written in terms of the old angle ϕ_0 and the new action I, i.e.,

$$\Phi_1(\phi_0, I; x) = \frac{q^4(\phi_0, I; x)}{4!} = \frac{I^2 \sin^4\phi_0}{6m^2\omega_0^2}. \tag{5.53}$$

The functions Φ_2 and Φ_3 can be obtained by the Taylor series expansion of the Hamiltonian, and they are

$$\Phi_2(\phi_0, I; x) = \frac{\partial W_1}{\partial \phi_0} \frac{\partial H_1}{\partial I}, \tag{5.54}$$

$$\Phi_3(\phi_0, I; x) = \frac{1}{2}\left(\frac{\partial W_1}{\partial \phi_0}\right)^2 \frac{\partial^2 H_1}{\partial I^2} + \frac{\partial W_2}{\partial \phi_0}\frac{\partial H_1}{\partial I}. \tag{5.55}$$

Also, since we have only one degree of freedom, the W_μ can be easily calculated by integrating (5.52). It turns out that

$$\Phi_2(\phi_0, I; x) = -\frac{I^3 \sin^4\phi_0 \left(8\sin^4\phi_0 - 3\right)}{144 m^4 \omega_0^5},$$

$$\Phi_3(\phi_0, I; x) = \frac{I^4 \sin^4\phi_0 \left(320\sin^8\phi_0 - 144\sin^4\phi_0 - 25\right)}{13824 m^6 \omega_0^8}, \tag{5.56}$$

and

$$W_1(\phi_0, I; x) = \frac{I^2(8\sin 2\phi_0 - \sin 4\phi_0)}{192 m^2 \omega_0^3},$$

$$W_2(\phi_0, I; x) = \frac{I^3(-384\sin 2\phi_0 + 132\sin 4\phi_0 - 32\sin 6\phi_0 + 3\sin 8\phi_0)}{55296 m^4 \omega_0^6},$$

$$W_3(\phi_0, I; x) = \frac{I^4(9264\sin 2\phi_0 - 4101\sin 4\phi_0 + 1624\sin 6\phi_0 - 441\sin 8\phi_0 + 72\sin 10\phi_0 - 5\sin 12\phi_0)}{5308416 m^6 \omega_0^9}. \tag{5.57}$$

With this at hand, we are able to calculate the energy series:

$$E = I\omega_0 + \lambda\frac{I^2}{16m^2\omega_0^2} - \lambda^2\frac{17I^3}{2304 m^4\omega_0^5} + \lambda^3\frac{125 I^4}{73728 m^6\omega_0^8} + \mathcal{O}(\lambda^4). \tag{5.58}$$

Notice that all the expressions we have found so far are written in terms of the old angle variable ϕ_0 and the new action variable I. In order to compute the metric tensor, we need to find the generators $G_i = p(\partial_i q)_{\phi,I} - (\partial_i S)_{\phi,I}$, where the derivatives are taken at fixed new action-angle variables (ϕ, I). This requires the manipulation of the derivatives to write them in the most convenient form for computation. Another issue to address is that we must find the generating function S of the transformation from variables (q, p) to (ϕ, I) and it is not evident how to do it, since we only have the function W that performs the transformation $(\phi_0, I_0) \to (\phi, I)$.

The first issue is solved by noting that given a function $f(\phi_0, I; x)$, we can differentiate the expression $f(\phi_0, I; x) = f(\phi(\phi_0, I; x), I; x)$ with respect to the parameters x to find

$$\left(\frac{\partial f}{\partial x^i}\right)_{\phi_0, I} = \left(\frac{\partial f}{\partial \phi}\right)_{I,x}\left(\frac{\partial \phi}{\partial x^i}\right)_{\phi_0, I} + \left(\frac{\partial f}{\partial x^i}\right)_{\phi, I}. \tag{5.59}$$

Now, we still have to apply a cyclic property to write the derivative of f with respect to ϕ at our convenience. This can be done through the identity

$$\left(\frac{\partial f}{\partial \phi}\right)_{I,x} = \frac{(\partial f/\partial\phi_0)_{I,x}}{(\partial\phi/\partial\phi_0)_{I,x}}. \tag{5.60}$$

Hence, we are finally able to express everything in terms of derivatives that we can calculate:

$$\left(\frac{\partial f}{\partial x^i}\right)_{\phi,I} = \left(\frac{\partial f}{\partial x^i}\right)_{\phi_0,I} - \frac{(\partial f/\partial\phi_0)_{I,x}}{(\partial\phi/\partial\phi_0)_{I,x}}\left(\frac{\partial\phi}{\partial x^i}\right)_{\phi_0,I}. \tag{5.61}$$

The second issue can be solved by noting that we already have the position and momentum in terms of the old action-angle variables (5.45). This leads us into thinking that we may first attempt to perform a transformation $(q,p)\to(\phi_0,I_0)$ through a generating function $S_0(q,I_0;x)$, and then perform the transformation $(\phi_0,I_0)\to(\phi,I)$ through our $W(\phi_0,I;x)$. The resulting generating function S for the composition of two canonical transformations is [71, 72]

$$S(q,I;x) = S_0(q,I_0;x) + W(\phi_0,I;x) - \phi_0 I_0, \tag{5.62}$$

and the function S_0 (which we write in terms of old action-angle variables for convenience) is

$$S_0(\phi_0,I_0;x) = I_0(\phi_0 + \sin\phi_0\cos\phi_0). \tag{5.63}$$

With these results at hand, we can now compute the classical metric $g_{ij} = \langle G_i G_j\rangle - \langle G_i\rangle\langle G_j\rangle$ through the use of (5.61) making $f = q$ or $f = S$. The generators G_i are given in Appendix A. Notice that since we have everything written in terms of the old angle ϕ_0, we need to calculate the averages that appear in the metric by making the change of variable

$$\phi = \phi(\phi_0,I;x), \quad \mathrm{d}\phi = \left(\frac{\partial\phi}{\partial\phi_0}\right)_{I,x}\mathrm{d}\phi_0. \tag{5.64}$$

After taking all this into account, we find the components

$$\begin{aligned}
g_{11} =& \frac{I^2}{32m^2} - \lambda\frac{I^3}{256\sqrt{m^5k^3}} + \lambda^2\frac{47I^4}{32768m^3k^3} + \mathcal{O}(\lambda^3),\\
g_{12} =& \frac{I^2}{32mk} - \lambda\frac{7I^3}{768\sqrt{m^3k^5}} + \lambda^2\frac{347I^4}{98304m^2k^4} + \mathcal{O}(\lambda^3),\\
g_{13} =& \frac{I^3}{192\sqrt{m^3k^3}} - \lambda\frac{103I^4}{49152m^2k^3} + \lambda^2\frac{15I^5}{16384\sqrt{m^5k^9}} + \mathcal{O}(\lambda^3),\\
g_{22} =& \frac{I^2}{32k^2} - \lambda\frac{11I^3}{768\sqrt{mk^7}} + \lambda^2\frac{1919I^4}{294912mk^5} + \mathcal{O}(\lambda^3),\\
g_{23} =& \frac{I^3}{192\sqrt{mk^5}} - \lambda\frac{439I^4}{147456mk^4} + \lambda^2\frac{7I^5}{4608\sqrt{m^3k^{11}}} + \mathcal{O}(\lambda^3),\\
g_{33} =& \frac{65I^4}{73728mk^3} - \lambda\frac{89I^5}{147456\sqrt{m^3k^9}} + \lambda^2\frac{130621I^6}{382205952m^2k^6} + \mathcal{O}(\lambda^3).
\end{aligned} \tag{5.65}$$

We can easily see that in order to match the quantum and classical metrics, we should set for the ground state: $I^2/\hbar^2 = 1$, $I^3/\hbar^3 = 3/2$. However, for powers greater or equal

to 4, we cannot find the appropriate quantization. For instance, equating each of the terms of both metrics that contain I^4, we find six different results:

$$\frac{I^4}{\hbar^4} \approx 2.4,\ 2.4328,\ 2.4466,\ 2.4544,\ 2.4726,\ 2.5106, \tag{5.66}$$

whereas for I^5, we have

$$\frac{I^5}{\hbar^5} \approx 4.1797,\ 4.2868,\ 4.3574. \tag{5.67}$$

Moreover, this quantization does not allow us to recover the energy (5.36). Indeed, it can be seen that the energy series follows the quantization

$$\frac{I}{\hbar} = \left(n+\frac{1}{2}\right), \quad \frac{I^2}{\hbar^2} = \left(n+\frac{1}{2}\right)^2 + \frac{1}{4}, \quad \frac{I^3}{\hbar^3} = \left(n+\frac{1}{2}\right)^3 + \frac{67}{68}\left(n+\frac{1}{2}\right), \tag{5.68}$$

which for the ground state reduces to

$$\frac{I}{\hbar} = \frac{1}{2}, \quad \frac{I^2}{\hbar^2} = \frac{1}{2}, \quad \frac{I^3}{\hbar^3} = \frac{21}{34}. \tag{5.69}$$

This result was determined by proposing a polynomial in n of the same degree as the power of the action variable and using the expression for the energies of the first four excited states given in [83]. It is important to comment that we have found the non-trivial result that through classical calculations we have reproduced the structure of the quantum metric. The mismatch is present since the quantum metric includes the quantum perturbative effects which the classical perturbative method fails to reproduce, hence the need of the empirical rules of quantization of the action variable. Finally, we should remark that the method based on canonical perturbation theory applied to the generalized harmonic oscillator with a linear term provides the same results.

5.3 Two-dimensional isotropic harmonic oscillator in polar coordinates

This is a very illustrative example since the isotropic harmonic oscillator in two dimensions can be effectively reduced to a one degree of freedom by using the conservation of angular momentum. For this system, the Schrödinger equation reads

$$-\frac{\hbar^2}{2m}\left(\frac{\partial^2}{\partial r^2} + \frac{1}{r}\frac{\partial}{\partial r} + \frac{1}{r^2}\frac{\partial^2}{\partial \theta^2}\right)\Psi + \frac{k}{2}r^2\Psi = E\Psi. \tag{5.70}$$

We take as our parameters the mass and the spring constant $x = \{x^i\} = (m, k)$ with $i = 1, 2$. The wave function can be separated in an angular part $\Theta(\theta)$ and a radial

part $\psi(r;x)$, such that $\Psi(r,\theta;x)=\psi(r;x)\Theta(\theta)$. In particular, for the ground state with energy $E=\hbar\omega$, the radial function is

$$\psi(r;x)=\sqrt{\frac{2\sqrt{mk}}{\hbar}}e^{-\frac{\sqrt{mk}}{2\hbar}r^2}, \tag{5.71}$$

whereas the angular part is only $\Theta(\theta)=1/\sqrt{2\pi}$. By convention, the normalization is taken separately so that the condition

$$\langle\Psi|\Psi\rangle=\int_0^{2\pi}\mathrm{d}\theta\,|\Theta(\theta)|^2\int_0^{\infty}\mathrm{d}r\,r|\psi(r;x)|^2=1 \tag{5.72}$$

means that every integral should be equal to one. Thus, in the simple case of the ground state the effective wave function is $\psi(r;x)$ and the inner product of two functions is given by

$$\langle f|g\rangle=\int_0^{\infty}\mathrm{d}r\,rf^*(r;x)g(r;x). \tag{5.73}$$

Since the wave function (5.71) is not complex, we automatically know that the connection, and consequently, the curvature, are zero. On the other hand, the metric tensor takes the form

$$g_{ij}^{(0)}=\frac{1}{16}\begin{pmatrix}\frac{1}{m^2} & \frac{1}{mk}\\ \frac{1}{mk} & \frac{1}{k^2}\end{pmatrix}. \tag{5.74}$$

The classical calculation is more involved, since it requires the knowledge of the equation of the orbit. We will follow an explicit approach which will be useful to summarize some steps in the next example. The first step is to obtain the action-angle variables for the system. The Hamiltonian is

$$H=\frac{p_r^2}{2m}+\frac{p_\theta^2}{2mr^2}+\frac{k}{2}r^2. \tag{5.75}$$

Using conservation of energy and angular momentum, we can see that

$$p_r=\sqrt{2mE-m^2\omega^2r^2-L^2/r^2},\quad p_\theta=L=constant, \tag{5.76}$$

where $\omega=\sqrt{k/m}$. From here, we get the angular action variable,

$$I_\theta=\frac{1}{2\pi}\oint\mathrm{d}\theta\,p_\theta=|L|. \tag{5.77}$$

On the other hand, the radial action variable is defined as

$$I_r=\frac{1}{2\pi}\oint\mathrm{d}r\,p_r=\frac{1}{2\pi}\oint\mathrm{d}r\,\sqrt{2mE-m^2\omega^2r^2-L^2/r^2}. \tag{5.78}$$

A standard procedure to solve this integral (which will be used in the Coulomb problem too) is to rewrite it as the sum of three integrals, M_1, M_2 and M_3 [69]

$$I_r = \frac{M_1 + M_2 + M_3}{2\pi}, \tag{5.79}$$

where

$$M_1 = \oint \mathrm{d}r\, \frac{mE - m^2\omega^2 r^2}{\sqrt{A}}, \quad M_2 = \oint \mathrm{d}r\, \frac{mE}{\sqrt{A}}, \quad M_3 = -\oint \mathrm{d}r\, \frac{L^2}{r^2\sqrt{A}}, \tag{5.80}$$

with $A = 2mE - m^2\omega^2 r^2 - L^2/r^2$. The first term is the integral of a total differential, so

$$M_1 = \oint \mathrm{d}\left(\frac{r\sqrt{2mE - m^2\omega^2 r^2 - L^2/r^2}}{2}\right) = 0. \tag{5.81}$$

The second integral, M_2, appears precisely when, through conservation of energy, one tries to solve for the motion $r = r(t)$, i.e.,

$$\frac{m}{2}\left(\frac{\mathrm{d}r}{\mathrm{d}t}\right)^2 + \frac{m\omega^2}{2}r^2 + \frac{L^2}{2mr^2} = E. \tag{5.82}$$

This leads to

$$\sqrt{\frac{2}{m}}t = \int \frac{\mathrm{d}r}{\sqrt{E - \frac{m\omega^2}{2}r^2 - \frac{L^2}{2mr^2}}} \tag{5.83}$$

We use the change of variable $s = r^2$ to turn the integral into

$$\sqrt{\frac{m}{2}}\frac{E}{2}\int \frac{\mathrm{d}s}{\sqrt{Es - \frac{m\omega^2}{2}s^2 - \frac{L^2}{2m}}}. \tag{5.84}$$

Since this leaves a second degree polynomial inside the radical, we can make use of the trigonometric substitution

$$s = \frac{E}{m\omega^2}\left(1 - \sqrt{1 - \frac{\omega^2 L^2}{E^2}}\cos\alpha\right) \tag{5.85}$$

to simplify everything. Evaluating the indefinite integral in a cycle, this becomes

$$M_2 = \frac{E}{2\omega}\oint \mathrm{d}\alpha = \frac{E}{2\omega}(2\pi) = \frac{E\pi}{\omega}, \tag{5.86}$$

since (5.85) indicates that in the phase space corresponding to r, the angle α moves 2π until r returns to its initial value. Now, notice that M_3 is the quadrature corresponding to the orbit equation

$$\frac{L^2}{2mr^4}\left(\frac{\mathrm{d}r}{\mathrm{d}\theta}\right)^2 + \frac{m\omega^2}{2}r^2 + \frac{L^2}{2mr^2} = E. \tag{5.87}$$

To solve this integral, we make the usual change of variable $u = 1/r$ and then we set

$$u^2 = \frac{mE}{L^2}\left(1 + \sqrt{1 - \frac{\omega^2 L^2}{E^2}}\cos\beta\right). \tag{5.88}$$

When we evaluate it in a cycle, we find

$$M_3 = -\frac{1}{2}\oint \mathrm{d}\beta\, L = -\frac{|L|}{2}(2\pi) = -|L|\pi, \tag{5.89}$$

because (5.88) returns to its initial value after β has advanced 2π. So, we conclude that

$$I_r = \frac{1}{2\pi}\left(\frac{E\pi}{\omega} - |L|\pi\right) = \frac{1}{2}\left(\frac{E}{\omega} - |L|\right). \tag{5.90}$$

By inverting this relation, we get the energy expressed in terms of the action variables as

$$E = \omega(2I_r + I_\theta). \tag{5.91}$$

The frequencies associated with the radial and angular motion are, respectively,

$$\omega_r = \frac{\partial E}{\partial I_r} = 2\omega, \quad \omega_\theta = \frac{\partial E}{\partial I_\theta} = \omega. \tag{5.92}$$

We would like to express the energy in terms of a single action variable which is the one that will correspond to the principal quantum number [76]. In order to do this, we consider the canonical transformation $(\phi_r, \phi_\theta, I_r, I_\theta) \to (\phi_1, \phi_2, I_1, I_2)$ generated by the type 2 function

$$F_2(\phi_r, \phi_\theta, I_1, I_2) = \left(\phi_\theta - \frac{\phi_r}{2}\right) I_1 + \phi_r I_2. \tag{5.93}$$

The equations of the transformation imply that

$$E = 2\omega I_2, \quad \phi_2 = \phi_r, \tag{5.94}$$

with $\omega_1 = 0$ and $\omega_2 = 2\omega$. Therefore, we have reduced our system to one effective degree of freedom. In what follows, we refer to I_2 only as I, and to ϕ_2 as ϕ.

Now we need to construct the generating function following a procedure that parallels the previous one. After the elimination of the angular degree of freedom through the conservation of angular momentum, we find that the function S which is the solution to the Hamilton-Jacobi equation has the form

$$S(r, E; x) = \int \mathrm{d}r\, \sqrt{2mE - m^2\omega^2 r^2 - L^2/r^2}. \tag{5.95}$$

We can read the result from the previous paragraphs:

$$S(r, E; x) = \frac{r\sqrt{2mE - m^2\omega^2 r^2 - L^2/r^2}}{2} + \frac{E}{2\omega}\alpha(r, E; x) - \frac{|L|}{2}\beta(r, E; x), \tag{5.96}$$

where α and θ should be substituted from (5.85) and (5.88) in terms of r, E and the parameters x. If we compare (5.85) with (5.83), we get that

$$\alpha = 2\omega t, \tag{5.97}$$

and thus we find that the solution for the motion $r(t)$ is given by

$$r^2(t) = \frac{E}{m\omega^2}\left(1 - \sqrt{1 - \frac{\omega^2 L^2}{E^2}}\cos 2\omega t\right). \tag{5.98}$$

From here, it is seen that $\alpha = 2\omega t$ is the angle variable $\phi = \phi_r$ corresponding to the radial degree of freedom. Furthermore, from (5.87) we find that $\beta = 2\theta$, so the orbit $r(\theta)$ is given by

$$\frac{1}{r^2(\theta)} = \frac{mE}{L^2}\left(1 + \sqrt{1 - \frac{\omega^2 L^2}{E^2}}\cos 2\theta\right), \tag{5.99}$$

which represents an ellipse with its geometrical center located at the origin. In order to proceed with the calculation of the classical analog of the metric tensor, we need to express the position r, the momentum p_r, and the generating function S in terms of action-angle variables. The rewriting of (5.98) using (5.94) results in

$$r(\phi, I; x) = \sqrt{\frac{2I}{\sqrt{mk}}}\left(1 - \sqrt{1 - L^2/4I^2}\cos\phi\right)^{1/2}, \tag{5.100}$$

and, since $p_r = m\dot{r}$,

$$p_r(\phi, I; x) = \sqrt{2I\sqrt{mk}}\frac{\sqrt{1 - L^2/4I^2}\sin\phi}{\left(1 - \sqrt{1 - L^2/4I^2}\cos\phi\right)^{1/2}}. \tag{5.101}$$

Moreover, the generating function becomes

$$S(\phi, I; x) = I\left(1 - L^2/4I^2\right)\sin\phi + I\phi - |L|\theta(\phi, I; x). \tag{5.102}$$

Now, we must relate the "physical angle" θ with the angle variable ϕ. A straightforward comparison of the solution $r(\phi, I; x)$ and the orbit $r(\theta, I; x)$ shows that

$$\frac{1}{1 - \sqrt{1 - L^2/4I^2}\cos\phi} = \frac{4I^2}{L^2}(1 + \sqrt{1 - L^2/4I^2}\cos 2\theta). \tag{5.103}$$

Hence, we see that the "physical angle" θ does not depend on the parameters x, and this leads us to conclude that the generating function does not depend on x either, i.e.,

$$S(\phi, I) = I\left(1 - L^2/4I^2\right)\sin\phi + I\phi - |L|\theta(\phi, I). \tag{5.104}$$

Therefore, the generators G_i are reduced to $G_i = p_r \partial_i r$. Remembering that $x^1 = m$ and $x^2 = k$, we find that

$$G_1 = -\frac{\sqrt{1 - L^2/4I^2}\, I \sin\phi}{2m} = -\frac{r p_r}{4m}, \tag{5.105}$$

$$G_2 = -\frac{\sqrt{1 - L^2/4I^2}\, I \sin\phi}{2k} = -\frac{r p_r}{4k}. \tag{5.106}$$

Finally, this allows us to compute the classical metric tensor which has the form

$$g_{ij} = \frac{4I^2 - L^2}{32} \begin{pmatrix} \frac{1}{m^2} & \frac{1}{mk} \\ \frac{1}{mk} & \frac{1}{k^2} \end{pmatrix}. \tag{5.107}$$

According to the EBK quantization rule [74], we should have $L = 0$ and $I = \hbar$ for the ground state, hence

$$g_{ij}(L = 0, I = \hbar) = \frac{\hbar^2}{8} \begin{pmatrix} \frac{1}{m^2} & \frac{1}{mk} \\ \frac{1}{mk} & \frac{1}{k^2} \end{pmatrix}, \tag{5.108}$$

and we see again that it differs from (5.74) by a factor of 2.

5.4 Two-dimensional attractive Coulomb problem

Now we address the two-dimensional attractive Coulomb problem whose Schrödinger equation is

$$-\frac{\hbar^2}{2m}\left(\frac{\partial^2}{\partial r^2} + \frac{1}{r}\frac{\partial}{\partial r} + \frac{1}{r^2}\frac{\partial^2}{\partial \theta^2}\right)\Psi - \frac{k}{r}\Psi = E\Psi \tag{5.109}$$

with $k > 0$. The parameters that we consider are $x = \{x^i\} = (m, k)$ with $i = 1, 2$. According to Zaslow and Zandler [84], the spectrum is given by

$$E_n = -\frac{mk^2}{2\hbar^2\left(n - \frac{1}{2}\right)^2}, \quad n = 1, 2, 3, \ldots. \tag{5.110}$$

Just as in the previous case, for the ground state, separation of variables dictates that the angular function $\Theta(\theta)$ is $1/\sqrt{2\pi}$. On the other hand, the radial wave function is

$$\psi(r; x) = \frac{4mk}{\hbar^2} e^{-\frac{2mk}{\hbar^2} r}. \tag{5.111}$$

We know that this will yield a zero connection so we move to the calculation of the quantum metric tensor. The inner product for this Hilbert space has the same form as (5.73), and this gives the metric tensor

$$g^{(0)}_{ij} = \frac{1}{2} \begin{pmatrix} \frac{1}{m^2} & \frac{1}{mk} \\ \frac{1}{mk} & \frac{1}{k^2} \end{pmatrix}. \tag{5.112}$$

For the classical computation, we consider the Hamiltonian

$$H = \frac{p_r^2}{2m} + \frac{L^2}{2mr^2} - \frac{k}{r}. \tag{5.113}$$

We know from the previous section that in order to calculate the classical metric, we require the motion as a function of time, $r(t)$, and the orbit equation, $r(\theta)$. However, we know that $r(t)$ cannot be explicitly obtained for the Coulomb problem [76], so we must work with the eccentric anomaly ψ rather than with the angle variable ϕ. The equation $r(t)$ is obtained, in principle, in two steps. First, we use Kepler's equation

$$\omega t = \psi - e \sin \psi, \tag{5.114}$$

to find $\psi(t)$. Here, $\omega = \frac{1}{k}\sqrt{\frac{-8E^3}{m}}$ is the frequency of revolution (remember that $E < 0$ for the bounded problem), and $e = \sqrt{1 + \frac{2EL^2}{mk^2}}$ is the eccentricity of the ellipse. Then, we substitute this result in the equation that defines the eccentric anomaly

$$r = -\frac{k}{2E}(1 - e \cos \psi). \tag{5.115}$$

It is straightforward to prove that the angle variable that corresponds to the radial degree of freedom is $\phi_r = \omega t$, just as we would anticipate from (5.114). On the other hand, the orbit equation $r(\theta)$ is given by

$$r(\theta) = \frac{L^2}{mk} \frac{1}{1 + e \cos \theta}, \tag{5.116}$$

and we know that it represents an ellipse with one of its foci located at the origin. We now use the same technique as the previous section to find the action variables for the system [69]. They are

$$I_r = \sqrt{-\frac{mk^2}{2E}} - |L|, \quad I_\theta = |L|. \tag{5.117}$$

From here we get

$$E = -\frac{mk^2}{2(I_r + I_\theta)^2}. \tag{5.118}$$

The frequencies for each degree of freedom are

$$\omega_r = \omega_\theta = \frac{1}{k}\sqrt{\frac{-8E^3}{m}}. \tag{5.119}$$

Again, we would like to express the energy in terms of a single action variable. In this case, we consider the canonical transformation $(\phi_r, \phi_\theta, I_r, I_\theta) \to (\phi_1, \phi_2, I_1, I_2)$ generated by

$$F_2(\phi_r, \phi_\theta, I_1, I_2) = (\phi_\theta - \phi_r) I_1 + \phi_r I_2. \tag{5.120}$$

This implies that

$$E = -\frac{mk^2}{2I_2^2}, \quad \phi_2 = \phi_r, \tag{5.121}$$

and $\omega_1 = 0$, $\omega_2 = \omega_r$. We will omit the subscript and refer to I_2 and ϕ_2 simply as I and ϕ, respectively. Carrying a similar procedure as that used in the previous section, we find that the generating function S is

$$S(\psi, I; x) = Ie\sin\psi + I\psi - L\theta(\psi, I; x), \tag{5.122}$$

where e is expressed as $\sqrt{1 - L^2/I^2}$. Since the angle variable ϕ does not appear explicitly, we need to calculate the averages in the definition of the metric by making the change of variable of integration

$$\phi = \psi - e\sin\psi \;\rightarrow\; \mathrm{d}\phi = (1 - e\cos\psi)\mathrm{d}\psi, \tag{5.123}$$

where e also takes values from 0 to 2π in one period of motion. Furthermore, we need to check if there is a dependence of the parameters in the expression $\theta(\psi, I; x)$. To do this, we only need to compare (5.115) with (5.116) to conclude that

$$\cos\theta = \frac{\cos\psi - e}{1 - e\cos\psi}. \tag{5.124}$$

From this expression, it is clearly seen that θ does not depend on the parameters x, so we have $G_i = p_r\partial_i r$. The position and momentum in terms of $(\psi, I; x)$ are

$$r(\psi, I; x) = -\frac{I^2}{mk}(1 - e\cos\psi), \quad p_r(\psi, I; x) = \frac{mk}{I}\frac{e\sin\psi}{1 - e\cos\psi}. \tag{5.125}$$

This allows us to calculate the generators,

$$G_1 = -\frac{Ie}{m}\sin\psi = -\frac{rp_r}{m}, \tag{5.126}$$

$$G_2 = -\frac{Ie}{k}\sin\psi = -\frac{rp_r}{k}, \tag{5.127}$$

and finally, the metric,

$$g_{ij} = \frac{I^2 - L^2}{2}\begin{pmatrix} \frac{1}{m^2} & \frac{1}{mk} \\ \frac{1}{mk} & \frac{1}{k^2} \end{pmatrix}. \tag{5.128}$$

Notice the resemblance of the metrics for the isotropic harmonic oscillator (5.107) and the attractive Coulomb problem (5.128). In Section 5.6, we will shed light on this issue through the Kustaanheimo-Stiefel transformation. We remind that the EBK rule [85] tells us that for the two-dimensional hydrogen atom we must have exactly $I = (n - 1/2)\hbar$ and $L = \ell\hbar$, with $n = 1, 2, 3, ...$, and $\ell = 0, \pm1, \pm2, ..., \pm(n-1)$. For the ground state, this means that the metric tensor is

$$g_{ij}(I = \hbar/2, L = 0) = \frac{\hbar^2}{8}\begin{pmatrix} \frac{1}{m^2} & \frac{1}{mk} \\ \frac{1}{mk} & \frac{1}{k^2} \end{pmatrix}, \tag{5.129}$$

which differs from (5.112) by a factor of 4.

5.5 Two-dimensional anisotropic harmonic oscillator

In this section we consider the two-dimensional anisotropic harmonic oscillator which has two degrees of freedom and three parameters. The Hamiltonian is

$$\hat{H} = \frac{\hat{p}_u^2 + \hat{p}_v^2}{2m} + \frac{k_u}{2}\hat{u}^2 + \frac{k_v}{2}\hat{v}^2, \tag{5.130}$$

and we take our parameters to be $x = \{x^i\} = (m, k_u, k_v)$ with $i = 1, 2, 3$. The angular momentum of this system is not conserved, so it cannot be reduced to a single degree of freedom, unless of course, the two spring constants are made equal.

For the quantum calculation, we employ the ground state only for simplicity. The normalized ground state wave function is just the product of the wave functions for each coordinate since the system is separable [86],

$$\psi(u, v; x) = \left(\frac{\sqrt{mk_u}}{\pi\hbar}\right)^{1/4} \left(\frac{\sqrt{mk_v}}{\pi\hbar}\right)^{1/4} \exp\left(-\frac{\sqrt{mk_u}}{2\hbar}u^2\right) \exp\left(-\frac{\sqrt{mk_v}}{2\hbar}v^2\right). \tag{5.131}$$

The inner product of two functions is now expressed as a double integral,

$$\langle f|g\rangle = \int_{-\infty}^{\infty} \mathrm{d}u \int_{-\infty}^{\infty} \mathrm{d}v\, f^*(u, v; x) g(u, v; x). \tag{5.132}$$

Of course, once again the connection and curvature are zero. On the other hand, the quantum metric tensor is

$$g_{ij}^{(0)} = \frac{1}{32} \begin{pmatrix} \frac{2}{m^2} & \frac{1}{mk_u} & \frac{1}{mk_v} \\ \frac{1}{mk_u} & \frac{1}{k_u^2} & 0 \\ \frac{1}{mk_v} & 0 & \frac{1}{k_v^2} \end{pmatrix}. \tag{5.133}$$

Now, moving to the classical quantities, we know that the Hamiltonian for this system can be expressed as

$$H = I_u\omega_u + I_v\omega_v, \tag{5.134}$$

where I_u and I_v denote the action variable of the respective coordinate, and where $\omega_u = \sqrt{k_u/m}$ and $\omega_v = \sqrt{k_v/m}$. The coordinates and the momenta are easily written in terms of action-angle variables as

$$u(\phi_u, I_u; x) = \sqrt{\frac{2I_u}{\sqrt{mk_u}}} \sin\phi_u, \quad v(\phi_v, I_v; x) = \sqrt{\frac{2I_v}{\sqrt{mk_v}}} \sin\phi_v \tag{5.135}$$

and

$$p_u(\phi_u, I_u; x) = \sqrt{2I_u\sqrt{mk_u}} \cos\phi_u, \quad p_v(\phi_v, I_v; x) = \sqrt{2I_v\sqrt{mk_v}} \cos\phi_v. \tag{5.136}$$

The generating function is just the sum of the functions for each degree of freedom [76],

$$S(\phi_u, \phi_v, I_u, I_v) = I_u(\phi_u + \sin\phi_u \cos\phi_u) + I_v(\phi_v + \sin\phi_v \cos\phi_v). \tag{5.137}$$

We see immediately that it does not depend on the parameters, so the generators will only be $G_i = p_u\partial_i u + p_v\partial_i v$. From here, we get the metric tensor

$$g_{ij} = \frac{1}{32}\begin{pmatrix} \frac{I_u^2+I_v^2}{m^2} & \frac{I_u^2}{mk_u} & \frac{I_v^2}{mk_v} \\ \frac{I_u^2}{mk_u} & \frac{I_u^2}{k_u^2} & 0 \\ \frac{I_v^2}{mk_v} & 0 & \frac{I_v^2}{k_v^2} \end{pmatrix}. \tag{5.138}$$

According to the EBK quantization rule, the actions are $I_u = (n_u + 1/2)\hbar$ and $I_v = (n_v+1/2)\hbar$, where $n_u, n_v = 0, 1, 2, \ldots$. Since we are considering the ground state only, the actions become $I_u = I_v = \hbar/2$. Again, we notice a discrepancy between the quantum and classical results. On a side note, in the case of an isotropic oscillator, i.e., $k_u = k_v = k$, the quantum metric tensor takes the form (cf. (5.74)),

$$g_{ij}(k_u = k_v = k) = \frac{1}{16}\begin{pmatrix} \frac{1}{m^2} & \frac{1}{mk} \\ \frac{1}{mk} & \frac{1}{k^2} \end{pmatrix}, \tag{5.139}$$

whereas its classical counterpart turns out to be (cf. (5.107))

$$g_{ij}(k_u = k_v = k) = \frac{I_u^2 + I_v^2}{32}\begin{pmatrix} \frac{1}{m^2} & \frac{1}{mk} \\ \frac{1}{mk} & \frac{1}{k^2} \end{pmatrix}. \tag{5.140}$$

5.6 Mapping of metrics through the Kustaanheimo-Stiefel transformation

The Kustaanheimo-Stiefel (KS) transformation allows one to relate the harmonic oscillator and the attractive Coulomb problem [87, 88]. In particular, we utilize the two-dimensional mapping (also known as the Levi-Civita transformation) to obtain in a straightforward manner the metric tensor of the Coulomb problem through the transformation rule of a second rank tensor. In this section, the barred parameters belong to the Coulomb problem.

Let us start with the attractive Coulomb Hamiltonian

$$\bar{H} = \frac{p_x^2 + p_y^2}{2\bar{m}} - \frac{\bar{k}}{\sqrt{x^2 + y^2}}, \tag{5.141}$$

where $\bar{k} > 0$.

The KS transformation is defined by

$$x = u^2 - v^2, \quad y = 2uv, \quad \frac{\mathrm{d}t}{\mathrm{d}s} = u^2 + v^2. \tag{5.142}$$

Notice that besides the transformation of coordinates, there is a time rescaling too. The momenta transform according to

$$p_x = \frac{up_u - vp_v}{2(u^2+v^2)}, \quad p_y = \frac{vp_u + up_v}{2(u^2+v^2)}. \tag{5.143}$$

The energy of the Coulomb problem (an integral of motion) in terms of variables (u, v, s) is

$$\bar{E} = \frac{p_u^2 + p_v^2}{8\bar{m}(u^2+v^2)} - \frac{\bar{k}}{u^2+v^2}, \tag{5.144}$$

or, after rearranging,

$$\bar{k} = \frac{p_u^2 + p_v^2}{8\bar{m}} - \bar{E}(u^2+v^2). \tag{5.145}$$

In order to have periodic orbits, we restrict ourselves to the bounded case so we take $\bar{E} < 0$. The above expression resembles the energy of the two-dimensional isotropic harmonic oscillator with mass $m = 4\bar{m}$ and spring constant $k = -2\bar{E}$. To verify that this is indeed the appropriate Hamiltonian, we can apply the KS transformation directly on the equations of motion for (5.141) which will take the form

$$u' = \frac{p_u}{4\bar{m}}, \quad p_u' = 2\bar{E}u, \tag{5.146}$$

$$v' = \frac{p_v}{4\bar{m}}, \quad p_v' = 2\bar{E}v. \tag{5.147}$$

where the prime denotes differentiation with respect to the time s. Therefore, we see that the transformation yields the Hamiltonian

$$H = \frac{p_u^2 + p_v^2}{2m} + \frac{k}{2}(u^2+v^2) = E. \tag{5.148}$$

So far, we have made the following identifications

$$m = 4\bar{m}, \quad k = -2\bar{E}, \quad E = \bar{k}. \tag{5.149}$$

It can easily be shown [87] that the angular momenta of the two systems are related as

$$L = 2\bar{L}. \tag{5.150}$$

Furthermore, the action variable is the same for both systems, since

$$I = \sqrt{\frac{m}{k}}\frac{E}{2} = \sqrt{\frac{4\bar{m}}{-2\bar{E}}}\frac{\bar{k}}{2} = \sqrt{-\frac{\bar{m}\bar{k}^2}{2\bar{E}}} = \bar{I}. \tag{5.151}$$

Thus, the spring constant k is given by

$$k = \frac{\bar{m}\bar{k}^2}{\bar{I}^2}. \tag{5.152}$$

Now, we are ready to obtain the metric tensor of the attractive Coulomb problem using the tensor transformation rule

$$\bar{g}_{ij} = \frac{\partial x^k}{\partial \bar{x}^i} \frac{\partial x^l}{\partial \bar{x}^j} g_{kl}, \tag{5.153}$$

or, in matrix form,

$$\bar{G} = A^T G A, \tag{5.154}$$

where A is the Jacobian matrix

$$A = \begin{pmatrix} \frac{\partial m}{\partial \bar{m}} & \frac{\partial m}{\partial \bar{k}} \\ \frac{\partial k}{\partial \bar{m}} & \frac{\partial k}{\partial \bar{k}} \end{pmatrix} = \begin{pmatrix} 4 & 0 \\ \frac{\bar{k}^2}{\bar{I}^2} & \frac{2\bar{m}\bar{k}}{\bar{I}^2} \end{pmatrix}. \tag{5.155}$$

Rewriting the metric tensor (5.107) in terms of the barred parameters and carrying out the matrix product (5.154) we get

$$\bar{g}_{ij} = \frac{\bar{I}^2 - \bar{L}^2}{2} \begin{pmatrix} \frac{1}{\bar{m}^2} & \frac{1}{\bar{m}\bar{k}} \\ \frac{1}{\bar{m}\bar{k}} & \frac{1}{\bar{k}^2} \end{pmatrix}, \tag{5.156}$$

which is precisely the metric of the Coulomb problem (5.128).

Chapter 6

Examples of the time-dependent approach to the classical metric

In this chapter, we employ the path integral approach to the quantum geometric tensor [58] and its classical time-dependent counterpart [68] to analyze some models. We see once again that the classical quantities contain all, or almost all, the parameter space structure modulo some identifications on the action variables. Moreover, some advantages of the time-dependent approach are manifest, such as not requiring explicitly the generating function of the transformation to action-angle variables. The results of this chapter have been published in [68].

6.1 Symmetric coupled harmonic oscillators

We begin by analyzing two coupled harmonic oscillators with Hamiltonian

$$\hat{H} = \frac{1}{2}(\hat{p}_1^2 + \hat{p}_2^2) + \frac{k}{2}(\hat{q}_1^2 + \hat{q}_2^2) + \frac{k'}{2}(\hat{q}_1 - \hat{q}_2)^2. \tag{6.1}$$

This system has been extensively employed to analyze quantum entanglement [89–91] and as a model toward understanding circuit complexity [26]. We take as our adiabatic parameters $x = \{x^i\} = (k, k')$. The corresponding deformation operators are

$$\hat{\mathcal{O}}_1 = \frac{\partial \hat{H}}{\partial k} = \frac{1}{2}\left(\hat{q}_1^2 + \hat{q}_2^2\right), \quad \hat{\mathcal{O}}_2 = \frac{\partial \hat{H}}{\partial k'} = \frac{1}{2}\left(\hat{q}_1 - \hat{q}_2\right). \tag{6.2}$$

To compute the expectation values that are required, we need to introduce new coordinates $(\hat{Q}_1, \hat{Q}_2)$ and momenta $(\hat{P}_1, \hat{P}_2)$ given by

$$\hat{q}_1 = \frac{1}{\sqrt{2}}(\hat{Q}_1 + \hat{Q}_2), \quad \hat{q}_2 = \frac{1}{\sqrt{2}}(\hat{Q}_1 - \hat{Q}_2), \tag{6.3}$$

$$\hat{p}_1 = \frac{1}{\sqrt{2}}(\hat{P}_1 + \hat{P}_2), \quad \hat{p}_2 = \frac{1}{\sqrt{2}}(\hat{P}_1 - \hat{P}_2), \tag{6.4}$$

such that the Hamiltonian acquires the diagonal form

$$H = \frac{1}{2}(\hat{P}_1^2 + \hat{P}_2^2) + \frac{\omega_1^2}{2}\hat{Q}_1^2 + \frac{\omega_2^2}{2}\hat{Q}_2^2, \tag{6.5}$$

where the frequencies are

$$\omega_1^2 = k, \quad \omega_2^2 = k + 2k'. \tag{6.6}$$

Given that the system is now separable, we can cast the position of the diagonal system in terms of time-dependent annihilation and creation operators $\hat{b}_a(t)$ and $\hat{b}_a^\dagger(t)$ $(a = 1, 2)$ as

$$\hat{Q}_a(t) = \sqrt{\frac{\hbar}{2\omega_a}}\left(\hat{b}_a^\dagger(t) + \hat{b}_a(t)\right). \tag{6.7}$$

This, in turn, allows us to express the operators $\hat{\mathcal{O}}_i(t)$ in terms of $\hat{b}_a(t)$ and $\hat{b}_a^\dagger(t)$. Taking into account the time dependence, the operators read $\hat{b}_a(t) = \hat{b}_a e^{-i\omega_a t}, \hat{b}_a^\dagger(t) = \hat{b}_a^\dagger e^{i\omega_a t}$, with which the resulting integrands $\Lambda_{ij}^{(0)} \equiv \langle\hat{\mathcal{O}}_i(t_1), \hat{\mathcal{O}}_j(t_2)\rangle_0 - \langle\hat{\mathcal{O}}_i(t_1)\rangle_0\langle\hat{\mathcal{O}}_j(t_2)\rangle_0$ are

$$\begin{aligned}
\Lambda_{11}^{(0)} &= \frac{\hbar^2}{8\omega_1^2}e^{-2i\omega_1(t_1-t_2)} + \frac{\hbar^2}{8\omega_2^2}e^{-2i\omega_2(t_1-t_2)}, \\
\Lambda_{12}^{(0)} &= \frac{\hbar^2}{4\omega_2^2}e^{-2i\omega_2(t_1-t_2)}, \\
\Lambda_{22}^{(0)} &= \frac{\hbar^2}{2\omega_2^2}e^{-2i\omega_2(t_1-t_2)}.
\end{aligned} \tag{6.8}$$

Plugging this in (2.55) and using the prescription (2.63) for the time integrals, we find the quantum geometric tensor for the ground state (which in this case is equal to the quantum metric tensor due to the lack of an imaginary part)

$$g_{ij}^{(0)} = \frac{1}{32}\begin{pmatrix} \frac{1}{\omega_1^4} + \frac{1}{\omega_2^4} & \frac{2}{\omega_2^4} \\ \frac{2}{\omega_2^4} & \frac{4}{\omega_1^4} \end{pmatrix}. \tag{6.9}$$

The metric has a non-vanishing determinant $\det g_{ij}^{(0)} = 1/(256\omega_1^4\omega_2^4)$. Of course, due to the reason stated above, the Berry curvature is zero. For a general state $|m, n\rangle$, $(m, n = 0, 1, 2, ...)$, the quantum metric is

$$g_{ij}^{(m,n)} = \frac{1}{32}\begin{pmatrix} \frac{m^2+m+1}{\omega_1^4} + \frac{n^2+n+1}{\omega_2^4} & \frac{2(n^2+n+1)}{\omega_2^4} \\ \frac{2(n^2+n+1)}{\omega_2^4} & \frac{4(n^2+n+1)}{\omega_2^4} \end{pmatrix}. \tag{6.10}$$

In the classical case, we use the Hamiltonian

$$H = \frac{1}{2}(p_1^2 + p_2^2) + \frac{k}{2}(q_1^2 + q_2^2) + \frac{k'}{2}(q_1 - q_2)^2. \tag{6.11}$$

A transformation analogous to (6.3) and (6.4) casts the Hamiltonian in the diagonal form $H = \frac{1}{2}(P_1^2 + P_2^2) + \frac{\omega_1^2}{2}Q_1^2 + \frac{\omega_2^2}{2}Q_2^2$. The solution as a function of time is easily expressed in terms of normal coordinates as

$$\begin{aligned} Q_1(t) &= Q_{10}\cos\omega_1 t + \frac{P_{10}}{\omega_1}\sin\omega_1 t \\ P_1(t) &= P_{10}\cos\omega_1 t - \omega_1 Q_{10}\sin\omega_1 t \\ Q_2(t) &= Q_{20}\cos\omega_2 t + \frac{P_{20}}{\omega_2}\sin\omega_2 t \\ P_2(t) &= P_{20}\cos\omega_2 t - \omega_2 Q_{20}\sin\omega_2 t, \end{aligned} \tag{6.12}$$

where we have taken the initial conditions $Q_1(0) = Q_{10}$, $P_1(0) = P_{10}$, and similarly for Q_2 and P_2.

First, we compute the Hannay curvature. The deformations functions $\mathcal{O}_i = \partial H/\partial x^i$ are written in terms of the normal coordinates as

$$\begin{aligned} \mathcal{O}_1(t) &= \frac{1}{2}\Bigg[\frac{P_{10}\left(P_{10}\sin^2\omega_1 t + \omega_1 Q_{10}\sin 2\omega_1 t\right)}{\omega_1^2} + \frac{P_{20}\left(P_{20}\sin^2\omega_2 t + \omega_2 Q_{20}\sin 2\omega_2 t\right)}{\omega_2^2} \\ &\quad + Q_{10}^2\cos^2\omega_1 t + Q_{20}^2\cos^2\omega_2 t\Bigg], \\ \mathcal{O}_2(t) &= \frac{(P_{20}\sin\omega_2 t + \omega_2 Q_{20}\cos\omega_2 t)^2}{\omega_2^2}. \end{aligned} \tag{6.13}$$

The Poisson bracket of the $\mathcal{O}_i$ evaluated at different times turns out to be

$$\{\mathcal{O}_1(t_1), \mathcal{O}_2(t_2)\} = -\frac{2\sin\omega_2(t_1 - t_2)[P_{20}\sin\omega_2 t_1 + \omega_2 Q_{20}\cos\omega_2 t_1][P_{20}\sin\omega_2 t_2 + \omega_2 Q_{20}\cos\omega_2 t_2]}{\omega_2^3}, \tag{6.14}$$

where we have taken advantage of their canonical invariance and calculated them with respect to the initial conditions (Q_0, P_0) rather than (q_0, p_0). Since the system is separable in normal coordinates, we can easily express the initial conditions in terms of initial action-angle variables as

$$Q_{10}(\phi, I) = \sqrt{\frac{2I_1}{\omega_1}}\sin\phi_{10}, \quad P_{10}(\phi, I) = \sqrt{2\omega_1 I_1}\cos\phi_{10}, \tag{6.15}$$

and similarly for Q_{20} and P_{20}. Substituting in (6.14), we find that

$$\{\mathcal{O}_1(t_1), \mathcal{O}_2(t_2)\} = -\frac{4I_2\sin\omega_2(t_1 - t_2)\sin(\omega_2 t_1 + \phi_{20})\sin(\omega_2 t_2 + \phi_{20})}{\omega_2^2}. \tag{6.16}$$

The next step is to compute the average. Since we have two degrees of freedom, the torus average of a function $f(\phi)$ takes the form

$$\langle f\rangle_0 \equiv \frac{1}{(2\pi)^2}\int_0^{2\pi} \mathrm{d}\phi_{10} \int_0^{2\pi} \mathrm{d}\phi_{20}\, f(\phi), \tag{6.17}$$

thus,

$$\langle\{\mathcal{O}_1(t_1),\mathcal{O}_2(t_2)\}\rangle_0 = -\frac{I_2\sin 2\omega_2(t_1-t_2)}{\omega_2^2}. \tag{6.18}$$

All that remains to compute the unique element of the curvature is to perform the time integrals. We see that

$$F_{12} = -\frac{I_2}{\omega_2^2}\int_{-\infty}^{0}\mathrm{d}t_1\int_{0}^{\infty}\mathrm{d}t_2\,\sin 2\omega_2(t_1-t_2) = 0, \tag{6.19}$$

due to our regularization prescription (2.63).

We now compute the classical metric. Making use of (6.12), we find the $\mathcal{O}_i$ as functions of time and initial action-angle variables:

$$\begin{aligned}\mathcal{O}_1(t) &= \frac{I_1\sin^2(\omega_1 t+\phi_{10})}{\omega_1}+\frac{I_2\sin^2(\omega_2 t+\phi_{20})}{\omega_2},\\ \mathcal{O}_2(t) &= \frac{2I_2\sin^2(\omega_2 t+\phi_{20})}{\omega_2}.\end{aligned} \tag{6.20}$$

We begin by evaluating the average of each $\mathcal{O}_i$:

$$\begin{aligned}\langle\mathcal{O}_1(t)\rangle_0 &= \int_0^{2\pi}\mathrm{d}\phi_{10}\int_0^{2\pi}\mathrm{d}\phi_{20}\left[\frac{I_1\sin^2(\omega_1 t+\phi_{10})}{\omega_1}+\frac{I_2\sin^2(\omega_2 t+\phi_{20})}{\omega_2}\right]\\ &= \frac{I_1\omega_2+I_2\omega_1}{2\omega_1\omega_2},\end{aligned} \tag{6.21}$$

$$\begin{aligned}\langle\mathcal{O}_2(t)\rangle_0 &= \int_0^{2\pi}\mathrm{d}\phi_{10}\int_0^{2\pi}\mathrm{d}\phi_{20}\left[\frac{2I_2\sin^2(\omega_2 t+\phi_{20})}{\omega_2}\right]\\ &= \frac{I_2}{\omega_2}.\end{aligned} \tag{6.22}$$

The averages of the products of $\mathcal{O}_i$ evaluated at different times are

$$\begin{aligned}\langle\mathcal{O}_1(t_1)\mathcal{O}_1(t_2)\rangle_0 &= \frac{I_1^2\omega_2^2\cos 2\omega_1(t_2-t_1)+I_2^2\omega_1^2\cos 2\omega_2(t_2-t_1)+2(I_1\omega_2+I_2\omega_1)^2}{8\omega_1^2\omega_2^2},\\ \langle\mathcal{O}_1(t_1)\mathcal{O}_2(t_2)\rangle_0 &= \frac{I_2\left[2I_1\omega_2+2I_2\omega_1+I_2\omega_1\cos 2\omega_2(t_2-t_1)\right]}{4\omega_1\omega_2^2},\\ \langle\mathcal{O}_2(t_1)\mathcal{O}_2(t_2)\rangle_0 &= \frac{I_2^2\left[\cos 2\omega_2(t_2-t_1)+2\right]}{2\omega_2^2}.\end{aligned} \tag{6.23}$$

The component g_{11} is

$$\begin{aligned} g_{11} &= -\int_{-\infty}^{0} \mathrm{d}t_1 \int_{0}^{\infty} \mathrm{d}t_2 \left[\frac{1}{8}\left(\frac{I_1^2 \cos 2\omega_1(t_2-t_1)}{\omega_1^2} + \frac{I_2^2 \cos 2\omega_2(t_2-t_1)}{\omega_2^2}\right)\right] \\ &= \frac{1}{32}\left(\frac{I_1^2}{\omega_1^4} + \frac{I_2^2}{\omega_2^4}\right), \end{aligned} \tag{6.24}$$

whereas the component g_{12} is

$$\begin{aligned} g_{12} &= -\int_{-\infty}^{0} \mathrm{d}t_1 \int_{0}^{\infty} \mathrm{d}t_2 \left[\frac{I_2^2 \cos 2\omega_2(t_2-t_1)}{4\omega_2^2}\right] \\ &= \frac{I_2^2}{16\omega_2^4}. \end{aligned} \tag{6.25}$$

Finally, we find the component g_{22}:

$$\begin{aligned} g_{22} &= -\int_{-\infty}^{0} \mathrm{d}t_1 \int_{0}^{\infty} \mathrm{d}t_2 \left[\frac{I_2^2 \cos 2\omega_2(t_2-t_1)}{2\omega_2^2}\right] \\ &= \frac{I_2^2}{8\omega_2^4}. \end{aligned} \tag{6.26}$$

The resulting classical metric has the form

$$g_{ij} = \frac{1}{32}\begin{pmatrix} \frac{I_1^2}{\omega_1^4} + \frac{I_2^2}{\omega_2^4} & \frac{2I_2^2}{\omega_2^4} \\ \frac{2I_2^2}{\omega_2^4} & \frac{4I_2^2}{\omega_2^4} \end{pmatrix}, \tag{6.27}$$

whose determinant is

$$\det g_{ij} = \frac{I_1^2 I_2^2}{256\omega_1^4\omega_2^4}, \tag{6.28}$$

and it is always different from zero. Comparing the classical and quantum metrics, (6.27) and (6.10) respectively, we see that they are related as

$$g_{ij}^{(m,n)} = \frac{g_{ij}}{\hbar^2}, \tag{6.29}$$

as long as we make the identifications $I_1^2 = (m^2+m+1)\hbar^2$ and $I_2^2 = (n^2+n+1)\hbar^2$. This confirms relation (4.74).

6.2 Linearly coupled harmonic oscillators

We now present a different system that is also important in the study of entanglement [92–94]. The Hamiltonian under consideration is

$$\hat{H} = \frac{1}{2}(\hat{p}_1^2 + \hat{p}_2^2) + \frac{A}{2}\hat{q}_1^2 + \frac{B}{2}\hat{q}_2^2 + \frac{C}{2}\hat{q}_1\hat{q}_2, \tag{6.30}$$

where the parameters are $x = \{x^i\} = (A, B, C)$ with $A \neq B$. This Hamiltonian is not a particular case of (6.1), so it must be treated separately.

We begin with the computation of the quantum metric. The deformation operators associated with the parameter space are

$$\hat{\mathcal{O}}_1(t) = \frac{\hat{q}_1^2}{2}, \quad \hat{\mathcal{O}}_2(t) = \frac{\hat{q}_2^2}{2}, \quad \hat{\mathcal{O}}_3(t) = \frac{\hat{q}_1\hat{q}_2}{2}. \tag{6.31}$$

The first step, as we have seen, is to carry out the diagonalization of the Hamiltonian. With that purpose, we introduce the transformation

$$\hat{q}_1 = \hat{Q}_1\cos\alpha + \hat{Q}_2\sin\alpha, \quad \hat{q}_2 = -\hat{Q}_1\sin\alpha + \hat{Q}_2\cos\alpha, \tag{6.32}$$

$$\hat{p}_1 = \hat{P}_1\cos\alpha + \hat{P}_2\sin\alpha, \quad \hat{p}_2 = -\hat{P}_1\sin\alpha + \hat{P}_2\cos\alpha), \tag{6.33}$$

Here, $\tan\alpha = \frac{\epsilon}{|\epsilon|}\sqrt{\epsilon^2+1} - \epsilon$ with $\epsilon = \frac{B-A}{C}$. Since $\tan\alpha \in (-1, 1)$, the angle is restricted as $-\frac{\pi}{4} < \alpha < \frac{\pi}{4}$. Once the transformation is effected, we end up with the Hamiltonian

$$H = \frac{1}{2}(\hat{P}_1^2 + \hat{P}_2^2) + \frac{\omega_1^2}{2}\hat{Q}_1^2 + \frac{\omega_2^2}{2}\hat{Q}_2^2, \tag{6.34}$$

where the normal frequencies are

$$\omega_1^2 = A - \frac{C}{2}\tan\alpha, \quad \omega_2^2 = B + \frac{C}{2}\tan\alpha. \tag{6.35}$$

The transformations (6.32) and (6.33) help us treat the three deformation operators at once by applying the chain rule:

$$\hat{\mathcal{O}}_i = \frac{\partial\hat{H}}{\partial x^i} = \omega_1\hat{Q}_1^2\partial_i\omega_1 + \omega_2\hat{Q}_2^2\partial_i\omega_2 - (\omega_1^2 - \omega_2^2)\hat{Q}_1\hat{Q}_2\partial_i\alpha, \tag{6.36}$$

and from here, we can write the $\hat{Q}_a$ in terms of creation and annihilation operators as in (6.7), but with the frequencies (6.35). The integrands $\Lambda_{ij}^{(0)} = \langle\hat{\mathcal{O}}_i(t_1), \hat{\mathcal{O}}_j(t_2)\rangle_0 - \langle\hat{\mathcal{O}}_i(t_1)\rangle_0\langle\hat{\mathcal{O}}_j(t_2)\rangle_0$ can then be obtained and have the form

$$\begin{aligned}\Lambda_{ij}^{(0)} =& \hbar^2\Bigg[\frac{\partial_i\omega_1\partial_j\omega_1}{2}e^{-2i\omega_1(t_1-t_2)} \\ &+ \frac{\partial_i\omega_2\partial_j\omega_2}{2}e^{-2i\omega_2(t_1-t_2)} + \partial_i\alpha\partial_j\alpha\frac{(\omega_1^2-\omega_2^2)^2}{4\omega_1\omega_2}e^{-i(\omega_1+\omega_2)(t_1-t_2)}\Bigg].\end{aligned} \tag{6.37}$$

Substituting this in (2.55), we get the quantum metric tensor

$$g_{ij}^{(0)} = \frac{\partial_i\omega_1\partial_j\omega_1}{8\omega_1^2} + \frac{\partial_i\omega_2\partial_j\omega_2}{8\omega_2^2} + \partial_i\alpha\partial_j\alpha\left[\frac{1}{4}\left(\frac{\omega_1}{\omega_2}+\frac{\omega_2}{\omega_1}\right)-\frac{1}{2}\right], \tag{6.38}$$

which explicitly reads

$$g_{ij}^{(0)} = \frac{1}{32\omega_1^4}M_{ij} + \frac{1}{32\omega_2^4}N_{ij} + \frac{L_{ij}}{4\left(\omega_2^2-\omega_1^2\right)^2}\left[\frac{1}{4}\left(\frac{\omega_1}{\omega_2}+\frac{\omega_2}{\omega_1}\right)-\frac{1}{2}\right], \tag{6.39}$$

where the matrices M_{ij}, N_{ij} and L_{ij} are

$$\begin{aligned}
M_{ij} &= \frac{1}{4}\begin{pmatrix} (1+\mu)^2 & \nu^2 & -(1+\mu)\nu \\ \nu^2 & (1-\mu)^2 & -(1-\mu)\nu \\ -(1+\mu)\nu & -(1-\mu)\nu & \nu^2 \end{pmatrix}, \\
N_{ij} &= \frac{1}{4}\begin{pmatrix} (1-\mu)^2 & \nu^2 & (1-\mu)\nu \\ \nu^2 & (1+\mu)^2 & (1+\mu)\nu \\ (1-\mu)\nu & (1+\mu)\nu & \nu^2 \end{pmatrix}, \\
L_{ij} &= \begin{pmatrix} \nu^2 & -\nu^2 & \mu\nu \\ -\nu^2 & \nu^2 & -\mu\nu \\ \mu\nu & -\mu\nu & \mu^2 \end{pmatrix},
\end{aligned} \tag{6.40}$$

with $\mu = \cos 2\alpha = \frac{\epsilon}{\sqrt{\epsilon^2+1}}$ and $\nu = \sin 2\alpha = \frac{1}{\sqrt{\epsilon^2+1}}$. Since the quantum geometric tensor is real, we have a vanishing Berry curvature

$$F_{ij}^{(0)} = 0. \tag{6.41}$$

For a general state $|m,n\rangle$, $(m,n = 0,1,2,...)$, one gets the quantum metric

$$\begin{aligned}
g_{ij}^{(m,n)} =& \frac{m^2+m+1}{32\omega_1^4}M_{ij} + \frac{n^2+n+1}{32\omega_2^4}N_{ij} + \frac{L_{ij}}{4\left(\omega_2^2-\omega_1^2\right)^2}\Bigg[\left(\frac{\omega_1}{\omega_2}+\frac{\omega_2}{\omega_1}\right) \\
&\times\left(m+\frac{1}{2}\right)\left(n+\frac{1}{2}\right)-\frac{1}{2}\Bigg],
\end{aligned} \tag{6.42}$$

and the Berry curvature

$$F_{ij}^{(m,n)} = 0. \tag{6.43}$$

We now compute the classical metric and the Hannay curvature. The Hamiltonian of the system is, naturally,

$$H = \frac{1}{2}(p_1^2+p_2^2) + \frac{A}{2}q_1^2 + \frac{B}{2}q_2^2 + \frac{C}{2}q_1q_{2.}. \tag{6.44}$$

As in the quantum case, we can use transformations analogous to (6.32) and (6.33) to diagonalize the Hamiltonian. The deformation functions will then take the form

$$\mathcal{O}_i = \omega_1 Q_1^2 \partial_i \omega_1 + \omega_2 Q_2^2 \partial_i \omega_2 + (\omega_2^2 - \omega_1^2) Q_1 Q_2 \partial_i \alpha. \tag{6.45}$$

The normal coordinates can be expressed in terms of initial action-angle variables (ϕ_0, I) and time as

$$Q_a(t) = \sqrt{\frac{2I_a}{\omega_a}} \sin(\omega_a t + \phi_{0a}), \quad a = 1, 2\,. \tag{6.46}$$

This allows us to form the integrands $\Lambda_{ij} = \langle \mathcal{O}_i(t_1)\mathcal{O}_j(t_2)\rangle_0 - \langle \mathcal{O}_i(t_1)\rangle_0 \langle \mathcal{O}_j(t_2)\rangle_0$ which turn out to be

$$\begin{aligned}\Lambda_{ij} =& \frac{I_1}{2}\partial_i\omega_1\partial_j\omega_1 \cos[2\omega_1(t_1 - t_2)] + \frac{I_2}{2}\partial_i\omega_2\partial_j\omega_2 \cos[2\omega_2(t_1 - t_2)] \\ &+ \frac{I_1 I_2}{\omega_1\omega_2}(\omega_2^2 - \omega_1^2)^2 \partial_i\alpha\partial_j\alpha \cos[\omega_1(t_1 - t_2)] \cos[\omega_2(t_1 - t_2)].\end{aligned} \tag{6.47}$$

Plugging them in (4.75), we obtain the classical metric

$$g_{ij} = \frac{\partial_i\omega_1\partial_j\omega_1}{8\omega_1^2} I_1^2 + \frac{\partial_i\omega_2\partial_j\omega_2}{8\omega_2^2} I_2^2 + I_1 I_2 \left(\frac{\omega_1}{\omega_2} + \frac{\omega_2}{\omega_1}\right) \partial_i\alpha\partial_j\alpha, \tag{6.48}$$

which explicitly reads

$$g_{ij} = \frac{I_1^2}{32\omega_1^4} M_{ij} + \frac{I_2^2}{32\omega_2^4} N_{ij} + \frac{I_1 I_2}{4\left(\omega_2^2 - \omega_1^2\right)^2} \left(\frac{\omega_1}{\omega_2} + \frac{\omega_2}{\omega_1}\right) L_{ij}, \tag{6.49}$$

where the matrices M_{ij}, N_{ij} and L_{ij} are the same as those of the quantum case (6.40).

We now want to compare the quantum and classical metrics, (6.42) and (6.49), respectively. By using the Bohr-Sommerfeld quantization rule $I_1 = \left(m + \frac{1}{2}\right)\hbar$, $I_2 = \left(n + \frac{1}{2}\right)\hbar$, and the identifications $I_1^2 = (m^2 + m + 1)\hbar^2$, $I_2^2 = (n^2 + n + 1)\hbar^2$, we find the relation

$$g_{ij}^{(m,n)} = \frac{1}{\hbar^2} g_{ij} - \frac{L_{ij}}{8(\omega_2^2 - \omega_1^2)^2}, \tag{6.50}$$

instead of our semiclassical relation (4.74). We see that the extra term in (6.50) does not involve the quantum numbers m, n, it only contains parameters and is of order $\hbar^0$. The reason behind this result is the ambiguity of operator ordering in some of the expectation values. They are

$$\langle \hat{Q}_1 \hat{P}_2 \hat{Q}_2 \hat{P}_1 \rangle_{m,n} = \frac{\hbar^2}{4}, \quad \langle \hat{Q}_2 \hat{P}_1 \hat{Q}_1 \hat{P}_2 \rangle_{m,n} = \frac{\hbar^2}{4}, \tag{6.51}$$

whereas the corresponding averages in the classical setting are

$$\langle Q_1 P_2 Q_2 P_1 \rangle_0 = 0, \quad \langle Q_2 P_1 Q_1 P_2 \rangle_0 = 0. \tag{6.52}$$

Finally, we compute the Hannay curvature. We need the non-equal-time Poisson brackets, which we choose to calculate in terms of the initial normal coordinates (Q_0, P_0):

$$\begin{aligned}\langle\{\mathcal{O}_i(t_1), \mathcal{O}_j(t_2)\}\rangle_0 = &- I_1 \cos[\omega_1(t_1 - t_2)]\Big(4\partial_i\omega_1\partial_j\omega_1 \sin[\omega_1(t_1 - t_2)] \\ &+ \partial_i\alpha\partial_j\alpha\frac{(\omega_1^2 - \omega_2^2)^2}{\omega_1\omega_2}\sin[\omega_2(t_1 - t_2)]\Big) \\ &- I_2 \cos[\omega_2(t_1 - t_2)]\Big(4\partial_i\omega_2\partial_j\omega_2 \sin[\omega_2(.t_1 - t_2)] \\ &+ \partial_i\alpha\partial_j\alpha\frac{(\omega_1^2 - \omega_2^2)^2}{\omega_1\omega_2}\sin[\omega_1(t_1 - t_2)]\Big).\end{aligned} \tag{6.53}$$

Substituting this in (4.77), we finally get that the Hannay curvature is zero, which coincides with its quantum counterpart.

6.3 Singular Euclidean oscillator

We now present the singular Euclidean oscillator. This model has been used in the study of quantum rings, which are semiconductor ring-shaped systems [95, 96]. The Hamiltonian of this oscillator is

$$H = \frac{\boldsymbol{p}^2}{2} + \frac{\alpha^2}{2r^2} + \frac{\omega^2\boldsymbol{r}^2}{2}. \tag{6.54}$$

We first solve for the ground state and then compute the quantum metric tensor. After that, we set out to solve the corresponding classical system and find the classical metric. At the end, we compare both results and establish some prescriptions for the action variables.

To solve the system, we shall restrict ourselves to the two-dimensional case, so we can introduce a polar coordinate system as

$$x = r\cos\theta, \quad y = r\sin\theta. \tag{6.55}$$

The Hamiltonian then reads

$$H = \frac{p_r^2}{2} + \frac{p_\theta^2 + \alpha^2}{2r^2} + \frac{\omega^2 r^2}{2}, \tag{6.56}$$

where we clearly see that θ is a cyclic coordinate and hence its conjugate momentum p_θ is a constant. The time-independent Schrödinger equation for the singular Euclidean oscillator is

$$\frac{\partial^2\psi}{\partial r^2} + \frac{1}{r}\frac{\partial\psi}{\partial r} + \frac{1}{r^2}\frac{\partial^2\psi}{\partial\theta^2} + \frac{2}{\hbar^2}\left[E - \left(\frac{\alpha^2}{2r^2} + \frac{\omega^2 r^2}{2}\right)\right]\psi = 0. \tag{6.57}$$

We can easily separate the angular part by substituting $\psi(r,\theta) = R(r)\Theta(\theta)$. This results in

$$\Theta(\theta) = \frac{e^{i\ell\theta}}{\sqrt{2\pi}}, \quad \ell = 0, \pm 1, \pm 2, \dots, \tag{6.58}$$

and the radial equation

$$\frac{\mathrm{d}^2 R}{\mathrm{d}r^2} + \frac{1}{r}\frac{\mathrm{d}R}{\mathrm{d}r} + \frac{2}{\hbar^2}\left[E - \left(\frac{\hbar^2\ell^2 + \alpha^2}{2r^2} + \frac{\omega^2 r^2}{2}\right)\right] R = 0. \tag{6.59}$$

The normalization condition on the wave function is

$$\langle\psi|\psi\rangle = \int_0^{2\pi} \mathrm{d}\theta\, |\Theta(\theta)|^2 \int_0^{\infty} \mathrm{d}r\, r|R(r)|^2 = 1. \tag{6.60}$$

As is usual, we require both the angular and the radial wave functions to be normalized. We see from (6.58) that the angular wave function automatically fulfills this condition, so we are only left effectively with the radial wave function. This means that our inner products will be of the form

$$\langle f|g\rangle = \int_0^{\infty} \mathrm{d}r\, r f^*(r) g(r). \tag{6.61}$$

Since we are only interested in the ground state, we set $\ell = 0$. From (6.59) we expect that when $r \to \infty$, we can recover the harmonic oscillator wave function. To account for the behavior for all r, we make the following ansatz

$$R_0(r) = N r^{\beta} e^{-\frac{\omega}{2\hbar} r^2}, \tag{6.62}$$

where N is a normalization constant, and β is a parameter we must determine. We plug our ansatz in (6.59), which leads to

$$-\alpha^2 + \hbar^2\beta^2 + 2r^2[E_0 - (\beta+1)\omega\hbar] = 0. \tag{6.63}$$

Equating each coefficient of a power of r to zero, we find that

$$\beta = \alpha/\hbar, \quad E_0 = (\alpha + \hbar)\omega. \tag{6.64}$$

We only need to find the constant N by solving the condition

$$\int_0^{\infty} \mathrm{d}r\, r R_0^2(r) = N^2 \int_0^{\infty} \mathrm{d}r\, r^{1+2\beta} e^{-\frac{\omega r^2}{\hbar}} = 1. \tag{6.65}$$

We obtain

$$N = \sqrt{\frac{2\omega}{\alpha\Gamma\left(\frac{\alpha}{\hbar}\right)}} \left(\frac{\omega}{\hbar}\right)^{\frac{\alpha}{2\hbar}}, \tag{6.66}$$

where $\Gamma(z)$ is the gamma function [97]

$$\Gamma(z) = \int_0^\infty \mathrm{d}t\, t^{z-1} e^{-t}, \quad \mathrm{Re} z > 0. \tag{6.67}$$

Hence, the radial ground state wave function reads

$$R_0(r) = \sqrt{\frac{2\omega}{\alpha \Gamma\left(\frac{\alpha}{\hbar}\right)}} \left(\frac{\omega}{\hbar}\right)^{\frac{\alpha}{2\hbar}} r^{\frac{\alpha}{\hbar}} e^{-\frac{\omega}{2\hbar} r^2}, \tag{6.68}$$

which has the energy

$$E_0 = (\alpha + \hbar)\omega. \tag{6.69}$$

We can readily corroborate that these results reduce to the two-dimensional harmonic oscillator (see [98]) when we take the limit $\alpha \to 0$:

$$E_0(\alpha = 0) = \hbar\omega, \quad R_0(r; \alpha = 0) = \sqrt{\frac{2\omega}{\hbar}} e^{-\frac{\omega}{2\hbar} r^2}. \tag{6.70}$$

Now that we have the solution, we proceed to compute the quantum metric tensor using (2.20):

$$g_{ij}^{(0)}(x) = \mathrm{Re}\left(\langle \partial_i \psi_0 | \partial_j \psi_0 \rangle - \langle \partial_i \psi_0 | \psi_0 \rangle \langle \psi_0 | \partial_j \psi_0 \rangle\right). \tag{6.71}$$

We take as our parameters $x = \{x^i\} = (\omega, \alpha)$, $i = 1, 2$. The fact that we have a real wave function implies that the Berry connection (and, of course, the Berry curvature) is zero [4]; hence, the second term vanishes, and the metric tensor simplifies to

$$g_{ij}^{(0)}(x) = \langle \partial_i \psi_0 | \partial_j \psi_0 \rangle. \tag{6.72}$$

Plugging the wave function (6.68) in this expression, we find the following components:

$$\begin{aligned} g_{11}^{(0)} &= \frac{\alpha + \hbar}{4\hbar\omega^2}, \\ g_{12}^{(0)} &= -\frac{1}{4\hbar\omega}, \\ g_{22}^{(0)} &= \frac{\psi_1(1 + \alpha/\hbar)}{4\hbar^2}, \end{aligned} \tag{6.73}$$

where $\psi_1(z)$ is the trigamma function defined as [97]

$$\psi_1(z) = \frac{\mathrm{d}^2}{\mathrm{d}z^2} \ln \Gamma(z), \tag{6.74}$$

which has the series representation

$$\psi_1(z) = \sum_{n=0}^{\infty} \frac{1}{(z+n)^2}. \tag{6.75}$$

The determinant of the quantum metric tensor is

$$\det g_{ij}^{(0)} = \frac{\left(1+\frac{\alpha}{\hbar}\right)\psi_1\left(1+\frac{\alpha}{\hbar}\right)-1}{16\hbar^2\omega^2}, \tag{6.76}$$

and it is different from zero for any α. By taking the limit, we can see that it only approaches zero when $\alpha \to \infty$.

In the classical setting, we consider the Hamiltonian

$$H = \frac{p_r^2}{2} + \frac{p_\theta^2+\alpha^2}{2r^2} + \frac{\omega^2 r^2}{2}, \tag{6.77}$$

and try to find the classical analog of the quantum metric tensor and the Berry curvature proposed in [67]. We note that in order to have orbits with a fixed energy E, the condition $E > \omega\sqrt{p_\theta^2+\alpha^2}$ needs to be fulfilled. This guarantees that the energy is greater than the minimum of the effective radial potential. Due to the presence of the parameter α, the Runge-Lenz vector will not be a constant of motion, and hence, the orbit will precess [76]. The action variables of the singular Euclidean oscillator are [95]

$$\begin{aligned} I_\theta &= \frac{1}{2\pi}\oint \mathrm{d}\theta\, p_\theta = p_\theta, \\ I_r &= \frac{1}{2\pi}\oint \mathrm{d}r\, p_r = \frac{E}{2\omega} - \frac{\tilde{p}_\theta}{2}, \end{aligned} \tag{6.78}$$

where $\tilde{p}_\theta \equiv \sqrt{p_\theta^2+\alpha^2} = \sqrt{I_\theta^2+\alpha^2}$. The condition for the orbits is then $E > \omega\tilde{p}_\theta$. From these expressions, we see that the energy in terms of action variables can be written as

$$E = \omega\left(2I_r + \sqrt{I_\theta^2+\alpha^2}\right). \tag{6.79}$$

Given that p_θ is a constant of the motion, the generating function that solves the time-independent Hamilton-Jacobi equation is given by [76]

$$S(r,\theta,E,p_\theta) = p_\theta\theta + \int \mathrm{d}r\, p_r. \tag{6.80}$$

From here, we get the angle variables [95]

$$\begin{aligned} \phi_\theta &= \left(\frac{\partial S}{\partial p_\theta}\right)_{r,\theta,E} + \left(\frac{\partial S}{\partial E}\right)_{r,\theta,p_\theta}\left(\frac{\partial E}{\partial p_\theta}\right)_{I_r} = \theta - \frac{p_\theta}{2\tilde{p}_\theta}\arcsin\frac{(\tilde{p}_\theta+\omega r^2)\sqrt{2Er^2-\tilde{p}_\theta^2-\omega^2r^4}}{(E+\omega\tilde{p}_\theta)r^2}, \\ \phi_r &= \left(\frac{\partial S}{\partial E}\right)_{r,\theta,p_\theta}\left(\frac{\partial E}{\partial I_r}\right)_{p_\theta} = -\arcsin\frac{E-\omega^2r^2}{\sqrt{E^2-\omega^2\tilde{p}_\theta^2}}. \end{aligned} \tag{6.81}$$

We notice that we can solve for r from the second equation:

$$r = \frac{\left(E+\sqrt{E^2-\omega^2\tilde{p}_\theta^2}\sin\phi_r\right)^{1/2}}{\omega}. \tag{6.82}$$

From the definition of the angle variable, we know that $\phi_r = \omega_r t - \beta$, where $\omega_r = \partial E/\partial I_r = 2\omega$, and β is a constant related to the initial position. With this result at hand, we can easily write the radial coordinate r and its conjugate momentum $p_r = \dot{r}$ as

$$\begin{aligned} r(t) &= \frac{\left[E + \sqrt{E^2 - \omega^2 \tilde{p}_\theta^2}\sin(2\omega t - \beta)\right]^{1/2}}{\omega}, \\ p_r(t) &= \frac{\sqrt{E^2 - \omega^2 \tilde{p}_\theta^2}\cos(2\omega t - \beta)}{\left[E + \sqrt{E^2 - \omega^2 \tilde{p}_\theta^2}\sin(2\omega t - \beta)\right]^{1/2}}. \end{aligned} \tag{6.83}$$

The next step is to use the initial conditions to solve for β. Setting $r(0) = r_0$ and $p_r(0) = p_{r0}$, we can solve for the sine and cosine:

$$\cos\beta = \frac{\omega r_0 p_{r0}}{\sqrt{E^2 - \omega^2 \tilde{p}_\theta^2}}, \quad \sin\beta = \frac{E - \omega^2 r_0^2}{\sqrt{E^2 - \omega^2 \tilde{p}_\theta^2}}. \tag{6.84}$$

Now, we find the explicit form of the deformation functions $\mathcal{O}_i$ expanding the trigonometric functions in (6.83) and substituting the above relations. Recall that the parameters we chose are $x = \{x^i\} = (\omega, \alpha)$. Thus,

$$\begin{aligned} \mathcal{O}_1 &= \frac{\partial H}{\partial \omega} = \omega r^2 = \frac{E + \omega r_0 p_{r0}\sin 2\omega t - (E - \omega^2 r_0^2)\cos 2\omega t}{\omega}, \\ \mathcal{O}_2 &= \frac{\partial H}{\partial \alpha} = \frac{\alpha}{r^2} = \frac{\alpha\omega^2}{E + \omega r_0 p_{r0}\sin 2\omega t - (E - \omega^2 r_0^2)\cos 2\omega t}. \end{aligned} \tag{6.85}$$

We still need to write the initial conditions, r_0 and p_{r0}, in terms of initial action-angle variables $(\phi_{r0}, \phi_{\theta 0}, I_{r0}, I_{\theta 0})$ as

$$r_0 = \frac{\left[E + \sqrt{E^2 - \omega^2 \tilde{p}_\theta^2}\sin\phi_{r0}\right]^{1/2}}{\omega}, \quad p_{r0} = \frac{\sqrt{E^2 - \omega^2 \tilde{p}_\theta^2}\cos\phi_{r0}}{\left[E + \sqrt{E^2 - \omega^2 \tilde{p}_\theta^2}\sin\phi_{r0}\right]^{1/2}}, \tag{6.86}$$

where E is given by (6.79). Finally, we substitute these expressions in (6.85) to find that

$$\begin{aligned} \mathcal{O}_1(t) &= \frac{E + \sqrt{E^2 - \omega^2 \tilde{p}_\theta^2}\sin(\phi_{r0} + 2\omega t)}{\omega}, \\ \mathcal{O}_2(t) &= \frac{\alpha\omega^2}{E + \sqrt{E^2 - \omega^2 \tilde{p}_\theta^2}\sin(\phi_{r0} + 2\omega t)}. \end{aligned} \tag{6.87}$$

Notice that, despite its appearance, $\mathcal{O}_2(t)$ is continuous everywhere, since the denominator is never zero. Introducing the parameter $a = \sqrt{1 - \omega^2 \tilde{p}_\theta^2/E^2}$, which has the range $0 < a < 1$, we can recast (6.87) in the form

$$\begin{aligned} \mathcal{O}_1(t) &= \frac{E}{\omega}\left[1 + a\sin(\phi_{r0} + 2\omega t)\right], \\ \mathcal{O}_2(t) &= \frac{\alpha\omega^2}{E}\frac{1}{1 + a\sin(\phi_{r0} + 2\omega t)}. \end{aligned} \tag{6.88}$$

The formula (4.77) for the Hannay curvature requires the evaluation of the Poisson bracket $\{\mathcal{O}_1(t_1), \mathcal{O}_2(t_2)\}$ with respect to the initial conditions. We take advantage of the canonical invariance of the bracket and choose to evaluate it in terms of action-angle variables, i.e.,

$$\{\mathcal{O}_1(t_1), \mathcal{O}_2(t_2)\} = \frac{\partial \mathcal{O}_1(t_1)}{\partial \phi_{r0}} \frac{\partial \mathcal{O}_2(t_2)}{\partial I_{r0}} - \frac{\partial \mathcal{O}_1(t_1)}{\partial I_{r0}} \frac{\partial \mathcal{O}_2(t_2)}{\partial \phi_{r0}}. \tag{6.89}$$

Since the $\mathcal{O}_i(t)$ do not depend on $\phi_{\theta 0}$, we omitted the derivatives with respect to it in this expression. Now, given (6.87) we can compute the Poisson bracket taking care of including the dependence on I_r of E and a. We obtain

$$\{\mathcal{O}_1(t_1), \mathcal{O}_2(t_2)\} = \frac{4\alpha\omega^2 \sin\omega(t_1 - t_2)}{E} \left\{ \frac{\cos\omega(t_1 - t_2) + a\sin[\omega(t_1 + t_2) + \phi_{r0}]}{[1 + a\sin(\phi_{r0} + 2\omega t_2)]^2} \right\}. \tag{6.90}$$

The torus average of a function $f(\phi_0)$ for the two degrees of freedom, ϕ_{r0} and $\phi_{\theta 0}$, is

$$\langle f \rangle_0 = \frac{1}{(2\pi)^2} \int_0^{2\pi} \mathrm{d}\phi_{r0} \int_0^{2\pi} \mathrm{d}\phi_{\theta 0}\, f(\phi_0). \tag{6.91}$$

However, the functions $\mathcal{O}_i(t)$ do not depend on $\phi_{\theta 0}$, thus, the average is taken only with respect to ϕ_{r0}. The average of the Poisson bracket, then, is

$$\langle \{\mathcal{O}_1(t_1), \mathcal{O}_2(t_2)\} \rangle_0 = \frac{2\alpha\omega^2 \sin 2\omega(t_1 - t_2)}{E\sqrt{1 - a^2}} = \frac{2\alpha\omega}{\tilde{p}_\theta} \sin 2\omega(t_1 - t_2). \tag{6.92}$$

The final step is to integrate this expression with respect to both t_1 and t_2. The result is easily found using the regularization prescription (2.63). We have that

$$F_{12} = \frac{2\alpha\omega}{\tilde{p}_\theta} \int_{-\infty}^{0} \mathrm{d}t_1 \int_0^{\infty} \mathrm{d}t_2\, \sin 2\omega(t_1 - t_2) = 0, \tag{6.93}$$

just as in the quantum case.

To compute the quantum metric tensor, let us evaluate the torus averages. We begin with the average of each $\mathcal{O}_i$:

$$\langle \mathcal{O}_1(t) \rangle_0 = \frac{1}{2\pi} \int_0^{2\pi} \mathrm{d}\phi_{r0}\, \mathcal{O}_1(t) = \frac{E}{2\pi\omega} \int_0^{2\pi} \mathrm{d}\phi_{r0}\, [1 + a\sin(\phi_{r0} + 2\omega t)] = \frac{E}{\omega}, \tag{6.94}$$

$$\langle \mathcal{O}_2(t) \rangle_0 = \frac{1}{2\pi} \int_0^{2\pi} \mathrm{d}\phi_{r0}\, \mathcal{O}_2(t) = \frac{\alpha\omega^2}{2\pi E} \int_0^{2\pi} \frac{\mathrm{d}\phi_{r0}}{1 + a\sin(\phi_{r0} + 2\omega t)} = \frac{\alpha\omega}{\tilde{p}_\theta}. \tag{6.95}$$

Now, we compute the average of the product of $\mathcal{O}_i$ evaluated at different times:

$$\begin{aligned}\langle \mathcal{O}_1(t_1)\mathcal{O}_1(t_2)\rangle_0 &= \frac{1}{2\pi}\int_0^{2\pi} \mathrm{d}\phi_{r0}\, \mathcal{O}_1(t_1)\mathcal{O}_1(t_2) \\ &= \frac{E^2}{2\pi\omega^2}\int_0^{2\pi} \mathrm{d}\phi_{r0}\, \left[1+a\sin(\phi_{r0}+2\omega t_1)\right]\left[1+a\sin(\phi_{r0}+2\omega t_2)\right] \\ &= \frac{E^2}{\omega^2}\left[1+\frac{a^2}{2}\cos 2\omega(t_2-t_1)\right] \\ &= \frac{E^2}{\omega^2}+\frac{E^2-\omega^2\tilde{p}_\theta^2}{2\omega^2}\cos 2\omega(t_2-t_1). \end{aligned} \tag{6.96}$$

$$\begin{aligned}\langle \mathcal{O}_1(t_1)\mathcal{O}_2(t_2)\rangle_0 &= \frac{1}{2\pi}\int_0^{2\pi} \mathrm{d}\phi_{r0}\, \mathcal{O}_1(t_1)\mathcal{O}_2(t_2) \\ &= \frac{\alpha\omega}{2\pi}\int_0^{2\pi} \mathrm{d}\phi_{r0}\, \frac{1+a\sin(\phi_{r0}+2\omega t_1)}{1+a\sin(\phi_{r0}+2\omega t_2)} \\ &= \alpha\omega\left[1-\frac{1}{\sqrt{1-a^2}}\cos 2\omega(t_2-t_1)\right] \\ &= \frac{\alpha E}{\tilde{p}_\theta}-\frac{\alpha}{\tilde{p}_\theta}\left(E-\omega\tilde{p}_\theta\right)\cos 2\omega(t_2-t_1). \end{aligned} \tag{6.97}$$

$$\begin{aligned}\langle \mathcal{O}_2(t_1)\mathcal{O}_2(t_2)\rangle_0 &= \frac{1}{2\pi}\int_0^{2\pi} \mathrm{d}\phi_{r0}\, \mathcal{O}_2(t_1)\mathcal{O}_2(t_2) \\ &= \frac{\alpha^2\omega^4}{2\pi E^2}\int_0^{2\pi} \frac{\mathrm{d}\phi_{r0}}{\left[1+a\sin(\phi_{r0}+2\omega t_1)\right]\left[1+a\sin(\phi_{r0}+2\omega t_2)\right]} \\ &= \frac{\alpha^2\omega^4}{E^2}\left[\frac{1}{\sqrt{1-a^2}}\frac{1}{1-a^2\cos^2\omega(t_2-t_1)}\right] \\ &= \frac{\alpha^2\omega^3}{E\tilde{p}_\theta}\frac{1}{1-a^2\cos^2\omega(t_2-t_1)}. \end{aligned} \tag{6.98}$$

With these results, we can start calculating the classical metric. The component g_{11} is

$$\begin{aligned} g_{11} &= -\int_{-\infty}^{0} \mathrm{d}t_1 \int_{0}^{\infty} \mathrm{d}t_2 \left[\frac{E^2}{\omega^2} + \frac{E^2-\omega^2\tilde{p}_\theta^2}{2\omega^2}\cos 2\omega(t_2-t_1) - \frac{E^2}{\omega^2}\right] \\ &= -\frac{E^2-\omega^2\tilde{p}_\theta^2}{2\omega^2}\int_{-\infty}^{0} \mathrm{d}t_1 \int_{0}^{\infty} \mathrm{d}t_2 \cos 2\omega(t_2-t_1) \\ &= -\frac{E^2-\omega^2\tilde{p}_\theta^2}{2\omega^2}\left(-\frac{1}{4\omega^2}\right) \\ &= \frac{E^2-\omega^2\tilde{p}_\theta^2}{8\omega^4} \\ &= \frac{I_r^2 + I_r\sqrt{I_\theta^2+\alpha^2}}{2\omega^2}, \end{aligned} \tag{6.99}$$

whereas the component g_{12} is

$$\begin{aligned} g_{12} &= -\int_{-\infty}^{0} \mathrm{d}t_1 \int_{0}^{\infty} \mathrm{d}t_2 \left[\frac{\alpha E}{\tilde{p}_\theta} - \frac{\alpha}{\tilde{p}_\theta}(E-\omega\tilde{p}_\theta)\cos 2\omega(t_2-t_1) - \frac{\alpha E}{\tilde{p}_\theta}\right] \\ &= \frac{\alpha}{\tilde{p}_\theta}(E-\omega\tilde{p}_\theta)\int_{-\infty}^{0} \mathrm{d}t_1 \int_{0}^{\infty} \mathrm{d}t_2 \cos 2\omega(t_2-t_1) \\ &= \frac{\alpha}{\tilde{p}_\theta}(E-\omega\tilde{p}_\theta)\left(-\frac{1}{4\omega^2}\right) \\ &= -\frac{\alpha}{4\omega^2\tilde{p}_\theta}(E-\omega\tilde{p}_\theta) \\ &= \frac{-\alpha I_r}{2\omega\sqrt{I_\theta^2+\alpha^2}}. \end{aligned} \tag{6.100}$$

We see that in both calculations the divergent terms cancel, analogous to the different examples that appear in [58]. Now, the component g_{22} is

$$\begin{aligned} g_{22} &= -\int_{-\infty}^{0} \mathrm{d}t_1 \int_{0}^{\infty} \mathrm{d}t_2 \left[\frac{\alpha^2\omega^3}{E\tilde{p}_\theta}\frac{1}{1-a^2\cos^2\omega(t_2-t_1)} - \frac{\alpha^2\omega^2}{\tilde{p}_\theta^2}\right] \\ &= \frac{\alpha^2\omega^2}{\tilde{p}_\theta^2}\int_{-\infty}^{0} \mathrm{d}t_1 \int_{0}^{\infty} \mathrm{d}t_2 \left[1 - \frac{\sqrt{1-a^2}}{1-a^2\cos^2\omega(t_2-t_1)}\right], \end{aligned} \tag{6.101}$$

where we have left the function inside the brackets in terms of a for easier manipulation. Given the complicated form of the integral and that the divergent terms do not seem to

be canceled, we try an expansion in Fourier series on the second term so that we have to integrate only trigonometric functions as the prescription (2.63) indicates. Defining $T \equiv t_2 - t_1$ and the function $f(T)$ as

$$f(T) \equiv \frac{1}{1 - a^2 \cos^2 \omega T}, \tag{6.102}$$

we Fourier expand it

$$f(T) = \frac{c_0}{2} + \sum_{n=1}^{\infty} c_n \cos\left(\frac{2n\pi T}{P}\right), \tag{6.103}$$

where

$$c_n = \frac{2}{P} \int_0^P \mathrm{d}T\, f(T) \cos\left(\frac{2n\pi T}{P}\right), \quad n = 0, 1, 2, \ldots, \tag{6.104}$$

and P is such that $f(T + P) = f(T)$. Notice that the function $f(T)$ is not singular because of the condition $0 < a < 1$. Since we are dealing with an even function of T, there is no need to include the sine terms in the series. The period P is easily seen to be π/ω, hence, the expression for the nth coefficient of the series is

$$c_n = \frac{2\omega}{\pi} \int_0^{\pi/\omega} \mathrm{d}T\, \frac{\cos 2n\omega T}{1 - a^2 \cos^2 \omega T}. \tag{6.105}$$

Here are listed the first three Fourier coefficients:

$$\begin{aligned} c_0 &= \frac{2}{\sqrt{1 - a^2}}, \\ c_1 &= -\frac{2}{\sqrt{1 - a^2}} + \frac{4}{a^2\sqrt{1 - a^2}} - \frac{4}{a^2}, \\ c_2 &= -\frac{16}{a^4} + \frac{2}{\sqrt{1 - a^2}} - \frac{16}{a^2\sqrt{1 - a^2}} + \frac{8}{a^2} + \frac{16}{a^4\sqrt{1 - a^2}}. \end{aligned} \tag{6.106}$$

With the Fourier expansion, the component g_{22} of the classical metric is

$$\begin{aligned} g_{22} &= \frac{\alpha^2\omega^2}{\tilde{p}_\theta^2} \int_{-\infty}^0 \mathrm{d}t_1 \int_0^{\infty} \mathrm{d}t_2 \left[1 - \sqrt{1 - a^2}\left(\frac{1}{\sqrt{1 - a^2}} + \sum_{n=1}^{\infty} c_n \cos 2n\omega T\right)\right] \\ &= -\frac{\alpha^2\omega^2}{\tilde{p}_\theta^2}\sqrt{1 - a^2} \sum_{n=1}^{\infty} c_n \int_{-\infty}^0 \mathrm{d}t_1 \int_0^{\infty} \mathrm{d}t_2\, \cos 2n\omega(t_2 - t_1) \\ &= \frac{\alpha^2}{4\tilde{p}_\theta^2}\sqrt{1 - a^2} \sum_{n=1}^{\infty} \frac{c_n}{n^2} \\ &= \frac{\alpha^2\omega}{4\tilde{p}_\theta E} \sum_{n=1}^{\infty} \frac{c_n}{n^2}. \end{aligned} \tag{6.107}$$

Here, it is evident how the divergent terms cancel each other. A closed expression for g_{22} can be given provided that we use the expression for the nth Fourier coefficient (6.105) and interchange the sum and integral symbols:

$$g_{22} = \frac{\alpha^2\omega^2}{2\pi\tilde{p}_\theta E}\int_0^{\pi/\omega} \mathrm{d}T \left(\sum_{n=1}^{\infty}\frac{\cos 2n\omega T}{n^2}\frac{1}{1-a^2\cos^2\omega T}\right). \tag{6.108}$$

Noting that the quadratic Bernoulli polynomial, $B_2(x) = x^2 - x + \frac{1}{6}$, has the series representation [99]

$$B_2(x) = \frac{1}{\pi^2}\sum_{n=1}^{\infty}\frac{\cos 2n\pi x}{n^2}, \quad 0 \le x \le 1, \tag{6.109}$$

we can set $x = \omega T/\pi$ to get

$$\sum_{n=1}^{\infty}\frac{\cos 2n\omega T}{n^2} = \pi\left(\frac{\pi}{6} - \omega T + \frac{\omega^2 T^2}{\pi}\right), \tag{6.110}$$

which, upon substitution into (6.108), yields

$$g_{22} = \frac{\alpha^2\omega^2}{2\tilde{p}_\theta E}\left(\frac{\pi}{6}\mathcal{I}_1 - \omega\mathcal{I}_2 + \frac{\omega^2}{\pi}\mathcal{I}_3\right). \tag{6.111}$$

The three integrals that appear are

$$\begin{aligned}
\mathcal{I}_1 &= \int_0^{\pi/\omega}\mathrm{d}T\,\frac{1}{1-a^2\cos^2\omega T},\\
\mathcal{I}_2 &= \int_0^{\pi/\omega}\mathrm{d}T\,\frac{T}{1-a^2\cos^2\omega T},\\
\mathcal{I}_3 &= \int_0^{\pi/\omega}\mathrm{d}T\,\frac{T^2}{1-a^2\cos^2\omega T}.
\end{aligned} \tag{6.112}$$

The first and the second have the simple results

$$\mathcal{I}_1 = \frac{\pi}{\omega\sqrt{1-a^2}} = \frac{\pi E}{\omega^2\tilde{p}_\theta}, \quad \mathcal{I}_2 = \frac{\pi^2}{2\omega^2\sqrt{1-a^2}} = \frac{\pi^2 E}{2\omega^3\tilde{p}_\theta}, \tag{6.113}$$

whereas the third one turns out to be

$$\mathcal{I}_3 = \frac{\pi}{\omega^3\sqrt{1-a^2}}\left[\frac{\pi^2}{3} + \mathrm{Li}_2\beta\right], \tag{6.114}$$

with $\beta \equiv \frac{2-a^2-2\sqrt{1-a^2}}{a^2}$ bounded between 0 and 1. The function $\mathrm{Li}_2(z)$ is the dilogarithm defined as [99]

$$\mathrm{Li}_2(z) = \int_z^0 \mathrm{d}t\, \frac{\ln(1-t)}{t}, \tag{6.115}$$

or, equivalently,

$$\mathrm{Li}_2(z) = \sum_{n=1}^{\infty} \frac{z^n}{n^2}, \quad |z| < 1. \tag{6.116}$$

Substitution of a gives

$$\mathcal{I}_3 = \frac{\pi E}{\omega^4 \tilde{p}_\theta} \left[\frac{\pi^2}{3} + \mathrm{Li}_2 \left(\frac{E - \omega \tilde{p}_\theta}{E + \omega \tilde{p}_\theta} \right) \right]. \tag{6.117}$$

Thus, the metric component g_{22} simplifies to

$$g_{22} = \frac{\alpha^2}{2\tilde{p}_\theta^2} \mathrm{Li}_2 \left(\frac{I_r}{I_r + \tilde{p}_\theta} \right). \tag{6.118}$$

The determinant of the classical metric is

$$\det g_{ij} = \frac{\alpha^2 I_r^2}{4\omega^2 \tilde{p}_\theta^2} \left[\left(1 + \frac{\tilde{p}_\theta}{I_r} \right) \mathrm{Li}_2 \left(\frac{I_r}{I_r + \tilde{p}_\theta} \right) - 1 \right]. \tag{6.119}$$

We now set out to compare the quantum and classical metrics. It is easily verified that the components g_{11} and g_{12} of both metrics follow the rule $g_{ij} = \hbar^2 g_{ij}^{(0)}$ provided that we use the quantization conditions

$$I_r = \frac{\hbar}{2}, \quad I_r^2 = \frac{\hbar^2}{2}, \quad I_\theta = 0. \tag{6.120}$$

Regarding the component g_{22} of the classical metric, we expand it in a Taylor series in I_r and find

$$g_{22} = \frac{I_r}{2\alpha} - \frac{3I_r^2}{8\alpha^2} + \frac{11I_r^3}{36\alpha^3} - \frac{25I_r^4}{96\alpha^4} + \frac{137I_r^5}{600\alpha^5} - \frac{49I_r^6}{240\alpha^6} + \mathcal{O}\left(I_r^7\right). \tag{6.121}$$

In order to contrast this result with the quantum computation, we try an expansion on the trigamma function that appears in the element $g_{22}^{(0)}$. We first define the variable $z \equiv \alpha/\hbar$, and employ the recurrence relation

$$\psi_1(1+z) = \psi_1(z) - \frac{1}{z^2}. \tag{6.122}$$

Now, we make use of the asymptotic expansion of the trigamma function [97]:

$$\psi_1(z) \approx \frac{1}{z} + \frac{1}{2z^2} + \frac{1}{6z^3} - \frac{1}{30z^5} + \frac{1}{42z^7} + \mathcal{O}\left(\frac{1}{z^9}\right), \tag{6.123}$$

which is valid when $z \to \infty$, or, equivalently, when $\hbar/\alpha \to 0$. This yields

$$\hbar^2 g_{22}^{(0)} \approx \frac{\hbar}{4\alpha} - \frac{\hbar^2}{8\alpha^2} + \frac{\hbar^3}{24\alpha^3} - \frac{\hbar^5}{120\alpha^5} + \mathcal{O}(\hbar^7). \tag{6.124}$$

If we want to match the classical and quantum results, we should set the following quantization rules:

$$I_r/\hbar = 1/2,\ I_r^2/\hbar^2 = 1/3,\ I_r^3/\hbar^3 = 3/22,\ I_r^4/\hbar^4 = 0,\ I_r^5/\hbar^5 = -\frac{5}{137}. \tag{6.125}$$

Notice that, analogous to the quartic anharmonic oscillator that appears in [67], we have different quantization conditions for every power of the action variable. This only indicates that in order to get a better concordance, the semiclassical approximation must get further contributions from superior powers of $\hbar$. Another possibility to compare the quantum and classical results is to take $I_r = \hbar/2$, which is suggested by the matching of the other metric components. Using this condition, we get

$$g_{22}(I_r = \hbar/2, I_\theta = 0) = \frac{\hbar}{4\alpha} - \frac{3\hbar^2}{32\alpha^2} + \frac{11\hbar^3}{288\alpha^3} - \frac{25\hbar^4}{1536\alpha^4} + \frac{137\hbar^5}{19200\alpha^5} - \frac{49\hbar^6}{15360\alpha^6} + \mathcal{O}(\hbar^7). \tag{6.126}$$

We can see that the first term is in perfect agreement with the quantum expression (6.124). In Table 6.1, subsequent terms corresponding to higher powers of $\hbar$ are shown for both the classical and quantum case.

Power of $\hbar$	Classical g_{22}	Quantum $g_{22}^{(0)}$
2	$-\frac{3}{32} \approx -0.09375$	$-\frac{1}{8} = -0.125$
3	$\frac{11}{288} \approx 0.03819$	$\frac{1}{24} \approx 0.04166$
4	$-\frac{25}{1536} \approx -0.0162$	0

Table 6.1: Comparison of the classical and quantum g_{22} components of the metric. In the classical case, we have taken $I_r = \hbar/2$.

6.4 Spin-half particle in an external magnetic field

We now consider a spin 1/2 particle in a magnetic field which varies adiabatically. This system was studied by Berry [6], who found the famous result that the geometrical phase is proportional to the solid angle subtended by the curve that the magnetic field vector traces in space during its adiabatic evolution. We would like now to address the classical counterpart of this system. To do so, we follow the analysis of Gozzi, Thacker and Rohrlich [100, 101], and from there, we compute the classical metric and the Hannay

curvature. We work with two complex Grassmann variables such that $\psi_a\psi_b + \psi_b\psi_a = 0$, $(a, b = 1, 2)$ to treat the spin from a classical standpoint (for details, see Appendix B). The Lagrangian of the systems is

$$L = i\psi^\dagger\dot{\psi} - \psi^\dagger M(\boldsymbol{B})\psi, \tag{6.127}$$

where $\psi = (\psi_1, \psi_2)^T$, $\boldsymbol{B} = (B_1, B_2, B_3)$ and

$$M(\boldsymbol{B}) = \sum_{i=1}^{3} B_i\sigma^i = \begin{pmatrix} B_3 & B_1 - iB_2 \\ B_1 + iB_2 & -B_3 \end{pmatrix}, \tag{6.128}$$

with σ^i the Pauli matrices. To build the associated Hamiltonian, we must find the momenta Π_a. We define them using the right derivative as

$$\Pi_a = L\frac{\overleftarrow{\partial}}{\partial\dot{\psi}_a} = i\psi_a^*, \tag{6.129}$$

so that the Hamiltonian is

$$H = \Pi_1\dot{\psi}_1 + \Pi_2\dot{\psi}_2 - L = \psi^\dagger M(\boldsymbol{B})\psi. \tag{6.130}$$

Hence, in expanded form, the Hamiltonian reads

$$H = B_3\psi_1^*\psi_1 + (B_1 - iB_2)\psi_1^*\psi_2 + (B_1 + iB_2)\psi_2^*\psi_1 - B_3\psi_2^*\psi_2. \tag{6.131}$$

The Poisson brackets of two functions $f(\psi, \psi^*)$ and $g(\psi, \psi^*)$ are defined as

$$\{f, g\} = i\sum_{a=1}^{2}\left(f\frac{\overleftarrow{\partial}}{\partial\psi_a^*}\frac{\overrightarrow{\partial}}{\partial\psi_a}g + f\frac{\overleftarrow{\partial}}{\partial\psi_a}\frac{\overrightarrow{\partial}}{\partial\psi_a^*}g\right), \tag{6.132}$$

which leads to the following fundamental brackets:

$$\{\psi_a, \psi_b\} = \{\psi_a^*, \psi_b^*\} = 0, \quad \{\psi_a, \psi_b^*\} = i\delta_{ab}. \tag{6.133}$$

To compute the classical metric, we take as our adiabatic parameters the three components of the magnetic field, i.e., $x = \{x^i\} = (B_1, B_2, B_3)$. First, we need the functions $\mathcal{O}_i(t)$, which are easily found to be

$$\mathcal{O}_i(t) = \left(\frac{\partial H}{\partial B_i}\right)_{\psi^\dagger,\psi} = \sum_{a,b}\psi_a^*(t)\sigma_{ab}^i\psi_b(t) = \psi^\dagger(t)\sigma^i\psi(t). \tag{6.134}$$

Since the Hamiltonian couples both degrees of freedom, it is necessary to find the normal modes by diagonalizing M through a unitary matrix U given by

$$U = \begin{pmatrix} \frac{B_1 - iB_2}{\sqrt{2B(B - B_3)}} & \frac{B_1 - iB_2}{\sqrt{2B(B + B_3)}} \\ \frac{\sqrt{B - B_3}}{\sqrt{2B}} & -\frac{\sqrt{B + B_3}}{\sqrt{2B}} \end{pmatrix}. \tag{6.135}$$

This yields

$$\tilde{M} = U^\dagger M U = \begin{pmatrix} \Omega_1 & 0 \\ 0 & \Omega_2 \end{pmatrix} = \begin{pmatrix} B & 0 \\ 0 & -B \end{pmatrix}, \tag{6.136}$$

where $B = \sqrt{B_1^2 + B_2^2 + B_3^2}$. The diagonalization procedure induces the transformation $\psi = U\tilde{\psi}$, so that the transformed Lagrangian and Hamiltonian now read

$$L = i(\tilde{\psi}_1^* \dot{\tilde{\psi}}_1 + \tilde{\psi}_2^* \dot{\tilde{\psi}}_2) - \Omega_1 \tilde{\psi}_1^* \tilde{\psi}_1 - \Omega_2 \tilde{\psi}_2^* \tilde{\psi}_2, \tag{6.137}$$

$$H = \Omega_1 \tilde{\psi}_1^* \tilde{\psi}_1 + \Omega_2 \tilde{\psi}_2^* \tilde{\psi}_2. \tag{6.138}$$

The momenta of the normal modes are

$$\tilde{\Pi}_a = L \frac{\overleftarrow{\partial}}{\partial \dot{\tilde{\psi}}_a} = i\tilde{\psi}_a^*, \tag{6.139}$$

and the equations of motion turn out to be

$$\dot{\tilde{\psi}}_a = \{H, \tilde{\psi}_a\} = -i\Omega_a \tilde{\psi}_a, \quad \dot{\tilde{\psi}}_a^* = \{H, \tilde{\psi}_a^*\} = i\Omega_a \tilde{\psi}_a^*, \tag{6.140}$$

which possess the solutions

$$\tilde{\psi}_a(t) = \tilde{\psi}_a(0) e^{-i\Omega_a t}, \quad \tilde{\psi}_a^*(t) = \tilde{\psi}_a^*(0) e^{i\Omega_a t}. \tag{6.141}$$

Thus, the action variables are

$$I_a = \frac{1}{2\pi} \oint \mathrm{d}t \tilde{\Pi}_a(t) \dot{\tilde{\psi}}_a(t) = \tilde{\psi}_a^*(0)\tilde{\psi}_a(0), \tag{6.142}$$

and the Hamiltonian takes the simple form

$$H = \Omega_1 I_1 + \Omega_2 I_2 = B(I_1 - I_2). \tag{6.143}$$

We can find the angle variables as

$$\dot{\phi}_a = \frac{\partial H}{\partial I_a} = \Omega_a, \tag{6.144}$$

which implies that

$$\phi_a(t) = \Omega_a t + \phi_{a0}, \tag{6.145}$$

where $\phi_{a0} \equiv \phi_a(0)$. Hence, the solutions in terms of initial angle variables and time are

$$\tilde{\psi}_a(t) = \tilde{\psi}_a(0) e^{-i\phi_{a0}} e^{-i\Omega_a t}, \tag{6.146}$$

and their corresponding complex conjugate. They allow us to express the $\mathcal{O}_i(t)$ in terms of normal coordinates as

$$\mathcal{O}_i(t) = \psi^\dagger(t)\sigma^i\psi(t) = \tilde{\psi}^\dagger(t) U^\dagger \sigma^i U \tilde{\psi}(t) = \tilde{\psi}^\dagger(t)\tilde{\sigma}^i\tilde{\psi}(t), \tag{6.147}$$

where we have defined $\tilde{\sigma}^i \equiv U^\dagger \sigma^i U$. Substituting (6.146), we find the $\mathcal{O}_i$ in terms of initial conditions as

$$\mathcal{O}_i(t) = \sum_{a,b} \tilde{\psi}_a^*(0)\tilde{\psi}_b(0) e^{i(\Omega_a - \Omega_b)t} e^{i(\phi_{a0}-\phi_{b0})} \tilde{\sigma}^i_{ab}. \tag{6.148}$$

The $\tilde{\sigma}^i$ are

$$\tilde{\sigma}^1 = \begin{pmatrix} \frac{B_1}{B} & -\frac{B_1 B_3 + iB_2 B}{B\sqrt{B_1^2+B_2^2}} \\ -\frac{B_1 B_3 - iB_2 B}{B\sqrt{B_1^2+B_2^2}} & -\frac{B_1}{B} \end{pmatrix}, \quad \tilde{\sigma}^2 = \begin{pmatrix} \frac{B_2}{B} & -\frac{B_2 B_3 - iB_1 B}{B\sqrt{B_1^2+B_2^2}} \\ -\frac{B_2 B_3 + iB_1 B}{B\sqrt{B_1^2+B_2^2}} & -\frac{B_2}{B} \end{pmatrix},$$
$$\tilde{\sigma}^3 = \begin{pmatrix} \frac{B_3}{B} & \frac{\sqrt{B_1^2+B_2^2}}{B} \\ \frac{\sqrt{B_1^2+B_2^2}}{B} & -\frac{B_3}{B} \end{pmatrix}. \tag{6.149}$$

We now calculate the average of $\mathcal{O}_i(t)$:

$$\langle \mathcal{O}_i(t) \rangle_0 = \sum_{a,b} \tilde{\psi}_a^*(0)\tilde{\psi}_b(0) e^{i(\Omega_a - \Omega_b)t} \tilde{\sigma}^i_{ab} \langle e^{i(\phi_{a0}-\phi_{b0})} \rangle. \tag{6.150}$$

Since $\langle e^{i(\phi_{a0}-\phi_{b0})} \rangle_0 = \delta_{ab}$, we have that

$$\langle \mathcal{O}_i(t) \rangle_0 = \sum_a \tilde{\psi}_a^*(0)\tilde{\psi}_a(0)\tilde{\sigma}^i_{aa} = \sum_a I_a \tilde{\sigma}^i_{aa}. \tag{6.151}$$

The remaining average is $\langle \mathcal{O}_i(t_1)\mathcal{O}_j(t_2) \rangle_0$. We find

$$\langle \mathcal{O}_i(t_1)\mathcal{O}_j(t_2) \rangle_0 = \sum_{a,b,c,d} \tilde{\psi}_a^*(0)\tilde{\psi}_b(0)\tilde{\psi}_c^*(0)\tilde{\psi}_d(0) e^{i[(\Omega_a-\Omega_b)t_1 + (\Omega_c-\Omega_d)t_2]} \tilde{\sigma}^i_{ab}\tilde{\sigma}^j_{cd} \langle e^{i(\phi_{a0}-\phi_{b0}+\phi_{c0}-\phi_{d0})} \rangle. \tag{6.152}$$

Taking into account that

$$\langle e^{i(\phi_{a0}-\phi_{b0}+\phi_{c0}-\phi_{d0})} \rangle_0 = \delta_{ab}\delta_{cd} + \delta_{a1}\delta_{b2}\delta_{c2}\delta_{d1} + \delta_{a2}\delta_{b1}\delta_{c1}\delta_{d2}, \tag{6.153}$$

this simplifies to

$$\begin{aligned} \langle \mathcal{O}_i(t_1)\mathcal{O}_j(t_2) \rangle_0 = \sum_{a,c} & \tilde{\psi}_a^*(0)\tilde{\psi}_a(0)\tilde{\psi}_c^*(0)\tilde{\psi}_c(0)\tilde{\sigma}^i_{aa}\tilde{\sigma}^j_{cc} \\ & + \tilde{\psi}_1^*(0)\tilde{\psi}_2(0)\tilde{\psi}_2^*(0)\tilde{\psi}_1(0) e^{i(\Omega_1-\Omega_2)(t_1-t_2)} \tilde{\sigma}^i_{12}\tilde{\sigma}^j_{21} \\ & + \tilde{\psi}_2^*(0)\tilde{\psi}_1(0)\tilde{\psi}_1^*(0)\tilde{\psi}_2(0) e^{-i(\Omega_1-\Omega_2)(t_1-t_2)} \tilde{\sigma}^i_{21}\tilde{\sigma}^j_{12}. \end{aligned} \tag{6.154}$$

Further simplification can be made by realizing that in the second line we can move $\tilde{\psi}_2^*(0)$ to the left of $\tilde{\psi}_2(0)$ at the cost of a minus sign, and similarly with $\tilde{\psi}_1^*(0)$ in the third line. This manipulation results in

$$\langle \mathcal{O}_i(t_1)\mathcal{O}_j(t_2) \rangle_0 = \sum_{a,c} I_a I_c \tilde{\sigma}^i_{aa}\tilde{\sigma}^j_{cc} - I_1 I_2 \left[e^{i(\Omega_1-\Omega_2)(t_1-t_2)} \tilde{\sigma}^i_{12}\tilde{\sigma}^j_{21} + e^{-i(\Omega_1-\Omega_2)(t_1-t_2)} \tilde{\sigma}^i_{21}\tilde{\sigma}^j_{12} \right]. \tag{6.155}$$

Hence, the integrands $\Lambda_{ij}(t_1,t_2) \equiv \langle \mathcal{O}_i(t_1)\mathcal{O}_j(t_2)\rangle_0 - \langle \mathcal{O}_i(t_1)\rangle_0\langle \mathcal{O}_j(t_2)\rangle_0$ reduce to

$$\Lambda_{ij}(t_1,t_2) = -I_1 I_2 \left[e^{i(\Omega_1-\Omega_2)(t_1-t_2)}\tilde{\sigma}^i_{12}\tilde{\sigma}^j_{21} + e^{-i(\Omega_1-\Omega_2)(t_1-t_2)}\tilde{\sigma}^i_{21}\tilde{\sigma}^j_{12}\right], \tag{6.156}$$

which, integrated in time gives

$$g_{ij} = -\frac{I_1 I_2}{4B^2}\left(\tilde{\sigma}^i_{12}\tilde{\sigma}^j_{21} + \tilde{\sigma}^i_{21}\tilde{\sigma}^j_{12}\right). \tag{6.157}$$

Expressed in matrix form, the classical metric tensor is

$$g_{ij} = -\frac{I_1 I_2}{2B^4}\begin{pmatrix} B_2^2+B_3^2 & -B_1B_2 & -B_1B_3 \\ -B_1B_2 & B_1^2+B_3^2 & -B_2B_3 \\ -B_1B_3 & -B_2B_3 & B_1^2+B_2^2 \end{pmatrix}. \tag{6.158}$$

In order to compare this result with the quantum metric tensor, we need to remember that the quantum system is described by a two-dimensional Hilbert space which is spanned by the eigenstates with spin projections $+1/2$ and $-1/2$. The calculations will not be shown here, but they can be consulted in [4]. The result, in spherical coordinates, is

$$g^{(+)}_{ij} = g^{(-)}_{ij} = \frac{1}{4}\begin{pmatrix} 0 & 0 & 0 \\ 0 & 1 & 0 \\ 0 & 0 & \sin^2\theta \end{pmatrix}, \tag{6.159}$$

where θ is the polar angle between the magnetic field $\boldsymbol{B}$ and the z axis. Using the tensor transformation rule, we find that in Cartesian coordinates, the quantum metric tensor has the form

$$g^{(+)}_{ij} = g^{(-)}_{ij} = \frac{1}{4B^4}\begin{pmatrix} B_2^2+B_3^2 & -B_1B_2 & -B_1B_3 \\ -B_1B_2 & B_1^2+B_3^2 & -B_2B_3 \\ -B_1B_3 & -B_2B_3 & B_1^2+B_2^2 \end{pmatrix}. \tag{6.160}$$

Notice that the quantum and classical metric tensors are related by

$$g_{ij} = -2I_1I_2 g^{(\pm)}_{ij}. \tag{6.161}$$

This shows that the classical metric reproduces the parameter structure of its quantum counterpart. Finally, it is not difficult to verify that the determinant of (6.158) is zero. We can obtain a non-vanishing determinant fixing one parameter, for instance, $B_1 = B_{10} = const.$, which has the effect of eliminating the first row and column of (6.158). Hence, we are left with a reduced metric

$$g^{\rm red}_{ij}(B_1 = B_{10}) = -\frac{I_1 I_2}{2B^4}\begin{pmatrix} B_{10}^2+B_3^2 & -B_2B_3 \\ -B_2B_3 & B_{10}^2+B_2^2 \end{pmatrix}, \tag{6.162}$$

with determinant

$$\det g_{ij}^{\rm red}(B_1 = B_{10}) = \frac{I_1^2 I_2^2 B_{10}^2}{4B^6}, \tag{6.163}$$

which is different from zero as long as $B_{10} \neq 0$.

To compute the Hannay curvature, we recall that the Poisson brackets are invariant under unitary transformations [101], which allows us to take the bracket with respect to the normal coordinates as

$$\{\mathcal{O}_i(t_1), \mathcal{O}_j(t_2)\} = i \sum_a \left(\mathcal{O}_i(t_1) \frac{\overleftarrow{\partial}}{\partial \tilde{\psi}_a^*(0)} \frac{\overrightarrow{\partial}}{\partial \tilde{\psi}_a(0)} \mathcal{O}_j(t_2) + \mathcal{O}_i(t_1) \frac{\overleftarrow{\partial}}{\partial \tilde{\psi}_a(0)} \frac{\overrightarrow{\partial}}{\partial \tilde{\psi}_a^*(0)} \mathcal{O}_j(t_2) \right). \tag{6.164}$$

This yields

$$\{\mathcal{O}_i(t_1), \mathcal{O}_j(t_2)\} = i \sum_{a,b,c} \tilde{\psi}_b^*(0) \tilde{\psi}_c(0) N_{abc}^{ij}(t_1, t_2) e^{i(\phi_{b0} - \phi_{c0})}, \tag{6.165}$$

where

$$N_{abc}^{ij}(t_1, t_2) \equiv -e^{i[(\Omega_a - \Omega_c)t_1 + (\Omega_b - \Omega_a)t_2]} \tilde{\sigma}_{ac}^i \tilde{\sigma}_{ba}^j + e^{i[(\Omega_b - \Omega_a)t_1 + (\Omega_a - \Omega_c)t_2]} \tilde{\sigma}_{ba}^i \tilde{\sigma}_{ac}^j. \tag{6.166}$$

The average results in

$$\begin{aligned} \langle \{\mathcal{O}_i(t_1), \mathcal{O}_j(t_2)\} \rangle_0 &= i \sum_{a,b} I_b \left[-e^{i(\Omega_a - \Omega_b)(t_1 - t_2)} \tilde{\sigma}_{ab}^i \tilde{\sigma}_{ba}^j + e^{-i(\Omega_a - \Omega_b)(t_1 - t_2)} \tilde{\sigma}_{ba}^i \tilde{\sigma}_{ab}^j \right] \\ &= i(I_1 - I_2) \left[e^{i(\Omega_1 - \Omega_2)(t_1 - t_2)} \tilde{\sigma}_{12}^i \tilde{\sigma}_{21}^j - e^{-i(\Omega_1 - \Omega_2)(t_1 - t_2)} \tilde{\sigma}_{21}^i \tilde{\sigma}_{12}^j \right] \end{aligned} \tag{6.167}$$

and, upon integration with respect to t_1 and t_2, it is found that

$$F_{ij} = \frac{i}{4B^2} (I_1 - I_2) \left(\tilde{\sigma}_{21}^i \tilde{\sigma}_{12}^j - \tilde{\sigma}_{12}^i \tilde{\sigma}_{21}^j \right) \tag{6.168}$$

In terms of components, we have

$$F_{23} = \frac{(I_1 - I_2)}{2B^3} B_1, \quad F_{31} = \frac{(I_1 - I_2)}{2B^3} B_2, \quad F_{12} = \frac{(I_1 - I_2)}{2B^3} B_3, \tag{6.169}$$

which matches the result that Gozzi and Thacker [100] found using the standard definition of the Hannay curvature. It is easily seen that the relationship between the classical and quantum curvatures is

$$F_{ij} = -(I_1 - I_2) F_{ij}^{(+)} = (I_1 - I_2) F_{ij}^{(-)}. \tag{6.170}$$

Chapter 7

Application to the Dicke model

In this chapter, we analyze the parameter space geometry of the Dicke model with the aid of the classical and quantum metrics, as well as their corresponding scalar curvatures. This is the first place where the developed geometric tools are applied to the study of quantum phase transitions. In particular, through the application of the truncated Holstein-Primakoff transformation, we find that in the thermodynamic limit, the classical and quantum metrics have the same divergent behavior near the quantum phase transition, as opposed to their corresponding scalar curvatures which approach the same value there. We also see that under resonance conditions, both scalar curvatures show a divergence at the critical point.

The Dicke model [102] is a well-known model in quantum optics. It describes a collection of $\mathcal{N}$ two-level atoms interacting with one mode of a bosonic field inside a cavity. Its quantum and classical dynamics have been explored [103–105], and it has been widely studied in the context of quantum and classical chaos [106–111], entanglement and fidelity-related measures [112–117].

The Hamiltonian of the Dicke model is

$$\hat{H} = \omega_0 \hat{J}_z + \omega \hat{a}^\dagger \hat{a} + \frac{\lambda}{\sqrt{\mathcal{N}}}(\hat{a}^\dagger + \hat{a})(\hat{J}_+ + \hat{J}_-), \tag{7.1}$$

where ω_0 is the splitting of the two levels, ω is the frequency of the bosonic mode, λ is the coupling of the dipole interaction between the field and the atoms, $\hat{a}$ and $\hat{a}^\dagger$ are the creation and annihilation operators of the field, and $\hat{J}_z$, $\hat{J}_\pm = \hat{J}_x \pm i\hat{J}_y$ are the collective spin operators. Also, we have chosen $\hbar = 1$. We see that the operator $\hat{J}^2 = \hat{J}_x^2 + \hat{J}_y^2 + \hat{J}_z^2$ commutes with the Hamiltonian, which implies that the total pseudospin is conserved and we can restrict ourselves, as usual, to the consideration of the maximum pseudospin $j = \mathcal{N}/2$. This has the effect of treating the collection of $\mathcal{N}$ two-level atoms as a single $(\mathcal{N}+1)$-level system with pseudospin $j = \mathcal{N}/2$ [106, 107]. We are interested in the thermodynamic limit $j \to \infty$, where the system undergoes a quantum phase transition at the critical coupling $\lambda = \lambda_c \equiv \frac{\sqrt{\omega\omega_0}}{2}$ that separates the normal phase, $\lambda < \lambda_c$, and the superradiant phase, $\lambda > \lambda_c$.

7.1 Analysis in the thermodynamic limit

7.1.1 Normal phase

To describe the system in the thermodynamic limit, we follow the work of Emary and Brandes [106, 107]. We first use the Holstein-Primakoff transformation [118]

$$\hat{J}_+ = \hat{b}^\dagger \sqrt{2j - \hat{b}^\dagger \hat{b}}, \quad \hat{J}_- = \sqrt{2j - \hat{b}^\dagger \hat{b}}\, \hat{b}, \quad \hat{J}_z = \hat{b}^\dagger \hat{b} - j, \tag{7.2}$$

which is a way to associate the bosonic operators $\hat{b}$ and $\hat{b}^\dagger$ to the angular momentum operators $\hat{J}_z, \hat{J}_\pm$. After performing this transformation, the Dicke Hamiltonian takes the form

$$\hat{H} = -j\omega_0 + \omega_0 \hat{b}^\dagger \hat{b} + \omega \hat{a}^\dagger \hat{a} + \lambda(\hat{a}^\dagger + \hat{a}) \left(\hat{b}^\dagger \sqrt{1 - \frac{\hat{b}^\dagger \hat{b}}{2j}} + \sqrt{1 - \frac{\hat{b}^\dagger \hat{b}}{2j}}\, \hat{b} \right). \tag{7.3}$$

Next, we expand the square roots and take the limit $j \to \infty$, keeping only the zeroth order term in $1/j$. This leads to the effective Hamiltonian

$$\hat{H}_n = -j\omega_0 + \omega_0 \hat{b}^\dagger \hat{b} + \omega \hat{a}^\dagger \hat{a} + \lambda(\hat{a}^\dagger + \hat{a})(\hat{b}^\dagger + \hat{b}), \tag{7.4}$$

which is valid for $\lambda < \lambda_c$, i.e., the normal phase. It is important to mention that this approach is valid only in the low energy region where the classical Hamiltonian corresponding to (7.1) has regular dynamics [110]. The term proportional to j, which is dominant as j increases, is identified as the ground state energy of the model in the normal phase. From (7.4), we readily recognize that this Hamiltonian corresponds to two coupled harmonic oscillators, as can be explicitly seen by applying the operator transformation

$$\begin{aligned} \hat{q}_1 &= \frac{1}{\sqrt{2\omega}}(\hat{a}^\dagger + \hat{a}), \qquad \hat{p}_1 = i\sqrt{\frac{\omega}{2}}(\hat{a}^\dagger - \hat{a}), \\ \hat{q}_2 &= \frac{1}{\sqrt{2\omega_0}}(\hat{b}^\dagger + \hat{b}), \qquad \hat{p}_2 = i\sqrt{\frac{\omega_0}{2}}(\hat{b}^\dagger - \hat{b}), \end{aligned} \tag{7.5}$$

which casts it in the position-momentum representation as

$$\hat{H}_n = -j\omega_0 - \frac{(\omega + \omega_0)}{2} + \frac{1}{2}\left(\hat{p}_1^2 + \hat{p}_2^2 + \omega^2 \hat{q}_1^2 + \omega_0^2 \hat{q}_2^2 + 4\lambda\sqrt{\omega\omega_0}\, \hat{q}_1 \hat{q}_2 \right). \tag{7.6}$$

We can uncouple the two oscillators by going to the normal coordinates $(\hat{Q}_1, \hat{Q}_2)$ through the transformation

$$\begin{pmatrix} \hat{q}_1 \\ \hat{q}_2 \end{pmatrix} = \begin{pmatrix} \cos\alpha_n & \sin\alpha_n \\ -\sin\alpha_n & \cos\alpha_n \end{pmatrix} \begin{pmatrix} \hat{Q}_1 \\ \hat{Q}_2 \end{pmatrix}, \tag{7.7}$$

and similarly for the corresponding conjugate normal momenta $(\hat{P}_1, \hat{P}_2)$. The angle α_n is such that

$$\tan 2\alpha_n = \frac{4\lambda\sqrt{\omega\omega_0}}{\omega_0^2 - \omega^2}, \tag{7.8}$$

with $\tan\alpha_n \in \left(-\frac{\pi}{4}, \frac{\pi}{4}\right)$, and we assume that $\omega_0 \neq \omega$. After performing this transformation, the Hamiltonian acquires the form

$$\hat{H}_n = -j\omega_0 - \frac{(\omega+\omega_0)}{2} + \frac{1}{2}\left(\hat{P}_1^2 + \hat{P}_2^2 + \varepsilon_{1n}^2\hat{Q}_1^2 + \varepsilon_{2n}^2\hat{Q}_2^2\right), \tag{7.9}$$

where the two (squared) normal frequencies are

$$\begin{aligned}\varepsilon_{1n}^2 &= \frac{1}{2}\left[\omega^2 + \omega_0^2 - \sqrt{(\omega^2-\omega_0^2)^2 + 16\lambda^2\omega\omega_0}\right], \\ \varepsilon_{2n}^2 &= \frac{1}{2}\left[\omega^2 + \omega_0^2 + \sqrt{(\omega^2-\omega_0^2)^2 + 16\lambda^2\omega\omega_0}\right].\end{aligned} \tag{7.10}$$

We clearly see that at the critical coupling $\lambda_c = \frac{\sqrt{\omega\omega_0}}{2}$, the normal frequency ε_{1n} vanishes and the system reduces effectively to only one normal mode. This feature signals the quantum phase transition of the model [106, 107].

7.1.2 Superradiant phase

In the case of the superradiant phase ($\lambda > \lambda_c$), one can derive an effective Hamiltonian $\hat{H}_s$ by letting the field and the set of atoms acquire macroscopic occupation numbers; one way to achieve this is by displacing the bosonic operators that appear in (7.3) and demanding that the linear terms in $\hat{a}$ and $\hat{a}^\dagger$ vanish. After expanding the square roots and changing to the position-momentum representation, we arrive to the Hamiltonian for the superradiant phase which reads [106, 107]

$$\hat{H}_s = -j\left(\frac{2\lambda^2}{\omega} + \frac{\omega_0^2\omega}{8\lambda^2}\right) - \frac{4\lambda^2+\omega^2}{2\omega} + \frac{1}{2}\left(\hat{p}_1^2 + \hat{p}_2^2 + \omega^2\hat{q}_1^2 + \frac{16\lambda^4}{\omega^2}\hat{q}_2^2 + 2\omega\omega_0\,\hat{q}_1\hat{q}_2\right). \tag{7.11}$$

As in the normal phase, we use the transformation (7.7), which casts the Hamiltonian in the form

$$\hat{H}_s = -j\left(\frac{2\lambda^2}{\omega} + \frac{\omega_0^2\omega}{8\lambda^2}\right) - \frac{4\lambda^2+\omega^2}{2\omega} + \frac{1}{2}\left(\hat{P}_1^2 + \hat{P}_2^2 + \varepsilon_{1s}^2\hat{Q}_1^2 + \varepsilon_{2s}^2\hat{Q}_2^2\right), \tag{7.12}$$

where now the rotation angle α_s is such that

$$\tan 2\alpha_s = \frac{2\omega^3\omega_0}{16\lambda^4 - \omega^4}, \tag{7.13}$$

and we have assumed that $\lambda \neq \pm\omega/2$. The two resulting (squared) normal frequencies are

$$\varepsilon_{1s}^2 = \frac{1}{2}\left[\frac{16\lambda^4+\omega^4}{\omega^2} - \sqrt{\left(\frac{16\lambda^4-\omega^4}{\omega^2}\right)^2 + 4\omega^2\omega_0^2}\right],$$
$$\varepsilon_{2s}^2 = \frac{1}{2}\left[\frac{16\lambda^4+\omega^4}{\omega^2} + \sqrt{\left(\frac{16\lambda^4-\omega^4}{\omega^2}\right)^2 + 4\omega^2\omega_0^2}\right]. \tag{7.14}$$

Notice, once more, that at the critical coupling $\lambda = \lambda_c$, the frequency ε_{1s} vanishes. Indeed, it can be easily verified that $\hat{H}_n(\lambda_c) = \hat{H}_s(\lambda_c)$. Furthermore, looking at the dominant term of order j in the Hamiltonians (7.6) and (7.11), we can read off the ground state energy for both phases:

$$\frac{E_g}{j} = \begin{cases} -\omega_0, & \lambda < \lambda_c \\ -\left(\frac{2\lambda^2}{\omega} + \frac{\omega_0^2\omega}{8\lambda^2}\right), & \lambda > \lambda_c \end{cases}. \tag{7.15}$$

This normalized ground state energy exhibits a discontinuity in its second derivative at $\lambda = \lambda_c$, which is precisely the hallmark of the quantum phase transition in this model. Interestingly, the main features of the transition were reproduced using only the quadratic approximation coming from the truncated Holstein-Primakoff transformation. This is one of the main virtues of this approach, which was precisely exploited by Emary and Brandes in their remarkable papers [106, 107]. We are also taking advantage of this simple method as a first step toward the understanding of the underlying geometry of the parameter space. In reference [119], some shortcomings of the truncated Holstein-Primakoff transformation are addressed.

7.2 Classical and quantum metric tensors

Our aim is now to compute the classical and quantum metrics for the normal and superradiant phases, and compare them to see how well the classical metric captures the essential information of the quantum system. After that, we analyze the scalar curvatures of both metrics. We fix $\omega_0 = \text{const.}$ and take as our adiabatic parameters the frequency ω and the strength of the dipole coupling λ, which results in a two dimensional parameter manifold with coordinates $x = \{x^i\} = (\omega, \lambda)$, $i = 1, 2$.

7.2.1 Normal phase

We begin our computation of the classical metric tensor for the normal phase using the time-dependent approach (4.75). The Hamiltonian of the normal phase is the classical counterpart of (7.6),

$$H_{n,cl} = -j\omega_0 - \frac{(\omega+\omega_0)}{2} + \frac{1}{2}\left(p_1^2 + p_2^2 + \omega^2 q_1^2 + \omega_0^2 q_2^2 + 4\lambda\sqrt{\omega\omega_0}\, q_1 q_2\right). \tag{7.16}$$

The deformation functions associated with the parameters are

$$\mathcal{O}_{1n} = \frac{\partial H_{n,cl}}{\partial \omega} = \omega q_1^2 + \lambda \sqrt{\frac{\omega_0}{\omega}}\, q_1 q_2,$$
$$\mathcal{O}_{2n} = \frac{\partial H_{n,cl}}{\partial \lambda} = 2\sqrt{\omega\omega_0}\, q_1 q_2, \tag{7.17}$$

where we have ignored the terms that do not depend on (q_a, p_a) since they would not contribute to the metric integrands $\Lambda_{ij}(t_1, t_2) := \langle \mathcal{O}_{in}(t_1)\mathcal{O}_{jn}(t_2)\rangle_0 - \langle \mathcal{O}_{in}(t_1)\rangle_0 \langle \mathcal{O}_{jn}(t_2)\rangle_0$. Actually, we can deal with both deformation functions simultaneously as in Section 6.2, and write them as

$$\mathcal{O}_{in}(t) = \varepsilon_{1n} Q_1^2(t)\partial_i \varepsilon_{1n} + \varepsilon_{2n} Q_2^2(t)\partial_i \varepsilon_{2n} + (\varepsilon_{2n}^2 - \varepsilon_{1n}^2) Q_1(t) Q_2(t) \partial_i \alpha_n, \tag{7.18}$$

where the $Q_a(t)$, $(a = 1, 2)$ are the normal coordinates that uncouple the two harmonic oscillators through the transformation (7.7), and ε_{an} are the normal frequencies (7.10). The next step is to write the $Q_a(t)$ as functions of the initial conditions (Q_{a0}, P_{a0}) and time as

$$Q_a(t) = Q_{a0} \cos \varepsilon_{an} t + \frac{P_{a0}}{\varepsilon_{an}} \sin \varepsilon_{an} t, \tag{7.19}$$

and then, the initial conditions in terms of initial action-angle variables (ϕ_{a0}, I_a) as

$$Q_{a0} = \sqrt{\frac{2I_a}{\varepsilon_{an}}} \sin \phi_{a0}, \qquad P_{a0} = \sqrt{2I_a \varepsilon_{an}} \cos \phi_{a0}. \tag{7.20}$$

Now, we use the classical torus average to form the integrands $\Lambda_{ij}(t_1, t_2)$ which turn out to be

$$\begin{aligned}\Lambda_{ij}(t_1, t_2) =& \frac{1}{2}\partial_i \varepsilon_{1n} \partial_j \varepsilon_{1n} I_1 \cos\left[2\varepsilon_{1n}(t_1 - t_2)\right] + \frac{1}{2}\partial_i \varepsilon_{2n} \partial_j \varepsilon_{2n} I_2 \cos\left[2\varepsilon_{2n}(t_1 - t_2)\right] \\ &+ \frac{\partial_i \alpha_n \partial_j \alpha_n}{\varepsilon_{1n}\varepsilon_{2n}} \left(\varepsilon_{1n}^2 - \varepsilon_{2n}^2\right)^2 \cos\left[2\varepsilon_{1n}(t_1 - t_2)\right] \cos\left[2\varepsilon_{2n}(t_1 - t_2)\right].\end{aligned} \tag{7.21}$$

With the regularization prescription (2.63), we carry out the time integrals and finally obtain the classical metric for the normal phase, whose components are

$$g_{ij} = \frac{\partial_i \varepsilon_{1n} \partial_j \varepsilon_{1n}}{8\varepsilon_{1n}^2} I_1^2 + \frac{\partial_i \varepsilon_{2n} \partial_j \varepsilon_{2n}}{8\varepsilon_{2n}^2} I_2^2 + \partial_i \alpha_n \partial_j \alpha_n \left(\frac{\varepsilon_{1n}}{\varepsilon_{2n}} + \frac{\varepsilon_{2n}}{\varepsilon_{1n}}\right) I_1 I_2. \tag{7.22}$$

It is clear from this expression that the appearance of ε_{1n} in the denominator causes a divergence in the metric components at $\lambda_c = \frac{\sqrt{\omega\omega_0}}{2}$, since ε_{1n} vanishes at the critical coupling (see equation (7.10)); this property of the classical metric signals the quantum phase transition in the Dicke model.

We now compute the quantum metric tensor (2.56) for the normal phase. From the Hamiltonian (7.6), we obtain the corresponding deformation operators, which can be written in compact form as

$$\hat{\mathcal{O}}_{in}(t) = \varepsilon_{1n} \hat{Q}_1^2(t)\partial_i \varepsilon_{1n} + \varepsilon_{2n} \hat{Q}_2^2(t)\partial_i \varepsilon_{2n} + (\varepsilon_{2n}^2 - \varepsilon_{1n}^2) \hat{Q}_1(t) \hat{Q}_2(t) \partial_i \alpha_n, \tag{7.23}$$

where $\hat{Q}_a(t)$, $(a = 1, 2)$ are the operators corresponding to the normal modes of the diagonal Hamiltonian, which can be written in terms of annihilation and creation operators as

$$\hat{Q}_a(t) = \frac{1}{\sqrt{2\varepsilon_{an}}}\left(\hat{b}^\dagger_{a0}\mathrm{e}^{i\varepsilon_{an}t} + \hat{b}_{a0}\mathrm{e}^{-i\varepsilon_{an}t}\right). \tag{7.24}$$

With these operators at hand, we can compute the combination $\frac{1}{2}\langle\{\hat{\mathcal{O}}_{in}(t_1), \hat{\mathcal{O}}_{jn}(t_2)\}\rangle_0 - \langle\hat{\mathcal{O}}_{in}(t_1)\rangle_0\langle\hat{\mathcal{O}}_{jn}(t_2)\rangle_0$ and then use the integral regularization (2.63) to arrive at the components of the quantum metric tensor, which turn out to be

$$g^{(0)}_{ij} = \frac{\partial_i\varepsilon_{1n}\partial_j\varepsilon_{1n}}{8\varepsilon^2_{1n}} + \frac{\partial_i\varepsilon_{2n}\partial_j\varepsilon_{2n}}{8\varepsilon^2_{2n}} + \partial_i\alpha_n\partial_j\alpha_n\left[\frac{1}{4}\left(\frac{\varepsilon_{1n}}{\varepsilon_{2n}} + \frac{\varepsilon_{2n}}{\varepsilon_{1n}}\right) - \frac{1}{2}\right]. \tag{7.25}$$

We notice, as with the classical metric, that the frequency ε_{1n} appears in the denominator in equation (7.25), causing a divergence when $\lambda = \lambda_c$ and signaling the quantum phase transition in the Dicke model. Moreover, with both metrics at our disposal (equations (7.22) and (7.25)), we find the relation

$$g^{(0)}_{ij} = g_{ij} - \frac{1}{2}\partial_i\alpha_n\partial_j\alpha_n, \tag{7.26}$$

where the identifications $I_1 = I_2 = 1/2$ and $I_1^2 = I_2^2 = 1$ were made. We observe that the quantum metric (7.25) has an extra parameter-dependent term that does not appear in its classical analog; this term has been related to an anomaly arising from the ordering of the operators in the quantum case [68].

7.2.2 Superradiant phase

The treatment of the superradiant phase is analogous to that of the normal phase in both the classical and quantum settings; the difference lies in the explicit expressions of the rotation angle (7.13) and the normal frequencies (7.14) in terms of the parameters. The classical counterpart of the Hamiltonian (7.11) is

$$H_{s,cl} = -j\left(\frac{2\lambda^2}{\omega} + \frac{\omega_0^2\omega}{8\lambda^2}\right) - \frac{4\lambda^2 + \omega^2}{2\omega} + \frac{1}{2}\left(p_1^2 + p_2^2 + \omega^2 q_1^2 + \frac{16\lambda^4}{\omega^2}q_2^2 + 2\omega\omega_0\, q_1 q_2\right), \tag{7.27}$$

and its deformation functions are

$$\begin{aligned}\mathcal{O}_{1s} &= \frac{\partial H_{s,cl}}{\partial\omega} = \omega q_1^2 - \frac{16\lambda^4}{\omega^3}q_2^2 + \omega_0\, q_1 q_2,\\ \mathcal{O}_{2s} &= \frac{\partial H_{s,cl}}{\partial\lambda} = \frac{32\lambda^3}{\omega^2}q_2^2.\end{aligned} \tag{7.28}$$

By following the same steps as in the normal phase, we arrive at the classical and quantum metrics, which turn out to be

$$g_{ij} = \frac{\partial_i\varepsilon_{1s}\partial_j\varepsilon_{1s}}{8\varepsilon^2_{1s}}I_1^2 + \frac{\partial_i\varepsilon_{2s}\partial_j\varepsilon_{2s}}{8\varepsilon^2_{2s}}I_2^2 + \partial_i\alpha_s\partial_j\alpha_s\left(\frac{\varepsilon_{1s}}{\varepsilon_{2s}} + \frac{\varepsilon_{2s}}{\varepsilon_{1s}}\right)I_1 I_2, \tag{7.29}$$

and

$$g_{ij}^{(0)} = \frac{\partial_i \varepsilon_{1s} \partial_j \varepsilon_{1s}}{8\varepsilon_{1s}^2} + \frac{\partial_i \varepsilon_{2s} \partial_j \varepsilon_{2s}}{8\varepsilon_{2s}^2} + \partial_i \alpha_s \partial_j \alpha_s \left[\frac{1}{4} \left(\frac{\varepsilon_{1s}}{\varepsilon_{2s}} + \frac{\varepsilon_{2s}}{\varepsilon_{1s}} \right) - \frac{1}{2} \right], \tag{7.30}$$

respectively. We see that these metrics have the same form as those of equations (7.22) and (7.25), and hence satisfy the relation (7.26), but with the normal frequencies ε_{1s} and ε_{2s} and the rotation angle α_s. Remarkably, due to the presence of ε_{1s} in the denominators of (7.29) and (7.30), both metrics exhibit a divergence at $\lambda = \lambda_c$, which reveals the existence of the quantum phase transition.

To gain more insight into this, in Figure 7.1 (a), (b), and (c) we show the components of the classical and quantum metrics for both phases and fixed values of ω and ω_0. Clearly, we see that both metrics diverge at λ_c, which signals the quantum phase transition, however, the metric component g_{22} of the classical metric at $\lambda = 0$ shows a different behavior than its quantum counterpart; this can be attributed to the anomalous extra term that appears in (7.25), making the classical metric more sensitive to the vanishing of the coupling term in the Hamiltonian (7.6).

The scalar curvatures, computed with the aid of equation (1.20), for both the classical and quantum metrics are shown in Figure 7.1 (d). We observe some features from the plots. First, the agreement between them is good in the superradiant phase ($\lambda > \lambda_c$). Second, an important difference between them appears in the normal phase ($\lambda < \lambda_c$): while in the quantum case the scalar curvature takes a constant value very close to -4, in the classical case the scalar curvature possesses a minimum around $\lambda = 0.16$. Such a difference can be related to the behavior of the component g_{22} at that phase. It would be interesting if an analysis of the exact model, for finite j, presents this behavior, as will be the case with the anisotropic Lipkin-Meshok-Glick in the next chapter. And third, in the limit $\lambda \to \lambda_c$ both scalar curvatures approach each other and tend to -4. Notice, however, that for $\lambda = \lambda_c$ they are not defined since the classical and quantum Hamiltonians used to compute the metrics are not valid at that point. This behavior of the scalar curvatures when $\lambda \to \lambda_c$ suggests that the singularity of the classical and quantum metrics at the phase transition could be created by the coordinates used. It is worth mentioning that the scalar curvature of the quantum metric resembles the one found in reference [17], the only difference being the method used to compute it and an overall sign due to a convention in formula (1.20).

7.2.3 Metrics under resonance

A special important case of the Dicke model is that of resonance, i.e., when $\omega = \omega_0$. We are unaware of previous geometric analyses in this case. In order to treat it, we take the limits $\alpha_n \to \pi/4$ and $\omega_0 \to \omega$ in the classical and quantum metrics corresponding to the normal phase (equations (7.22) and (7.25)), whereas in the superradiant phase we only set $\omega_0 \to \omega$ in the associated metrics (equations (7.29) and (7.30)). The resulting metric components in terms of the parameters are greatly simplified, and we find that in the normal phase, the components g_{12} and g_{22} of the classical and quantum metrics

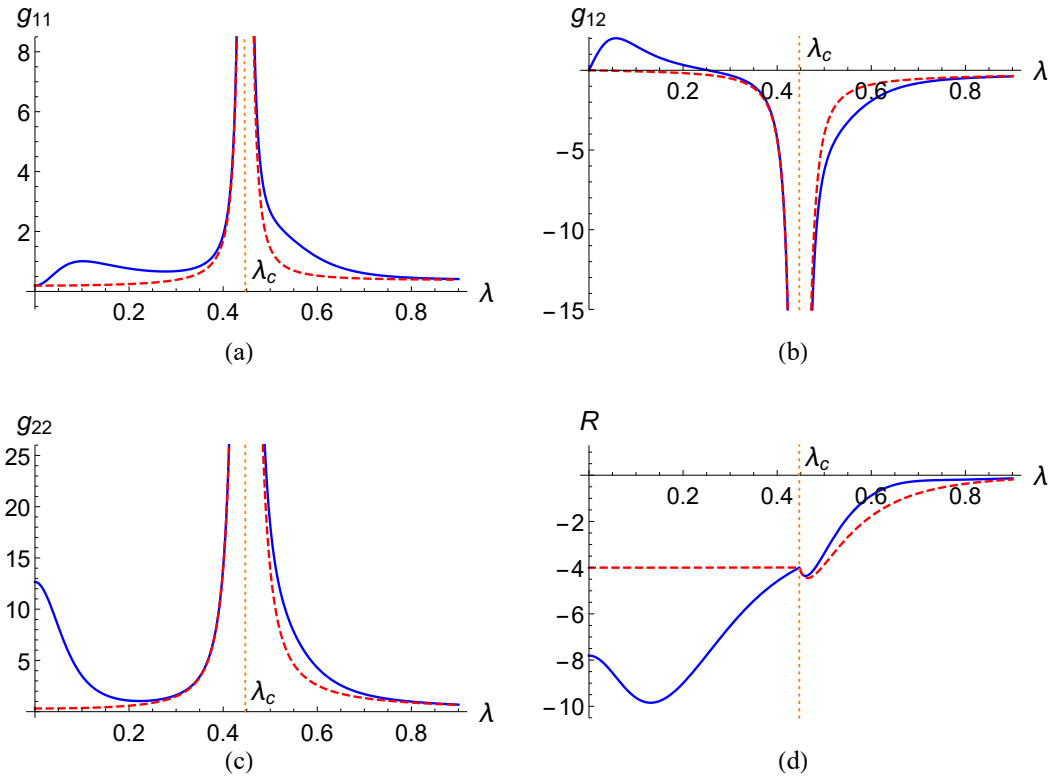

Figure 7.1: Metric components and scalar curvature of the classical metric (solid blue) and the quantum metric (dashed red) as a function of λ when $\omega_0 = 1$ and $\omega = 0.8$. All the components show a divergence at the phase transition (dotted orange) with critical coupling $\lambda_c = 0.447$, whereas the scalar curvature does not.

perfectly match when the identifications $I_1^2 = I_2^2 = 1$ and $I_1 = I_2 = 1/2$ are used. These components are

$$g_{12} = g_{12}^{(0)} = \frac{\lambda(4\lambda^2 - 3\omega^2)}{8\omega(\omega^2 - 4\lambda^2)^2}, \tag{7.31}$$

$$g_{22} = g_{22}^{(0)} = \frac{4\lambda^2 + \omega^2}{4(\omega^2 - 4\lambda^2)^2}. \tag{7.32}$$

On the other hand, the g_{11} components do not match, as we can see below

$$g_{11} = \frac{16\lambda^4\omega^3 - 8\lambda^2\omega^5 + \omega^7 + \lambda^2\sqrt{\omega^2 - 4\lambda^2}(8\lambda^4 - 6\lambda^2\omega^2 + 2\omega^4)}{32\lambda^2\omega^2\left(\omega^2 - 4\lambda^2\right)^{5/2}}, \tag{7.33}$$

$$g_{11}^{(0)} = \frac{-16\lambda^6 + 48\lambda^4\omega^2 - 23\lambda^2\omega^4 + 3\omega^6 - \omega\sqrt{\omega^2 - 4\lambda^2}(4\lambda^4 - 3\lambda^2\omega^2 + \omega^4)}{16\omega^2(\omega^2 - 4\lambda^2)^{5/2}\left(\omega + \sqrt{\omega^2 - 4\lambda^2}\right)}. \tag{7.34}$$

In the superradiant phase, the classical and quantum metric components are more complicated and do not match, however, it can be seen that all of them diverge at the

critical coupling $\lambda_c = \omega/2$. We show in Figure 7.2 (a), (b), and (c) the components of the metrics under the resonance condition $\omega = \omega_0$. We can see that the component g_{11} has a divergence at $\lambda = 0$. Moreover, we observe that in the normal phase, the components g_{12} and g_{22} of the classical metric are exactly the same as those of the quantum metric, just as we mentioned earlier. It is also worth noting that both metrics show the same behavior in the limiting cases $\lambda \to \lambda_c$ and $\lambda \to \infty$.

In Figure 7.2 (d), we show the scalar curvatures associated with the classical and quantum metrics. We notice that the scalar curvature in the classical case presents a divergence at $\lambda = 0$, which is inherited from the g_{11} metric component. Once again, we see that the effect of the anomaly is to get rid of that behavior in the quantum result. Additionally, in contrast to the non resonant analysis, both scalar curvatures diverge at the quantum phase transition in exactly the same way. There is, however, an alternative approach to the metrics under the resonance condition. One could set $\omega_0 = \omega$ in the Hamiltonian from the very beginning, and from there, derive the corresponding $\mathcal{O}_i$. The resulting deformation operators are different from those we have used and lead to different expressions for both the classical and quantum metrics as functions of ω and λ. As a matter of fact, it turns out that both metrics have zero scalar curvature in the whole range of ω and λ, which is not particularly illuminating. We are unaware of the physical reason behind this result and consider that it deserves further analysis.

To conclude, we would like to stress the fact that both the classical and quantum metrics exhibit a divergent behavior at the phase transition for the resonant and non-resonant cases. This is a remarkable result since it shows that the classical metric can be used to get a first insight into the information contained in the quantum metric tensor. On the other hand, according to the (classical and quantum) scalar curvatures, the metric for the resonant case involve a genuine singularity, whereas in the non-resonant case there seems to be a spurious singularity. This effect could be a consequence of the fact that the Holstein-Primakoff approximation fails at the quantum phase transition [119]. Then, in order to clarify this point it would be valuable to carry out a study of the parameter space of the Dicke model for finite j using the original Hamiltonian (7.1). This model has features that make the study for finite j subtle, although some authors have successfully employed techniques that can be implemented numerically and allow the exploration of the system in various regimes (including chaotic regions) [105, 108, 109]. In the classical setting, we could explore the mean-field Dicke Hamiltonian constructed with coherent states using as a first approach the perturbative analysis developed in [67] to find corrections to the quadratic approximation in the thermodynamic limit. The results should then be compared with the quantum counterpart using a perturbative approach to the quantum metric tensor [120]. Besides, the chaotic region could be approached through the study of the adiabatic gauge potential (which is deeply related to the quantum metric tensor), since it has been found recently that it serves as a sensitive measure of quantum chaos [121].

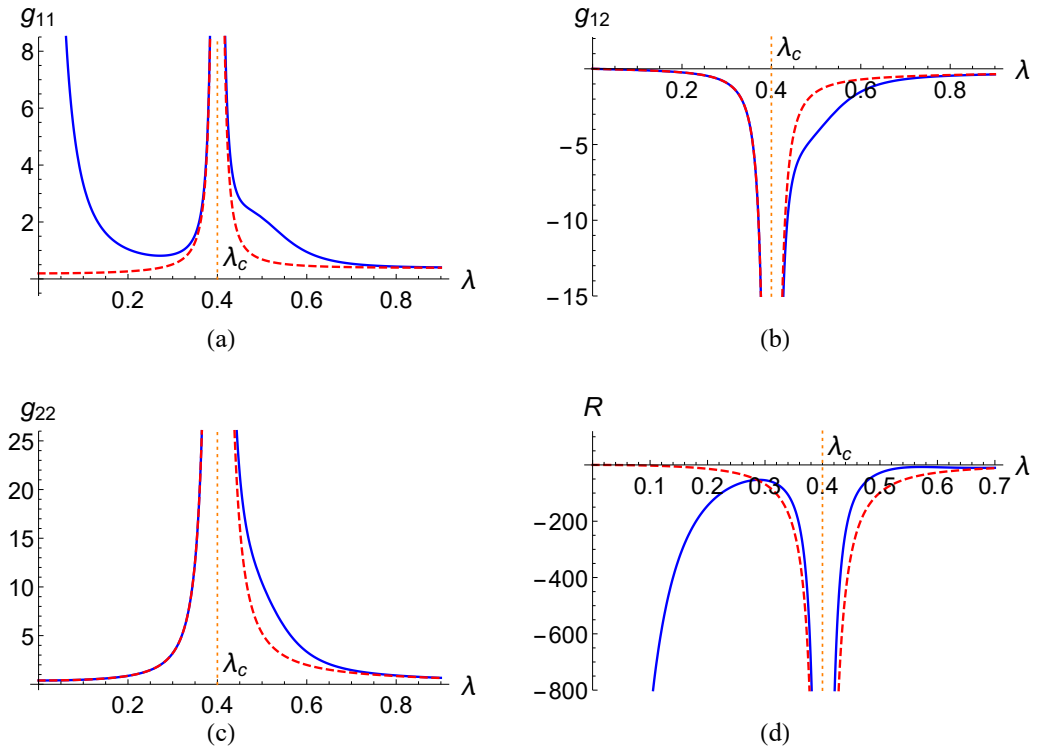

Figure 7.2: Metric components and scalar curvature of the classical metric (solid blue) and the quantum metric (dashed red) for the resonant case as a function of λ when $\omega = 0.8$. All of them show a divergence at the phase transition (dotted orange) with critical coupling $\lambda_c = 0.4$.

Chapter 8

Application to the anisotropic Lipkin-Meshkov-Glick model

In this chapter, we study the parameter space geometry of the anisotropic Lipkin-Meshkov-Glick (LMG) model. Some quantum information concepts like fidelity and fidelity susceptibility have already been applied to the study of classical and quantum phase transitions in this model [114, 122–128], but a complete geometrical characterization of the parameter space geometry is lacking. To do so, we analyze both the classical and the quantum metrics as well as their scalar curvatures. First, we consider the thermodynamic limit using Bloch coherent states in the classical case and the truncated Holstein-Primakoff transformation on the quantum side, and see that the classical metric is exactly the same as its quantum counterpart after making an identification of the action variable. Two of the three metric components show a divergence at the quantum phase transition and the scalar curvature is also singular there. Nevertheless, we find that the metric is not invertible in one phase of the system, and as a consequence, the scalar curvature is not defined in that phase. We finally perform a numerical analysis for finite sizes of the system that shows the precursors of the quantum phase transition and allows their characterization as functions of the parameters and of the system's size.

The LMG model consists of $\mathcal{N}$ mutually interacting spin-half particles that are also affected by a transverse magnetic field. It was first introduced in the context of nuclear physics [129–131], and it has been deeply studied through various analytic and numerical techniques [128, 132–136]. It has also been used as a model for Floquet time crystals [137], in the study of out-of-time order correlators [117], and to illustrate the orthogonality catastrophe and its relation to quantum speed limit [138].

The Hamiltonian that we shall consider is [123]

$$\hat{H} = -h\sum_i \sigma_z^i - \frac{1}{\mathcal{N}}\sum_{i<j}(\sigma_x^i\sigma_x^j + \gamma\sigma_y^i\sigma_y^j), \tag{8.1}$$

where $\{\sigma_\alpha^i\}$, $\alpha = x, y, z$ are the Pauli spin matrices for the ith spin, h, γ are real parameters, and we have set $\hbar = 1$. From here, it is customary to define the pseudospin

(collective spin) operators as $\hat{J}_\alpha = \sum_i \sigma_\alpha^i/2$ and cast the Hamiltonian into the form

$$\hat{H} = -2h\hat{J}_z - \frac{1}{j}\left(\hat{J}_x^2 + \gamma \hat{J}_y^2\right), \tag{8.2}$$

where, as usual, we restrict ourselves to the maximum pseudospin representation with $j = \mathcal{N}/2$. We also consider $h \geq 0$ and $-1 < \gamma < 1$, and analyze the system in the thermodynamic limit $j \to \infty$ where a quantum phase transition occurs.

8.1 Analysis in the thermodynamic limit

The description of the LMG model when $j \to \infty$ begins by taking the expectation value of the Hamiltonian (8.2) in spin coherent states $|z\rangle$ given by [117, 124, 139, 140]

$$|z\rangle = \frac{e^{z\hat{J}_+}}{(1+|z|^2)^j}|j,-j\rangle, \tag{8.3}$$

where $|j,-j\rangle$ is the state with the lowest pseudospin projection and z is a complex number parameterized in terms of the two angles of the Bloch sphere as $z = e^{i\phi}\tan\frac{\theta}{2}$ (for details, see Appendix C). The function thus obtained is

$$H_{cl}(\theta,\phi) := \langle z|\hat{H}|z\rangle = -2hJ_z - \frac{1}{j}(J_x^2 + \gamma J_y^2), \tag{8.4}$$

and it defines the classical energy surface where the dynamics of the pseudospin vector $\boldsymbol{J} = j(\sin\theta\cos\phi, \sin\theta\sin\phi, \cos\theta)$ will take place. Explicitly, in terms of the angles (θ,ϕ), the function

$$H_{cl} = -j[2h\cos\theta + \sin^2\theta(\cos^2\phi + \gamma\sin^2\phi)] \tag{8.5}$$

possesses two extrema, each of them defining a phase of the system. The two phases are:

- Symmetric phase: $\theta_0 = 0$. It corresponds to a classical pseudospin vector aligned with the z axis. The ground state energy is $E_g := H_{cl}(0,\phi_0) = -2hj$.
- Broken phase: $\theta_0 = \cos^{-1}h$ with $\phi_0 = 0$ or $\phi_0 = \pi$. It corresponds to two possible configurations of the pseudospin vector, signaling two ground states with degenerate energy $E_g := H_{cl}(\cos^{-1}h, 0) = H_{cl}(\cos^{-1}h, \pi) = -(1+h^2)j$. In this case, the classical pseudospin is not aligned with the z axis.

The ground state energy $E_g = E_g(h)$ is thus the piecewise function

$$\frac{E_g}{j} = \begin{cases} -(1+h^2), & h < 1 \\ -2h, & h > 1 \end{cases}, \tag{8.6}$$

which has a discontinuous second derivative at $h = 1$, signaling a second order quantum phase transition [41]. The region $h > 1$ corresponds to the symmetric phase where the ground state is unique, whereas the region $h < 1$ is the broken phase which has a degenerate ground state energy.

8.1.1 Symmetric phase

To carry out the analysis of the symmetric phase in the thermodynamic limit, we will use the Holstein-Primakoff transformation [118]:

$$\hat{J}_+ = \sqrt{2j}\sqrt{1-\frac{\hat{a}^\dagger\hat{a}}{2j}}\,\hat{a}, \qquad \hat{J}_- = \sqrt{2j}\hat{a}^\dagger\sqrt{1-\frac{\hat{a}^\dagger\hat{a}}{2j}}, \qquad \hat{J}_z = j-\hat{a}^\dagger\hat{a}, \tag{8.7}$$

which is then truncated to zeroth order in $1/j$ under the assumption that $j\to\infty$. Hence, we have

$$\hat{J}_+ \simeq \sqrt{2j}\,\hat{a}, \qquad \hat{J}_- \simeq \sqrt{2j}\,\hat{a}^\dagger, \qquad \hat{J}_z = j-\hat{a}^\dagger\hat{a}. \tag{8.8}$$

Taking this into account and using $\hat{J}_\pm = \hat{J}_x \pm i\hat{J}_y$, the resulting quadratic Hamiltonian that corresponds to (8.2) is

$$\hat{H} \simeq -\frac{1+\gamma}{2} - 2hj - (1+\gamma-2h)\hat{a}^\dagger\hat{a} - \frac{1-\gamma}{2}\left(\hat{a}^{\dagger 2}+\hat{a}^2\right), \tag{8.9}$$

which in terms of $\hat{Q}$ and $\hat{P}$ can be written as

$$\hat{H} \simeq -h - 2hj + (h-\gamma)\hat{P}^2 + (h-1)\hat{Q}^2. \tag{8.10}$$

From (8.9), it is clear that the Hamiltonian can be diagonalized through the Bogoliubov transformation from operators $(\hat{a},\hat{a}^\dagger)$ to $(\hat{b},\hat{b}^\dagger)$ as

$$\hat{a} = \cosh\alpha\,\hat{b} + \sinh\alpha\,\hat{b}^\dagger, \qquad \hat{a}^\dagger = \sinh\alpha\,\hat{b} + \cosh\alpha\,\hat{b}^\dagger, \tag{8.11}$$

with $\tanh 2\alpha = \frac{1-\gamma}{2h-\gamma-1}$. By doing this, the Hamiltonian takes the form

$$\hat{H} \simeq -h - 2hj + 2\sqrt{(h-1)(h-\gamma)}\left(\hat{b}^\dagger\hat{b}+\frac{1}{2}\right). \tag{8.12}$$

It is readily noted here that at the phase transition, $h=1$, the frequency of the resulting harmonic oscillator vanishes.

8.1.2 Broken phase

In the case of the broken phase, we need to perform a rotation around the y axis to align the z axis with the pseudospin ground state configuration. Hence, we shall transform the operators $(\hat{J}_x,\hat{J}_y,\hat{J}_z)$ to a new set of operators $(\hat{J}'_x,\hat{J}'_y,\hat{J}'_z)$ as

$$\begin{pmatrix}\hat{J}_x\\ \hat{J}_y\\ \hat{J}_z\end{pmatrix} = \begin{pmatrix}\cos\theta_0 & 0 & \sin\theta_0\\ 0 & 1 & 0\\ -\sin\theta_0 & 0 & \cos\theta_0\end{pmatrix}\begin{pmatrix}\hat{J}'_x\\ \hat{J}'_y\\ \hat{J}'_z\end{pmatrix}, \tag{8.13}$$

where $\cos\theta_0 = h$ and $\sin\theta_0 = \sqrt{1-h^2}$, which is the ground state configuration that corresponds to $(\theta_0, \phi_0) = (\cos^{-1} h, 0)$. Thus, the Hamiltonian of the broken phase turns out to be [132, 133]

$$\begin{aligned}\hat{H}' = &-2h^2\hat{J}'_z + 2h\sqrt{1-h^2}\hat{J}'_x - \frac{1}{j}(1-h^2)\hat{J}'^2_z \\ &- \frac{1}{j}\left[h^2\hat{J}'^2_x + h\sqrt{1-h^2}(\hat{J}'_x\hat{J}'_z + \hat{J}'_z\hat{J}'_x) + \gamma\hat{J}'^2_y\right].\end{aligned} \tag{8.14}$$

Next, we apply the truncated Holstein-Primakoff transformation (8.8) to these rotated operators to find the quadratic Hamiltonian for the broken phase. The resulting Hamiltonian is given by

$$\hat{H}' \simeq -(1+h^2)j + (1-\gamma)\hat{P}^2 + (1-h^2)\hat{Q}^2, \tag{8.15}$$

or, in terms of the creation and annihilation operators $\hat{b}$ and $\hat{b}^\dagger$,

$$\hat{H}' \simeq -(1+h^2)j + 2\sqrt{(1-h^2)(1-\gamma)}\left(\hat{b}^\dagger\hat{b} + \frac{1}{2}\right). \tag{8.16}$$

We observe once more that at the critical point, $h = 1$, the frequency of the resulting harmonic oscillator vanishes, which signals the quantum phase transition. Now that we have at hand the effective quadratic Hamiltonians for both the symmetric and the broken phase, we proceed to the calculation of the classical and quantum metric tensors.

8.2 Classical and quantum metric tensors

We are now ready to compute the classical and quantum metrics in the thermodynamic limit $j \to \infty$. In what follows, we take $x = \{x^i\} = (h, \gamma)$, $i = 1, 2$ to be the adiabatic parameters. To build the classical metric, we nee to derive the deformation functions from the Hamiltonian (8.4). They are

$$\begin{aligned}\mathcal{O}_1 &= \frac{\partial H_{cl}}{\partial h} = -2J_z, \\ \mathcal{O}_2 &= \frac{\partial H_{cl}}{\partial \gamma} = -\frac{J_y^2}{j}.\end{aligned} \tag{8.17}$$

At this point, we introduce canonical coordinates for the description of the classical system. It is easy to see that the coordinates (ϕ, J_z) are canonical in the sense that they reproduce the angular momentum algebra $\{J_i, J_j\} = \epsilon_{ijk}J_k$, where

$$\{f, g\} = \frac{\partial f}{\partial \phi}\frac{\partial g}{\partial J_z} - \frac{\partial f}{\partial J_z}\frac{\partial g}{\partial \phi}. \tag{8.18}$$

Then, we perform a canonical transformation and move to the (Q, P) representation, where

$$Q = \sqrt{2(j - J_z)}\cos\phi, \qquad P = \sqrt{2(j - J_z)}\sin\phi. \tag{8.19}$$

After this, the resulting classical LMG Hamiltonian is

$$H_{cl} = -2hj + h(P^2 + Q^2) - (\gamma P^2 + Q^2)\left(1 - \frac{P^2 + Q^2}{4j}\right). \tag{8.20}$$

In Figure 8.1, we can see the level curves of the classical Hamiltonian H_{cl} in terms of the (Q, P) coordinates for the two different phases of the model. Once the mean field Hamiltonian H_{cl} is constructed with the coherent states, the analysis is purely classical in terms of fixed points and their stability. This highlights the importance of the classical methods for quantum systems.

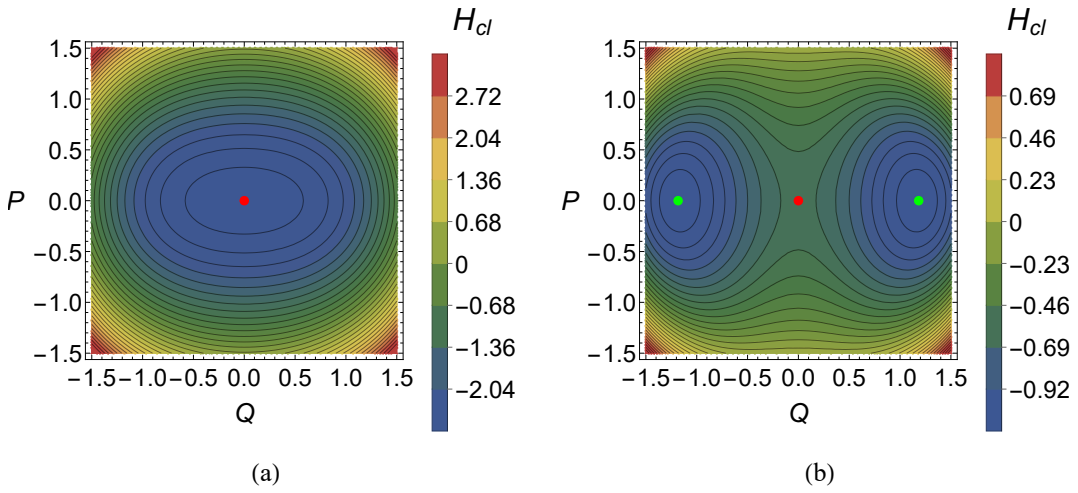

Figure 8.1: Phase space corresponding to the classical Hamiltonian H_{cl} for $\gamma = 0.1$ and (a) $h = 1.3$, or (b) $h = 0.3$. In (a), the red point is the only minimum; this is the symmetric phase. On the other hand, in (b), the red point becomes a local maximum and the green points appear as two degenerate minima; this is the broken phase.

8.2.1 Metrics for the symmetric phase

We first consider the symmetric phase. The quadratic Hamiltonian associated with (8.20) is

$$H_{cl} \simeq -2hj + (h - \gamma)P^2 + (h - 1)Q^2. \tag{8.21}$$

Notice that when $Q = P = 0$, only the ground state energy of the symmetric phase, $E_g = -2hj$, survives. We need to express the deformation functions (8.17) in terms of initial action-angle variables and time. To do this, we find the solution to the equations of motion of (8.21), which are

$$\begin{aligned} Q(t) =& Q_0 \cos\omega t + \frac{P_0}{\omega}\sin\omega t, \\ P(t) =& P_0 \cos\omega t - \omega Q_0 \sin\omega t, \end{aligned} \tag{8.22}$$

where we have identified the frequency as $\omega = \sqrt{(h-1)(h-\gamma)}$. From here, we readily find the action-angle variables (ϕ_0, I) and write the initial conditions in terms of them as

$$Q_0 = \sqrt{\frac{2I\sqrt{h-\gamma}}{\sqrt{h-1}}}\,\sin\phi_0, \qquad P_0 = \sqrt{\frac{2I\sqrt{h-1}}{\sqrt{h-\gamma}}}\,\cos\phi_0. \tag{8.23}$$

We substitute (8.23) in (8.22) and use (4.75) to find the classical metric. The resulting metric components are

$$\begin{aligned} g_{11} &= \frac{I^2}{32}\left[\frac{1-\gamma}{(h-1)(h-\gamma)}\right]^2, \\ g_{12} &= \frac{I^2(1-\gamma)}{32(h-1)(h-\gamma)^2}, \\ g_{22} &= \frac{I^2}{32(h-\gamma)^2}. \end{aligned} \tag{8.24}$$

We see that at the quantum phase transition, $h = 1$, the components g_{11} and g_{12} diverge. Besides, one can easily note that the determinant of the classical metric is zero.

Now, to compute the quantum metric in the thermodynamic limit, we use the Hamiltonian (8.2) which leads to the deformation operators

$$\begin{aligned} \hat{\mathcal{O}}_1 &= \frac{\partial \hat{H}}{\partial h} = -2\hat{J}_z, \\ \hat{\mathcal{O}}_2 &= \frac{\partial \hat{H}}{\partial \gamma} = -\frac{\hat{J}_y^2}{j}. \end{aligned} \tag{8.25}$$

Recall that when $j \to \infty$, the truncated Holstein-Primakoff transformation allows us to cast the angular momentum operators in the $(\hat{Q}, \hat{P})$ representation, as suggested by equation (8.8). Thus, the deformation operators read

$$\begin{aligned} \hat{\mathcal{O}}_1 &= \hat{P}^2 + \hat{Q}^2 - 2j - 1, \\ \hat{\mathcal{O}}_2 &= -\hat{P}^2. \end{aligned} \tag{8.26}$$

We express them in terms of creation and annihilation operators and time, and read off the spectrum from the effective quadratic Hamiltonian (8.10). This information is then substituted into equation (2.56), which yields the following metric components:

$$\begin{aligned} g_{11}^{(0)} &= \frac{1}{32}\left[\frac{1-\gamma}{(h-1)(h-\gamma)}\right]^2, \\ g_{12}^{(0)} &= \frac{1-\gamma}{32(h-1)(h-\gamma)^2}, \\ g_{22}^{(0)} &= \frac{1}{32(h-\gamma)^2}. \end{aligned} \tag{8.27}$$

This quantum metric has already been obtained in reference [17] by using another method, hence, we corroborate it with our approach. We also see that the metric determinant is zero, which was noted in the same reference and implies that information geometry is ill-defined in the symmetric phase of this model. Comparing equations (8.24) and (8.27), it is easy to see that the classical and quantum results have exactly the same parameter dependence and that the classical metric reproduces the singularities of the quantum metric. Moreover, both metrics match perfectly if the identification $I^2 = 1$ is made. This is a remarkable result, because the classical metric is easier to compute: it only requires the parameterization of the canonical coordinates (Q, P) in terms of action-angle variables (see equation (8.23)), instead of the introduction of creation and annihilation operators. Furthermore, it uses the classical average instead of expectation values of operators.

8.2.2 Metrics for the broken phase

For the broken phase, the classical Hamiltonian is obtained by taking the expectation value of equation (8.14) in spin coherent states $|z\rangle$, which leads to

$$\begin{aligned} H'_{cl} =& -j(1+h^2) + (1-\gamma)P^2 + (1-h^2)Q^2 \\ &+ \frac{h}{\sqrt{j}}\sqrt{1-h^2}Q(P^2+Q^2)\sqrt{1-\frac{P^2+Q^2}{4j}} \\ &+ \frac{1}{4j}(P^2+Q^2)\left[\gamma P^2 + h^2Q^2 - (1-h^2)(P^2+Q^2)\right]. \end{aligned} \tag{8.28}$$

The quadratic approximation of this Hamiltonian is given by

$$H'_{cl} \simeq -j(1+h^2) + (1-\gamma)P^2 + (1-h^2)Q^2. \tag{8.29}$$

In this case, the evaluation of H'_{cl} at $Q = P = 0$ yields the broken phase ground state $E_g = -j(1+h^2)$. The deformation functions are the same as (8.17), however, they must be expressed in terms of rotated quantities, in which case they take the following form:

$$\begin{aligned} \mathcal{O}'_1 &= 2\sqrt{1-h^2}J'_x - 2hJ'_z, \\ \mathcal{O}'_2 &= -\frac{J'^2_y}{j}. \end{aligned} \tag{8.30}$$

From here, we move to the position-momentum representation through the transformation (8.19) and find that the deformation functions are

$$\begin{aligned} \mathcal{O}'_1 &= h(P^2+Q^2) + 2\sqrt{j(1-h^2)}Q - 2hj - h, \\ \mathcal{O}'_2 &= -P^2. \end{aligned} \tag{8.31}$$

We use (8.22) and (8.23), and substitute (8.31) into (4.75), which yields the metric components

$$\begin{aligned} g_{11} &= \frac{jI}{\sqrt{(1-h^2)(1-\gamma)}} + \frac{I^2}{32}\left[\frac{h(h^2-\gamma)}{(1-h^2)(1-\gamma)}\right]^2, \\ g_{12} &= \frac{I^2 h\,(h^2-\gamma)}{32\,(1-h^2)\,(1-\gamma)^2}, \\ g_{22} &= \frac{I^2}{32(1-\gamma)^2}. \end{aligned} \tag{8.32}$$

As for the quantum metric in the broken phase, we use the deformation operators (8.25), rewrite them in terms of the rotated angular momenta (8.13), and use the truncated Holstein-Primakoff transformation (8.8) to compute the metric. The resulting quantum metric tensor is

$$\begin{aligned} g_{11}^{(0)} &= \frac{j}{2\sqrt{(1-h^2)(1-\gamma)}} + \frac{1}{32}\left[\frac{h(h^2-\gamma)}{(1-h^2)(1-\gamma)}\right]^2, \\ g_{12}^{(0)} &= \frac{h(h^2-\gamma)}{32(1-h^2)(1-\gamma)^2}, \\ g_{22}^{(0)} &= \frac{1}{32(1-\gamma)^2}. \end{aligned} \tag{8.33}$$

Again, it is remarkable that both the classical and quantum metrics have the same parameter structure and match perfectly with the identifications $I = 1/2$ and $I^2 = 1$. In contrast to the symmetric phase, both metrics are now invertible and have the determinants

$$\begin{aligned} \det g_{ij} &= \frac{I^3}{32\sqrt{(1-h^2)(1-\gamma)^5}}, \\ \det g_{ij}^{(0)} &= \frac{j}{64\sqrt{(1-h^2)(1-\gamma)^5}}, \end{aligned} \tag{8.34}$$

which, at the critical point, $h = 1$, diverge. This is a new result, since reference [17] did not analyze the broken phase of the model. Thus, we have found that the broken phase has a well-defined metric structure that allows a further geometric characterization with the aid of the scalar curvature. In addition to this, we see once more that the classical metric provides the same information as its the quantum counterpart but with a simpler method. The scalar curvature for either of these two metrics can be computed with equation (1.20), giving as a result

$$R = -4 + \frac{7h^4 - (9\gamma - 2)h^2 - 4(1-\gamma)}{j\sqrt{(1-h^2)(1-\gamma)^3}}. \tag{8.35}$$

From this expression, we observe that for large values of j (as expected in the thermodynamic limit), the scalar curvature practically takes on the constant value -4, and it diverges at $h = 1$, which indicates the presence of the quantum phase transition. It is interesting to observe that the singularity of the metric is independent of the coordinate system for this phase since it also appears in the scalar curvature. To investigate more details of this phenomenon, we consider in the next section a numerical analysis for finite j.

8.2.3 Finite-size analysis

We now want to address the effects of having a finite j directly and without resorting to any approximations. The Hamiltonian (8.2) can be numerically diagonalized, so we can compare the classical metric (equations (8.24) and (8.32)) with the quantum metric (equations (8.27) and (8.33)) for a given value of j and see how well the analytic computation via the truncated Holstein-Primakoff transformation agrees with the exact quantum metric tensor[1]. We obtain the numerical results by employing the so called perturbative form (2.64), which reads

$$g_{ij}^{(0)}(x) = \sum_{n\neq 0} \frac{\langle 0|\hat{\mathcal{O}}_i|n\rangle\langle n|\hat{\mathcal{O}}_j|0\rangle}{(E_n - E_0)^2}. \tag{8.36}$$

The evaluation of this formula requires the time-independent deformation operators, as opposed to equation (2.56), but at the cost of summing over all the elements of the eigenspace of $\hat{H}$. The Wolfram Mathematica code that was used to implement equation (8.36) is shown in Appendix D. In Figure 8.2, we show the three components of the quantum metric tensor for $j = 100$ and the scalar curvature obtained through numerical differentiation over a mesh in the parameter space (see Appendix D). We see the appearance of peaks near $h = 1$, which we identify as the precursors of the quantum phase transition. This is most clearly seen in Figure 8.3, where we show the quantum metric and its scalar curvature for a fixed γ and different values of j. We notice that the peaks of the metric components and the scalar curvature become narrower and get closer to $h = 1$ as j increases, which corroborates their identification as the precursors of the quantum phase transition.

In Figure 8.4, we compare the classical metric in the thermodynamic limit with the exact quantum metric tensor for $j = 500$ and $\gamma = -0.5$. We see that the agreement between them is acceptable as long as we are not close to the phase transition, where the Holstein-Primakoff approximation fails [128]. At the transition, the analytic metric components g_{11} and g_{12} show a divergence that is not present in their finite j counterparts coming from equation (8.36). Nevertheless, they still bear a resemblance given that, as we mentioned, the exact metric components have peaks that grow and get closer to

[1] In this context, by "exact" we mean that we can reach sufficiently high digit accuracy with the use of numerical diagonalization.

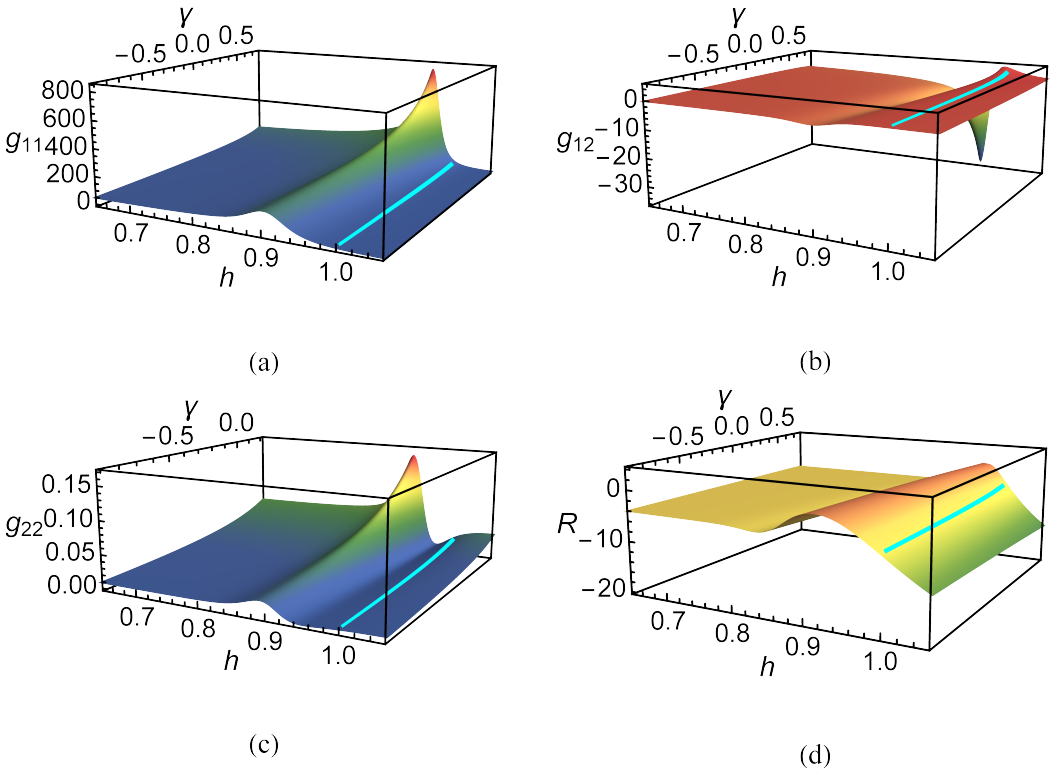

Figure 8.2: Metric components and scalar curvature for $j = 100$. The plots clearly show the presence of the precursors of the quantum phase transition. The critical line $h = 1$ is shown in cyan.

$h = 1$ as j increases. Actually, this suggests that for large values of j and $h = 1$, the components g_{11} and g_{12} will evolve to a divergent behavior. On the other hand, g_{22} does not seem to have such a good agreement with its analytic counterpart near the phase transition; this is because g_{22} (see equations (8.24) and (8.32)) is not sensitive to the critical value $h = 1$, unlike the other components. For the scalar curvature, we see in Figure 8.4 (d), that the analytic plot has a divergence at $h = 1$, and that it does not exist in the region $h > 1$, which was expected from equation (8.35). However, the numerical result indicates that the scalar curvature is smooth after $h = 1$ and Figure 8.3 shows that the slope of the descending curve for $h > 1$ gets steeper as j increases. Thus, for large values of j and $h = 1$, the scalar curvature will be an almost vertical line that falls off to large negative values. This dissimilar behavior between the analytic and numerical results is a consequence of the failure of the Holstein-Primakoff truncation at $h = 1$.

To better understand the behavior of the numerical quantum metric and its scalar curvature, we close this section by presenting a fundamental result of our work: an analysis of the quantum metric and its scalar curvature near the phase transition for finite j. In Figure 8.5, we plot the height of the peaks of the metric components as a

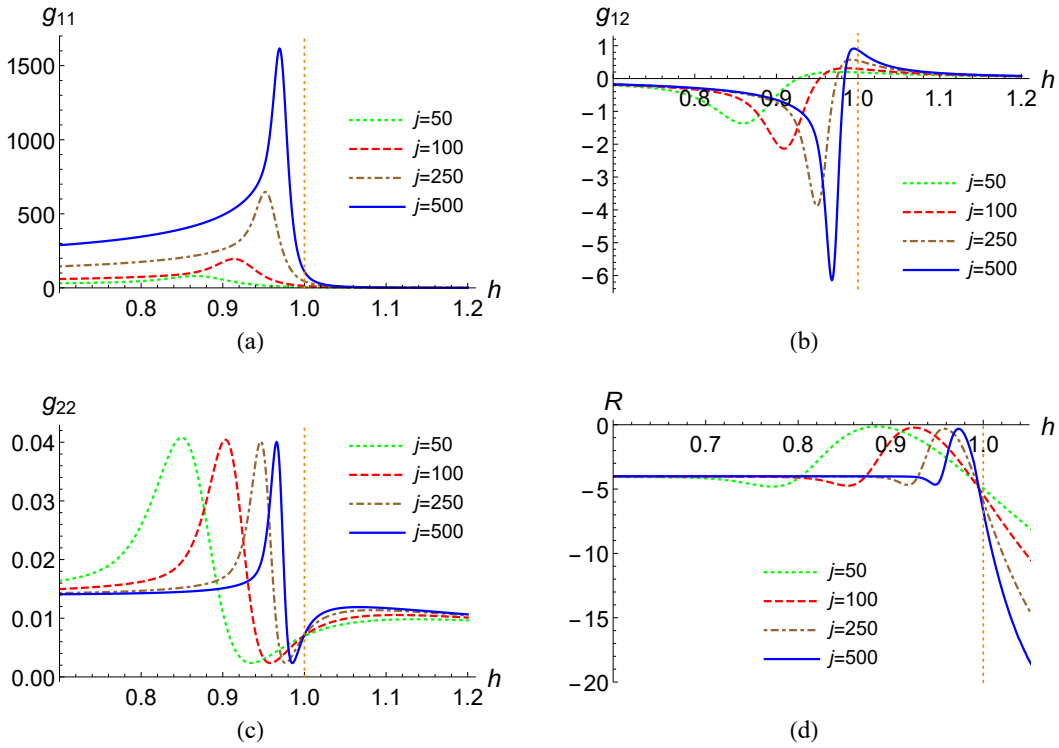

Figure 8.3: Quantum metric tensor and its scalar curvature for different values of j when $\gamma = -0.5$. The peaks in the components g_{11} and g_{12} become narrower as j increases.

function of h while we fix $\gamma = -0.5$[2]. The curves that interpolate the points have the following form:

- g_{11} peak

$$g_{11}^{(\text{peak})} = -22.5317 + \frac{1.5333}{(h-1)^2}. \tag{8.37}$$

- g_{12} peaks

$$\begin{aligned} g_{12}^{(\text{peak 1})} &= 0.0608 + \frac{0.1990}{h-1}, \\ g_{12}^{(\text{peak 2})} &= -0.0103 - \frac{0.0048}{h-1}. \end{aligned} \tag{8.38}$$

- g_{22} peaks

$$\begin{aligned} g_{22}^{(\text{peak 1})} &= 0.0498 - 0.0142h + 0.0042h^2, \\ g_{22}^{(\text{peak 2})} &= 0.0046 - 0.0042h + 0.0019h^2, \\ g_{22}^{(\text{peak 3})} &= 0.0207 - 0.0125h - 0.0194h^2. \end{aligned} \tag{8.39}$$

[2]The peaks are numbered from left to right (see Figures 8.3 and 8.4).

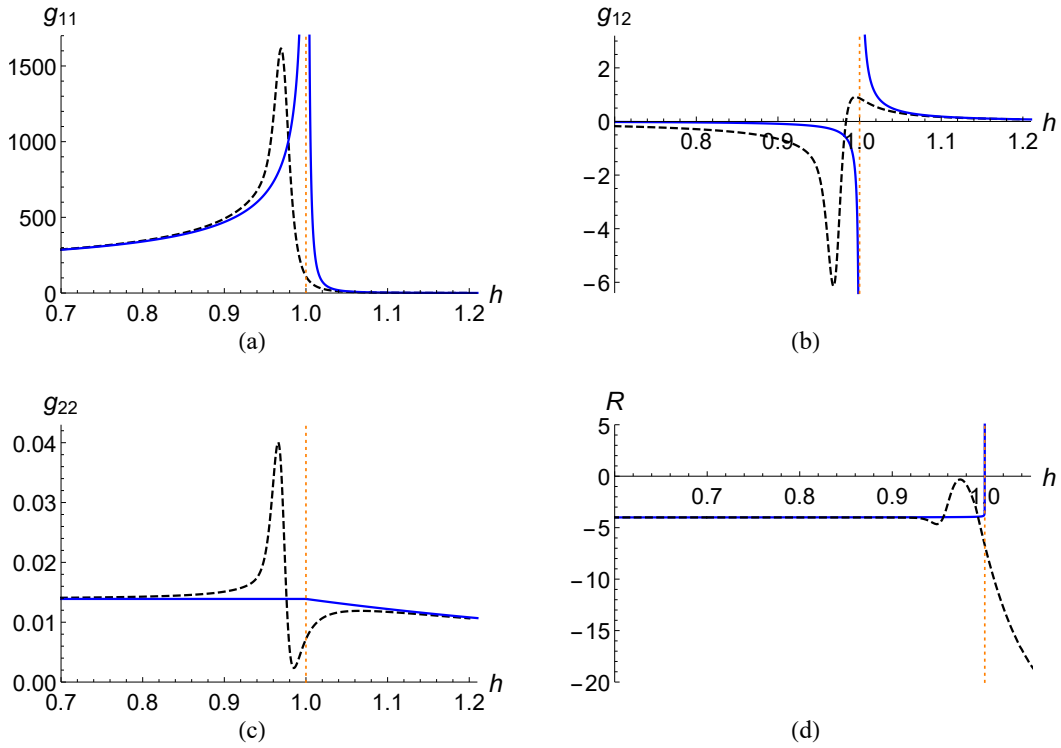

Figure 8.4: Metric components and scalar curvature of the classical (or quantum) metric in the thermodynamic limit (solid blue) and the exact quantum metric for $j = 500$ (dashed black) as a function of h when $\gamma = -0.5$. The g_{11} and g_{12} components of the thermodynamic limit diverge at the phase transition (dotted orange), while the quantum metric is always smooth.

From the functions (8.37) and (8.38), it is clear that in the limit $h = 1$, the metric components g_{11} and g_{12} exhibit a divergent behavior, which is in accordance with the corresponding classical (or quantum) metric components in the thermodynamic limit.

In Figure 8.6, we plot the height of the peaks as a function of j for $\gamma = -0.5$. A linear relation between these quantities is evident when using a log-log scale. The function we use to fit the points is

$$\ln(g_{ij}^{(\text{peak})}) = m \ln(j) + n, \tag{8.40}$$

where the parameters m and n are shown in Table 8.1 for every peak. We reproduce the value $m \approx 1.3$ for the metric component g_{11} that was obtained in references [123, 132, 133]. In addition to this, we analyze the other components, finding that the sum of the m values for the two peaks of g_{12} is 1.3142, which is a similar result to that of the g_{11} component. This is because g_{12} has mixed information about the parameters h and γ. Accordingly, the m values of g_{22} do not relate with those of the other components.

Now, we study the scalar curvature for two representative values of γ. This will allow us to characterize R for finite j and infer its behavior in the $j \to \infty$ limit. We first analyze the behavior of the extrema as functions of h. In Figure 8.7, we plot the two

Peak	m	n
$g_{11}^{(peak)}$	1.3103	-0.7480
$g_{12}^{(peak\,1)}$	0.6549	-2.2513
$g_{12}^{(peak\,2)}$	0.6593	-4.1853
$g_{22}^{(peak\,1)}$	-0.0081	-3.1676
$g_{22}^{(peak\,2)}$	-0.0037	-6.0269
$g_{22}^{(peak\,3)}$	0.0731	-4.9007

Table 8.1: Values of m and n in equation (8.40) for $\gamma = -0.5$. Notice that the two peaks of g_{12} have the property that their values of m sum up to 1.3142, which is close to the m value of g_{11} peak.

peaks of R for $\gamma = -0.5$ and $\gamma = -0.1$. One of the peaks is a local minimum (peak 1) and the other is a maximum (peak 2). The functions that interpolate the points of the minima are

$$\begin{aligned} R^{(\text{peak}\,1)}(h, \gamma = -0.5) &= -3.407 - \frac{2.197}{h + 0.795}, \\ R^{(\text{peak}\,1)}(h, \gamma = -0.1) &= -3.443 - \frac{1.525}{h + 0.285}, \end{aligned} \tag{8.41}$$

whereas for the maxima they are

$$\begin{aligned} R^{(\text{peak}\,2)}(h, \gamma = -0.5) &= -2.972 + \frac{3.674}{h + 0.412}, \\ R^{(\text{peak}\,2)}(h, \gamma = -0.1) &= -2.685 + \frac{2.145}{h - 0.073}. \end{aligned} \tag{8.42}$$

At $h = 1$, where the quantum phase transition appears in the thermodynamic limit, the first peak of R takes the value of -4.631 when $\gamma = -0.5$ and -4.630 when $\gamma = -0.1$, whereas the second peak goes to -0.370 when $\gamma = -0.5$ and to -0.371 when $\gamma = -0.1$. The value of the first peak in both cases is very close to the one predicted by the truncated Holstein-Primakoff approximation. Also, notice that at $h = 1$, the minima for the two different values of γ are similar, which is also the case for the maxima. This is seen in Figure 8.7, where both lines intersect.

If we now analyze the value of the peaks as a function of j, we can fit the data for the minima as follows:

$$\begin{aligned} R^{(\text{peak}\,1)}(j, \gamma = -0.5) &= -4.645 - \frac{3.882}{j^{0.812}}, \\ R^{(\text{peak}\,1)}(j, \gamma = -0.1) &= -4.655 - \frac{6.100}{j^{0.879}}. \end{aligned} \tag{8.43}$$

For the maxima, the functions take the form

$$R^{(\text{peak }2)}(j,\gamma=-0.5) = -0.365 + \frac{3.408}{j^{0.695}},$$
$$R^{(\text{peak }2)}(j,\gamma=-0.1) = -0.360 + \frac{4.749}{j^{0.726}}. \tag{8.44}$$

We show in Figure 8.8 the behavior of the two peaks of R as a function of j when $\gamma = -0.5$ and $\gamma = -0.1$. Two main features are seen. First, the minimum (peak 1) grows as j increases and the maximum (peak 2) decreases with j. Second, the functions (8.43) reveal that the minimum reaches a value around -4.6 when $j \to \infty$, whereas the maximum (8.44) goes to -0.36. This is also confirmed by equations (8.41) and (8.42), since the limits $h = 1$ and $j \to \infty$ predict the same results. The persistence of both peaks when $j \to \infty$ seems to indicate that the scalar curvature is not singular in the thermodynamic limit; perhaps a more detailed analysis for higher values of j can help understand this issue. Nevertheless, it is important to remark that despite the scalar curvature's smoothness for finite j, its peaks function as precursors of the quantum phase transition.

A comment can be made regarding the change of sign in the maximum of R. Solving the condition $R^{(\text{peak }2)} = 0$ yields the value of j for which the maximum is zero. When $\gamma = -0.5$, this value is $j = 25$, while for $\gamma = -0.1$, the result is $j = 35$. This indicates a local change in the geometry of the parameter space, i.e., a change in curvature from spherical-type to hyperbolic-type, although we do not attribute any special interpretation to those values of j.

We close by remarking that in reference [123], the authors found the fidelity susceptibility related to the parameter h, however, we contributed with the exploration of the parameter γ through the other two components of the quantum metric tensor. In this way, we closed the geometric study with the analytic and numerical computation of the scalar curvature, as well as with the analysis of their peaks.

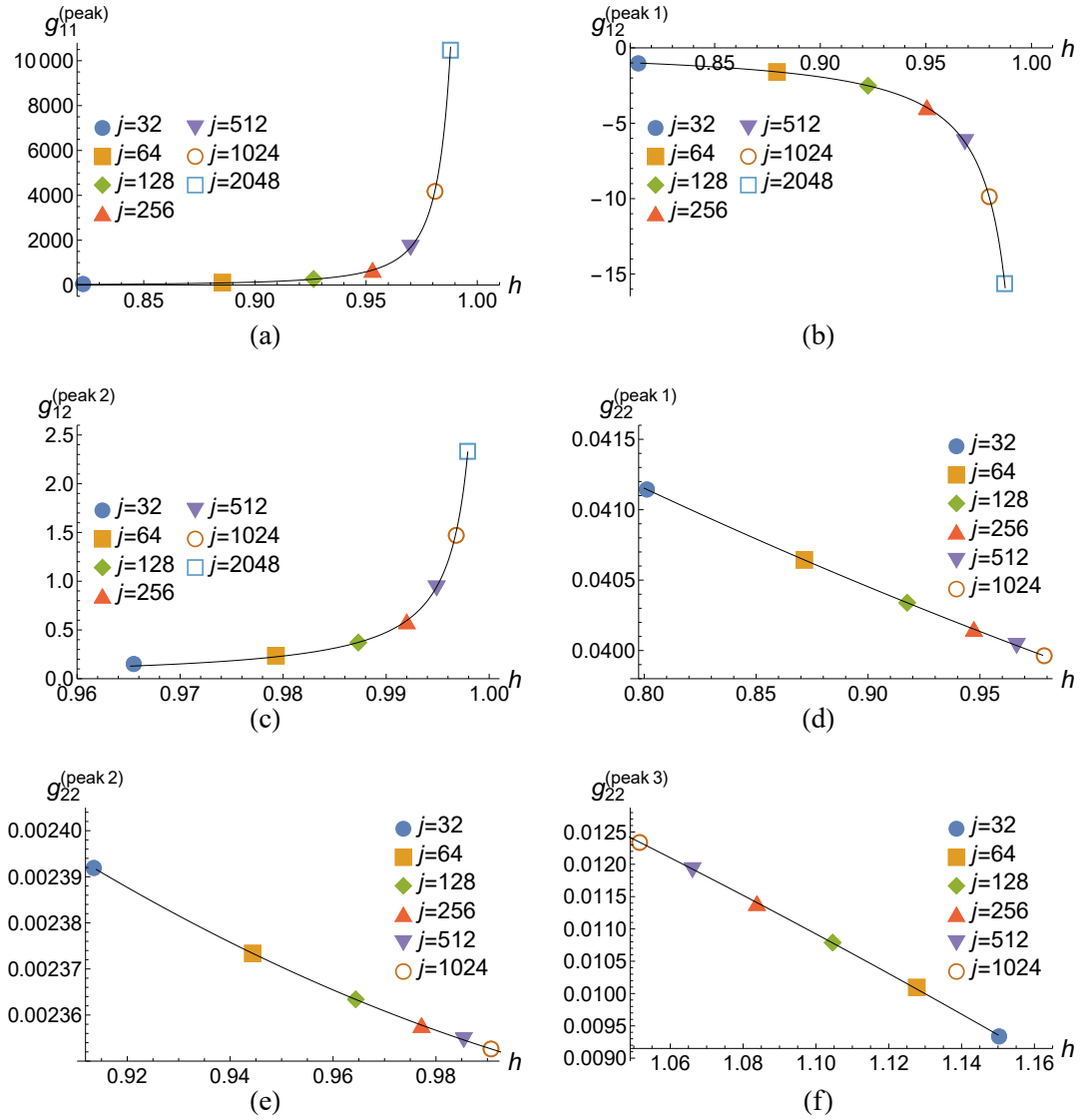

Figure 8.5: Peaks of the components of the quantum metric as functions of h when $\gamma = -0.5$. The value of j is indicated for each point. The g_{11} component has only one peak, g_{12} has two peaks, and g_{22} has three peaks.

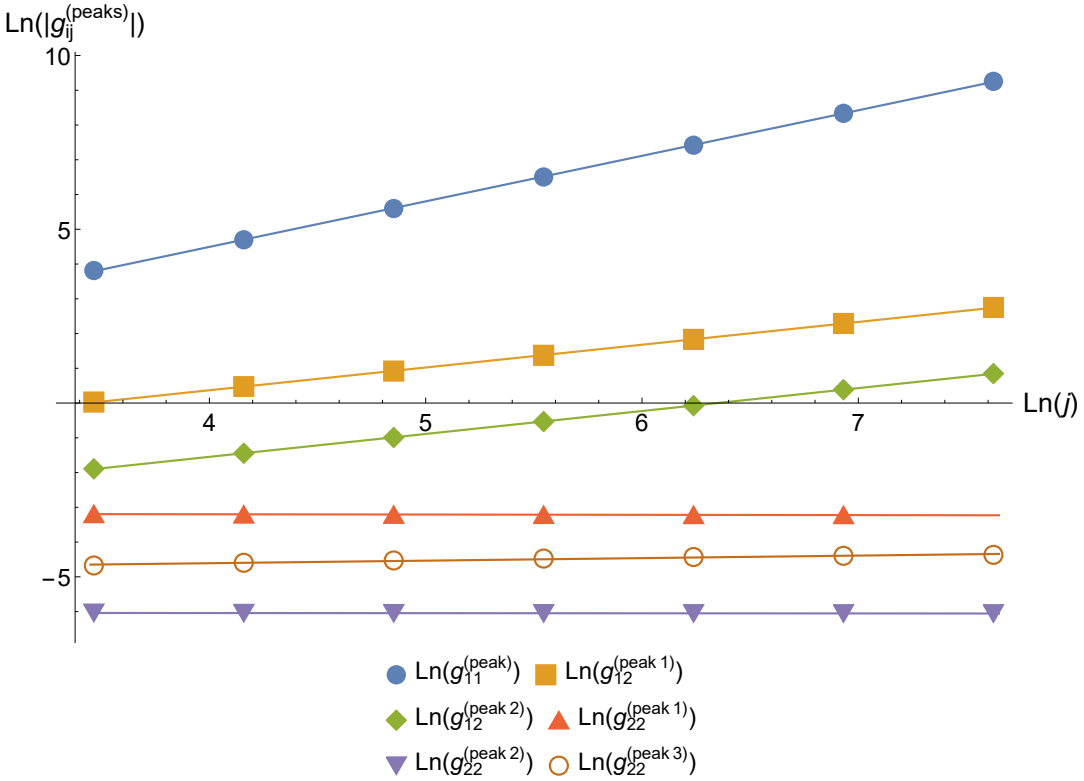

Figure 8.6: Peaks of the components of the quantum metric as functions of j when $\gamma = -0.5$. The axes are presented in logarithmic scale.

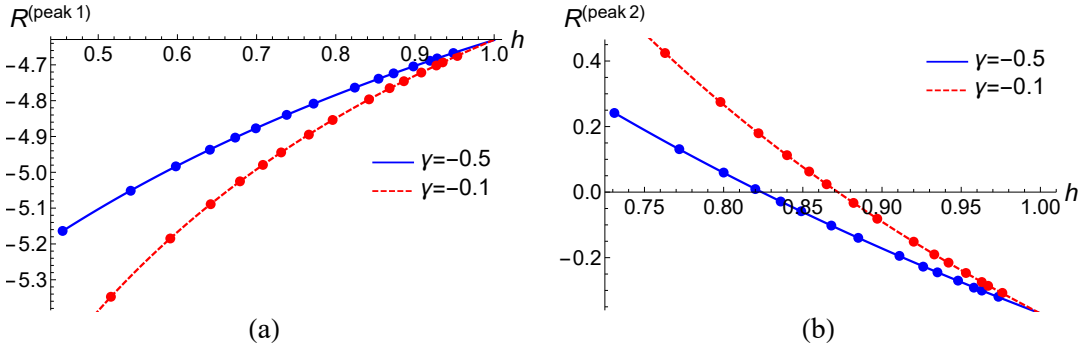

Figure 8.7: Peaks of the scalar curvature as functions of h for $\gamma = -0.5$ and $\gamma = -0.1$. The values of j=12,16,20,24,28,32,40,50,75,100,125,175,250,300,500 were considered. In both plots, j grows with h.

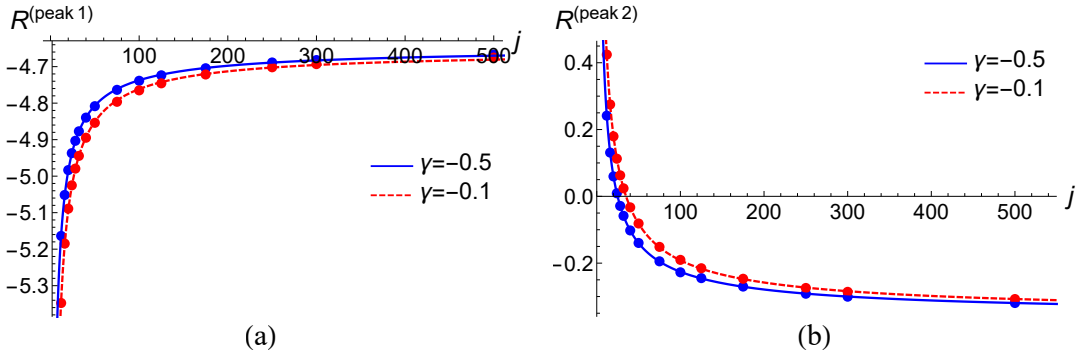

Figure 8.8: Peaks of the scalar curvature as functions of j for $\gamma = -0.5$ and $\gamma = -0.1$. The minimum is shown in (a) and the maximum is shown in (b).

Chapter 9

Application to a modified Lipkin-Meshkov-Glick model

In this chapter, we present a Lipkin-Meshkov-Glick (LMG) model with a linear term in $\hat{J}_x$. In this case, the parameter space provides an invertible metric in both phases, and therefore, a well-defined scalar curvature across the parameter space. We first build the classical Hamiltonian using Bloch coherent states and find its fixed points. We will focus on the quantum phase transition that appears in the highest energy state, so we compute the quantum geometric tensor for this state using the truncated Holstein-Primakoff transformation. As a result, we observe a divergence in the metric components at the phase transition and we find that the Berry curvature only exists in one of the phases. We then compute the scalar curvature and show that it has a singularity at the phase transition. We then contrast the analytic results with their finite-size counterparts obtained through exact numeric diagonalization, and find a good agreement between them, except in points near the phase transition where the Holstein-Primakoff approximation ceases to be valid. We finally include a detailed analysis of the precursors of the quantum phase transition that appear in the metric and its scalar curvature.

The modified LMG model that we propose has the Hamiltonian

$$\hat{H}_{\mathrm{LMG}} = \Omega \hat{J}_z + \Omega_x \hat{J}_x + \frac{\xi_y}{j} \hat{J}_y^2, \tag{9.1}$$

where $\hat{J}_{x,y,z} = (1/2)\sum_i \sigma^{(i)}_{x,y,z}$ are the collective pseudo-spin operators and $j = \mathcal{N}/2$, with j coming from the eigenvalue $j(j+1)$ of the total spin operator $\hat{J}^2 = \hat{J}_x^2 + \hat{J}_y^2 + \hat{J}_z^2$. Also, Ω, Ω_x and ξ_y are real parameters, and we put $\hbar = 1$. We begin by studying the properties of this model when $j \to \infty$, i.e., the thermodynamic limit.

9.1 Analysis in the thermodynamic limit

The classical LMG Hamiltonian, which gives an exact description of the quantum system for $j \to \infty$, is obtained by taking the expectation value of $\hat{H}_{\mathrm{LMG}}/j$ in Bloch coherent

states $|z\rangle = \left(1+|z|^2\right)^{-j} e^{z\hat{J}_+}|j,-j\rangle$, where $|j,-j\rangle$ is the state with the lowest pseudo-spin projection, and $\hat{J}_+$ is the raising operator (for details, see Appendix C). Defining $z = e^{-i\phi}\tan\frac{\theta}{2}$, the classical LMG Hamiltonian has the simple form

$$H_{cl} = \frac{\langle z|\hat{H}_{\rm LMG}|z\rangle}{j} = -\Omega\cos\theta + \Omega_x \sin\theta\cos\phi + \xi_y \sin^2\theta\sin^2\phi, \tag{9.2}$$

or, in terms of the canonical variables

$$Q = \sqrt{2(1-\cos\theta)}\cos\phi, \qquad P = -\sqrt{2(1-\cos\theta)}\sin\phi, \tag{9.3}$$

it reads

$$H_{cl}(Q,P) = \frac{\Omega}{2}\left(P^2+Q^2\right) - \Omega + \Omega_x Q\sqrt{1-\frac{P^2+Q^2}{4}} + \xi_y P^2\left(1-\frac{P^2+Q^2}{4}\right). \tag{9.4}$$

We now set out to find the fixed points of the Hamiltonian (9.4). To simplify the analysis, we consider only two independent parameters (Ω_x and ξ_y), setting from now on $\Omega = 1$. Notice that the Hamiltonian (9.2) is invariant under $\phi \to -\phi$, which has as a consequence the invariance of (9.4) under $P \to -P$. This implies that all the fixed points are doubly degenerate if $\phi \neq 0$ or $\phi = \pi$.

The fixed points of (9.4) are found by imposing the conditions $\dot{Q} = 0$ and $\dot{P} = 0$ on the Hamilton equations in the region $0 \le \theta \le \pi$, $0 \le \phi < 2\pi$, which means that

$$\begin{aligned}
\dot{Q} &= \frac{\partial H_{cl}}{\partial P} = \frac{P}{2}\left[2\Omega - \xi_y(2P^2+Q^2-4) - \frac{\Omega_x Q}{\sqrt{4-(P^2+Q^2)}}\right] = 0,\\
\dot{P} &= -\frac{\partial H_{cl}}{\partial Q} = \frac{1}{2}\left[\xi_y P^2 Q + \frac{\Omega_x Q^2}{\sqrt{4-(P^2+Q^2)}} - \Omega_x\sqrt{4-(P^2+Q^2)} - 2\Omega Q\right] = 0,
\end{aligned} \tag{9.5}$$

The valid solutions of this system are:

1. For any value of Ω_x and ξ_y:
   - $\mathbf{x}_1 = (Q_1,P_1) = \left(\sqrt{2+\frac{2}{\sqrt{\Omega_x^2+1}}},0\right)$ with $(\theta_1,\phi_1) = \left(\arccos\left(-\frac{1}{\sqrt{\Omega_x^2+1}}\right),0\right)$.
   - $\mathbf{x}_2 = (Q_2,P_2) = \left(-\sqrt{2-\frac{2}{\sqrt{\Omega_x^2+1}}},0\right)$ with $(\theta_2,\phi_2) = \left(\arccos\left(\frac{1}{\sqrt{\Omega_x^2+1}}\right),\pi\right)$.
2. For $\xi_y \le -\frac{\sqrt{\Omega_x^2+1}}{2}$:
   - $\mathbf{x}_3 = (Q_3,P_3) = \left(-\frac{\Omega_x}{\sqrt{\xi_y(2\xi_y-1)}}, -\sqrt{\frac{4\xi_y^2-\Omega_x^2-1}{\xi_y(2\xi_y-1)}}\right)$
     with $(\theta_3,\phi_3) = \left(\arccos\left(-\frac{1}{2\xi_y}\right), \arccos\left(-\frac{\Omega_x}{\sqrt{4\xi_y^2-1}}\right)\right)$ and $\sin\phi_3 = \sqrt{1-\cos^2\phi_3}$.

- $\mathbf{x}_3' = (Q_3', P_3') = \left(-\frac{\Omega_x}{\sqrt{\xi_y(2\xi_y-1)}}, \sqrt{\frac{4\xi_y^2-\Omega_x^2-1}{\xi_y(2\xi_y-1)}} \right)$
  with $(\theta_3', \phi_3') = \left(\arccos\left(-\frac{1}{2\xi_y}\right), \arccos\left(-\frac{\Omega_x}{\sqrt{4\xi_y^2-1}}\right) \right)$ and $\sin\phi_3' = -\sqrt{1-\cos^2\phi_3'}$.

3. For $\xi_y \geq \frac{\sqrt{\Omega_x^2+1}}{2}$:

- $\mathbf{x}_4 = (Q_4, P_4) = \left(\frac{\Omega_x}{\sqrt{\xi_y(2\xi_y-1)}}, -\sqrt{\frac{4\xi_y^2-\Omega_x^2-1}{\xi_y(2\xi_y-1)}} \right)$
  with $(\theta_4, \phi_4) = \left(\arccos\left(-\frac{1}{2\xi_y}\right), \arccos\left(\frac{\Omega_x}{\sqrt{4\xi_y^2-1}}\right) \right)$ and $\sin\phi_4 = \sqrt{1-\cos^2\phi_4}$.

- $\mathbf{x}_4' = (Q_4', P_4') = \left(\frac{\Omega_x}{\sqrt{\xi_y(2\xi_y-1)}}, \sqrt{\frac{4\xi_y^2-\Omega_x^2-1}{\xi_y(2\xi_y-1)}} \right)$
  with $(\theta_4', \phi_4') = \left(\arccos\left(-\frac{1}{2\xi_y}\right), \arccos\left(\frac{\Omega_x}{\sqrt{4\xi_y^2-1}}\right) \right)$ and $\sin\phi_4' = -\sqrt{1-\cos^2\phi_4'}$.

The energies $h_i = H_{cl}(\mathbf{x}_i)$ associated with each fixed point are given in Table 9.1.

Point	Energy
$\mathbf{x_1}$	$\sqrt{\Omega_x^2+1}$
$\mathbf{x_2}$	$-\sqrt{\Omega_x^2+1}$
$\mathbf{x_3}$ and $\mathbf{x_3'}$	$(4\xi_y^2+\Omega_x^2+1)/(4\xi_y)$
$\mathbf{x_4}$ and $\mathbf{x_4'}$	$(4\xi_y^2+\Omega_x^2+1)/(4\xi_y)$

Table 9.1: Classical energies at each fixed point.

Some properties of the energies are:

- The energies h_1 and h_2 are defined for any value of Ω_x and ξ_y.
- The energy h_3 is only defined in the region $\xi_y \leq -\frac{\sqrt{\Omega_x^2+1}}{2}$, where it satisfies $h_3 \leq h_2$.
- The energy h_4 is only defined in the region $\xi_y \geq \frac{\sqrt{\Omega_x^2+1}}{2}$, where it satisfies $h_4 \geq h_1$.

Each of the curves $\xi_y = \pm\frac{\sqrt{\Omega_x^2+1}}{2}$ is the separatrix between different regions which correspond to different quantum phases of the LMG model in the thermodynamic limit. Accordingly, for a fixed ξ_y, the values $\Omega_x = \pm\Omega_{xc} = \pm\sqrt{4\xi_y^2-1}$ represent the critical coupling at which the quantum phase transition occurs. To understand this, we show in Figure 9.1 the energies as functions of Ω_x for a fixed ξ_y. In (a), for negative ξ_y, we clearly see that the ground state energy has the value h_3 when $-\Omega_{xc} < \Omega_x < \Omega_{xc}$, while it takes

the value h_2 when $\Omega_x < -\Omega_{xc}$ or $\Omega_x > \Omega_{xc}$; this indicates the presence of a quantum phase transition in the ground state. However, for positive ξ_y, the ground state energy is given only by h_2 in the whole region, as clearly shown in (b), thus, no phase transition appears in this case.

Regarding the highest energy, for negative ξ_y, we see in (a) that it takes the value h_1 for any Ω_x so it does not present a phase transition. On the other hand, when ξ_y is positive, (b) shows that the highest energy is h_4 in the region $-\Omega_{xc} < \Omega_x < \Omega_{xc}$, whereas for $\Omega_x < -\Omega_{xc}$ or $\Omega_x > \Omega_{xc}$, it takes the value h_1; therefore, we have a quantum phase transition in this case.

In what follows, we only consider positive values of ξ_y so that we have the quantum phase transition occurring in the highest energy state. Due to the symmetries of the model, reversing the sign of ξ_y would generate an analogous description for the ground state. For $\xi_y < \frac{\sqrt{\Omega_x^2+1}}{2}$, the highest energy state is unique and we call it the symmetric phase. On the contrary, when $\xi_y > \frac{\sqrt{\Omega_x^2+1}}{2}$, the highest energy state is doubly degenerate and we call it the broken phase.

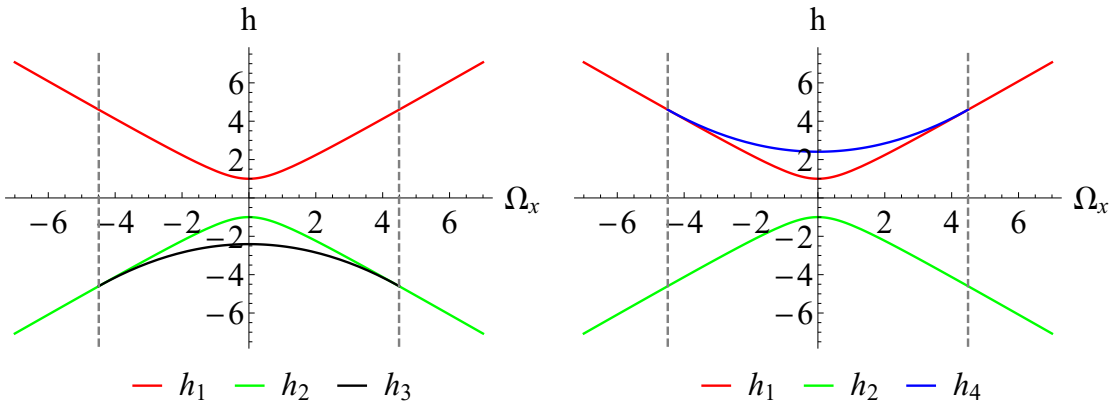

(a) (b)

Figure 9.1: Classical energies as functions of Ω_x when (a) $\xi_y = -2.3$ and (b) $\xi_y = 2.3$. The energies h_3 and h_4 are only defined in the region $-4.490 \leq \Omega_x \leq 4.490$ whose extreme values are marked with the dashed gray lines.

We show in Figure 9.2 the expectation values of some observables in Bloch coherent states and their comparison with the expectation values taken in the highest energy eigenstate. The quantum phase transition manifests as a discontinuity in the first derivative of the plots at $\Omega_{xc} = 4.490$ for (b), (c), and (d), whereas as a discontinuity in the second derivative at $\Omega_{xc} = 4.490$ for (a). The coherent states give an excellent description of the system even for $j = 128$.

To further illustrate the quantum phase transition, we show in Figure 9.3 the fixed points $\mathbf{x}_1$, $\mathbf{x}_2$, $\mathbf{x}_4$, and $\mathbf{x}_4'$. We can see how the fixed points move and how the phase space trajectories change around them when the parameter Ω_x is varied leaving ξ_y fixed.

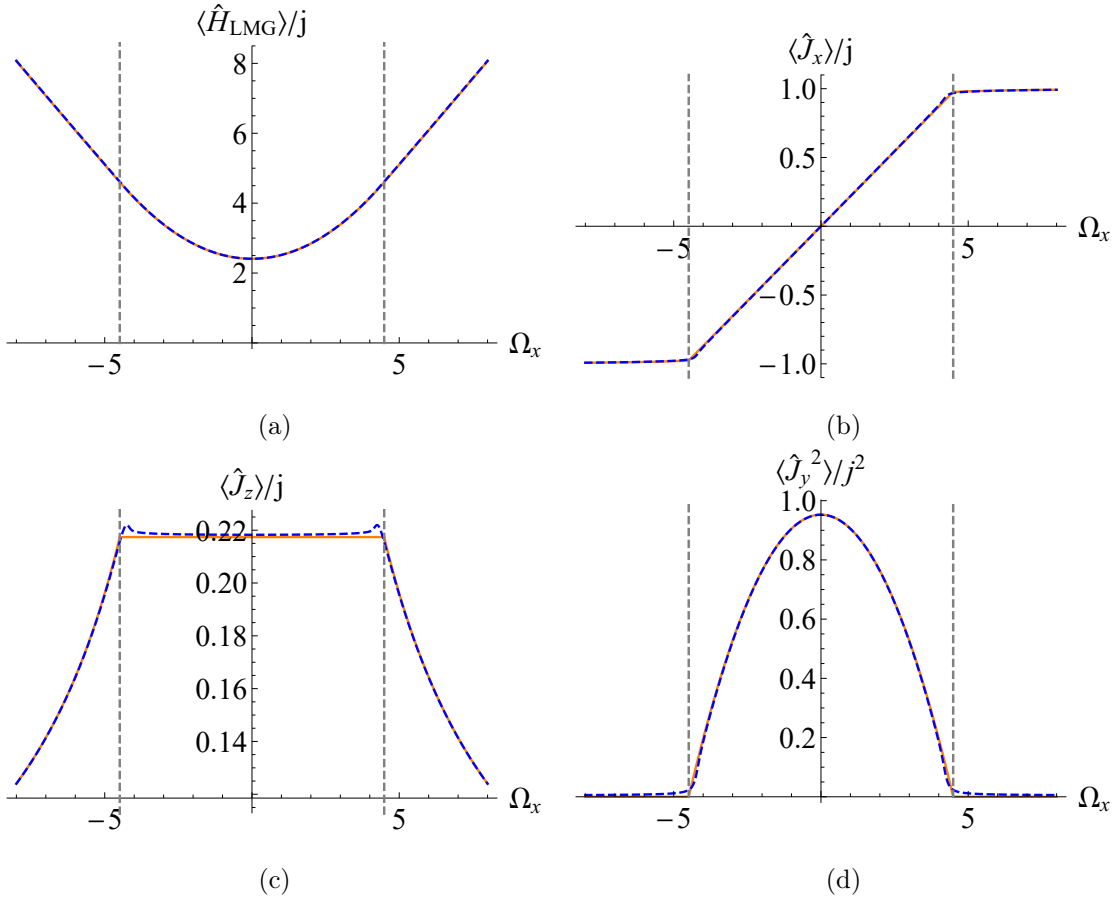

Figure 9.2: Comparison of the expectation values of different observables taken in the highest energy eigenstate (dashed blue) and in spin coherent states (solid orange) for $j = 128$ and $\xi_y = 2.3$. The critical values $\pm\Omega_{xc} = \pm 4.490$ are signaled with the gray dashed lines.

The green point is $\mathbf{x}_2$ and it corresponds to the ground state of the system; as we know, for positive values of ξ_y the ground state does not present a quantum phase transition, thus preserving a center stability. The two blue points are $\mathbf{x}_4$ and $\mathbf{x}_4'$, and for $\Omega_x < \Omega_{xc}$, they correspond to the highest energy states; they are stable center points in this region. As we increase Ω_x, we see that the two blue points become closer until they disappear at the phase transition when $\Omega_x = \Omega_{xc}$. Finally, the red point is $\mathbf{x}_1$ and it corresponds to the highest energy state when $\Omega_x > \Omega_{xc}$, where it is stable center point. However, note that at $\Omega_x = \Omega_{xc}$ it changes its stability, becoming an unstable hyperbolic point for $\Omega_x < \Omega_{xc}$ and having a positive Lyapunov exponent given by

$$\lambda = \sqrt{\sqrt{1+\Omega_x^2}\,(2\xi_y - \sqrt{1+\Omega_x^2})}. \tag{9.6}$$

Figure 9.4 shows the Lyapunov exponent of $\mathbf{x}_1$ as a function of the parameters Ω_x and ξ_y. It is important to mention that the Hamiltonian (9.4) is integrable and thus has regular dynamics. The Lyapunov exponent is therefore not associated to chaos but to

an instability.

In the quantum domain, the instability of $\mathbf{x}_1$ is associated with an excited-state quantum phase transition (ESQPT). A main signature of ESQPTs is the divergence of the density of states at an energy denoted by E_c. In the mean-field approximation, it has been shown that this energy coincides with the energy of the classical system at the saddle point [141, 142], in this case, $E_c = jH_{cl}(\mathbf{x}_1) = jh_1 = j\sqrt{\Omega_x^2 + 1}$. In Figure 9.5, we show the density of states for the LMG model taking $j = 256$, $\xi_y = 2$ and $\Omega_x = 0.774$. These parameters correspond to the unstable region where there is a non-zero Lyapunov exponent (see Figure 9.4). The peak in the density of states associated with the ESQPT is clearly visible at h_1, marked with a vertical red dashed line.

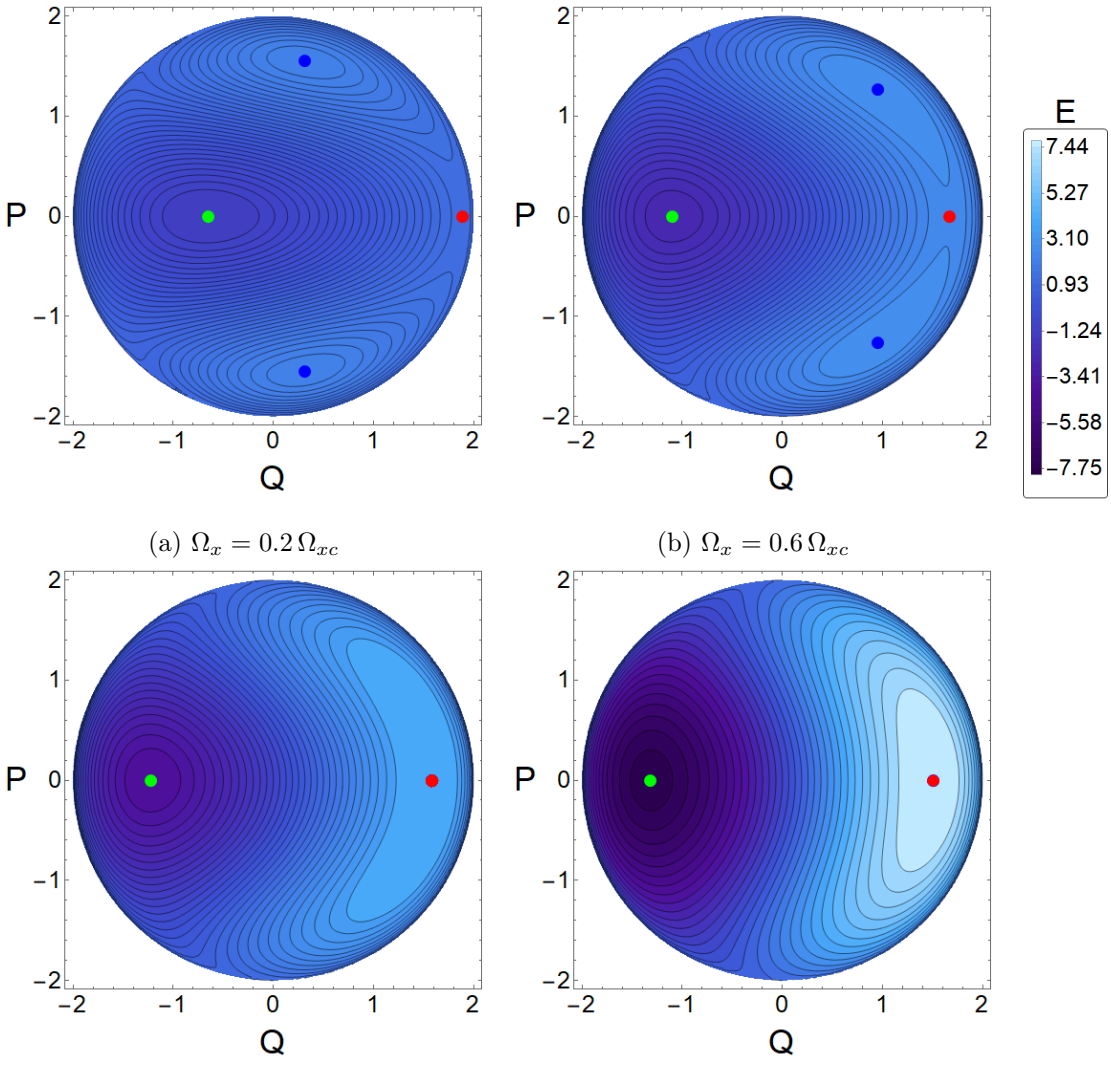

(a) $\Omega_x = 0.2\,\Omega_{xc}$ (b) $\Omega_x = 0.6\,\Omega_{xc}$

(c) $\Omega_x = \Omega_{xc}$ (d) $\Omega_x = 2\,\Omega_{xc}$

Figure 9.3: Level curves of the classical LMG Hamiltonian $H_{cl}(Q,P) = E$ for different values of Ω_x and fixing $\xi_y = 2$. The green point is $\mathbf{x}_2$ and is stable; the blue points are $\mathbf{x}_4$ and $\mathbf{x}_4'$ and are also stable; the red point is stable when $\Omega_x > \Omega_{xc}$ (d), but unstable when $\Omega_x < \Omega_{xc}$ ((a) and (b)), where it has a positive Lyapunov exponent.

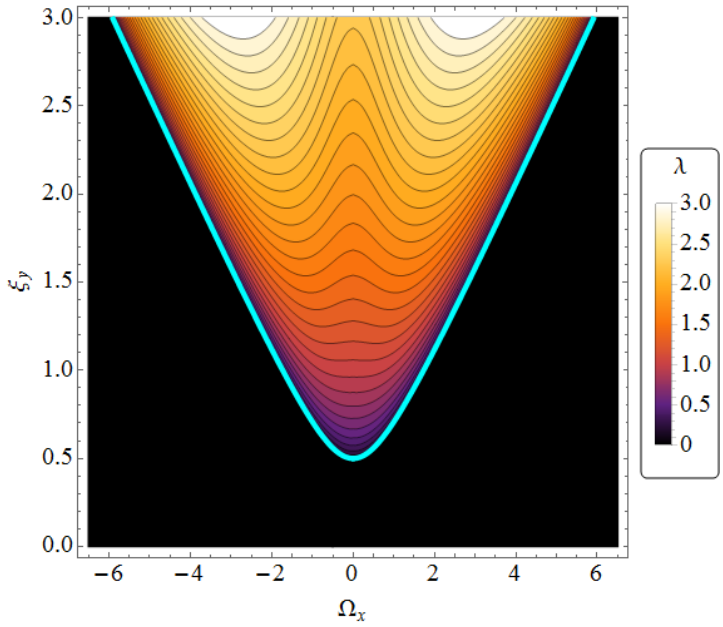

Figure 9.4: Lyapunov exponent for the critical point $\mathbf{x}_1$ as a function of the coupling parameters Ω_x and ξ_y. The black zone indicates a null Lyapunov exponent.

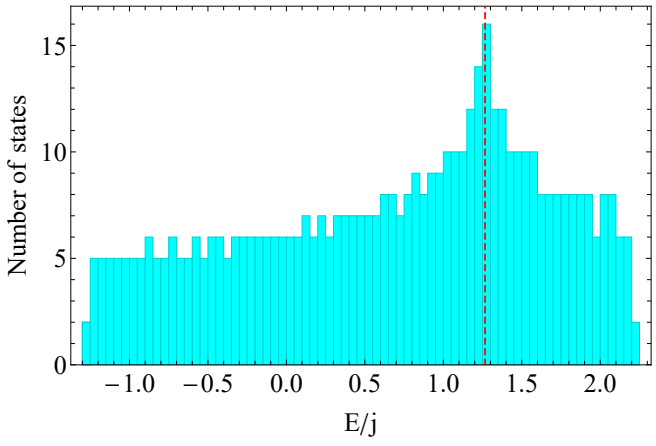

Figure 9.5: Density of states when $\xi_y = 2$ and $\Omega_x = 0.2\,\Omega_{xc}$ for $j = 256$. The red dashed line indicates the classical energy $h_1 = \sqrt{\Omega_x^2 + 1} = 1.265$ where the ESQPT takes place.

9.2 Quantum geometric tensor for the LMG model

In this section, we study the geometry of the ground state and the highest energy states of the LMG model. While the semiclassical analysis performed above employing SU(2) coherent states provides rich and valuable information about the system, it is not well suited to study the geometry of the parameter space of this system. As shown in Appendix E, the metric obtained employing coherent states is ill-defined for $\xi_y < \frac{\sqrt{\Omega_x^2+1}}{2}$ since it has a vanishing determinant. To overcome this difficulty, we first compute the quantum metric tensor and its scalar curvature in the thermodynamic limit via the truncated Holstein-Primakoff transformation [118]. This approximation becomes exact in this limit as long as we are not close to a phase transition, where spurious divergences may appear [128]. After the analytic computation, we carry out an exact diagonalization and compare the analytic and numeric results.

In what follows, we take $x = \{x^i\} = (\Omega_x, \xi_y)$ with $i = 1, 2$ as the adiabatic parameters. As we said before, we only focus on positive values of ξ_y, so that the phase transition occurs for the highest energy state.

9.2.1 Ground state

We begin our analysis with the ground state, which corresponds via the classical Hamiltonian (9.4) to the fixed point $\mathbf{x}_2$ (the green one in Figure 9.3) with angular coordinates $(\theta_2, \phi_2) = \left(\arccos\left(\frac{1}{\sqrt{\Omega_x^2+1}}\right), \pi\right)$. The first step is to align the classical pseudospin of the ground state with the z axis. To do this, we perform a rotation of the spin operators around the y axis as follows [132, 133]

$$\begin{pmatrix} \hat{J}_x \\ \hat{J}_y \\ \hat{J}_z \end{pmatrix} = \begin{pmatrix} \cos\theta_2 & 0 & \sin\theta_2 \\ 0 & 1 & 0 \\ -\sin\theta_2 & 0 & \cos\theta_2 \end{pmatrix} \begin{pmatrix} \hat{J}'_x \\ \hat{J}'_y \\ \hat{J}'_z \end{pmatrix}. \tag{9.7}$$

With this rotation, the Hamiltonian (9.1) takes the form

$$\hat{H} = \sqrt{1+\Omega_x^2}\,\hat{J}'_z + \frac{\xi_y}{j}\hat{J}'^2_y, \tag{9.8}$$

which is suitable for applying the Holstein-Primakoff transformation that maps angular momentum operators into bosonic operators as

$$\hat{J}'_z = \hat{a}^\dagger\hat{a} - j, \qquad \hat{J}'_+ = \sqrt{2j}\,\hat{a}^\dagger\sqrt{1-\frac{\hat{a}^\dagger\hat{a}}{2j}}, \qquad \hat{J}'_- = \sqrt{2j}\sqrt{1-\frac{\hat{a}^\dagger\hat{a}}{2j}}\,\hat{a}. \tag{9.9}$$

It is readily verified that this representation satisfies the SU(2) algebra as long as $[\hat{a}, \hat{a}^\dagger] = 1$. Now, we consider the thermodynamic limit $j \to \infty$ and expand the square roots

retaining only the zeroth order term in $1/j$ [123, 132, 133]. The Cartesian components of the angular momentum turn out to be

$$\hat{J}'_x \simeq \sqrt{\frac{j}{2}}\left(\hat{a}^\dagger + \hat{a}\right), \qquad \hat{J}'_y \simeq -i\sqrt{\frac{j}{2}}\left(\hat{a}^\dagger - \hat{a}\right), \qquad \hat{J}'_z = \hat{a}^\dagger\hat{a} - j. \tag{9.10}$$

In principle, we may substitute these expressions into equation (9.8) and perform a Bogoliubov transformation to creation and annihilation operators $(\hat{b}, \hat{b}^\dagger)$ that diagonalize the Hamiltonian. However, for illustrative purposes, we make first the intermediate transformation $\hat{Q} = \frac{1}{\sqrt{2}}\left(\hat{a}^\dagger + \hat{a}\right)$, $\hat{P} = \frac{i}{\sqrt{2}}\left(\hat{a}^\dagger - \hat{a}\right)$ to find that the Hamiltonian takes the form

$$\hat{H} \simeq -j\sqrt{\Omega_x^2+1} + \left(\frac{\sqrt{\Omega_x^2+1}+2\xi_y}{2}\right)\hat{P}^2 + \frac{\sqrt{\Omega_x^2+1}}{2}\hat{Q}^2. \tag{9.11}$$

This suggests the use of the following transformation

$$\hat{Q} = \left(\frac{\sqrt{1+\Omega_x^2}+2\xi_y}{4\sqrt{1+\Omega_x^2}}\right)^{1/4}\left(\hat{b}^\dagger + \hat{b}\right), \qquad \hat{P} = i\left(\frac{\sqrt{1+\Omega_x^2}}{4\left(\sqrt{1+\Omega_x^2}+2\xi_y\right)}\right)^{1/4}\left(\hat{b}^\dagger - \hat{b}\right), \tag{9.12}$$

that will cast the Hamiltonian (9.11) into the harmonic oscillator

$$\hat{H} \simeq -j\sqrt{\Omega_x^2+1} + \sqrt{\sqrt{\Omega_x^2+1}\left(\sqrt{\Omega_x^2+1}+2\xi_y\right)}\left(\hat{b}^\dagger\hat{b} + \frac{1}{2}\right), \tag{9.13}$$

which has the frequency $\omega = \sqrt{\sqrt{\Omega_x^2+1}\left(\sqrt{\Omega_x^2+1}+2\xi_y\right)}$ and energy $E = -j\sqrt{\Omega_x^2+1}$. The quantum metric tensor can now be calculated with the aid of equation (2.64) setting $n = 0$ and employing the operators

$$\begin{aligned}\frac{\partial \hat{H}_{\mathrm{LMG}}}{\partial \Omega_x} &= \hat{J}_x = \frac{1}{\sqrt{\Omega_x^2+1}}\hat{J}'_x + \frac{\Omega_x}{\sqrt{\Omega_x^2+1}}\hat{J}'_z,\\ \frac{\partial \hat{H}_{\mathrm{LMG}}}{\partial \xi_y} &= \frac{\hat{J}_y^2}{j} = \frac{\hat{J}_y'^2}{j},\end{aligned} \tag{9.14}$$

provided that they are expressed in terms of $(\hat{b}, \hat{b}^\dagger)$ to act on the eigenstates of $\hat{H}$. After doing this, we find the components

$$\begin{aligned} g_{11} &= \frac{j}{2\left(\Omega_x^2+1\right)^{7/4}\sqrt{\sqrt{\Omega_x^2+1}+2\xi_y}} + \frac{\xi_y^2\Omega_x^2}{8\left(\Omega_x^2+1\right)^2\left(\sqrt{\Omega_x^2+1}+2\xi_y\right)^2},\\ g_{12} &= -\frac{\xi_y\Omega_x}{8\left(\Omega_x^2+1\right)\left(\sqrt{\Omega_x^2+1}+2\xi_y\right)^2},\\ g_{22} &= \frac{1}{8\left(\sqrt{\Omega_x^2+1}+2\xi_y\right)^2}, \end{aligned} \tag{9.15}$$

and the determinant

$$g = \frac{j}{16\left(\Omega_x^2+1\right)^{7/4}\left(\sqrt{\Omega_x^2+1}+2\xi_y\right)^{5/2}}. \tag{9.16}$$

We see that a singularity appears in all the components when $\xi_y = -\frac{\sqrt{\Omega_x^2+1}}{2}$. Also, we observe that g_{11} consists of two terms, one of them is proportional to j and dominant as $j \to \infty$. Retaining all the terms and using equation (1.20), we find that the scalar curvature associated of the metric (9.15) simplifies to

$$R = -4. \tag{9.17}$$

Remarkably, the scalar curvature is constant despite the non-trivial dependence of the metric components on the parameters. Furthermore, there is no sign of the singularity that appeared in the metric, at least in the region of the parameter space under consideration. We must mention that if we had considered only the dominant term in j in g_{11} for the computation of the scalar curvature, the result would have been different; therefore, we choose to retain all the terms. This constant negative curvature signals that the parameter space of the ground state possesses a hyperbolic geometry and is isomorphic to the Lobachevsky space [51].

In Figure 9.6, we plot the metric components and the scalar curvature for $\xi_y = 2.3$ and $j = 120$. We see that the numeric results agree well with their analytic counterparts coming from the Holstein-Primakoff approximation. Figure 9.7 shows a map of the scalar curvature for different values of j, where we see a tendency to the analytic result as j increases. Notice that the singularity predicted by the metric components (9.15) is outside the range of the parameters employed in the plots ($\xi_y > 0$).

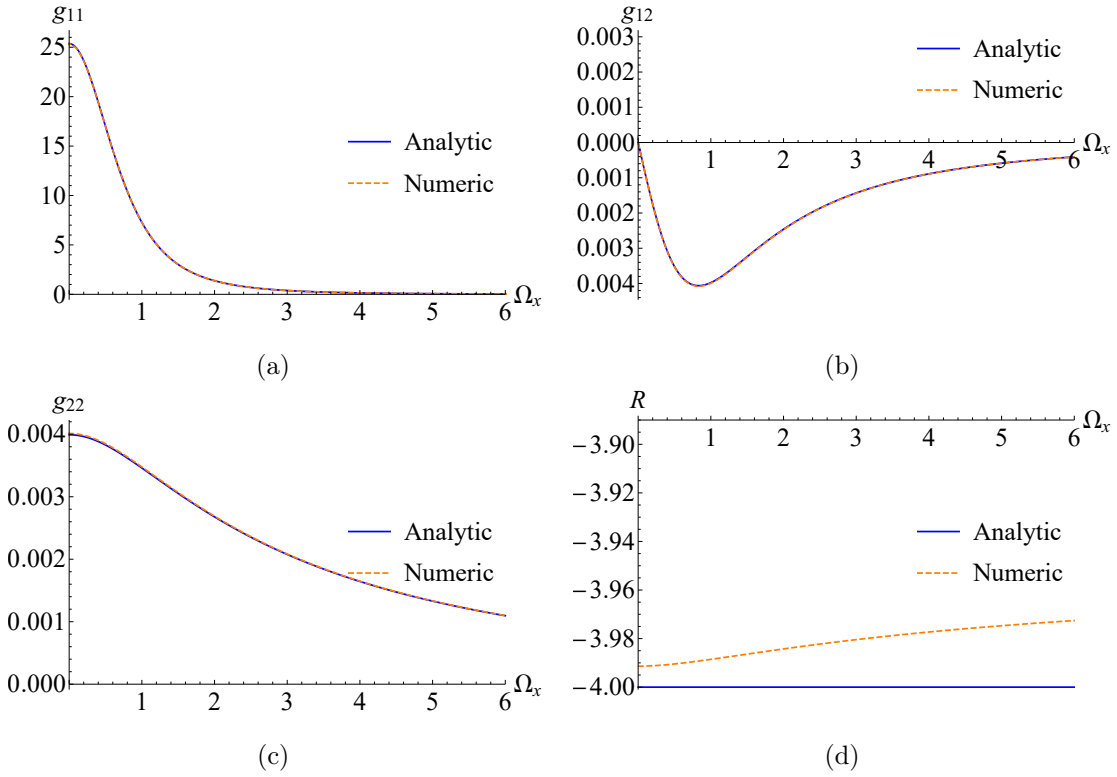

Figure 9.6: Metric components and scalar curvature for the ground state when $j = 120$ and $\xi_y = 2.3$.

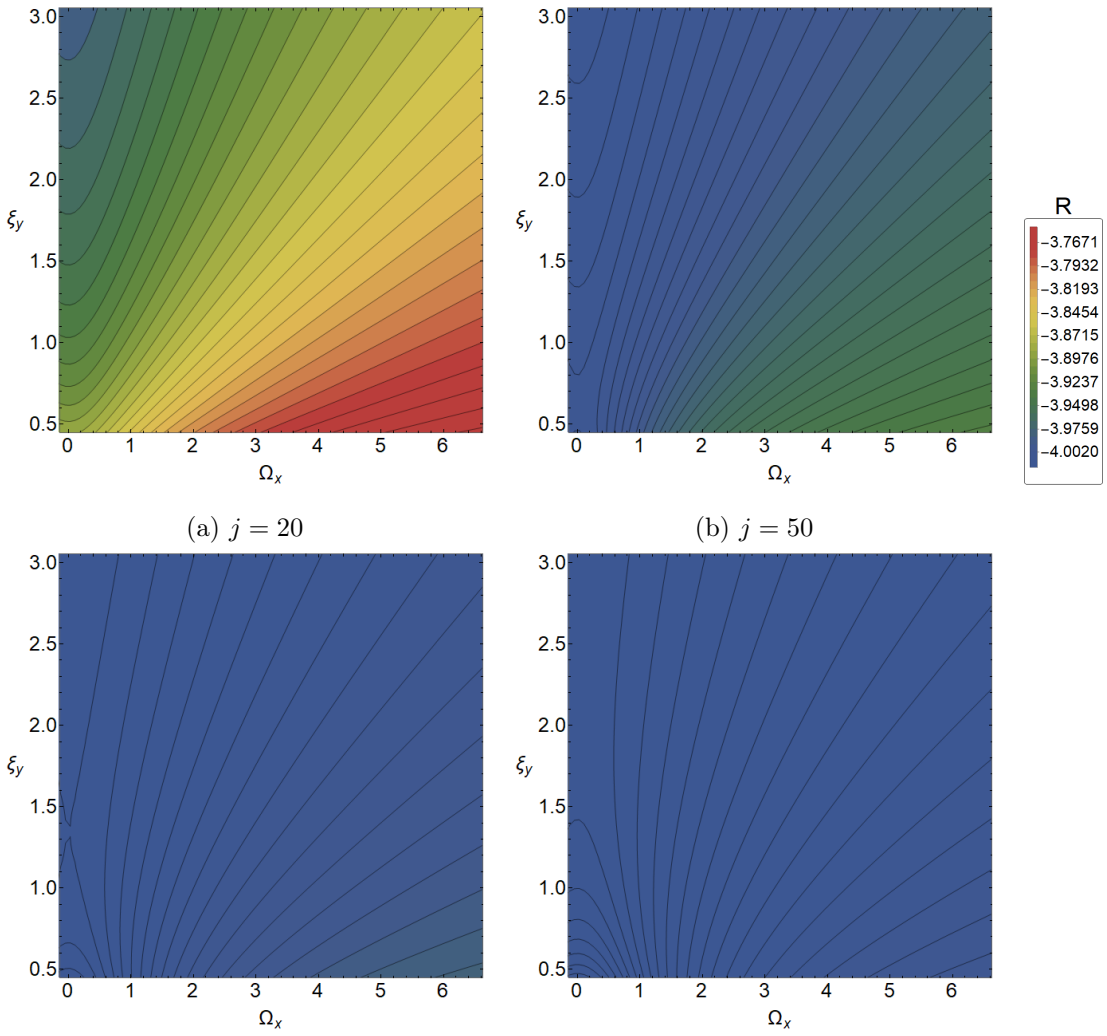

(a) $j = 20$ (b) $j = 50$

(c) $j = 80$ (d) $j = 120$

Figure 9.7: Scalar curvature map of the ground state for different values of j.

9.2.2 Highest energy state

We now study the highest energy state for which the quantum phase transition occurs. We divide the parameter space into regions above and below the separatrix, and thus, treat each phase separately. The energy of the maximum is (see Figure 9.1)

$$\frac{E_h}{j} = \begin{cases} \frac{4\xi_y^2+\Omega_x^2+1}{4\xi_y} & , \ \Omega_x < \Omega_{xc} \\ \sqrt{\Omega_x^2+1} & , \ \Omega_x > \Omega_{xc} \end{cases}, \tag{9.18}$$

The energy E_h and its first derivative are continuous as a function of Ω_x at the critical point $\Omega_x = \Omega_{xc}$, whereas its second derivative presents a discontinuity. This signals a second order quantum phase transition.

9.2.2.1 Symmetric phase

We begin with the region in parameter space for $\xi_y < \frac{\sqrt{\Omega_x^2+1}}{2}$ (symmetric phase). Here, the procedure to find the quantum metric tensor is similar to that of the ground state. The angular coordinates of the corresponding fixed point $\mathbf{x}_1$ (the red one in Figure 9.3) are $(\theta_1, \phi_1) = \left(\arccos\left(-\frac{1}{\sqrt{1+\Omega_x^2}}\right), 0\right)$, and the rotation that aligns the classical pseudospin with the z axis is

$$\begin{pmatrix} \hat{J}_x \\ \hat{J}_y \\ \hat{J}_z \end{pmatrix} = \begin{pmatrix} \cos\theta_1 & 0 & -\sin\theta_1 \\ 0 & 1 & 0 \\ \sin\theta_1 & 0 & \cos\theta_1 \end{pmatrix} \begin{pmatrix} \hat{J}'_x \\ \hat{J}'_y \\ \hat{J}'_z \end{pmatrix}. \tag{9.19}$$

Making use of the truncated Holstein-Primakoff transformation, we arrive at the quadratic Hamiltonian

$$\hat{H} \simeq j\sqrt{\Omega_x^2+1} - \left(\frac{\sqrt{\Omega_x^2+1}-2\xi_y}{2}\right)\hat{P}^2 - \frac{\sqrt{\Omega_x^2+1}}{2}\hat{Q}^2, \tag{9.20}$$

which is a harmonic oscillator with frequency $\omega = \sqrt{\sqrt{\Omega_x^2+1}\left(\sqrt{\Omega_x^2+1}-2\xi_y\right)}$ and energy $E = j\sqrt{\Omega_x^2+1}$. Notice that there is a minus sign in the last two terms of equation (9.20) due to this fixed point being a maximum of energy, although the dynamics is still

oscillatory. The components of the metric are

$$
\begin{aligned}
g_{11} &= \frac{j}{2\left(\Omega_x^2+1\right)^{7/4}\sqrt{\sqrt{\Omega_x^2+1}-2\xi_y}} + \frac{\xi_y^2\Omega_x^2}{8\left(\Omega_x^2+1\right)^2\left(\sqrt{\Omega_x^2+1}-2\xi_y\right)^2}, \\
g_{12} &= -\frac{\xi_y\Omega_x}{8\left(\Omega_x^2+1\right)\left(\sqrt{\Omega_x^2+1}-2\xi_y\right)^2}, \\
g_{22} &= \frac{1}{8\left(\sqrt{\Omega_x^2+1}-2\xi_y\right)^2},
\end{aligned}
\tag{9.21}
$$

and the determinant is

$$
g = \frac{j}{16\left(\Omega_x^2+1\right)^{7/4}\left(\sqrt{\Omega_x^2+1}-2\xi_y\right)^{5/2}}. \tag{9.22}
$$

We can easily identify a singularity in all the components of the metric and the determinant which occurs at $\xi_y = \frac{\sqrt{\Omega_x^2+1}}{2}$. This is precisely the critical point where the quantum phase transition takes place, and confirms the usefulness of the quantum metric tensor to detect a quantum phase transition. With the quantum metric tensor (9.21) at hand, we compute its scalar curvature with the aid of (1.20) and find

$$
R = -4, \tag{9.23}
$$

which again means that the underlying geometry is hyperbolic.

9.2.2.2 Broken phase

Now, when $\xi_y > \frac{\sqrt{\Omega_x^2+1}}{2}$ (broken phase), there are two fixed points that correspond to the highest energy (the blue ones in Figure 9.3). Choosing $\mathbf{x}_4$, which has the angular coordinates $(\theta_4, \phi_4) = \left(\arccos\left(-\frac{1}{2\xi_y}\right), \arccos\left(\frac{\Omega_x}{\sqrt{4\xi_y^2-1}}\right)\right)$, the rotation that aligns the classical pseudospin with the z axis is

$$
\begin{pmatrix} \hat{J}_x \\ \hat{J}_y \\ \hat{J}_z \end{pmatrix} = \begin{pmatrix} \cos\phi_4 & -\sin\phi_4 & 0 \\ \sin\phi_4 & \cos\phi_4 & 0 \\ 0 & 0 & 1 \end{pmatrix} \begin{pmatrix} \cos\theta_4 & 0 & -\sin\theta_4 \\ 0 & 1 & 0 \\ \sin\theta_4 & 0 & \cos\theta_4 \end{pmatrix} \begin{pmatrix} \hat{J}'_x \\ \hat{J}'_y \\ \hat{J}'_z \end{pmatrix}. \tag{9.24}
$$

Following similar steps as with the normal phase, we find that the quadratic Hamiltonian now is

$$
\begin{aligned}
\hat{H} \simeq & j\frac{4\xi_y^2+\Omega_x^2+1}{4\xi_y} - \frac{\xi_y\left(4\xi_y^2-\Omega_x^2-1\right)}{4\xi_y^2-1}\hat{P}^2 + \frac{\Omega_x\sqrt{4\xi_y^2-\Omega_x^2-1}}{2\left(4\xi_y^2-1\right)}\left(\hat{Q}\hat{P}+\hat{P}\hat{Q}\right) \\
& - \frac{16\xi_y^4-8\xi_y^2+\Omega_x^2+1}{4\xi_y\left(4\xi_y^2-1\right)}\hat{Q}^2.
\end{aligned}
\tag{9.25}
$$

This Hamiltonian has the form of a generalized harmonic oscillator. In order to remove the crossed term in $\hat{Q}$ and $\hat{P}$, we make the further linear transformation

$$\hat{Q} = \sqrt{\frac{2\xi_y\left(4\xi_y^2-\Omega_x^2-1\right)}{4\xi_y^2-1}}\,\hat{Q}', \quad \hat{P} = \sqrt{\frac{4\xi_y^2-1}{2\xi_y\left(4\xi_y^2-\Omega_x^2-1\right)}}\,\hat{P}' + \frac{\Omega_x}{\sqrt{2\xi_y\left(4\xi_y^2-1\right)}}\hat{Q}'. \tag{9.26}$$

The Hamiltonian then turns into a simple harmonic oscillator

$$\hat{H} = j\frac{4\xi_y^2+\Omega_x^2+1}{4\xi_y} - \frac{\hat{P}'^2}{2} - \frac{\omega^2}{2}\hat{Q}'^2, \tag{9.27}$$

with frequency $\omega = \sqrt{4\xi_y^2-\Omega_x^2-1}$ and energy $E = j\frac{4\xi_y^2+\Omega_x^2+1}{4\xi_y}$. Again, two minus signs appear since we are considering a maximum of energy, although the dynamics is still oscillatory.

The resulting expressions for the metric components in this case are cumbersome, however, all of them are singular at points on the separatrix. Also, the computation of the scalar curvature via equation (1.20) yields a cumbersome expression. In Figure 9.8, we show the quantum metric tensor and its scalar curvature as well as their numeric counterparts, observing a good agreement between them, except for g_{11} near $\Omega_x = 0$. This component has a maximum at $\Omega_x = 0$ which is not observed in the result of the analytic Holstein-Primakoff calculation and it seems to be related to the vanishing of $\langle \hat{J}_x \rangle$ when Ω_x changes sign as observed in Figure 9.2 (b). In any case, this strong difference does not affect much the scalar curvature, which approaches to zero in the broken phase in both the analytic and numeric results. We must say, as explained in detail in Appendix F, that the numerical evaluation of the metric demands extremely high precision (from 15 to 60 decimal digits), involving extensive computational resources.

Now, it turns that under the analytic computation the broken phase exhibits a Berry curvature, whose only component is given by

$$F_{12} = -\frac{2j+1}{4\xi_y^2\sqrt{4\xi_y^2-\Omega_x^2-1}} + \frac{16\xi_y^2-\Omega_x^2+1}{16\xi_y^3\left(4\xi_y^2-\Omega_x^2-1\right)}. \tag{9.28}$$

We observe, as expected, that the Berry curvature is also singular at the separatrix. On the other hand, the numeric analysis yields a zero Berry curvature. The reason for this discrepancy is that the Berry phase appeared due to the rotation that was performed to align the highest energy state with the classical pseudospin, introducing in this way the crossed term in $\hat{Q}$ and $\hat{P}$ in the Hamiltonian (9.25).

In Figure 9.9, the plots of the metric components and the scalar curvature for the highest energy state are shown in 3D, while Figure 9.10 contains their maps. We see that in the symmetric phase, the scalar curvature has a value around -4, just as the Holstein-Primakoff calculation predicts. However, as Ω_x decreases, the scalar curvature begins growing, passes the separatrix, takes small positive values, reaches a maximum and then descends to near zero values.

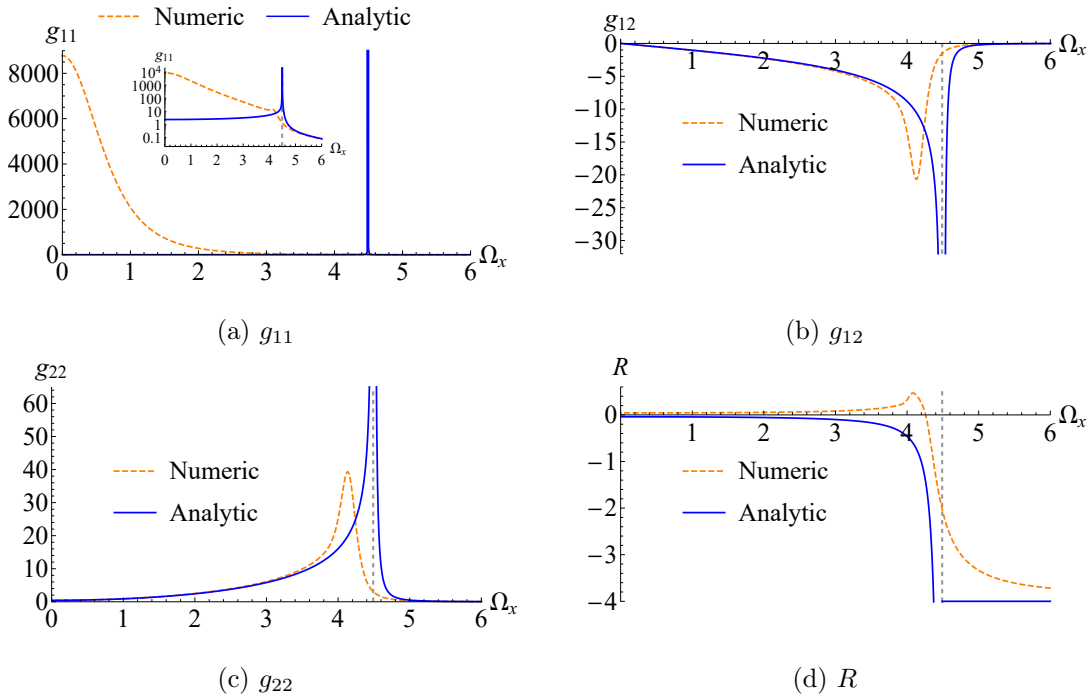

(a) g_{11} (b) g_{12}

(c) g_{22} (d) R

Figure 9.8: Comparison of the metric components and the scalar curvature with the analytic results for $\xi_y = 2.3$ and $j = 96$. The inset shows the g_{11} component in logarithmic scale. The agreement is excellent except near to the quantum phase transition (dashed gray). Notice the difference in g_{11}between the analytic and numeric curves as $\Omega_x \to 0$. Also, the analytic plots show a divergence at Ω_{xc} due to the unreliability of the truncated Holstein-Primakoff approximation at that point.

Now a question arises. How can we interpret the change of sign near the separatrix? Does it mean that there is a change in the topology of the parameter space and that it switches between a closed and an open shape? To answer this, we must recall that a fundamental quantity in the study of two-dimensional surfaces is the Gaussian curvature K, which is related to the scalar curvature as $K = R/2$. It is defined as the product of the two principal curvatures, κ_1 and κ_2, which quantify the bending of the surface along each direction [143]. If both principal curvatures, κ_1 and κ_2, have the same sign, then the Gaussian curvature is positive and the local geometry is spherical. On the contrary, when both principal curvatures have opposite signs, the Gaussian curvature is negative and the surface is locally hyperbolic. A change in topology would imply that the metric becomes singular at some point [144], which means that its determinant should vanish there. Since we do not observe that the metric determinant is zero (see Figure 9.9 (e)), we conclude that a change in topology does not take place. Instead, there is only a sign change in one of the two principal curvatures, κ_1 or κ_2, producing a local change between dome-like and saddle-like shapes.

In Figure 9.11, we show the plots of the quantum metric tensor and its scalar curvature for various values of j when $\xi_y = 2.3$. We can see how the peaks of the metric

components get sharper and closer to the critical value $\Omega_{xc} = 4.490$ as j increases, thus anticipating that in the limit $j \to \infty$ they will diverge (they are the precursors of the quantum phase transition for finite j). Also, the maximum of the scalar curvature gets closer to the separatrix, and the transition region between the asymptotic values -4 on one side and 0 on the other becomes thinner, suggesting that a discontinuity will appear at Ω_{xc} in the thermodynamic limit. In the next section, we carry out a detailed analysis to extract more relevant information about this behavior.

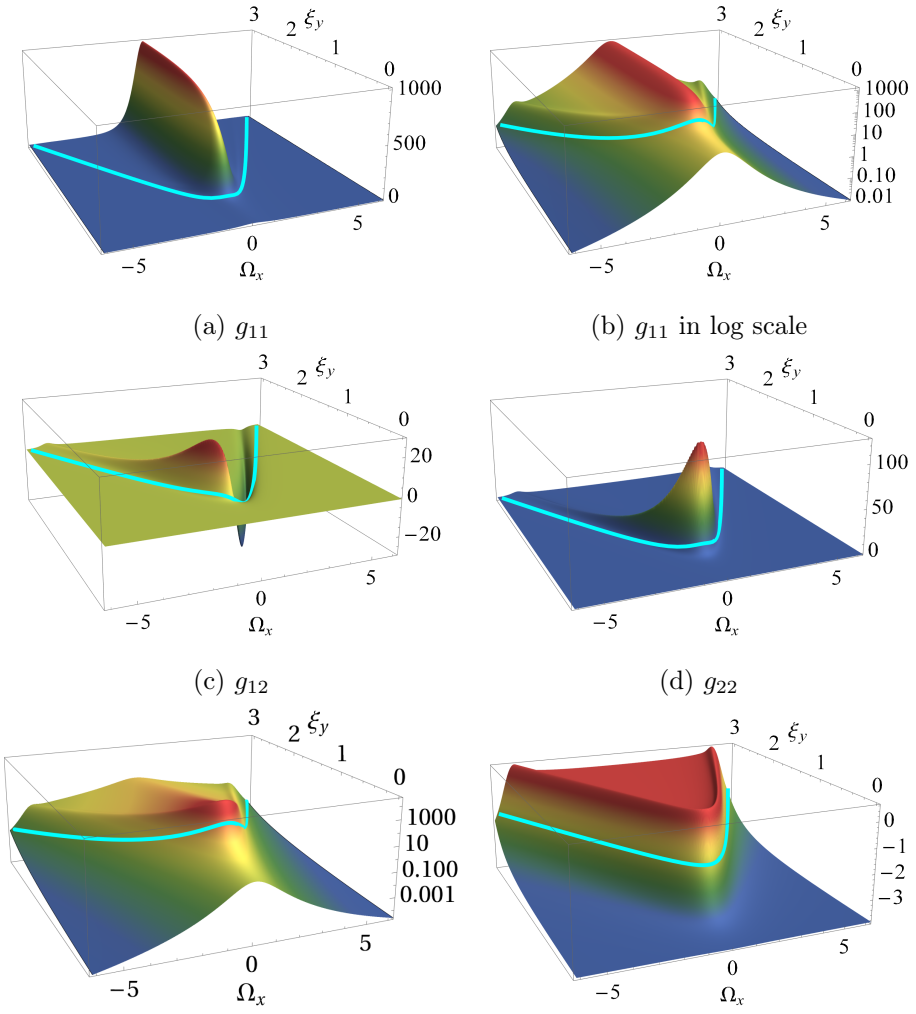

(a) g_{11} (b) g_{11} in log scale

(c) g_{12} (d) g_{22}

(e) g in log scale (f) R

Figure 9.9: Metric components, determinant, and scalar curvature for the highest energy state with $j = 32$. The cyan line is the separatrix $\xi_y = \frac{\sqrt{1+\Omega_x^2}}{2}$.

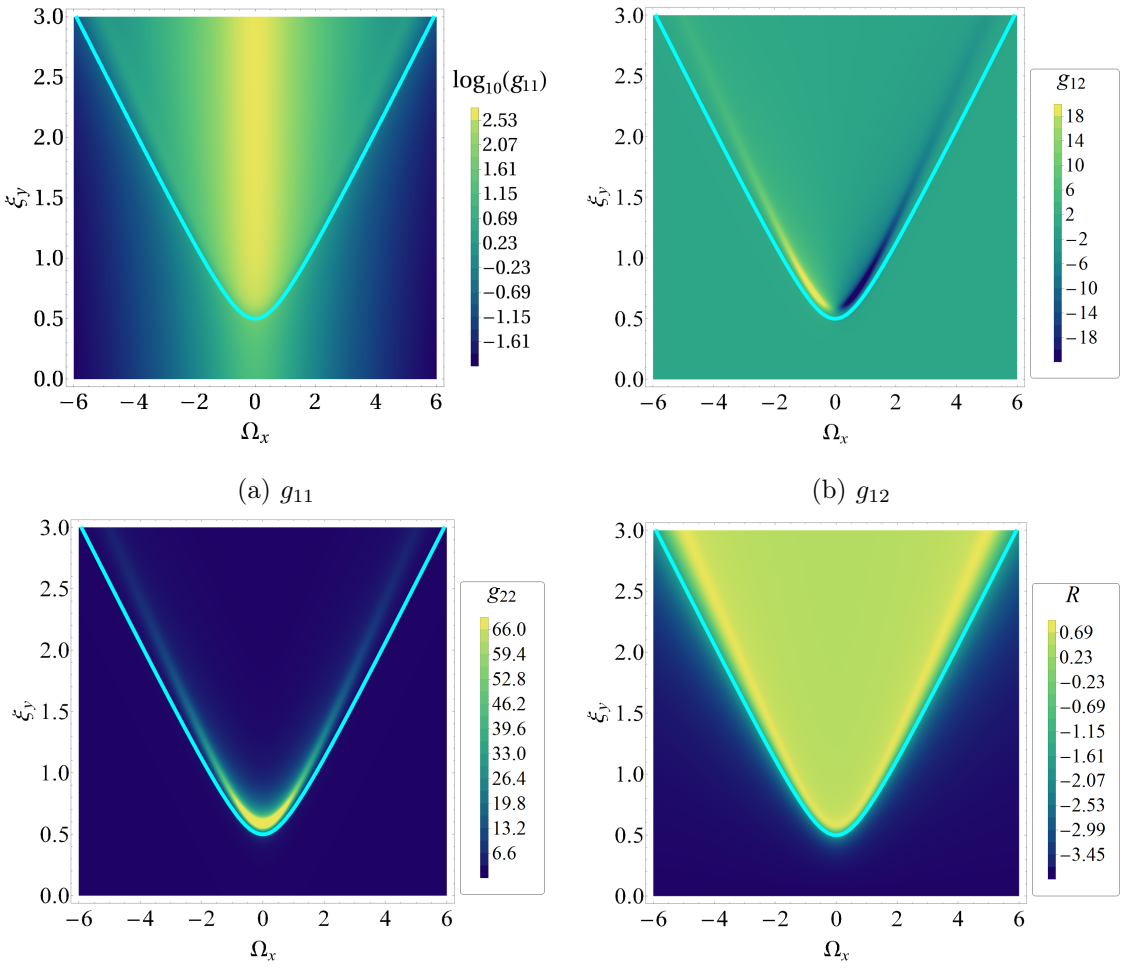

(a) g_{11} (b) g_{12}

(c) g_{22} (d) R

Figure 9.10: Maps of the metric components and the scalar curvature for the highest energy state with $j = 32$.

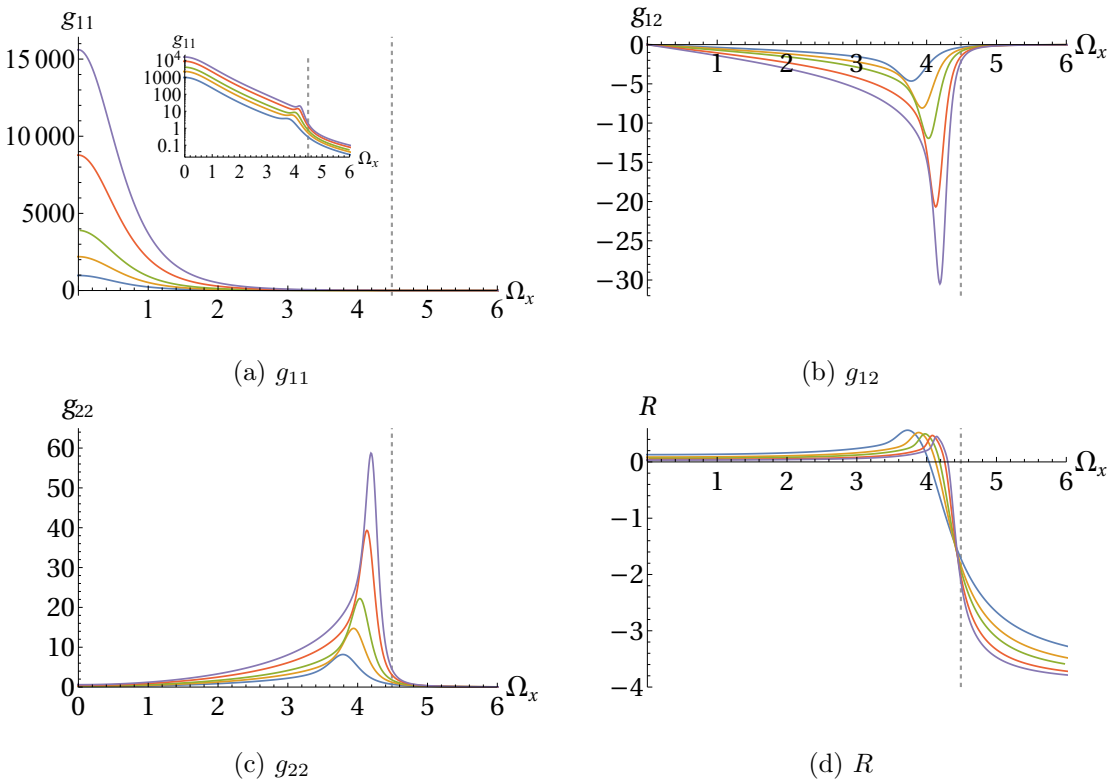

(a) g_{11} (b) g_{12}

(c) g_{22} (d) R

Figure 9.11: Metric components and scalar curvature for the highest energy state with $\xi_y = 2.3$ and $j = 32, 48, 64, 96, 128$. The inset shows the g_{11} component in logarithmic scale.

9.2.3 Analysis of the peaks

We now analyze the peaks of the metric components and the scalar curvature to infer their behavior in the thermodynamic limit. We consider three interesting cases: (i) fixing $\xi_y = 2.3$, (ii) fixing Ω_x =0, and (iii) fixing $\xi_y = 0.5$.

9.2.3.1 Case 1: $\xi_y = 2.3$

In Figure 9.12, we plot the peak (maximum or minimum) of every metric component and of the scalar curvature as a function of Ω_x for $\xi_y = 2.3$ and increasing values of j. The functions used to fit the data are:

$$\begin{aligned} g_{11}^{(\max)} &= 0.582 + \frac{2.051}{(\Omega_x - 4.490)^2}, \\ g_{12}^{(\min)} &= 2.249 - \frac{2.966}{(\Omega_x - 4.490)^2}, \\ g_{22}^{(\max)} &= -7.170 + \frac{5.931}{(\Omega_x - 4.490)^2}, \\ R^{(\max)} &= -0.083 + 2.470\, e^{-0.356\Omega_x}. \end{aligned} \tag{9.29}$$

We see that at the critical point, $\Omega_{xc} = 4.490$, the metric components are singular, just as the analytic formulas (9.21) predict. On the other hand, the maximum of the scalar curvature takes the value 0.416. This is an indication that the maximum of the scalar curvature persists and that there is not a singularity when $j \to \infty$, but rather a discontinuity produced by a sudden change of sign across the quantum phase transition, which is implied by the increasing slope of R seen in Figure 9.11 (d).

Next, in Figure 9.13, we show the peaks of the metric components and the scalar curvature as functions of j. In this case, the functions used to fit the data are:

$$\begin{aligned} \log(g_{11}^{(\max)}) &= -3.102 + 1.267 \log(j), \\ \log(g_{12}^{(\min)}) &= -3.134 + 1.349 \log(j), \\ \log(g_{22}^{(\max)}) &= -2.702 + 1.394 \log(j), \\ R^{(\max)} &= 0.418 + \frac{1.563}{(j - 0.913)^{0.680}}. \end{aligned} \tag{9.30}$$

In the thermodynamic limit $j \to \infty$, the metric components diverge, whereas the scalar curvature approaches 0.418, which agrees with the prediction of the previous analysis when $\Omega_x = \Omega_{xc}$. Once again, this confirms that R is not singular across the quantum phase transition and that it just presents a sudden sign change, i.e., a discontinuity. As a consequence, it can be said that the singularity that appears in the metric is removable and is not a true singularity of the parameter space.

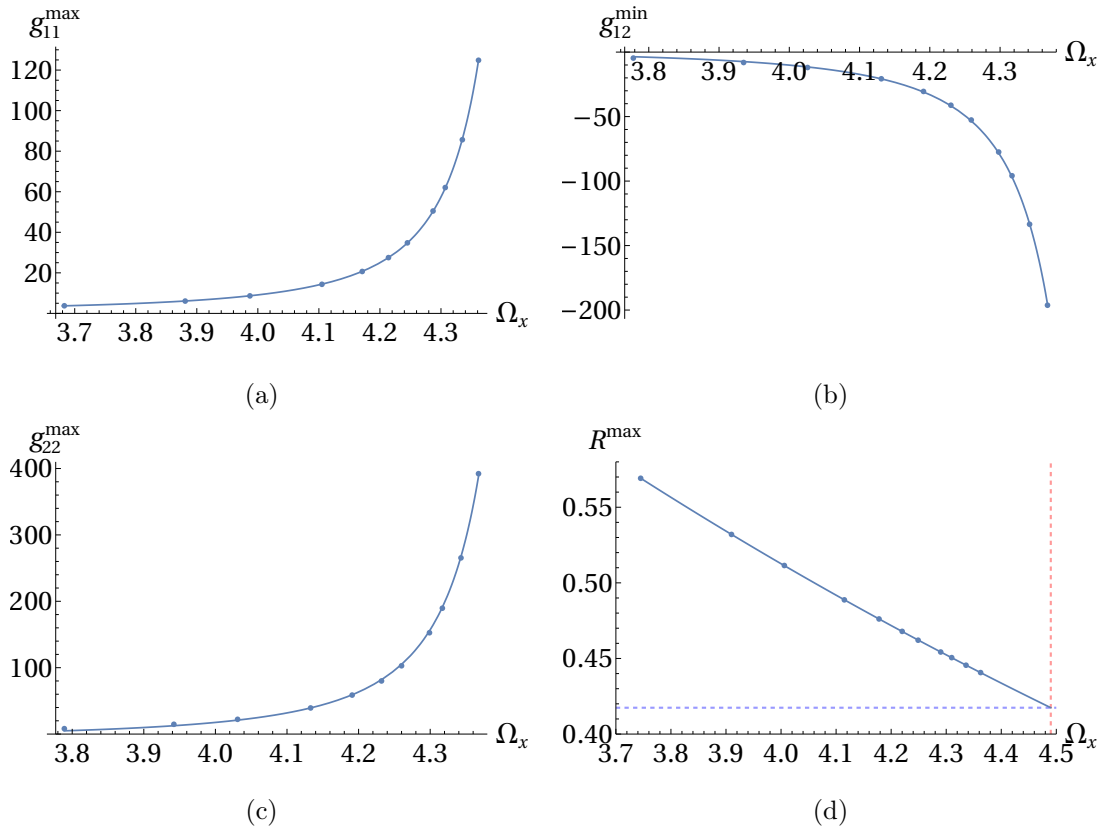

Figure 9.12: Behavior of the maximum of each metric component and the scalar curvature with respect to Ω_x for $\xi_y = 2.3$. The points correspond to $j = 32, 48, 64, 96, 128, 160, 192, 256, 300, 384, 512$.

9.2.3.2 Case 2: $\Omega_x = 0$

Now, we analyze the value of the metric components g_{11} and g_{22}, and the scalar curvature when $\Omega_x = 0$. The plots are shown in Figure 9.14 and the functions that fit the data are:

$$\begin{aligned} g_{11}^0 &= (-0.013 + 0.976j)^2, \\ g_{22}^0 &= 0.005 + 0.005j, \\ R^0 &= \frac{1}{0.131 + 0.238j}. \end{aligned} \tag{9.31}$$

Notice that g_{12} does not appear because its value at $\Omega_x = 0$ is zero. Remarkably, the scalar curvature goes to zero as $j \to \infty$, which is precisely the prediction of the coherent-state approach shown in Appendix E (see equation E.6).

9.2.3.3 Case 3: $\xi_y = 0.5$

Finally, we show in Figure 9.15 the peaks of the metric components g_{11} and g_{22}, as well as the scalar curvature for $\xi_y = 0.5$. This case is particularly interesting, since

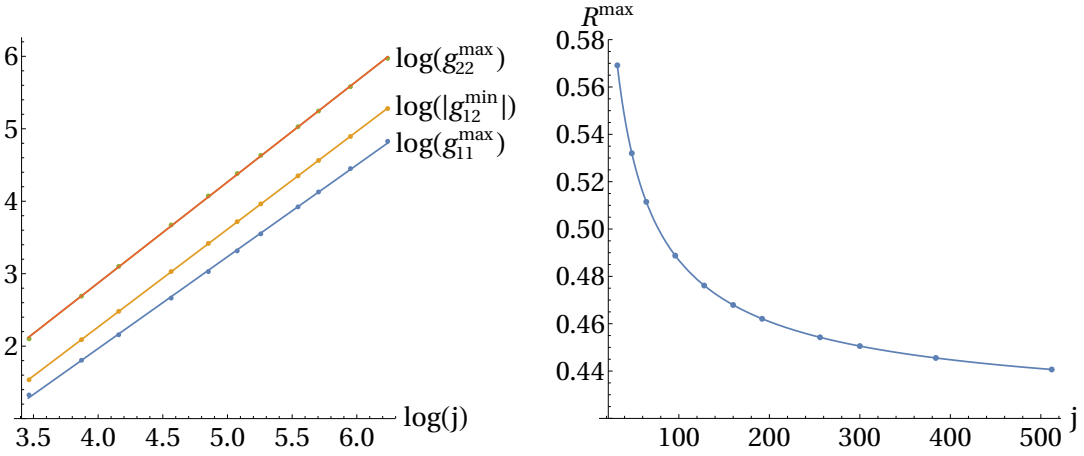

(a) Maxima of $|g_{ij}|$.

(b) $R^{(\max)}$.

Figure 9.13: Maximum of each metric component and the scalar curvature with respect to j for $\xi_y = 2.3$.

at $\xi_y = 0.5$ the peaks of the quantum metric tensor and the scalar curvature occur at $\Omega_x = 0$ regardless of the value of j. The functions used to fit the data in Figure 9.15 are:

$$\begin{aligned} \log(g^0_{11}) &= -0.480 + 1.325\log(j), \\ \log(g^0_{22}) &= -1.881 + 1.327\log(j), \\ R^0 &= -2.183 + \frac{3.430}{(j^2 - 6.206)^{0.284}}. \end{aligned} \tag{9.32}$$

In this case, in the thermodynamic limit $j \to \infty$, the metric components also diverge, whereas the scalar curvature approaches -2.183. This is a limiting point, over the separatrix, where R takes an intermediate value between the asymptotic ones in the two phases (0 and -4). Once again, this confirms that R is not singular at the quantum phase transition.

In summary, in this chapter we obtained a geometrical characterization of the modified LMG model with the aid of the quantum metric tensor and its scalar curvature. In particular, our analysis for finite j allows us to deduce that the second-order quantum phase transition in this model is indicated by the sudden sign chane in the scalar curvature. Thus, the singularity predicted by the analytic scalar curvature at Ω_{xc} is a consequence of the unreliability of the truncated Holstein-Primakoff approximation in a close vicinity of the phase transition. In this sense, one may try to use the resummation of the Holstein-Primakoff series proposed in [145] and see if the results obtained with this technique coincide with the numerical predictions.

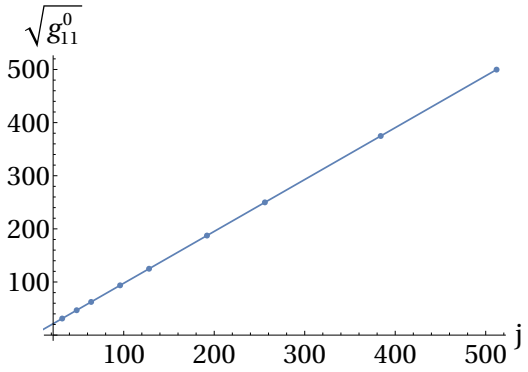

(a)

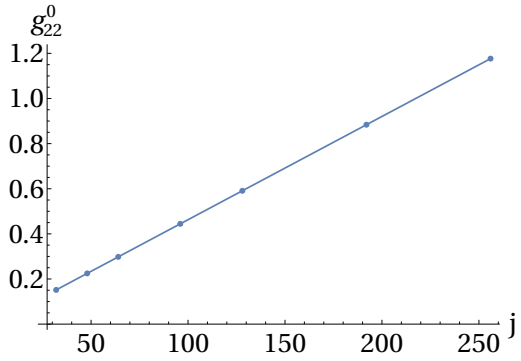

(b)

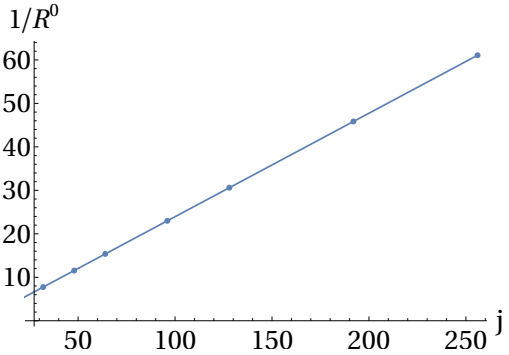

(c)

Figure 9.14: Plots of g_{11}, g_{22}, and R with respect to j for $\xi_y = 2.3$ and $\Omega_x = 0$.

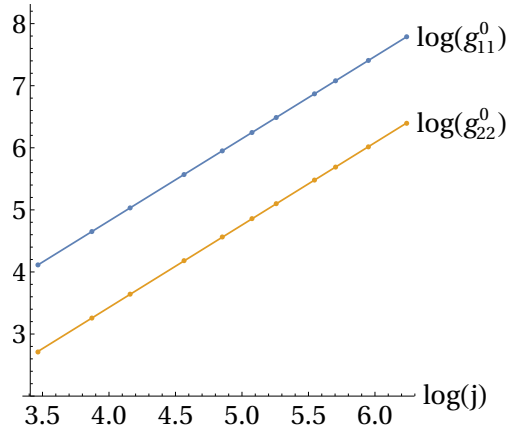

(a) Maxima of g_{ij}.

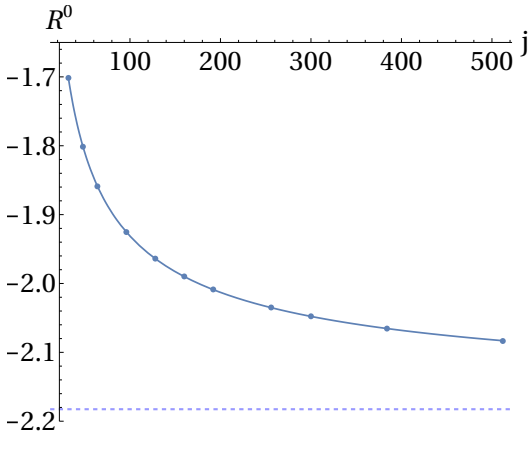

(b) R^0.

Figure 9.15: Maximum of each metric component and the scalar curvature with respect to j for $\xi_y = 0.5$.

Chapter 10

Relativistic Coulomb problem from $\mathcal{N} = 4$ super Yang-Mills

In this chapter, we analyze how to generalize the Runge-Lenz (RL) vector to the relativistic Coulomb problem. In Section 5.4, we discussed the two-dimensional attractive Coulomb problem in the non-relativistic setting. Although we did not use it, the RL vector can be introduced to find straightforwardly the equation of trajectory. In the relativistic case, the minimal coupling prescription on the Klein-Gordon equation destroys the SO(4) symmetry and hence no RL vector exists. Thus, our interest is the modification of the coupling prescription to allow for a RL vector that restores the SO(4) symmetry.

We see in this chapter that $\mathcal{N} = 4$ super Yang-Mills (SYM) gives rise to a modified Klein-Gordon equation by means of a specific Higgs mechanism. In particular, we present the simplest spontaneous breaking of symmetry that allows one to extract this integrable system where the Coulomb potential is coupled to both the mass and the energy of the particle. Then, we see the deduction of this equation from a modified action principle for a relativistic particle. Next, we obtain the RL vector and show that it generates, along with the angular momentum, the SO(4) algebra, providing the relativistic spectrum of the modified Klein-Gordon equation. Our results confirm previous analyses using different approaches [146–148]. We finally make use of the Kustaanheimo-Stiefel (KS) transformation and show that the relativistic spectrum of the hydrogen-like atom in two dimensions is related to the relativistic harmonic oscillator spectrum in two dimensions. Again, we confirm the analysis where the spectrum of the relativistic harmonic oscillator was constructed by directly solving the modified Klein-Gordon equation [149]. The results of this chapter have been published in references [150] and [151].

10.1 Modified Klein-Gordon equation from $\mathcal{N} = 4$ SYM

Our interest in this section is to make more transparent the extraction of the modified Klein-Gordon equation (Klein-Gordon equation with scalar and vector potentials of

equal magnitude, which is useful to describe the pseudospin symmetry in atomic nuclei [152]) from $\mathcal{N}=4$ SYM. The usual Klein-Gordon equation describing a charged spinless particle in a Coulomb field is obtained by the minimal coupling prescription $\partial_\mu \to D_\mu = \partial_\mu + \frac{i}{\hbar c}A_\mu$, where a particular reference frame is chosen to have $A^\mu = (-\alpha/r, \mathbf{0})$,

$$-\left(\frac{1}{c}\frac{\partial}{\partial t} - \frac{i}{\hbar c}\frac{\alpha}{r}\right)^2 \phi + \nabla^2\phi - \left(\frac{mc}{\hbar}\right)^2 \phi = 0. \tag{10.1}$$

Expanding, we get

$$-\frac{1}{c^2}\frac{\partial^2\phi}{\partial t^2} + \nabla^2\phi + \frac{2i\alpha}{\hbar c^2 r}\frac{\partial\phi}{\partial t} + \frac{\alpha^2}{\hbar^2 c^2 r^2}\phi - \left(\frac{mc}{\hbar}\right)^2 \phi = 0. \tag{10.2}$$

Now, the modified Klein-Gordon equation includes a non-minimal coupling through the mass,

$$-\left(\frac{1}{c}\frac{\partial}{\partial t} - \frac{i}{\hbar c}\frac{\alpha}{r}\right)^2 \phi + \nabla^2\phi - \left(\frac{mc}{\hbar} - \frac{\alpha}{\hbar c r}\right)^2 \phi = 0. \tag{10.3}$$

Expanding this equation, it can be seen that the modification of the mass results in the cancellation of the quadratic potential term,

$$-\frac{1}{c^2}\frac{\partial^2\phi}{\partial t^2} + \nabla^2\phi + \frac{2i\alpha}{\hbar c^2 r}\frac{\partial\phi}{\partial t} + \frac{2\alpha m}{\hbar^2 r}\phi - \left(\frac{mc}{\hbar}\right)^2 \phi = 0. \tag{10.4}$$

For future treatment, we write the relativistic form of this equation,

$$\partial_\mu\partial^\mu\phi - 2iA_\mu\partial^\mu\phi - A_\mu A^\mu\phi - \left(m - \frac{\alpha}{r}\right)^2 \phi = 0, \tag{10.5}$$

where $\hbar = c = 1$ and the metric is $\eta_{\mu\nu} = \mathrm{diag}(-1,1,1,1)$.

To undertake the spontaneous breaking of symmetry that will allow us to extract the above equation, we consider only the bosonic sector of $\mathcal{N}=4$ SYM which has the following Lagrangian density [153]

$$\mathcal{L} = \mathrm{Tr}\left\{-\frac{1}{4}F^{\mu\nu}F_{\mu\nu} - \frac{1}{2}\sum_{i=1}^{6} D_\mu\Phi_i D^\mu\Phi_i + \frac{g^2}{4}\sum_{i,j=1}^{6}[\Phi_i,\Phi_j]^2\right\}. \tag{10.6}$$

Here, the six scalar fields are $N\times N$ traceless Hermitian matrices in the adjoint representation of SU(N). The action of the covariant derivative on a generic field W is given by

$$D_\mu W = \partial_\mu W - ig[A_\mu, W], \tag{10.7}$$

where under a gauge transformation U, the gauge field A_μ and the scalar fields Φ_i transform as

$$\Phi_i \to U\Phi_i U^\dagger, \qquad A_\mu \to UA_\mu U^\dagger - \frac{i}{g}(\partial_\mu U)U^\dagger, \tag{10.8}$$

and as usual, the field strength $F_{\mu\nu}$ is defined by the commutator of the covariant derivatives

$$F_{\mu\nu} = \frac{i}{g}[D_\mu, D_\nu] = \partial_\mu A_\nu - \partial_\nu A_\mu - ig[A_\mu, A_\nu]. \tag{10.9}$$

The resulting equations of motion are [154]

$$D_\mu F^{\nu\mu} = ig\sum_{i=1}^{6}[\Phi_i, D^\nu \Phi_i], \tag{10.10}$$

$$D_\mu D^\mu \Phi_i = g^2 \sum_{j=1}^{6}[\Phi_j,[\Phi_j, \Phi_i]]. \tag{10.11}$$

We choose to work with the group SU(2) for simplicity. Therefore, the fields will be expressible in terms of the Pauli matrices τ^a as

$$\Phi_i = \Phi_i^a \frac{\tau^a}{2} = \frac{1}{2}\begin{pmatrix} \Phi_i^0 & \Phi_i^- \\ \Phi_i^+ & -\Phi_i^0 \end{pmatrix}, \qquad A_\mu = A_\mu^a \frac{\tau^a}{2} = \frac{1}{2}\begin{pmatrix} A_\mu^3 & A_\mu^1 - iA_\mu^2 \\ A_\mu^1 + iA_\mu^2 & -A_\mu^3 \end{pmatrix}, \tag{10.12}$$

where $\Phi_i^\pm = \Phi_i^1 \pm i\Phi_i^2$. We introduce the Higgs mechanism by giving a vacuum expectation value v to Φ_1 [148, 155, 156]

$$\Phi_1 = \frac{1}{2}\begin{pmatrix} \Phi_i^0 + v & 0 \\ 0 & -\Phi_i^0 - v \end{pmatrix}, \tag{10.13}$$

and taking the other fields as

$$\Phi_2 = \frac{1}{2}\begin{pmatrix} 0 & \Phi_2^- \\ \Phi_2^+ & 0 \end{pmatrix}, \quad \Phi_i = 0,\ i = 3,4,5,6; \quad A_\mu = A_\mu^a \frac{\tau^a}{2} = \frac{1}{2}\begin{pmatrix} A_\mu^3 & 0 \\ 0 & -A_\mu^3 \end{pmatrix}. \tag{10.14}$$

Now, the Lagrangian (10.6) reads

$$\begin{aligned}\mathcal{L} = &-\frac{1}{8}F^{\mu\nu}F_{\mu\nu} - \frac{1}{4}\partial_\mu\Phi_2^-\partial^\mu\Phi_2^+ - \frac{1}{4}\partial_\mu\Phi_1^0\partial^\mu\Phi_1^0 + \frac{ig}{4}A^\mu(\Phi_2^-\partial_\mu\Phi_2^+ - \Phi_2^+\partial_\mu\Phi_2^-) \\ &- \frac{g^2}{4}\Phi_2^-\Phi_2^+A_\mu A^\mu - \frac{g^2}{4}(\Phi_1^0 + v)^2\Phi_2^-\Phi_2^+.\end{aligned} \tag{10.15}$$

Here, we have defined $A_\mu = A_\mu^3$ and $F_{\mu\nu} = \partial_\mu A_\nu - \partial_\nu A_\mu$. A crucial step is to implement the constraint

$$\Phi_1^0 + \frac{\alpha}{r} = 0 \tag{10.16}$$

in the previous Lagrangian. After the strong implementation of the constraint, we obtain[1]

$$\begin{aligned}\mathcal{L} = &-\frac{1}{8}F^{\mu\nu}F_{\mu\nu} - \frac{1}{4}\partial_\mu\Phi_2^-\partial^\mu\Phi_2^+ + \frac{ig}{4}A^\mu(\Phi_2^-\partial_\mu\Phi_2^+ - \Phi_2^+\partial_\mu\Phi_2^-) \\ &- \frac{g^2}{4}\Phi_2^-\Phi_2^+A_\mu A^\mu - \frac{g^2}{4}\left(v - \frac{\alpha}{r}\right)^2\Phi_2^-\Phi_2^+\end{aligned} \tag{10.17}$$

[1]This constraint can be interpreted as a second class constraint in Dirac's sense.

up to a boundary term. Thus, the field content of our theory has been reduced to one vector field A_μ and one complex scalar Φ_2^-. It is worth noting that this Lagrangian is not Lorentz-invariant unless the coupling α is allowed to transform in such a way that it cancels the contribution of $1/r$.

The equation of motion for the scalar field Φ_2^- arising from (10.17) is

$$\partial_\mu\partial^\mu\Phi_2^- - ig(\partial_\mu A^\mu)\Phi_2^- - 2igA_\mu\partial^\mu\Phi_2^- - g^2A_\mu A^\mu\Phi_2^- - g^2(v+\Phi_1^0)^2\Phi_2^- = 0. \tag{10.18}$$

Of course, the equation for Φ_2^+ will be the complex conjugate of this one. Denoting $\Phi_2^- = \phi$ and taking the Coulomb potential $A^\mu = (-\alpha/r, \mathbf{0})$ with $g = 1$,[2] this equation becomes

$$\partial_\mu\partial^\mu\phi - 2iA_\mu\partial^\mu\phi - A_\mu A^\mu\phi - \left(m - \frac{\alpha}{r}\right)^2\phi = 0, \tag{10.19}$$

which is clearly (10.5). We see that the vacuum expectation value of Φ_1 is the mass m of the scalar field ϕ, and that the imposed constraint provides the non-minimal coupling $m \to m - \alpha/r$ necessary to enhance the symmetry of the field theory from SO(3) to SO(4). The Lagrangian (10.17) can be rewritten as

$$\mathcal{L} = \frac{1}{2}\left[-\frac{1}{4}F^{\mu\nu}F_{\mu\nu} - \frac{1}{2}(D_\mu\phi)^*(D^\mu\phi) - \frac{1}{2}\left(m - \frac{\alpha}{r}\right)^2\phi^*\phi\right], \tag{10.20}$$

where the covariant derivative is given by $D_\mu = \partial_\mu - iA_\mu$. We can recognize this as one half the Lagrangian for scalar electrodynamics with modified mass. Now, we obtain the equation of motion for the gauge field (10.10),

$$-\partial_\mu\partial^\mu A^\nu + \partial^\nu(\partial\cdot A) = \frac{i}{2}(\phi\,\partial^\nu\phi^* - \phi^*\partial^\nu\phi) - A^\nu|\phi|^2. \tag{10.21}$$

The application of the divergence to (10.21) reveals that the conserved current is

$$J^\nu = \frac{i}{2}(\phi\,\partial^\nu\phi^* - \phi^*\partial^\nu\phi) - A^\nu|\phi|^2, \tag{10.22}$$

which means that the density ρ is

$$\rho = \frac{i}{2}(\phi^*\partial_t\phi - \phi\,\partial_t\phi^*) + \frac{\alpha}{r}|\phi|^2. \tag{10.23}$$

On the other hand, if we set $A^\mu = (-\alpha/r, \mathbf{0})$ in the equation of motion (10.21), we find

$$\nabla^2\left(\frac{\alpha}{r}\right) = \frac{i}{2}(\phi^*\partial_t\phi - \phi\,\partial_t\phi^*) + \frac{\alpha}{r}|\phi|^2, \tag{10.24}$$

which implies

$$\rho = \nabla^2\left(\frac{\alpha}{r}\right), \tag{10.25}$$

just as expected, or, upon integration,

$$\int \mathrm{d}^3r\,\rho = -4\pi\alpha. \tag{10.26}$$

[2] This is equivalent to absorbing the coupling constant into α.

10.2 Modified relativistic particle

In this section, we will see how the equation (10.19) possesses an enhanced symmetry SO(4) that allows to write it in a Schrödinger-like form. We start by considering the action for a relativistic particle with electromagnetic coupling

$$S = \int \mathrm{d}\tau\, L = \int \mathrm{d}\tau\, \left(-mc\sqrt{-\eta_{\mu\nu}\dot{x}^\mu \dot{x}^\nu} + \frac{1}{c} A_\mu \dot{x}^\mu \right). \tag{10.27}$$

The momentum p_μ conjugate to x^μ is

$$p_\mu = \frac{\partial L}{\partial \dot{x}^\mu} = \frac{mc\dot{x}_\mu}{\sqrt{-\eta_{\alpha\beta}\dot{x}^\alpha \dot{x}^\beta}} + \frac{1}{c} A_\mu. \tag{10.28}$$

Therefore, by considering the square of $p_\mu - A_\mu/c$, we obtain the constraint

$$\left(p_\mu - \frac{1}{c} A_\mu \right) \left(p^\mu - \frac{1}{c} A^\mu \right) + m^2 c^2 = 0. \tag{10.29}$$

Taking $A^\mu = (-\alpha/r, \mathbf{0})$, the constraint reads

$$(p^0)^2 + \frac{2\alpha}{cr} p^0 + \frac{\alpha^2}{c^2 r^2} - \boldsymbol{p}^2 - m^2 c^2 = 0. \tag{10.30}$$

If we apply the quantization prescription $p_\mu \to -i\hbar\partial_\mu$ and let this constraint act on a scalar field ϕ, we obtain (10.1). Following the method of separation of variables, we write the wave function as

$$\phi(\boldsymbol{r}, t) = \exp\left(-\frac{i}{\hbar} E t \right) \varphi(\boldsymbol{r}). \tag{10.31}$$

This leads to the stationary Klein-Gordon equation with Coulomb potential that has the well known spectrum [148, 157]

$$E_{n\ell} = m \left[1 + \left(\frac{\gamma}{n - (\ell + 1/2) + \sqrt{(\ell + 1/2)^2 - \gamma^2}} \right)^2 \right]^{-1/2}, \quad n = 0, 1, 2, \ldots, \tag{10.32}$$

where $\gamma = \alpha/\hbar c$. We can see the breaking of the n^2 degeneracy of the hydrogen atom due to the appearance of the orbital quantum number ℓ in the spectrum.

The classical stationary problem with conserved angular momentum L and energy $E = cp^0$ is given by the constraint (10.30)

$$-\frac{(E + \alpha/r)^2}{c^2} + (p_r^2 + L^2/r^2) + m^2 c^2 = 0. \tag{10.33}$$

The solutions of this equation for bounded orbits are rosettes [158], in contrast with the non-relativistic problem where the orbits are ellipses [76]. As a consequence, the RL

vector is not conserved. Now comes the question of finding the action that upon the application of the previous method, will yield the modified Klein-Gordon equation that possesses the SO(4) symmetry. It is clear from (10.3) that the mass should be affected by the addition of the potential, so that now

$$S=\int \mathrm{d}\tau\, L=\int \mathrm{d}\tau\, \left[-mc\sqrt{-\left(1-\frac{\alpha}{mc^2r}\right)^2\eta_{\mu\nu}\dot{x}^\mu\dot{x}^\nu}+\frac{1}{c}A_\mu\dot{x}^\mu\right]. \tag{10.34}$$

This action corresponds to a relativistic particle interacting with a Coulomb potential in a curved spacetime described by the conformally flat metric

$$g_{\mu\nu}=\left(1-\frac{\alpha}{mc^2r}\right)^2\eta_{\mu\nu}. \tag{10.35}$$

The momentum now becomes

$$p_\mu=mc\left(1-\frac{\alpha}{mc^2r}\right)\frac{\dot{x}_\mu}{\sqrt{-\eta_{\alpha\beta}\dot{x}^\alpha\dot{x}^\beta}}+\frac{1}{c}A_\mu, \tag{10.36}$$

so that

$$\left(p_\mu-\frac{1}{c}A_\mu\right)\left(p^\mu-\frac{1}{c}A^\mu\right)+m^2c^2\left(1-\frac{\alpha}{mc^2r}\right)^2=0. \tag{10.37}$$

Again, taking $A^\mu=(-\alpha/r,\mathbf{0})$, the constraint is reduced to

$$(p^0)^2+\frac{2\alpha}{cr}p^0+\frac{2\alpha m}{r}-\boldsymbol{p}^2-m^2c^2=0, \tag{10.38}$$

which reproduces the modified Klein-Gordon equation (10.4) after quantization. Applying separation of variables in the resulting equation (10.4), we find

$$\frac{E^2}{\hbar^2c^2}\varphi+\nabla^2\varphi+\frac{2\alpha E}{\hbar^2c^2r}\varphi+\frac{2\alpha m}{\hbar^2r}\varphi-\left(\frac{mc}{\hbar}\right)^2\varphi=0. \tag{10.39}$$

This can be cast in the form of a Schrödinger-like equation

$$-\frac{\hbar^2}{(E/c^2+m)}\nabla^2\varphi-\frac{2\alpha}{r}\varphi=(E-mc^2)\varphi \tag{10.40}$$

with the spectrum [148]

$$E_n=m\left(1-\frac{2\gamma^2}{n^2+\gamma^2}\right),\quad n=1,2,3,\dots. \tag{10.41}$$

It is noteworthy that we have recovered the degeneracy since the orbital quantum number ℓ does not appear in this formula. This points to the existence of an additional integral of motion, i.e., the relativistic generalization of the RL vector which will enable us to

recover the hidden SO(4) symmetry. In this case, the constraint (10.38) leads to the classical problem

$$\frac{p_r^2 + L^2/r^2}{E/c^2 + m} - \frac{2\alpha}{r} = E - mc^2. \tag{10.42}$$

The quantum and classical equations suggest that we should make the identifications

$$E/c^2 + m \leftrightarrow 2m_s, \quad E - mc^2 \leftrightarrow E_s, \quad 2\alpha \leftrightarrow \alpha_s, \tag{10.43}$$

to recover a Schrödinger equation with mass m_s, energy E_s, and coupling constant α_s. Notice that under the previous substitutions, the spectrum (10.41) can be easily obtained from that of the hydrogen atom. In the next section, we will construct the relativistic RL vector and obtain the energy levels à la Pauli [159].

10.3 Relativistic SO(4) algebra using the relativistic Runge-Lenz vector

In this section, we obtain the relativistic RL vector associated with the modified relativistic Coulomb problem and we show that the orbit can be reconstructed using this conserved quantity. We then proceed to the construction of the infinitesimal Noether symmetries generated by the relativistic RL vector. We also describe the complete SO(4) algebra generated by the angular momentum and the RL vector and recover the correct relativistic spectrum of the corresponding hydrogen-like atom. We shall take units such that $\hbar = c = 1$.

Using as a model the non-relativistic construction [76] we find

$$\frac{\mathrm{d}}{\mathrm{d}t}\left[\boldsymbol{p} \times \boldsymbol{L} - (E + m)\,\frac{\alpha \boldsymbol{r}}{r}\right] = 0, \tag{10.44}$$

where $\boldsymbol{L}$ is the angular momentum that generates the SO(3) algebra. This indicates that the relativistic generalization of the RL vector is

$$\boldsymbol{A} = \boldsymbol{p} \times \boldsymbol{L} - (E + m)\,\frac{\alpha \boldsymbol{r}}{r}. \tag{10.45}$$

The vector $\boldsymbol{A}$ enhances the symmetry from SO(3) to SO(4), and in this way we have shown that the non-minimal coupling $m \to m - \alpha/r$, or equivalently, the transformation to a conformally flat space with metric (10.35) allows us to restore the SO(4) symmetry in the relativistic case. Notice that by taking the non-relativistic limit of the RL vector, we obtain

$$\boldsymbol{A}_{NR} = \boldsymbol{p} \times \boldsymbol{L} - \frac{2\alpha m \boldsymbol{r}}{r}, \tag{10.46}$$

which is the usual RL vector with a coupling constant twice as larger. We observe that the analogous procedure to obtain the classical non relativistic orbit of the Coulomb

problem can also be implemented in the relativistic case. If we take the dot product of the RL vector with $\boldsymbol{r}$, we get

$$\boldsymbol{A}\cdot\boldsymbol{r} = Ar\cos\theta = (\boldsymbol{p}\times\boldsymbol{L})\cdot\boldsymbol{r} - (E+m)\,\frac{\alpha\boldsymbol{r}\cdot\boldsymbol{r}}{r}, \tag{10.47}$$

or

$$\frac{1}{r} = \frac{\alpha(E+m)}{L^2}\left[1+\frac{A}{\alpha(E+m)}\cos\theta\right]. \tag{10.48}$$

This is precisely the equation of an ellipse with one of its foci at the origin. The eccentricity and semi-latus rectum are given, respectively by

$$e = \frac{A}{\alpha\,(E+m)}, \quad p = \frac{L^2}{\alpha(E+m)}, \tag{10.49}$$

while the semi-major and semi-minor axes are

$$a = \frac{\alpha L^2(E+m)}{\alpha^2(E+m)^2 - A^2}, \quad b = \frac{L^2}{\sqrt{\alpha^2(E+m)^2 - A^2}}. \tag{10.50}$$

Now, we focus on the infinitesimal transformations associated with the position x^i and the canonical momentum p^i that are generated by our relativistic RL vector. We find that

$$\delta x^i = \left\{x^i, \epsilon^j A^j\right\} = 2(\boldsymbol{\epsilon}\cdot\boldsymbol{r})p^i - x^i(\boldsymbol{\epsilon}\cdot\boldsymbol{p}) - (\boldsymbol{r}\cdot\boldsymbol{p})\epsilon^i,$$

$$\delta p^i = \left\{p^i, \epsilon^j A^j\right\} = -\boldsymbol{p}^2\epsilon^i + (\boldsymbol{p}\cdot\boldsymbol{\epsilon})p^i - (E+m)\,\alpha\left(\frac{\boldsymbol{\epsilon}\cdot\boldsymbol{r}}{r^3}x^i - \frac{\epsilon^i}{r}\right).$$

The RL vector also acts on the magnitude r as

$$\delta r = \left\{\sqrt{x^l x^l}, \epsilon^i A^i\right\} = \frac{(\boldsymbol{p}\cdot\boldsymbol{r})\,(\boldsymbol{r}\cdot\boldsymbol{\epsilon})}{r} - (\boldsymbol{\epsilon}\cdot\boldsymbol{p})r. \tag{10.51}$$

These infinitesimal symmetries do not exactly correspond with the symmetry transformations previously written in [40]. A crucial difference is that in the approach given in [40] the symmetry transformation acts in a dual momentum space (dual conformal transformation) that is appropriate to reveal the symmetries of scattering amplitudes in SYM theory.

We turn to the spectrum. It turns out that it can also be constructed from the relativistic SO(4) algebra generalizing the non relativistic result as presented in [160]. We introduce a redefinition of the RL vector (10.45)

$$\boldsymbol{A}' = \frac{2}{E+m}\boldsymbol{A} = \frac{1}{E+m}(\boldsymbol{p}\times\boldsymbol{L} - \boldsymbol{L}\times\boldsymbol{p}) - 2\alpha\frac{\boldsymbol{r}}{r}.$$

This vector $\boldsymbol{A}'$ satisfies

$$[\boldsymbol{A}', H] = 0, \quad \boldsymbol{L}\cdot\boldsymbol{A}' = \boldsymbol{A}'\cdot\boldsymbol{L},$$

and

$$\boldsymbol{A}'^2 = 4\left[\alpha^2 + \frac{E-m}{E+m}(1+L^2)\right]. \tag{10.52}$$

We can see that the corresponding relativistic algebra closes as

$$[L_i, L_j] = i\varepsilon_{ijk}L_k,$$

$$[A'_i, L_j] = i\varepsilon_{ijk}A'_k,$$

$$[A'_i, A'_j] = -4i\left(\frac{E-m}{E+m}\right)\varepsilon_{ijk}L_k.$$

Defining

$$\boldsymbol{D} = \sqrt{-\frac{E+m}{4(E-m)}}\boldsymbol{A}'$$

and

$$\boldsymbol{M} = \frac{1}{2}(\boldsymbol{L}-\boldsymbol{D}), \quad \boldsymbol{N} = \frac{1}{2}(\boldsymbol{L}+\boldsymbol{D}),$$

it is easy to show that the original algebra splits into the product of two SO(3) algebras

$$[M_i, M_j] = i\varepsilon_{ijk}M_k, \quad [N_i, N_j] = i\varepsilon_{ijk}N_k,$$

with the constraint

$$\boldsymbol{M}^2 = \boldsymbol{N}^2. \tag{10.53}$$

The operator $\boldsymbol{M}^2 + \boldsymbol{N}^2$ will have the eigenvalues $2\ell(\ell+1)$ with $\ell = 0, 1, 2, ...$ because of the constraint (10.53). On the other hand, we can find that

$$\boldsymbol{M}^2 + \boldsymbol{N}^2 = \frac{1}{2}\left[L^2 - \frac{E+m}{4(E-m)}\boldsymbol{A}'^2\right] = -\frac{1}{2}\left(\frac{E+m}{E-m}\alpha^2 + 1\right),$$

where we used (10.52). With this at hand, we can find the spectrum

$$E_n = m\left(1 - \frac{2\alpha^2}{n^2+\alpha^2}\right). \tag{10.54}$$

This is the same spectrum that we obtained through the identifications (10.43) and that is reported in [148], reproduced here with $n = 2\ell + 1$. Due to the hidden symmetry lying under this non-minimal coupling which reveals the existence of the relativistic RL vector, $\mathcal{N} = 4$ SYM is dubbed as the "hydrogen atom quantum field theory" [161].

10.4 Relativistic Kustaanheimo-Stiefel duality

In this section, we relate the wave functions and the spectra of the modified Coulomb problem and the modified relativistic harmonic oscillator. We consider the illustrative case of two dimensions (for the treatment of an arbitrary number of dimensions see [150]). At the end, we see how the integrals of motion of both problems are related by the KS duality.

The KS transformation relates the original variables (x, y, t) with new ones (u, v, s) by [87]

$$x = u^2 - v^2, \quad y = 2uv, \quad \frac{\mathrm{d}t}{\mathrm{d}s} = u^2 + v^2 = r. \tag{10.55}$$

We denote by $\bar{\phi}(u, v, s)$ the field that results from evaluating the original field in terms of the new variables,

$$\bar{\phi}(u, v, s) = \phi(x(u, v), y(u, v), t(s)). \tag{10.56}$$

Then, the transformation of the differential operators is

$$\frac{\partial \phi}{\partial t} = \frac{\partial \bar{\phi}}{\partial s}\frac{\mathrm{d}s}{\mathrm{d}t} = \frac{1}{u^2 + v^2}\frac{\partial \bar{\phi}}{\partial s}, \tag{10.57}$$

$$\frac{\partial^2 \phi}{\partial t^2} = \frac{1}{(u^2 + v^2)^2}\frac{\partial^2 \bar{\phi}}{\partial s^2}, \tag{10.58}$$

$$\nabla^2 \phi = \frac{1}{4(u^2 + v^2)}\nabla_u^2 \bar{\phi}, \tag{10.59}$$

where

$$\nabla_u^2 \bar{\phi} = \frac{\partial^2 \bar{\phi}}{\partial u^2} + \frac{\partial^2 \bar{\phi}}{\partial v^2}. \tag{10.60}$$

Thus, the modified Klein-Gordon equation (10.4) becomes

$$-\frac{1}{c^2(u^2 + v^2)^2}\frac{\partial^2 \bar{\phi}}{\partial s^2} + \frac{1}{4(u^2 + v^2)}\nabla_u^2 \bar{\phi} + \frac{2i\alpha}{\hbar c^2(u^2 + v^2)}\frac{\partial \bar{\phi}}{\partial s} + \frac{2\alpha m}{\hbar^2(u^2 + v^2)}\bar{\phi} - \left(\frac{mc}{\hbar}\right)^2 \bar{\phi} = 0. \tag{10.61}$$

The separation (10.31) in terms of new variables is

$$\bar{\phi}(u, v, s) = \exp\left[-\frac{i}{\hbar}E\int^s \mathrm{d}s' \, (u^2 + v^2)\right]\bar{\varphi}(u, v). \tag{10.62}$$

Substituting it in (10.61) we get

$$-\frac{\hbar^2}{4\,(E/c^2 + m)}\nabla_u^2 \bar{\varphi} - (E - mc^2)(u^2 + v^2)\bar{\varphi} = 2\alpha\bar{\varphi}. \tag{10.63}$$

This is the stationary Schrödinger equation for a two-dimensional harmonic oscillator with mass $2(E/c^2 + m)$, energy 2α, and frequency

$$\omega = c\sqrt{-\frac{E - mc^2}{E + mc^2}}. \tag{10.64}$$

Now, the time-dependent Schrödinger equation for the harmonic oscillator is

$$-\frac{\hbar^2}{4\mathcal{M}}\nabla_u^2\bar{\xi}+\frac{\mathcal{M}\omega^2}{2}(u^2+v^2)\bar{\xi}=i\hbar\frac{\partial\bar{\xi}}{\partial s}, \tag{10.65}$$

where

$$\bar{\xi}(u,v,s)=\exp\left(-\frac{i}{\hbar}\mathcal{E}s\right)\bar{\varphi}(u,v)=\exp\left(-\frac{i}{\hbar}2\alpha s\right)\bar{\varphi}(u,v). \tag{10.66}$$

Using (10.62) to substitute $\bar{\varphi}$ in terms of $\bar{\phi}$ we get

$$\begin{aligned}\bar{\xi}(u,v,s)&=\exp\left[-\frac{i}{\hbar}\left(2\alpha s-E\int^s \mathrm{d}s'\,(u^2+v^2)\right)\right]\bar{\phi}(u,v,s)\\&=\exp\left[-\frac{i}{\hbar}F(s)\right]\bar{\phi}(u,v,s).\end{aligned} \tag{10.67}$$

Here, $F(s)$ is the generating function of the canonical (and non-holonomic) KS transformation on the extended phase space [162]. Thus, we have related the wave functions $\bar{\phi}$ of the Coulomb problem (written in terms of new variables) with the wave functions $\bar{\xi}$ of the harmonic oscillator. It is also seen that the wave function φ solves both stationary equations. A final word of caution is that there will be sums in (10.67) over both E and 2α so the correspondence between the two wave functions is not one-to-one.

Now, we try to establish the relation between the spectra of the modified relativistic harmonic oscillator and the modified Coulomb problem. In the Schrödinger case, the relation between the harmonic oscillator mass, coupling constant, energy, and angular momentum $(\mathcal{M}_s, k_s, \mathcal{E}_s, \mathcal{L}_s)$ and the same variables of the Coulomb problem $(m_s, \alpha_s, E_s, L_s)$ is

$$\mathcal{M}_s=4m_s,\quad k_s=-2E_s,\quad \mathcal{E}_s=\alpha_s,\quad \mathcal{L}_s=2L_s. \tag{10.68}$$

We know that the identification (10.43) allows us to map the relativistic problem onto the non relativistic one, so this suggests the following steps to recover the spectrum of the modified relativistic Coulomb problem from that of the modified relativistic harmonic oscillator:

1. Make the identification (10.43) in the modified relativistic harmonic oscillator spectrum.
2. Apply the KS duality (10.68).
3. Make again the identification (10.43) in the opposite sense to obtain the modified Coulomb problem spectrum.

We start with the spectrum of the modified relativistic harmonic oscillator in two dimensions [149]

$$\frac{(\mathcal{E}/c^2+\mathcal{M})(\mathcal{E}-\mathcal{M}c^2)^2}{\hbar^2 k}=(4q+2|\mathcal{L}|+2)^2,\quad q=0,1,2,\ldots. \tag{10.69}$$

After carrying out step 1, we get the Schrödinger spectrum of the two-dimensional harmonic oscillator

$$\mathcal{E}_s = \hbar\sqrt{\frac{k_s}{\mathcal{M}_s}}(2q+|\mathcal{L}|+1). \tag{10.70}$$

Now, step 2 yields

$$E_s = -\frac{m_s\alpha_s^2}{2\hbar^2(q+|L|+1/2)^2}, \tag{10.71}$$

which is the spectrum of the non relativistic two-dimensional hydrogen atom. Finally, implementation of step 3 results in

$$E = mc^2\left[1-\frac{2\gamma^2}{(q+|L|+1/2)^2+\gamma^2}\right], \tag{10.72}$$

where $\gamma=\alpha/\hbar c$. By making $n=q+|L|$, we readily recognize this as the spectrum of the modified relativistic Coulomb problem in two dimensions. With these results at hand, we are able to build the relativistic KS transformation duality (cf. (10.68)):

$$\begin{aligned} E/c^2+m &= \frac{1}{4}(\mathcal{E}/c^2+\mathcal{M}),\\ E-mc^2 &= -k,\\ \alpha &= \frac{1}{2}(\mathcal{E}-\mathcal{M}c^2), \end{aligned} \tag{10.73}$$

which performs the mapping

$$\frac{\boldsymbol{\mathcal{P}}^2}{\mathcal{E}/c^2+\mathcal{M}}+k(u^2+v^2)=\mathcal{E}-\mathcal{M}c^2 \implies \frac{\boldsymbol{p}^2}{E/c^2+m}-\frac{2\alpha}{r}=E-mc^2. \tag{10.74}$$

Let us now address the issue of how the integrals of motion of both problems are related. We start with the non-relativistic case and then through the replacements (10.43) we move to the modified relativistic problem. We have already seen that the energy of a system becomes the coupling constant of the other one, so we analyze only the remaining integrals of motion. For the two-dimensional Coulomb problem, they are the Runge-Lenz vector $\boldsymbol{A}_s$ and the angular momentum L. The Runge-Lenz vector is

$$\begin{aligned} A_{s\,x} &= xp_y^2-yp_xp_y-\frac{m_s\alpha_s x}{\sqrt{x^2+y^2}},\\ A_{s\,y} &= yp_x^2-xp_xp_y-\frac{m_s\alpha_s y}{\sqrt{x^2+y^2}}, \end{aligned} \tag{10.75}$$

and the angular momentum reads $L_s = xp_y-yp_x$. On the other hand, for the two-dimensional harmonic oscillator we can find a conserved tensor $C_{s\,ij}$ whose components are [76]

$$C_{s\,11}=\frac{\mathcal{P}_u^2}{2\mathcal{M}_s}+\frac{k}{2}u^2,$$

$$C_{s\,12} = \frac{\mathcal{P}_u \mathcal{P}_v}{2\mathcal{M}_s} + \frac{k}{2} uv,$$
$$C_{s\,22} = \frac{\mathcal{P}_v^2}{2\mathcal{M}_s} + \frac{k}{2} v^2, \tag{10.76}$$

and the angular momentum $\mathcal{L}_s = up_v - vp_u$. A straightforward calculation employing the non-relativistic KS duality (10.68) shows that the mapping is

$$C_{s\,11} = \frac{\mathcal{P}_u^2}{2\mathcal{M}_s} + \frac{k}{2} u^2 = -\frac{A_{s\,x}}{2m_s} + \frac{\alpha_s}{2},$$
$$C_{s\,12} = \frac{\mathcal{P}_u \mathcal{P}_v}{2\mathcal{M}_s} + \frac{k}{2} uv = -\frac{A_{s\,y}}{2m_s},$$
$$C_{s\,22} = \frac{\mathcal{P}_v^2}{2\mathcal{M}_s} + \frac{k}{2} v^2 = \frac{A_{s\,x}}{2m_s} + \frac{\alpha_s}{2},$$
$$\mathcal{L}_s = 2L_s. \tag{10.77}$$

Finally, we apply (10.43) to find the relativistic mapping:

$$\frac{\mathcal{P}_u^2}{\mathcal{E}/c^2 + \mathcal{M}} + \frac{k}{2} u^2 = -\frac{A_x}{E/c^2 + m} + \alpha,$$
$$\frac{\mathcal{P}_u \mathcal{P}_u}{\mathcal{E}/c^2 + \mathcal{M}} + \frac{k}{2} uv = -\frac{A_y}{E/c^2 + m},$$
$$\frac{\mathcal{P}_v^2}{\mathcal{E}/c^2 + \mathcal{M}} + \frac{k}{2} v^2 = \frac{A_x}{E/c^2 + m} + \alpha,$$
$$\mathcal{L} = 2L. \tag{10.78}$$

Chapter 11

Conclusions

In this thesis, we have studied the geometry of a given system's parameter space from classical and quantum points of view. We did this with the aid of the quantum metric tensor and the Berry curvature on the quantum side, and with the classical metric and the Hannay curvature on the classical side. Different formulations of these important geometric objects have been presented and have been thoroughly discussed and exemplified, showing their relevance in the study of quantum and classical systems.

In Chapter 2, we mainly described the basic elements of the parameter space geometry, i.e., the quantum metric tensor and the Berry curvature. Our contribution here was the proof of the equivalence between the original Hilbert space formulation of the quantum geometric tensor (2.25) and the path integral approach (2.58). The proof is fundamental because it puts on a solid ground this approach and opens its confident applicability to different quantum systems. As a byproduct, we saw that the path integral approach can be used for a general quantum state, not only for the ground state.

Chapter 3 contains an important addition to the literature of the quantum geometric tensor. We presented a novel formulation in the phase space that accounts for the Abelian and non-Abelian quantum geometric tensor. The phase space function $\mathcal{A}_i(q,p;x)$ was shown to possess all the relevant information of the parameter space, and remarkably, it was seen that to build the quantum metric tensor we only require the Wigner functions.

Chapter 4 is at the heart of this thesis. We introduced for the first time the classical analog of the quantum metric tensor with the simple, but crucial observation, that the displacements of the parameters in the phase space coordinates are canonically generated. In this way, we established a parallelism with the quantum expressions, and thus, proposed the classical metric. We also contributed with the introduction of the time-dependent approach to the Hannay curvature and the classical metric, and showed how both of them emerged from the semiclassical approximation of their quantum counterparts. Here, too, we provided the proof of the equivalence of both approaches, which validates our initial proposal of the classical metric.

In the examples presented in Chapters 5 and 6, we explored a wide range of systems to get acquainted with the quantum and classical methods and established a comparison between them. We particularly highlight the quartic anharmonic oscillator and the spin-

half particle in an external field. In the first case, we proposed an algorithm to adapt canonical perturbation theory to the computation of the classical metric and found a good agreement with the quantum metric. As for the second case, the use of Grassmann variables allowed us to reproduce the quantum results.

The application of the geometric methods to the study of quantum phase transitions in the Dicke and Lipkin-Meshkov-Glick models was carried out in Chapters 7, 8 and 9. The analysis is especially relevant, because it shows that the classical description of the parameter space geometry is powerful and contains all, or almost all the elements as its quantum counterpart. For the Dicke model, the classical metric and its scalar curvature were obtained for the first time. In the Lipkin-Meshkov-Glick model, we obtained the quantum and classical metrics in the thermodynamic limit, and showed that from the finite-size analysis, it can be inferred that the scalar curvature does not diverge at the critical point, although it clearly indicates a precursor of the quantum phase transition.

Finally, in Chapter 10, our contribution was the construction of the Higgs mechanism on the $\mathcal{N} = 4$ super Yang-Mills theory that accounts for the emergence of a hydrogen-like relativistic theory. We saw that the hidden SO(4) symmetry in this system is restored, and through the introduction of a relativistic Runge-Lenz vector, we found the quantum and classical solutions. We also built the infinitesimal canonical transformations generated by the relativistic Runge-Lenz vector and we were able to reconstruct the spectrum of the system by means of a natural identification of relativistic and non-relativistic quantities. As an additional contribution, we employed the Kustaanheimo-Stiefel transformation to relate the spectra of the modified relativistic harmonic oscillator and the modified relativistic Coulomb problem, thus promoting the duality between these systems to the relativistic realm.

Many interesting lines for future research are opened with this work. For instance, the application of the path integral formulation to excited states may have interesting implications in field theory which are worth studying. Regarding the phase space formulation, a further analysis of the quantum geometric tensor might shed light on the parameter space of many-body systems and quantum optics models where the Wigner function formulation is heavily used, and in this sense, it may be useful in the quest for chaos indicators. As often seen along this work, the classical metric contains all, or almost all the information of the parameter space of a given system. Therefore, the classical methods can be used in a variety of many-body models by employing different tools such as coherent states, Grassmann variables and perturbation theory with the hope that the analysis of the deviations from the quantum results can help understand how quantum corrections arise. Naturally, the geometric analysis is not restricted to the metric tensor only and more elements such as its geodesics, its Riemann tensor, and a variety of scalars in higher-dimensional parameter spaces can be further examined with the hope that a connection with the phenomenon of entanglement, which is of great relevance in quantum information, can be found.

Appendices

Appendix A

Classical generators for the quartic anharmonic oscillator

In this appendix, we give the expression for the generators G_i of the quartic anharmonic oscillator (see Section 5.2) with Hamiltonian

$$H = \frac{p^2}{2m} + \frac{k}{2}q^2 + \frac{\lambda}{4!}q^4. \tag{A.1}$$

The parameters are $x = \{x^i\} = (m, k, \lambda)$, $i = 1, 2, 3$. To order $\mathcal{O}(\lambda^2)$, the generator G_i has the form

$$G_i(\phi_0, I; x) = \alpha_{i0} + \alpha_{i1}\lambda + \alpha_{i2}\lambda^2, \tag{A.2}$$

where in the case $i = 1$:

$$\begin{aligned}
\alpha_{10} &= -\frac{I \sin\phi_0 \cos\phi_0}{2m}, \\
\alpha_{11} &= -\frac{I^2 \sin^3\phi_0 \cos\phi_0 (2\cos\phi_0 - 3)}{48\sqrt{m^3k^3}}, \\
\alpha_{12} &= -\frac{I^3 \cos\phi_0 (647\sin\phi_0 - 329\sin 3\phi_0 + 125\sin 5\phi_0 - 30\sin 7\phi_0 + 3\sin 9\phi_0)}{27648m^2k^3},
\end{aligned} \tag{A.3}$$

while for $i = 2$:

$$\begin{aligned}
\alpha_{20} &= -\frac{I \sin\phi_0 \cos\phi_0}{2k}, \\
\alpha_{21} &= -\frac{I^2 \sin 2\phi_0 (7\cos 2\phi_0 - \cos 4\phi_0 - 12)}{192\sqrt{mk^5}}, \\
\alpha_{22} &= -\frac{I^3 \cos\phi_0 (583\sin\phi_0 - 221\sin 3\phi_0 + 65\sin 5\phi_0 - 12\sin 7\phi_0 + \sin 9\phi_0)}{9216mk^4},
\end{aligned} \tag{A.4}$$

and for $i = 3$:

$$\begin{aligned}
\alpha_{30} =& -\frac{I^2 \cos\phi_0(9\sin\phi_0 - \sin 3\phi_0)}{96\sqrt{mk^3}},\\
\alpha_{31} =& \frac{I^3 \cos\phi_0(551\sin\phi_0 - 167\sin 3\phi_0 + 35\sin 5\phi_0 - 3\sin 7\phi_0)}{13824mk^3},\\
\alpha_{32} =& \frac{I^4 \sin 2\phi_0(4547\cos 2\phi_0 - 1696\cos 4\phi_0 + 446\cos 6\phi_0 - 72\cos 8\phi_0 + 5\cos 10\phi_0 - 5480)}{884736\sqrt{m^3k^9}}.
\end{aligned} \tag{A.5}$$

Appendix B

Grassmann variables

The Grassmann variables are anticommuting numbers. In physics, they appear in the path integral formulation of a fermionic field [53]. When quantizing a classical theory, one promotes the phase space variables (q, p) to operators $(\hat{q}, \hat{p})$ acting on states $|\psi\rangle$ that belong to a Hilbert space. Additionally, the fundamental Poisson brackets

$$\{q^a, q^b\}_P = 0, \quad \{p_a, p_b\}_P = 0, \quad \{q^a, p_b\}_P = \delta^a_b \tag{B.1}$$

are promoted to commutation relations through the replacement $\{\cdot,\cdot\}_P \to \frac{1}{i\hbar}[\cdot,\cdot]$, which means that

$$[\hat{q}^a, \hat{q}^b] = 0, \quad [\hat{p}_a, \hat{p}_b] = 0, \quad [\hat{q}^a, \hat{p}_b] = i\hbar\delta^a_b. \tag{B.2}$$

Nevertheless, this process applies only to bosonic degrees of freedom. In the case of fermions, we must take into account the Pauli exclusion principle, and as a consequence, we must impose the anticommutation relations

$$\{\hat{q}^a, \hat{q}^b\} = 0, \quad \{\hat{p}_a, \hat{p}_b\} = 0, \quad \{\hat{q}^a, \hat{p}_b\} = i\hbar\delta^a_b. \tag{B.3}$$

The classical version of such a theory requires anticommuting numbers, thus, the product between two Grassmann numbers θ and θ' satisfies

$$\theta\theta' = -\theta'\theta, \tag{B.4}$$

which implies that $\theta^2 = 0$. If we have a set of n generators $\theta = \{\theta_1, ...\theta_n\}$ that satisfy the anticommutation relations

$$\{\theta_i, \theta_j\} = 0, \quad (i, j = 1, ..., n), \tag{B.5}$$

then the set of linear combinations of θ with c-number coefficients (usual commuting numbers) is called a Grassmann number, and the algebra generated by θ is called the Grassmann algebra Λ^n. Therefore, a function $f \in \Lambda^n$ has the expansion

$$f(\theta) = f_0 + \sum_{i=1}^{n} f_i\theta_i + \sum_{i<j} f_{ij}\theta_i\theta_j + ... + \sum_{i<j<k} f_{ijk}\theta_i\theta_j\theta_k + ... + f_{1\cdots n}\theta_1...\theta_n, \tag{B.6}$$

where the coefficients $f_{ij\cdots}$ are completely antisymmetric. Of course, a Grassmann number θ_i commutes with a c-number.

Two types of linear operators can be introduced to differentiate a function $f(\theta)$: the left derivative $\frac{\vec{\partial}}{\partial\theta_i}f(\theta)$ and the right derivative $f(\theta)\frac{\overleftarrow{\partial}}{\partial\theta_i}$. Their action on the generators yields

$$\frac{\vec{\partial}}{\partial\theta_i}\theta_j = \delta_{ij}, \quad \theta_j\frac{\overleftarrow{\partial}}{\partial\theta_i} = \delta_{ij}. \tag{B.7}$$

The derivatives anticommute with θ_i, thus the Leibniz rule takes the form

$$\frac{\vec{\partial}}{\partial\theta_i}(\theta_j\theta_k) = \frac{\vec{\partial}\theta_j}{\partial\theta_i}\theta_k - \theta_j\frac{\vec{\partial}\theta_k}{\partial\theta_i} = \delta_{ij}\theta_k - \delta_{ik}\theta_j, \tag{B.8}$$

and analogously for the right derivative. For higher orders, the following relations hold:

$$\frac{\vec{\partial}}{\partial\theta_i}\frac{\vec{\partial}}{\partial\theta_j} + \frac{\vec{\partial}}{\partial\theta_j}\frac{\vec{\partial}}{\partial\theta_i} = 0, \quad \frac{\overleftarrow{\partial}}{\partial\theta_i}\frac{\overleftarrow{\partial}}{\partial\theta_j} + \frac{\overleftarrow{\partial}}{\partial\theta_j}\frac{\overleftarrow{\partial}}{\partial\theta_i} = 0. \tag{B.9}$$

If besides the n generators θ of the Grassmann algebra Λ^n, we add n more generators denoted as θ^* and introduce an involution $*$, then the resulting algebra Λ^{2n} has the properties

$$\begin{aligned} \{\theta_i, \theta_j^*\} &= 0, \\ (\theta_i^*)^* &= \theta_i, \\ (\theta_i\theta_j)^* &= \theta_j^*\theta_i^*, \\ (f_{i_1\cdots i_n}\theta_{i_1}\cdots\theta_{i_n})^* &= f^*_{i_1\cdots i_n}\theta^*_{i_n}\cdots\theta^*_{i_1}, \end{aligned} \tag{B.10}$$

where $f^*_{i_1\cdots i_n}$ is the complex conjugate of $f_{i_1\cdots i_n}$.

Appendix C

Bloch coherent states

The Bloch coherent states (or SU(2) coherent states) [139, 140] can be defined through a displacement operator parameterized by a complex number ζ. In units where $\hbar = 1$, the displacement operator is

$$\hat{\Omega}(\zeta) = e^{\zeta \hat{J}_+ - \zeta^* \hat{J}_-}. \tag{C.1}$$

The form of this operator is reminiscent of the corresponding displacement operator for the harmonic oscillator coherent states. In the case of angular momentum, the role of the creation and annihilation operators is played by $\hat{J}_+$ and $\hat{J}_-$, respectively. Choosing the parameterization $\zeta = \frac{\theta}{2} e^{-i\phi}$, it is easy to see that the operator $\hat{\Omega}(\zeta)$ takes the form

$$\hat{\Omega}(\zeta) = e^{-i\theta(\hat{J}_x \sin\phi - \hat{J}_y \cos\phi)}, \tag{C.2}$$

which represents a rotation by an angle θ around the axis $\boldsymbol{n} = (\sin\phi, -\cos\phi, 0)$.

Now, using the disentangling theorem for angular momentum operators [140], we can recast $\hat{\Omega}(\zeta)$ in a more useful form as

$$\hat{\Omega}(\zeta) = e^{\zeta \hat{J}_+ - \zeta^* \hat{J}_-} = e^{z\hat{J}_+} e^{\ln(1+|z|^2)\hat{J}_z} e^{-z^* \hat{J}_-}, \tag{C.3}$$

where, if $\zeta = \frac{\theta}{2} e^{-i\phi}$, then z is parameterized as $z = e^{-i\phi} \tan\frac{\theta}{2}$. Following the convention of reference [140], a Bloch coherent state $|z\rangle$ is defined by the application of the displacement operator (C.1) to the state with the lowest angular momentum projection, i.e.,

$$|z\rangle = \hat{\Omega}(\zeta)|j, -j\rangle = e^{z\hat{J}_+} e^{\ln(1+|z|^2)\hat{J}_z} e^{-z^* \hat{J}_-} |j, -j\rangle. \tag{C.4}$$

We can get rid of two operators by noticing that the only contribution in the series expansion of the rightmost exponential is the identity. Thus, we are left with

$$\begin{aligned} |z\rangle &= e^{z\hat{J}_+} e^{\ln(1+|z|^2)\hat{J}_z} |j, -j\rangle \\ &= e^{z\hat{J}_+} e^{-j\ln(1+|z|^2)} |j, -j\rangle \\ &= \frac{1}{(1+|z|^2)^j} e^{z\hat{J}_+} |j, -j\rangle. \end{aligned} \tag{C.5}$$

Expanding the remaining exponential and using

$$\hat{J}_+^k|j,-j\rangle = \sqrt{\frac{k!(2j)!}{(2j-k)!}}|j,-j+k\rangle, \quad k=0,1,...,2j\,, \tag{C.6}$$

we finally arrive at the expression of the Bloch coherent states in terms of $|j,m\rangle$ states:

$$|z\rangle = \frac{1}{(1+|z|^2)^j}\sum_{m=-j}^{j}\binom{2j}{j+m}^{1/2} z^{j+m}|j,m\rangle. \tag{C.7}$$

With this equation at hand, it is not hard to show that the overlap between two Bloch coherent states is

$$\langle z|z'\rangle = \frac{(1+z^*z')^{2j}}{(1+|z|^2)^j(1+|z'|^2)^j}, \tag{C.8}$$

which implies that $\langle z|z\rangle = 1$. Furthermore, their completeness relation has the form

$$\frac{2j+1}{4\pi}\int \mathrm{d}\theta\mathrm{d}\phi\,\sin\theta\,|z\rangle\langle z| = \hat{\mathbb{1}}, \tag{C.9}$$

where the parameterization $z = e^{-i\phi}\tan\frac{\theta}{2}$ has been used.

One of the most important features of the Bloch coherent states is that the expectation values of the angular momentum components take on a simple and intuitive form. Let us first consider the expectation value of $\hat{J}_z$. Using (C.7), we get

$$\begin{aligned}
\langle z|\hat{J}_z|z\rangle &= \frac{1}{(1+|z|^2)^{2j}}\sum_{m'=-j}^{j}\binom{2j}{j+m'}^{1/2} z^{*j+m'}\sum_{m=-j}^{j}\binom{2j}{j+m}^{1/2} z^{j+m}\langle j,m'|\hat{J}_z|j,m\rangle \\
&= \frac{1}{(1+|z|^2)^{2j}}\sum_{m=-j}^{j}\binom{2j}{j+m} m|z|^{2(j+m)} \\
&= \frac{1}{(1+|z|^2)^{2j}}\sum_{k=0}^{2j}\binom{2j}{k} k|z|^{2k} - j\frac{1}{(1+|z|^2)^{2j}}\sum_{k=0}^{2j}\binom{2j}{k}|z|^{2k} \\
&= \frac{|z|^2}{(1+|z|^2)^{2j}}\frac{\partial}{\partial(|z|^2)}\sum_{k=0}^{2j}\binom{2j}{k}|z|^{2k} - j\frac{1}{(1+|z|^2)^{2j}}\sum_{k=0}^{2j}\binom{2j}{k}|z|^{2k}.
\end{aligned} \tag{C.10}$$

Recognizing the binomial expansion

$$\sum_{k=0}^{2j}\binom{2j}{k}|z|^{2k} = (1+|z|^2)^{2j}, \tag{C.11}$$

we arrive at

$$\begin{aligned}
\langle z|\hat{J}_z|z\rangle &= \frac{|z|^2}{(1+|z|^2)^{2j}}(2j)(1+|z|^2)^{2j-1} - j \\
&= -j\frac{1-|z|^2}{1+|z|^2}.
\end{aligned} \tag{C.12}$$

Proceeding in an analogous fashion with $\hat{J}_+$ and $\hat{J}_-$, we find that

$$\begin{aligned}
\langle z|\hat{J}_+|z\rangle &= j\frac{2z^*}{1+|z|^2},\\
\langle z|\hat{J}_-|z\rangle &= j\frac{2z}{1+|z|^2},\\
\langle z|\hat{J}_x|z\rangle &= j\frac{2\mathrm{Re}z}{1+|z|^2},\\
\langle z|\hat{J}_y|z\rangle &= -j\frac{2\mathrm{Im}z}{1+|z|^2},\\
\langle z|\hat{J}_z|z\rangle &= -j\frac{1-|z|^2}{1+|z|^2}.
\end{aligned} \tag{C.13}$$

which upon using the parameterization $z = e^{-i\phi}\tan\frac{\theta}{2}$ can be recast as

$$\begin{aligned}
\langle z|\hat{J}_+|z\rangle &= je^{i\phi}\sin\theta,\\
\langle z|\hat{J}_-|z\rangle &= je^{-i\phi}\sin\theta,\\
\langle z|\hat{J}_x|z\rangle &= j\sin\theta\cos\phi,\\
\langle z|\hat{J}_y|z\rangle &= j\sin\theta\sin\phi,\\
\langle z|\hat{J}_z|z\rangle &= -j\cos\theta.
\end{aligned} \tag{C.14}$$

These expressions allow us to define the classical angular momentum variables J_x,J_y, and J_z as the corresponding expectation values $\langle z|\hat{J}_x|z\rangle$, $\langle z|\hat{J}_y|z\rangle$, and $\langle z|\hat{J}_z|z\rangle$. Thus, we see that $J_x^2+J_y^2+J_z^2 = j^2$. The canonical coordinates can be found by requiring that (J_x, J_y, J_z) satisfy the SU(2) algebra

$$\{J_i, J_j\} = i\epsilon_{ijk}J_k. \tag{C.15}$$

It turns out that the pair $(\phi, -j\cos\theta) = (\phi, J_z)$ is canonical in this sense, therefore, writing the angular momentum variables as

$$J_x = \sqrt{j^2-J_z^2}\cos\phi, \quad J_y = \sqrt{j^2-J_z^2}\sin\phi, \tag{C.16}$$

we can readily see that the Poisson brackets

$$\{J_i, J_j\} = \frac{\partial J_i}{\partial\phi}\frac{\partial J_j}{\partial J_z} - \frac{\partial J_i}{\partial J_z}\frac{\partial J_j}{\partial\phi} \tag{C.17}$$

reproduce the relations (C.15). The canonical pair (ϕ, J_z) can be thought of as the action-angle variables of the classical Hamiltonian H_{cl} that corresponds to $\hat{H} \propto \hat{J}_z$, which in terms of the canonical coordinates $Q = \sqrt{2(j+J_z)}\cos\phi$, $P = -\sqrt{2(j+J_z)}\sin\phi$ has the form of the harmonic oscillator, i.e., $H_{cl} \propto \frac{1}{2}(P^2+Q^2)$.

Appendix D

Wolfram Mathematica codes

Here, we show the codes to compute the quantum metric tensor in the anisotropic LMG model (see Chapter 8) for a given j and a specified mesh in h and γ . The code was first run using a kernel for each metric component, then the determinant was computed, and finally, the scalar curvature.

D.1 Quantum metric tensor

```
In[•]:= SetDirectory[NotebookDirectory[]];

    j = 20;
    Jp = IdentityMatrix[2 j + 1];
    Jm = IdentityMatrix[2 j + 1];
    Jz = IdentityMatrix[2 j + 1]; Do[Do[Jz[[j - m + 1, j - mp + 1]] = mp KroneckerDelta[m, mp] , {mp, j, -j, -1}], {m, j, -j, -1}]
    Do[Do[Jp[[j - m + 1, j - mp + 1]] = √((j - mp) (j + mp + 1)) KroneckerDelta[m, mp + 1], {mp, j, -j, -1}], {m, j, -j, -1}]
    Do[Do[Jm[[j - m + 1, j - mp + 1]] = √((j + mp) (j - mp + 1)) KroneckerDelta[m, mp - 1], {mp, j, -j, -1}], {m, j, -j, -1}]
    Jx = Simplify[(1 / 2) (Jp + Jm)];
    Jy = Simplify[(1 / (2 I)) (Jp - Jm)];
    H = Simplify[-2 h Jz - (1/j) (Jx.Jx + γ Jy.Jy)];
    O1 = -2 Jz;
    O2 = -(1/j) (Jy.Jy);
```

Quantum metric for the ground state

```
In[•]:= G11ground[x_, y_] := Module[{Hnum, system, Ener, vec}, Hnum = H /. {h → x, γ → y};
      system = Transpose[SortBy[Transpose[Eigensystem[Hnum]], First]];
      Ener = Part[system, 1];
      vec[m_] := Part[system, 2, m];
      Sum[(vec[1].O1.vec[m])^2 / (Ener[[m]] - Ener[[1]])^2, {m, 2, 2 j + 1}]]
    G12ground[x_, y_] := Module[{Hnum, system, Ener, vec}, Hnum = H /. {h → x, γ → y};
      system = Transpose[SortBy[Transpose[Eigensystem[Hnum]], First]];
      Ener = Part[system, 1];
      vec[m_] := Part[system, 2, m];
      Sum[((vec[1].O1.vec[m]) (vec[m].O2.vec[1])) / (Ener[[m]] - Ener[[1]])^2, {m, 2, 2 j + 1}]]
    G22ground[x_, y_] := Module[{Hnum, system, Ener, vec}, Hnum = H /. {h → x, γ → y};
      system = Transpose[SortBy[Transpose[Eigensystem[Hnum]], First]];
      Ener = Part[system, 1];
      vec[m_] := Part[system, 2, m];
      Sum[(vec[1].O2.vec[m])^2 / (Ener[[m]] - Ener[[1]])^2, {m, 2, 2 j + 1}]]
```

h ∈ [ai,af] with step size Δ1
γ ∈ [bi,bf] with step size Δ2

```
ai = 0.6;
af = 1.2;
bi = -0.6;
bf = -0.4;
Δ1 = 0.001;
Δ2 = 0.001;
hline = Table[m, {m, ai, af, Δ1}];
γline = Table[m, {m, bi, bf, Δ2}];
G11 = Array[0 &, {Length[hline] × Length[γline], 3}];

i = 1;
Do[Do[Part[G11, i] = {hline[[m]], γline[[n]], G11ground[hline[[m]], γline[[n]]]};
   i++, {n, 1, Length[γline]}], {m, 1, Length[hline]}] // AbsoluteTiming
Export["G11_j20.csv", G11]
```

```
In[•]:= Clear[Jp, Jm, Jx, Jy, Jz, H, O1, O2, hline, γline, G11]
```

D.2 Determinant

```
SetDirectory[NotebookDirectory[]];
datG11 = Import["G11_j20.csv"];
datG12 = Import["G12_j20.csv"];
datG22 = Import["G22_j20.csv"];
```

Number of points in h

```
N1 = 601;
```

Number of points in γ

```
N2 = 201;
```

Determinant

```
G = Array[0 &, {N1 N2, 3}];
Do[Part[G, i] = {datG11[[i, 1]], datG11[[i, 2]], datG11[[i, 3]] * datG22[[i, 3]] - datG12[[i, 3]]^2}, {i, 1, N1 N2}]
Export["G_j20.csv", G]
```

```
In[•]:= Clear[datG11, datG12, datG22, G]
```

D.3 Scalar curvature

```
SetDirectory[NotebookDirectory[]];
datg11 = Import["G11_j20.csv"];
datg12 = Import["G12_j20.csv"];
datg22 = Import["G22_j20.csv"];
datg = Import["G_j20.csv"];
```

h ∈ [ai,af] with step size Δ1
γ ∈ [bi,bf] with step size Δ2

```
ai = 0.6;
af = 1.2;
bi = -0.6;
bf = -0.4;
Δ1 = 0.001;
Δ2 = 0.001;
hline = Table[m, {m, ai, af, Δ1}];
γline = Table[m, {m, bi, bf, Δ2}];
```

Converts the metric and determinant from 3-column format to mesh format

```
In[•]:= g11 = Array[0 &, {Length[hline], Length[γline]}];
g12 = Array[0 &, {Length[hline], Length[γline]}];
g22 = Array[0 &, {Length[hline], Length[γline]}];
g = Array[0 &, {Length[hline], Length[γline]}];
Ain = Array[0 &, {Length[hline], Length[γline]}];
Bin = Array[0 &, {Length[hline], Length[γline]}];
R = Array[0 &, {Length[hline], Length[γline]}];

In[•]:= k = 1;
Do[Do[
  g11[[i, j]] = datg11[[k, 3]];
  g12[[i, j]] = datg12[[k, 3]];
  g22[[i, j]] = datg22[[k, 3]];
  g[[i, j]] = datg[[k, 3]];
  k++, {j, 1, Length[γline]}], {i, 1, Length[hline]}]
Clear[k]
```

Computation of the scalar curvature

```
Der10G11 = NDSolve`FiniteDifferenceDerivative[{1, 0}, {hline, γline}, g11];
Der01G11 = NDSolve`FiniteDifferenceDerivative[{0, 1}, {hline, γline}, g11];
Der10G12 = NDSolve`FiniteDifferenceDerivative[{1, 0}, {hline, γline}, g12];
Der10G22 = NDSolve`FiniteDifferenceDerivative[{1, 0}, {hline, γline}, g22];
```

```
Do[Do[Ain[[i, j]] = (1 / (√g[[i, j]])) ((g12[[i, j]] / g11[[i, j]]) Der01G11[[i, j]] - Der10G22[[i, j]]);
  Bin[[i, j]] = (1 / (√g[[i, j]])) (2 Der10G12[[i, j]] - Der01G11[[i, j]] - (g12[[i, j]] / g11[[i, j]]) Der10G11[[i, j]]), {j, 1, Length[γline]}],
 {i, 1, Length[hline]}]
```

```
A = NDSolve`FiniteDifferenceDerivative[{1, 0}, {hline, γline}, Ain];
B = NDSolve`FiniteDifferenceDerivative[{0, 1}, {hline, γline}, Bin];
```

```
Do[Do[R[[i, j]] = (1 / (√g[[i, j]])) (A[[i, j]] + B[[i, j]]), {j, 1, Length[γline]}], {i, 1, Length[hline]}]
```

```
Clear[g11, g12, g22, g, Ain, Bin, Der10G11, Der01G11, Der10G12, Der10G22, A, B]
```

Converts the scalar curvature from mesh format to 3-column format

```
datR = Array[0 &, {Length[hline] × Length[γline], 3}];
```

```
k = 1;
Do[Do[
  Part[datR, k] = {hline[[i]], γline[[j]], R[[i, j]]}; k ++, {j, 1, Length[γline]}], {i, 1, Length[hline]}]
Clear[k]
```

```
Clear[R]
```

```
Export["R_j20.csv", datR]
```

```
Clear[datg11, datg12, datg22, datg, datR]
```

Appendix E

Quantum geometric tensor for Bloch coherent states in the modified LMG model

In this section, we compute the quantum geometric tensor for the modified LMG model (see Chapter 9) using Bloch coherent states. These states are parameterized by the complex number $z = e^{-i\phi}\tan\frac{\theta}{2}$ and are given by

$$|z\rangle = \frac{e^{z\hat{J}_+}|j,-j\rangle}{(1+|z|^2)^j} = \sum_{m=-j}^{j} c_m^{(j)}|j,m\rangle, \tag{E.1}$$

where

$$c_m^{(j)} := \binom{2j}{j+m}^{1/2} \sin^{j+m}\frac{\theta}{2}\cos^{j-m}\frac{\theta}{2}\, e^{-i(j+m)\phi}. \tag{E.2}$$

The angles on the Bloch sphere are functions of the parameters, i.e., $\theta = \theta(x)$ and $\phi = \phi(x)$, with $x = \{x^i\} = (\Omega_x, \xi_y)$, $i = 1, 2$. The coherent state $|z\rangle$ that corresponds to the highest energy state has the coordinates:

- $(\theta_4, \phi_4) = \left(\arccos\left(-\frac{1}{2\xi_y}\right), \arccos\left(\frac{\Omega_x}{\sqrt{4\xi_y^2-1}}\right)\right)$ for $\xi_y > \frac{\sqrt{\Omega_x^2+1}}{2}$.
- $(\theta_1, \phi_1) = \left(\arccos\left(-\frac{1}{\sqrt{1+\Omega_x^2}}\right), 0\right)$ for $\xi_y \leq \frac{\sqrt{\Omega_x^2+1}}{2}$.

The quantum geometric tensor for the coherent state $|z\rangle$ is given by

$$G_{ij}^{(z)} = \langle\partial_i z|\partial_j z\rangle - \langle\partial_i z|z\rangle\langle z|\partial_j z\rangle = \sum_{m=-j}^{j}\partial_i c_m^{*(j)}\partial_j c_m^{(j)} - \sum_{m=-j}^{j}\partial_i c_m^{*(j)} c_m^{(j)} \sum_{n=-j}^{j} c_n^{*(j)}\partial_j c_n^{(j)}. \tag{E.3}$$

With this at hand, we find the metric tensor, its determinant, and the Berry curvature for both phases.

-For $\xi_y > \frac{\sqrt{\Omega_x^2+1}}{2}$ (broken phase):

$$\begin{aligned} F_{12}^{(z)} &= -\frac{j}{2}\frac{1}{\xi_y^2\sqrt{4\xi_y^2-\Omega_x^2-1}}, \\ g_{11}^{(z)} &= \frac{j}{2}\frac{4\xi_y^2-1}{4\xi_y^2(4\xi_y^2-\Omega_x^2-1)}, \\ g_{12}^{(z)} &= -\frac{j}{2}\frac{\Omega_x}{\xi_y(4\xi_y^2-\Omega_x^2-1)}, \\ g_{22}^{(z)} &= \frac{j}{2}\frac{\Omega_x^2+1}{\xi_y^2(4\xi_y^2-\Omega_x^2-1)}, \\ g^{(z)} &= \frac{j^2}{16\xi_y^4(4\xi_y^2-\Omega_x^2-1)}. \end{aligned} \tag{E.4}$$

-For $\xi_y < \frac{\sqrt{\Omega_x^2+1}}{2}$ (symmetric phase):

$$\begin{aligned} F_{12}^{(z)} &= 0, \\ g_{11}^{(z)} &= \frac{j}{2}\frac{1}{(\Omega_x^2+1)^2}, \\ g_{12}^{(z)} &= 0, \\ g_{22}^{(z)} &= 0, \\ g^{(z)} &= 0. \end{aligned} \tag{E.5}$$

Since for the symmetric phase, $\xi_y < \frac{\sqrt{\Omega_x^2+1}}{2}$, the determinant of the metric is zero, the scalar curvature is not defined there. On the other hand, in the broken phase, $\xi_y > \frac{\sqrt{\Omega_x^2+1}}{2}$, it is possible to compute it using (1.20), which yields

$$R = 4/j. \tag{E.6}$$

In Figure E.1, we plot the resulting quantum metric tensors and their scalar curvature. In [5], the authors found the scalar curvature for the Bloch coherent states taking (θ, ϕ) as parameters, obtaining the same result (E.6). Due to the invariant nature of R under coordinate transformations, we conclude that the metric (E.4) is actually the metric of a sphere (see Chapter 1) in more complicated coordinates.

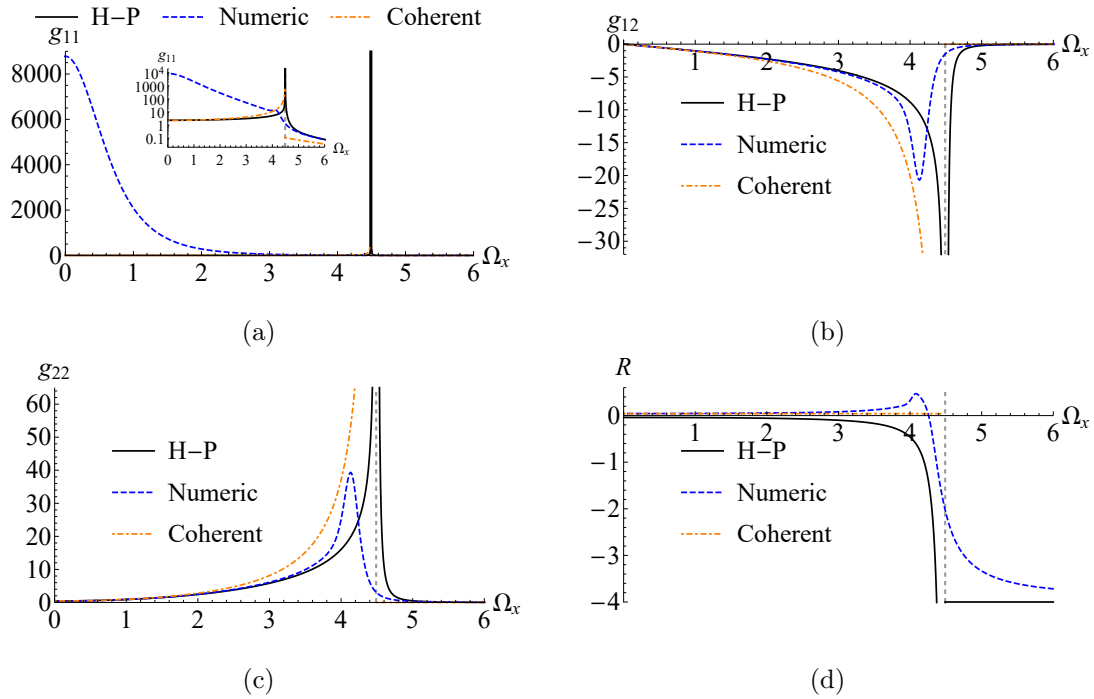

Figure E.1: Comparison of the quantum metric tensor and the scalar curvature obtained with the truncated Holstein-Primakoff approximation (solid black), coherent states (dot-dashed orange), and exact diagonalization (dashed blue). We fixed $j = 96$ and $\xi_y = 2.3$.

Appendix F

Precision considerations in the modified LMG model

In this section, our aim is to give some details regarding precision requirements for the computation of the quantum metric tensor in the modified LMG model (see Chapter 9). We only explore the energy levels, which is sufficient to provide insight into the phenomenon. To that end, consider the following Hamiltonian

$$\hat{H}^* = \Omega_x \hat{J}_x + \frac{\xi_y}{j} \hat{J}_y^2. \tag{F.1}$$

This Hamiltonian has an exact degeneracy when $\Omega_x = 0$, in contrast to the LMG Hamiltonian (9.1). In Figure F.1, we show the energy of the four upper eigenstates for both Hamiltonians. We notice that the energy levels begin getting together near the critical Ω_x where the quantum phase transition takes place in the thermodynamic limit.

To further characterize the level crossing for both Hamiltonians, we take the logarithm of the difference in energies between the maximum state ($n = 2j+1$) and the state closest to the maximum ($n = 2j$). We show in Figure F.2 the plots for $j = 32$ and $\xi_y = 2.3$. Some crucial features can be observed from the plots. As Figure F.2 (a) and (c) clearly show, machine precision of 15 decimal digits is not enough to have a good resolution of the energy difference; as a consequence, the computation of the quantum metric tensor is affected, since the denominator of equation (2.64) blows up. Now, if we raise the machine precision to a digit accuracy of 60[1], then Figure F.2 (b) and (d) are obtained. We thus see that the energy difference of the two upper levels of the LMG Hamiltonian (9.1) is now resolved, as opposed to the Hamiltonian $\hat{H}^*$, which continues unresolved due to its exact degeneracy. This brief analysis shows the importance of incorporating digit accuracy in the numerical computations, otherwise, the results would show a high degree of noise and conclusions could not be extracted with certainty. Naturally, as j increases, the precision requirement and the computing time is higher. This restricts the possibility to study higher values of j.

[1]The Wolfram Mathematica 12.1 software was used to undertake this task.

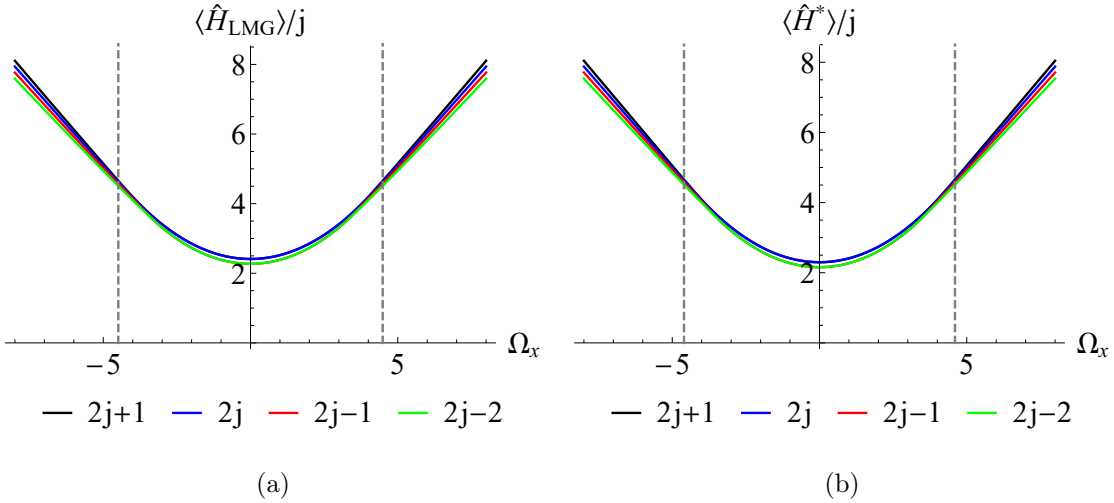

Figure F.1: Expectation value of $\hat{H}_{\mathrm{LMG}}$ taken in the upper four eigenstates (a), and of $\hat{H}^*$ (b). We fixed $j = 32$ and $\xi_y = 2.3$. The levels begin getting together near $\Omega_{xc} = 4.490$.

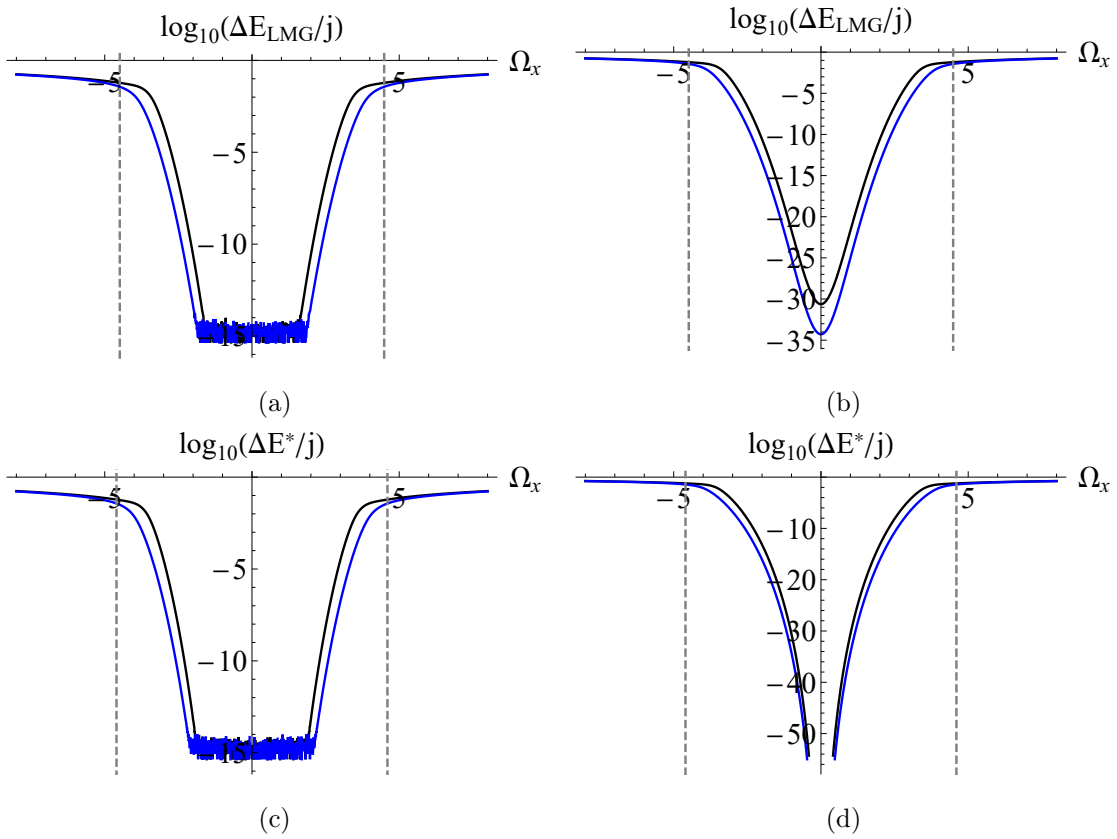

Figure F.2: Energy difference between the states $n = 2j+1$ and $n = 2j$ (blue) and between the states $n = 2j-1$ and $n = 2j-2$ (black) for the Hamiltonian $\hat{H}_{\mathrm{LMG}}$ ((a) and (b)) and for the Hamiltonian $\hat{H}^*$ ((c) and (d)). We fixed $j = 32$ and $\xi_y = 2.3$. The Hamiltonian $\hat{H}^*$ presents a level crossing at $\Omega_x = 0$, in contrast to $\hat{H}_{\mathrm{LMG}}$, which has an avoided crossing there. The plots in the left column were computed with machine precision, whereas those in the right have a precision of 60 decimal digits.

References

[1]A. Carollo, D. Valenti, and B. Spagnolo, "Geometry of quantum phase transitions", Physics Reports **838**, 1 (2020).

[2]P. Facchi, R. Kulkarni, V. Man'ko, G. Marmo, E. Sudarshan, and F. Ventriglia, "Classical and quantum Fisher information in the geometrical formulation of quantum mechanics", Physics Letters A **374**, 4801 (2010).

[3]J. Dittmann, "Explicit formulae for the Bures metric", Journal of Physics A: Mathematical and General **32**, 2663 (1999).

[4]D. Chruściński and A. Jamiołkowski, *Geometric phases in classical and quantum mechanics* (Springer Science+Business Media, 2004).

[5]J. P. Provost and G. Vallee, "Riemannian structure on manifolds of quantum states", Communications in Mathematical Physics **76**, 289 (1980).

[6]M. V. Berry, "Quantal phase factors accompanying adiabatic changes", Proceedings of the Royal Society of London A: Mathematical, Physical and Engineering Sciences **392**, 45 (1984).

[7]B. Simon, "Holonomy, the quantum adiabatic theorem, and Berry's phase", Physical Review Letters **51**, 2167 (1983).

[8]J. H. Hannay, "Angle variable holonomy in adiabatic excursion of an integrable Hamiltonian", Journal of Physics A: Mathematical and General **18**, 221 (1985).

[9]M. V. Berry, "Classical adiabatic angles and quantal adiabatic phase", Journal of Physics A: Mathematical and General **18**, 15 (1985).

[10]Y. Aharonov and J. Anandan, "Phase change during a cyclic quantum evolution", Physical Review Letters **58**, 1593 (1987).

[11]J. Anandan and Y. Aharonov, "Geometry of quantum evolution", Physical Review Letters **65**, 1697 (1990).

[12]A. K. Pati, "Relation between 'phases' and 'distance' in quantum evolution", Physics Letters A **159**, 105 (1991).

[13]S.-J. Gu, "Fidelity approach to quantum phase transitions", International Journal of Modern Physics B **24**, 4371 (2010).

[14]P. Zanardi and N. Paunković, "Ground state overlap and quantum phase transitions", Physical Review E **74**, 031123 (2006).

[15]P. Zanardi, P. Giorda, and M. Cozzini, "Information-theoretic differential geometry of quantum phase transitions", Physical Review Letters **99**, 100603 (2007).

[16]L. Campos Venuti and P. Zanardi, "Quantum critical scaling of the geometric tensors", Physical Review Letters **99**, 095701 (2007).

[17]A. Dey, S. Mahapatra, P. Roy, and T. Sarkar, "Information geometry and quantum phase transitions in the Dicke model", Physical Review E **86**, 031137 (2012).

[18]P. Kumar, S. Mahapatra, P. Phukon, and T. Sarkar, "Geodesics in information geometry: Classical and quantum phase transitions", Physical Review E **86**, 051117 (2012).

[19]P. Kumar and T. Sarkar, "Geometric critical exponents in classical and quantum phase transitions", Physical Review E **90**, 042145 (2014).

[20]R. Maity, S. Mahapatra, and T. Sarkar, "Information geometry and the renormalization group", Physical Review E **92**, 052101 (2015).

[21]M. Kolodrubetz, V. Gritsev, and A. Polkovnikov, "Classifying and measuring geometry of a quantum ground state manifold", Physical Review B **88**, 064304 (2013).

[22]M. Iskin, "Quantum-metric contribution to the pair mass in spin-orbit-coupled Fermi superfluids", Physical Review A **97**, 033625 (2018).

[23]L. Liang, S. Peotta, A. Harju, and P. Törmä, "Wave-packet dynamics of Bogoliubov quasiparticles: Quantum metric effects", Physical Review B **96**, 064511 (2017).

[24]M. A. Nielsen, "A geometric approach to quantum circuit lower bounds", arXiv:quant-ph/0502070 (2005).

[25]M. A. Nielsen, M. R. Dowling, M. Gu, and A. C. Doherty, "Quantum computation as geometry", Science **311**, 1133 (2006).

[26]R. A. Jefferson and R. C. Myers, "Circuit complexity in quantum field theory", Journal of High Energy Physics **2017**, 107 (2017).

[27]D. Felice, C. Cafaro, and S. Mancini, "Information geometric methods for complexity", Chaos: An Interdisciplinary Journal of Nonlinear Science **28**, 032101 (2018).

[28]F. Weinhold, "Metric geometry of equilibrium thermodynamics", The Journal of Chemical Physics **63**, 2479 (1975).

[29]G. Ruppeiner, "Thermodynamics: A Riemannian geometric model", Physical Review A **20**, 1608 (1979).

[30]L. Diósi, G. Forgács, B. Lukács, and H. L. Frisch, "Metricization of thermodynamic-state space and the renormalization group", Physical Review A **29**, 3343 (1984).

[31]G. Ruppeiner, "Riemannian geometry in thermodynamic fluctuation theory", Reviews of Modern Physics **67**, 605 (1995).

[32]H. Quevedo, "Geometrothermodynamics", Journal of Mathematical Physics **48**, 013506 (2007).

[33]H. Quevedo, A. Sánchez, S. Taj, and A. Vázquez, "Phase transitions in geometrothermodynamics", General Relativity and Gravitation **43**, 1153 (2010).

[34]T. Ozawa, "Steady-state Hall response and quantum geometry of driven-dissipative lattices", Physical Review B **97**, 041108 (2018).

[35]O. Bleu, D. D. Solnyshkov, and G. Malpuech, "Measuring the quantum geometric tensor in two-dimensional photonic and exciton-polariton systems", Physical Review B **97**, 195422 (2018).

[36]T. Ozawa and N. Goldman, "Extracting the quantum metric tensor through periodic driving", Physical Review B **97**, 201117 (2018).

[37]T. Ozawa and N. Goldman, "Probing localization and quantum geometry by spectroscopy", Physical Review Research **1**, 032019 (2019).

[38]A. Gianfrate, O. Bleu, L. Dominici, V. Ardizzone, M. D. Giorgi, D. Ballarini, G. Lerario, K. W. West, L. N. Pfeiffer, D. D. Solnyshkov, D. Sanvitto, and G. Malpuech, "Measurement of the quantum geometric tensor and of the anomalous Hall drift", Nature **578**, 381 (2020).

[39]Z. Bern, J. J. M. Carrasco, L. J. Dixon, H. Johansson, and R. Roiban, "Complete four-loop four-point amplitude in N=4 super-Yang-Mills theory", Physical Review D **82**, 125040 (2010).

[40]S. Caron-Huot and J. M. Henn, "Solvable relativistic hydrogenlike system in supersymmetric Yang-Mills theory", Physical Review Letters **113**, 161601 (2014).

[41]S. Sachdev, *Quantum phase transitions*, 2nd ed (Cambridge University Press, 2011).

[42]I. Bengtsson and K. Życzkowski, *Geometry of quantum states: An introduction to quantum entanglement*, 2nd ed (Cambridge University Press, 2017).

[43]M. Wilde, *Quantum information theory*, 2nd ed (Cambridge University Press, 2017).

[44]A. Uhlmann, "The 'transition probability' in the state space of a $*$-algebra", Reports on Mathematical Physics **9**, 273 (1976).

[45]G. Fubini, *Sulle metriche definite da una forma hermitiana: nota* (Office graf. C. Ferrari, 1904).

[46]E. Study, "Kürzeste Wege im komplexen Gebiet", Mathematische Annalen **60**, 321 (1905).

[47]D. Bures, "An extension of Kakutani's theorem on infinite product measures to the tensor product of semifinite w^*-algebras", Transactions of the American Mathematical Society **135**, 199 (1969).

[48]S. M. Carroll, *Spacetime and geometry: An introduction to General Relativity* (Cambridge University Press, 2004).

[49]T. Eguchi, P. B. Gilkey, and A. J. Hanson, "Gravitation, gauge theories and differential geometry", Physics Reports **66**, 213 (1980).

[50]I. Sokolnikoff, *Tensor analysis: theory and applications* (Wiley, 1951).

[51]D. V. Alekseevskij, E. B. Vinberg, and A. S. Solodovnikov, "Geometry of spaces of constant curvature", in *Geometry II*, edited by E. B. Vinberg (Springer-Verlag, 1993).

[52]D. J. Fernández C and N. Bretón, "Is there a prescribed parameter's space for the adiabatic geometric phase?", Europhysics Letters **21**, 147 (1993).

[53]M. Nakahara, *Geometry, topology and physics* (IOP Publishing Ltd, 2003).

[54]Y.-Q. Ma, S. Chen, H. Fan, and W.-M. Liu, "Abelian and non-Abelian quantum geometric tensor", Physical Review B **81**, 245129 (2010).

[55]F. Wilczek and A. Zee, "Appearance of gauge structure in simple dynamical systems", Physical Review Letters **52**, 2111 (1984).

[56]M. Kolodrubetz, D. Sels, P. Mehta, and A. Polkovnikov, "Geometry and non-adiabatic response in quantum and classical systems", Physics Reports **697**, 1 (2017).

[57]M. Miyaji, T. Numasawa, N. Shiba, T. Takayanagi, and K. Watanabe, "Distance between quantum states and gauge-gravity duality", Physical Review Letters **115**, 261602 (2015).

[58]J. Alvarez-Jimenez, A. Dector, and J. D. Vergara, "Quantum information metric and Berry curvature from a Lagrangian approach", Journal of High Energy Physics **2017**, 44 (2017).

[59]D. Gonzalez, D. Gutiérrez-Ruiz, and J. D. Vergara, "Phase space formulation of the Abelian and non-Abelian quantum geometric tensor", Journal of Physics A: Mathematical and Theoretical **53**, 505305 (2020).

[60]E. Wigner, "On the quantum correction for thermodynamic equilibrium", Physical Review **40**, 749 (1932).

[61]H. Weyl, *The theory of groups and quantum mechanics* (Dover, 1950).

[62]M. Hillery, R. O'Connell, M. Scully, and E. Wigner, "Distribution functions in physics: Fundamentals", Physics Reports **106**, 121 (1984).

[63]W. B. Case, "Wigner functions and Weyl transforms for pedestrians", American Journal of Physics **76**, 937 (2008).

[64]D. Chruściński, "Phase-space approach to Berry phases", Open Systems & Information Dynamics **13**, 67 (2006).

[65]D. T. Smithey, M. Beck, M. G. Raymer, and A. Faridani, "Measurement of the Wigner distribution and the density matrix of a light mode using optical homodyne tomography: Application to squeezed states and the vacuum", Physical Review Letters **70**, 1244 (1993).

[66]T. Curtright, D. Fairlie, and C. Zachos, *Quantum mechanics in phase space: an overview with selected papers* (World Scientific, 2005).

[67]D. Gonzalez, D. Gutiérrez-Ruiz, and J. D. Vergara, "Classical analog of the quantum metric tensor", Physiscal Review E **99**, 032144 (2019).

[68]J. Alvarez-Jimenez, D. Gonzalez, D. Gutiérrez-Ruiz, and J. D. Vergara, "Geometry of the parameter space of a quantum system: Classical point of view", Annalen der Physik **532**, 1900215 (2020).

[69]M. Calkin, *Lagrangian and Hamiltonian Mechanics* (World Scientific, 1996).

[70]P. Kramer, M. Moshinsky, and T. Seligman, "Complex extensions of canonical transformations and quantum mechanics", in *Group theory and its applications*, edited by E. M. Loebl (Academic Press, 1975).

[71]D. Anselmi, "Some reference formulas for the generating functions of canonical transformations", The European Physical Journal C **76**, 49 (2016).

[72]E. D. Davis and G. I. Ghandour, "Canonical transformations and non-unitary evolution", Journal of Physics A: Mathematical and General **35**, 5875 (2002).

[73]V. Maslov, M. Fedoriuk, M. Fedoriuk, J. Niederle, and J. Tolar, *Semi-classical approximation in quantum mechanics* (D. Reidel Publishing C., 1981).

[74]M. Brack and R. K. Bhaduri, *Semiclassical physics* (Addison-Wesley Publishing C., 1997).

[75]M. Maamache, J. P. Provost, and G. Vallee, "Berry's phase and Hannay's angle from quantum canonical transformations", Journal of Physics A: Mathematical and General **24**, 685 (1991).

[76]H. Goldstein, C. Poole, and J. Safko, *Classical mechanics*, 3rd ed (Pearson, 2013).

[77]L. Schiff, *Quantum mechanics* (McGraw-Hill, 1965).

[78]J. J. Sakurai, *Modern quantum mechanics*, 2nd ed (Addison-Wesley Publishing C., 1994).

[79]A. V. Turbiner, "The eigenvalue spectrum in quantum mechanics and the nonlinearization procedure", Soviet Physics Uspekhi **27**, 668 (1984).

[80]C. M. Bender and T. T. Wu, "Anharmonic oscillator", Physical Review **184**, 1231 (1969).

[81]C. M. Bender and T. T. Wu, "Anharmonic oscillator II. A study of perturbation theory in large order", Physical Review D **7**, 1620 (1973).

[82]W. Dittrich and M. Reuter, *Classical and quantum dynamics: from classical paths to path integrals*, 3rd ed (Springer, 2001).

[83]J. E. Drummond, "The anharmonic oscillator: perturbation series for cubic and quartic energy distortion", Journal of Physics A: Mathematical and General **14**, 1651 (1981).

[84]B. Zaslow and M. E. Zandler, "Two-dimensional analog to the hydrogen atom", American Journal of Physics **35**, 1118 (1967).

[85]L. J. Curtis and D. G. Ellis, "Use of the Einstein–Brillouin–Keller action quantization", American Journal of Physics **72**, 1521 (2004).

[86]C. Cohen-Tannoudji, B. Diu, and F. Laloë, *Quantum mechanics Vol. 1* (Wiley, 1991).

[87]S. A. Hojman, S. Chayet, D. Núñez, and M. A. Roque, "An algorithm to relate general solutions of different bidimensional problems", Journal of Mathematical Physics **32**, 1491 (1991).

[88]H. Kleinert, *Path integrals in quantum mechanics, statistics, polymer physics, and financial markets*, 5th ed (World Scientific, 2009).

[89]L. Bombelli, R. K. Koul, J. Lee, and R. D. Sorkin, "Quantum source of entropy for black holes", Physical Review D **34**, 373 (1986).

[90]M. Srednicki, "Entropy and area", Physical Review Letters **71**, 666 (1993).

[91]L. A. P. Zayas and N. Quiroz, "Left-right entanglement entropy of boundary states", Journal of High Energy Physics **2015**, 110 (2015).

[92]Y. S. Kim and M. E. Noz, "Coupled oscillators, entangled oscillators, and Lorentz-covariant harmonic oscillators", Journal of Optics B: Quantum and Semiclassical Optics **7**, S458 (2005).

[93]J. P. Paz and A. J. Roncaglia, "Dynamics of the entanglement between two oscillators in the same environment", Physical Review Letters **100**, 220401 (2008).

[94]D. N. Makarov, "Coupled harmonic oscillators and their quantum entanglement", Physical Review E **97**, 042203 (2018).

[95]S. Bellucci, A. Nersessian, A. Saghatelian, and V. Yeghikyan, "Quantum ring models and action-angle variables", Journal of Computational and Theoretical Nanoscience **8**, 769 (2011).

[96]J. Simonin, C. R. Proetto, Z. Barticevic, and G. Fuster, "Single-particle electronic spectra of quantum rings: A comparative study", Physical Review B **70**, 205305 (2004).

[97]G. Arfken, H. Weber, and F. Harris, *Mathematical methods for physicists*, 6th ed (Elsevier, 2005).

[98]R. Shankar, *Principles of quantum mechanics*, 2nd ed (Plenum Press, 1994).

[99]M. Abramowitz and I. Stegun, *Handbook of mathematical functions: with formulas, graphs, and mathematical tables* (Dover Publications, 1965).

[100]E. Gozzi and W. D. Thacker, "Classical adiabatic holonomy in a Grassmannian system", Physical Review D **35**, 2388 (1987).

[101]E. Gozzi, D. Rohrlich, and W. D. Thacker, "Classical adiabatic holonomy in field theory", Physical Review D **42**, 2752 (1990).

[102]R. H. Dicke, "Coherence in spontaneous radiation processes", Physical Review **93**, 99 (1954).

[103]Q.-H. Chen, Y.-Y. Zhang, T. Liu, and K.-L. Wang, "Numerically exact solution to the finite-size Dicke model", Physical Review A **78**, 051801 (2008).

[104]T. Liu, Y.-Y. Zhang, Q.-H. Chen, and K.-L. Wang, "Large-N scaling behavior of the ground-state energy, fidelity, and the order parameter in the Dicke model", Physical Review A **80**, 023810 (2009).

[105]L. Bakemeier, A. Alvermann, and H. Fehske, "Dynamics of the Dicke model close to the classical limit", Physical Review A **88**, 043835 (2013).

[106]C. Emary and T. Brandes, "Quantum chaos triggered by precursors of a quantum phase transition: the Dicke model", Physical Review Letters **90**, 044101 (2003).

[107]C. Emary and T. Brandes, "Chaos and the quantum phase transition in the Dicke model", Physical Review E **67**, 066203 (2003).

[108]M. A. Bastarrachea-Magnani, S. Lerma-Hernández, and J. G. Hirsch, "Comparative quantum and semiclassical analysis of atom-field systems. I. Density of states and excited-state quantum phase transitions", Physical Review A **89**, 032101 (2014).

[109]M. A. Bastarrachea-Magnani, S. Lerma-Hernández, and J. G. Hirsch, "Comparative quantum and semiclassical analysis of atom-field systems. II. Chaos and regularity", Physical Review A **89**, 032102 (2014).

[110]M. A. Bastarrachea-Magnani, B. López-del-Carpio, S. Lerma-Hernández, and J. G. Hirsch, "Chaos in the Dicke model: quantum and semiclassical analysis", Physica Scripta **90**, 068015 (2015).

[111]S. Lerma-Hernández, D. Villaseñor, M. A. Bastarrachea-Magnani, E. J. Torres-Herrera, L. F. Santos, and J. G. Hirsch, "Dynamical signatures of quantum chaos and relaxation time scales in a spin-boson system", Physical Review E **100**, 012218 (2019).

[112]N. Lambert, C. Emary, and T. Brandes, "Entanglement and the phase transition in single-mode superradiance", Physical Review Letters **92**, 073602 (2004).

[113]N. Lambert, C. Emary, and T. Brandes, "Entanglement and entropy in a spin-boson quantum phase transition", Physical Review A **71**, 053804 (2005).

[114]H. T. Quan and F. M. Cucchietti, "Quantum fidelity and thermal phase transitions", Physical Review E **79**, 031101 (2009).

[115]T.-L. Wang, L.-N. Wu, W. Yang, G.-R. Jin, N. Lambert, and F. Nori, "Quantum Fisher information as a signature of the superradiant quantum phase transition", New Journal of Physics **16**, 063039 (2014).

[116]R. Lewis-Swan, A. Safavi-Naini, J. J. Bollinger, and A. M. Rey, "Unifying scrambling, thermalization and entanglement through measurement of fidelity out-of-time-order correlators in the Dicke model", Nature Communications **10**, 1 (2019).

[117]S. Pilatowsky-Cameo, J. Chávez-Carlos, M. A. Bastarrachea-Magnani, P. Stránský, S. Lerma-Hernández, L. F. Santos, and J. G. Hirsch, "Positive quantum Lyapunov exponents in experimental systems with a regular classical limit", Physical Review E **101**, 010202 (2020).

[118]T. Holstein and H. Primakoff, "Field dependence of the intrinsic domain magnetization of a ferromagnet", Physical Review **58**, 1098 (1940).

[119]O. Castaños, E. Nahmad-Achar, R. López-Peña, and J. G. Hirsch, "No singularities in observables at the phase transition in the Dicke model", Physical Review A **83**, 051601 (2011).

[120]J. Alvarez-Jimenez and J. D. Vergara, "The quantum geometric tensor from generating functions", International Journal of Quantum Information **17**, 1950017 (2019).

[121]M. Pandey, P. W. Claeys, D. K. Campbell, A. Polkovnikov, and D. Sels, "Adiabatic eigenstate deformations as a sensitive probe for quantum chaos", Physical Review X **10**, 041017 (2020).

[122]O. Castaños, R. López-Peña, J. G. Hirsch, and E. López-Moreno, "Phase transitions and accidental degeneracy in nonlinear spin systems", Physical Review B **72**, 012406 (2005).

[123]H.-M. Kwok, W.-Q. Ning, S.-J. Gu, and H.-Q. Lin, "Quantum criticality of the Lipkin-Meshkov-Glick model in terms of fidelity susceptibility", Physical Review E **78**, 032103 (2008).

[124]O. Castaños, R. López-Peña, J. G. Hirsch, and E. López-Moreno, "Classical and quantum phase transitions in the Lipkin-Meshkov-Glick model", Physical Review B **74**, 104118 (2006).

[125]D. D. Scherer, C. A. Müller, and M. Kastner, "Finite-temperature fidelity-metric approach to the Lipkin-Meshkov-Glick model", Journal of Physics A: Mathematical and Theoretical **42**, 465304 (2009).

[126]O. Castaños, R. López-Peña, E. Nahmad-Achar, and J. G. Hirsch, "Quantum phase transitions in the LMG model by means of quantum information concepts", Journal of Physics: Conference Series **387**, 012021 (2012).

[127]O. Castaños, R. López-Peña, E. Nahmad-Achar, and J. G. Hirsch, "Quantum information approach to the description of quantum phase transitions", Journal of Physics: Conference Series **403**, 012003 (2012).

[128]J. G. Hirsch, O. Castaños, R. López-Peña, and E. Nahmad-Achar, "Virtues and limitations of the truncated Holstein-Primakoff description of quantum rotors", Physica Scripta **87**, 038106 (2013).

[129]H. Lipkin, N. Meshkov, and A. Glick, "Validity of many-body approximation methods for a solvable model: (I). Exact solutions and perturbation theory", Nuclear Physics **62**, 188 (1965).

[130]N. Meshkov, A. Glick, and H. Lipkin, "Validity of many-body approximation methods for a solvable model: (II). Linearization procedures", Nuclear Physics **62**, 199 (1965).

[131]A. Glick, H. Lipkin, and N. Meshkov, "Validity of many-body approximation methods for a solvable model: (III). Diagram summations", Nuclear Physics **62**, 211 (1965).

[132]S. Dusuel and J. Vidal, "Finite-size scaling exponents of the Lipkin-Meshkov-Glick model", Physical Review Letters **93**, 237204 (2004).

[133]S. Dusuel and J. Vidal, "Continuous unitary transformations and finite-size scaling exponents in the Lipkin-Meshkov-Glick model", Physical Review B **71**, 224420 (2005).

[134]F. Leyvraz and W. D. Heiss, "Large-N scaling behavior of the Lipkin-Meshkov-Glick model", Physical Review Letters **95**, 050402 (2005).

[135]P. Ribeiro, J. Vidal, and R. Mosseri, "Thermodynamical limit of the Lipkin-Meshkov-Glick model", Physical Review Letters **99**, 050402 (2007).

[136]P. Ribeiro, J. Vidal, and R. Mosseri, "Exact spectrum of the Lipkin-Meshkov-Glick model in the thermodynamic limit and finite-size corrections", Phys. Rev. E **78**, 021106 (2008).

[137]A. Russomanno, F. Iemini, M. Dalmonte, and R. Fazio, "Floquet time crystal in the Lipkin-Meshkov-Glick model", Physical Review B **95**, 214307 (2017).

[138]T. Fogarty, S. Deffner, T. Busch, and S. Campbell, "Orthogonality catastrophe as a consequence of the quantum speed limit", Physical Review Letters **124**, 110601 (2020).

[139]J. M. Radcliffe, "Some properties of coherent spin states", Journal of Physics A: General Physics **4**, 313 (1971).

[140]F. T. Arecchi, E. Courtens, R. Gilmore, and H. Thomas, "Atomic coherent states in quantum optics", Physical Review A **6**, 2211 (1972).

[141]P. Cejnar, M. Macek, S. Heinze, J. Jolie, and J. Dobeš, "Monodromy and excited-state quantum phase transitions in integrable systems: collective vibrations of nuclei", Journal of Physics A: Mathematical and General **39**, L515 (2006).

[142]M. Caprio, P. Cejnar, and F. Iachello, "Excited state quantum phase transitions in many-body systems", Annals of Physics **323**, 1106 (2008).

[143]M. Spivak, *A comprehensive introduction to differential geometry*, Vol. 3 (Publish or Perish, Incorporated, 1975).

[144]S. Hawking, "Spacetime foam", Nuclear Physics B **144**, 349 (1978).

[145]M. Vogl, P. Laurell, H. Zhang, S. Okamoto, and G. A. Fiete, "Resummation of the Holstein-Primakoff expansion and differential equation approach to operator square roots", Physical Review Research **2**, 043243 (2020).

[146]Q. Wen-Chao, "Bound states of the Klein-Gordon and Dirac equations for potential V(r)=Arˆ-2-Brˆ-1", Chinese Physics **12**, 1054 (2003).

[147]A. Alhaidari, H. Bahlouli, and A. Al-Hasan, "Dirac and Klein–Gordon equations with equal scalar and vector potentials", Physics Letters A **349**, 87 (2006).

[148]Y. Sakata, R. Schneider, Y. Tachikawa, and T. Yamaura, "On hydrogen-like bound states in N=4 super Yang-Mills", Journal of High Energy Physics **2017**, 15 (2017).

[149]Q. Wen-Chao, "Bound states of the Klein-Gordon and Dirac equations for scalar and vector harmonic oscillator potentials", Chinese Physics **11**, 757 (2002).

[150]J. Alvarez-Jimenez, I. Cortese, J. A. García, D. Gutiérrez-Ruiz, and J. D. Vergara, "Relativistic Runge-Lenz vector: from N=4 SYM to SO(4) scalar field theory", Journal of High Energy Physics **2018**, 153 (2018).

[151]J. Alvarez-Jimenez, I. Cortese, J. A. García, D. Gutiérrez-Ruiz, and J. D. Vergara, "Reestablishment of SO(4) symmetry in the relativistic Coulomb problem from N=4 SYM", Journal of Physics: Conference Series **1194**, 012057 (2019).

[152]H. Liang, J. Meng, and S.-G. Zhou, "Hidden pseudospin and spin symmetries and their origins in atomic nuclei", Physics Reports **570**, 1 (2015).

[153]L. Brink, J. H. Schwarz, and J. Scherk, "Supersymmetric Yang-Mills theories", Nuclear Physics B **121**, 77 (1977).

[154]N. Beisert, "The dilatation operator of N=4 super Yang–Mills theory and integrability", Physics Reports **405**, 1 (2004).

[155]R. M. Schabinger, "Scattering on the moduli space of N=4 super Yang-Mills", arXiv:0801.1542 (2015).

[156]L. F. Alday, J. Henn, J. Plefka, and T. Schuster, "Scattering into the fifth dimension of N=4 super Yang-Mills", Journal of High Energy Physics **2010**, 77 (2010).

[157]H. A. Bethe and R. W. Jackiw, *Intermediate quantum mechanics*, 3rd ed (Westview Press, 1997).

[158]L. Landau and E. Lifshitz, *Mechanics*, 3rd ed (Elsevier Science, 1982).

[159]W. Pauli, "Über das Wasserstoffspektrum vom Standpunkt der neuen Quantenmechanik", Zeitschrift für Physik **36**, 336 (1926).

[160]R. Gilmore, *Lie groups, physics, and geometry: An introduction for physicists, engineers and chemists* (Cambridge University Press, 2008).

[161]R. Brüser, S. Caron-Huot, and J. M. Henn, "Subleading Regge limit from a soft anomalous dimension", Journal of High Energy Physics **2018**, 47 (2018).

[162]A. Garcia-Chung, D. Gutiérrez-Ruiz, and J. D. Vergara, "Dirac's formalism for time-dependent Hamiltonian systems in the extended phase space", arXiv:1701.07120 (2021).